CONTROL OF MICROTUBULE ASSEMBLY IN 'DROSOPHILA' AND MDCK CELLS

Paul Hartley

A Thesis Submitted for the Degree of PhD
at the
University of St Andrews

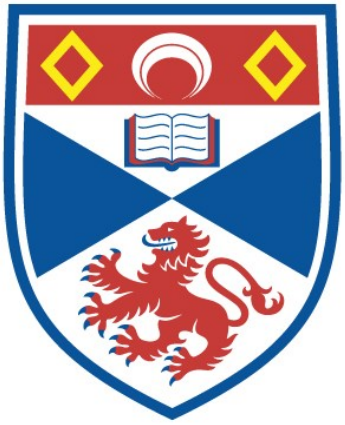

1996

Control of microtubule assembly in *Drosophila* and MDCK cells

A thesis submitted for the degree of Doctor of Philosophy to

the University of St. Andrews

by

Paul Hartley, B.Sc.

May 1995

Declarations

I Paul Andrew Hartley hereby certify that this thesis which is approximately 41000 words in length has been written by me, that it is the record of work carried out by me, and that it has not been submitted in any previous application for a higher degree.

date....10th May 1995.....signature of candidate.....

I hereby certify that the candidate has fulfilled the conditions of the Resolution and Regulations appropriate to the degree of Ph.D. of the University of St Andrews and that he is qualified to submit this thesis in application for that degree.

date....10-5-95.....signature of supervis

I was admitted as a research student under Ordinance No.12 on 1st October, 1991 and as a candidate for the degree of Ph.D. on 21st October, 1994; the higher study for which this is a record was carried out in the University of St Andrews between 1991 and 1995.

date....10th May 1995.....signature of candidate.....

Copyright

In submitting this thesis to the University of St. Andrews I understand that I am giving permission for it to be made available for use in accordance with the regulations of the University Library for the time being in force, subject to any copyright vested in the work not being affected thereby. I also understand that the title and the abstract will be published, and that a copy of the work may be made and supplied to any *bona fide* library or research worker.

date 10th May 1995 signature of candidate .....

Acknowledgements

I would like to thank the following people who have contributed their time, knowledge and technical expertise throughout the duration of my Postgraduate research,
Professor John Tucker, especially for his guidance and motivation.
Dr Mette Mogensen who taught me immunocytochemistry and whose advice has always been helpful.
Mr John Mackie, M.Sc. who taught me electron microscopy and how not to swing a golf club.

I would like to thank the following people who have contributed their time and technical expertise during my Postgraduate research,
Mr Ian Laurie who taught me cell culture techniques.
Dr John Sommerville and Mr Michael Ladomery, B.Sc. who both taught me how to perform SDS-gel electrophoresis and Western blots.
Mr Andrew Miller, B.Sc. who taught me how to culture a *Drosophila* cell line and how to climb a mountain with a hang-over.

I would like to thank the following people for supplying materials and suggesting protocols for various experiments,
Dr Steve Doxsey for supplying anti-pericentrin antibodies.
Dr Tim Stearns for supplying anti-γ-tubulin antibodies.
Dr Martin Milner for making available a *Drosophila* cell line and *Drosophila* pupae.
Dr Cayetano Gonzalez for making available an immunofluorescence protocol to be used on *Drosophila* neuroblasts.

I would like to thank the following person who has contributed his time (in the pub), knowledge (of horses) and technical expertise (golf swing) throughout the duration of my undergraduate and postgraduate days; its always been a constant source of amusement , Dr Craig Henderson.

I would also like to thank,
Dr D. Hawley for inspiring me to become involved in science.
My mother, father, sister and brother for their love and support.

And finally, a special thank you to
Steffanie for getting us both through the past several months.

Contents

Abstract

Various aspects of microtubule nucleation and organization have been investigated in *Drosophila* and MDCK cells.

Drosophila indirect fibrillar flight muscles (IFMs) do not possess centriole-containing centrosomes. The ends of both microtubules and developing myofibrils closely associate with specialized cell junctions called myotendon junctions which are located at the ends of developing muscle cells. Antisera raised against pericentrin, a protein involved in microtubule nucleation, stain myotendon junctions throughout myofibrillogenesis. The antisera also stain the centrosome/spindle poles of *Drosophila* embryos and cultured *Drosophila* epithelial cells. Hence, microtubules may be nucleated at the myotendon junctions of IFMs rather than by sites associated with nuclear envelopes as in vertebrate muscle cells.

Incipient MDCK daughter cells form an extremely short intercellular bridge. This contains the midbody and ends of two midbody-associated microtubule bundles. Eventually the two microtubule bundles completely lose contact with the midbody. These microtubules may have been severed. Consequently, the furrow base can constrict around the midbody to complete daughter cell separation. A non-affinity purified γ-tubulin antiserum stains an antigen closely associated with both sides of the midbody. This antigen is not γ-tubulin. The antigen appears to be associated with a recently discovered mitotic organelle (the telophase disc).

Taxol induced microtubule arrays contain 'chains' of microtubules in interphase neuroblast cells of *Drosophila* third instar larvae. Adjacent microtubules in these 'chains' appear to share several protofilaments. Preliminary results indicate that microtubules of taxol induced asters are composed of 12 rather than the normal 13 protofilaments in MDCK cells.

The centrosome may nucleate and release microtubules in interphase MDCK cells. γ-Tubulin is only concentrated at the centrosome of control and taxol-incubated interphase MDCK cells. Microtubule ends do not focus at the centrosome in either case. The

centrosomally-associated microtubule array increases substantially in size from anaphase to late telophase. At late telophase the array spreads throughout each incipient daughter cell. Subsequently, the array ceases to focus at the centrosome.

γ-Tubulin and pericentrin initially concentrate at the centre of two of the several taxol-induced microtubule asters in each mitotically arrested MDCK cell. Subsequently, γ-tubulin and pericentrin are concentrated at two closely associated discrete spherical sites. These sites are not associated with microtubule asters. This may represent a very clear example of microtubule release from the centrosomes in these cells.

Chapter 1

Introduction

This thesis deals with the control of microtubule assembly and disassembly in certain *Drosophila* tissue cells *in vivo* and during certain microtubule associated events during the cell cycle of Madin-Darby Canine kidney cells (MDCK cells) in culture. This introduction deals first with (A) molecular aspects of microtubule organization, and then (B) certain microtubule-associated events, which are pertinent to the investigations which have been undertaken. The investigations which have been undertaken and the objectives of these investigations are outlined below.

The organization of microtubules during myofibrillogenesis in *Drosophila* indirect fibrillar flight muscle has been investigated. Are these microtubules organized by a centriole-containing centrosome or alternatively an acentriolar microtubule nucleating-site? This investigation has also included an analysis of *Drosophila* embryos and a *Drosophila* epithelial cell line to monitor the localization of certain proteins (γ-tubulin and pericentrin) which are apparently involved in microtubule nucleation.

Microtubules associated with the midbody during telophase and the terminal stages of daughter cell separation have been investigated to learn more about how their organization is controlled. The midbody-associated microtubules of MDCK cells have been investigated. How is the disassembly of the hyperstable midbody-associated microtubules controlled during the terminal stages of daughter cell separation?

The effect of taxol on microtubule structure and distribution has been investigated. *Drosophila* neuroblast cells and MDCK cells contain centriole-containing centrosomes. Therefore under normal conditions these centrosomes are likely to nucleate 13 protofilament microtubules. Does taxol perturb the protofilament number of microtubules which are normally composed of 13 protofilaments? The impact of taxol

on centrosomal activity has also been investigated. Does the centrosome nucleate microtubules in the presence of taxol in MDCK cells?

Section A : Molecular organization of microtubules

1.1 An introduction to microtubules

A microtubule is a long hollow tube, with an exterior diameter of about 24nm and present in eucaryotic cells. Microtubules are initiated at microtubule-organizing centres (MTOC's). Microtubules are involved in a diverse range of cellular functions. They are a major component of the cell cytoskeleton, which controls cell shape and movement. For example, cilia and flagella beat through the sliding interactions of their constituent microtubules (Warner and Satir,1974). Microtubules, in conjunction with actin filaments, appear to be involved in establishing cell polarity (Buendia *et al.*,1990). Microtubule based-motors transport certain cellular organelles and membrane-bound vesicles along microtubules (Vale,1987). Chromosome separation during mitosis is also facilitated by microtubules (Gorbsky *et al.*,1988).

1.2 Tubulin

The basic building blocks of microtubules are tubulin subunits. The tubulin subunits form a distinct protein family. The tubulin subunits of alpha and beta are associated as heterodimers and upon polymerization form the linear protofilaments of each microtubule. A third subunit, γ-tubulin, has recently been discovered (Oakley and Oakley,1989). It is apparently not found in the interior of a microtubule (Bass and

Joshi,1992). Instead, γ-tubulin is localized at the ends of microtubules which are associated with microtubule-organizing centres. It appears to play an important role in the initiation of microtubules at MTOC's. γ-Tubulin is introduced in detail in section 1.12.1.

The tubulin subunits share around 35% to 40% sequence homology. They are also highly conserved across species. For example, a β-tubulin of yeast and that of chickens share approximately 70% homology (Sullivan,1988). There is a large degree of diversity within both α- and β-tubulins. For instance, there are at least six different isoforms of α-tubulin and six different isoforms of β-tubulin (Raff,1984; Sullivan,1988) and each is encoded by a different gene. However, there is only sparse evidence of a γ-tubulin gene family. The cloning experiments which resulted in the identification of γ-tubulin genes in several species only detected one γ-tubulin gene in each species (Oakley and Oakley,1989; Stearns *et al.*,1991; Horio *et al.*,1991; Zheng *et al.*,1991a). However, two γ-tubulin genes have been discovered in *Drosophila* (Zheng *et al.* 1991b).

The functional significance of the expression of different isoforms of tubulin is not clear. In a small number of instances it has been found that a particular form of tubulin can be present at a particular location (isoform sorting) and perform a specific function. For example, isoform sorting has been reported in several different cultured neuronal cell types (Burgoyne *et al.*,1988; Joshi and Cleveland,1989) and also in the developing wing blade of *Drosophila* (Kimble *et al.*, 1989).

1.3 Microtubule assembly and polarity

Most microtubules are composed of thirteen protofilaments (Tilney *et al.*,1973) which are bundled together in parallel and form a hollow tube (Fig.1). A protofilament is constructed from α β-heterodimers of tubulin which are arranged in a polar fashion.

The β-tubulin subunit of one heterodimer is associated with the α-tubulin subunit of another heterodimer and this association is repeated along the length of a protofilament.

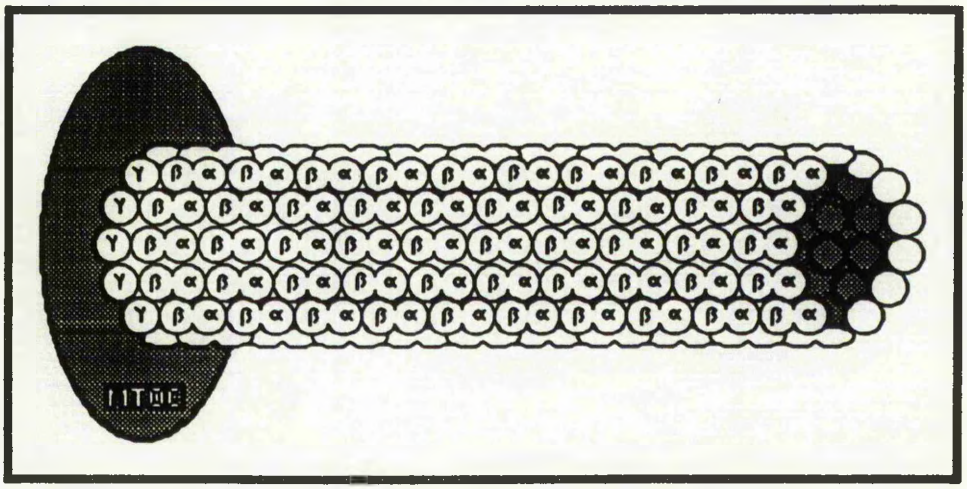

Fig.1 *Basic microtubule structure. Microtubule composed of thirteen linear protofilaments. Each protofilament is constructed from αβ-heterodimer. One end of the microtubule is associated with a microtubule-organizing centre where it may be bound to γ-tubulin.*

Thus, one end of a microtubule must terminate with α-tubulin and the other end must terminate with β-tubulin. Consequently, either β-tubulin or α-tubulin terminates at a MTOC (Fig.2). Recent evidence based on image reconstruction of microtubules decorated with kinesin indicates that β-tubulin terminates at microtubule ends which are associated with the MTOC (Song and Mandlekow,1995). While α-tubulin terminates at the other end of microtubules. This appears to be supported by the genetic linkage which exists between β-tubulin and γ-tubulin (which concentrates at MTOC's) (Oakley, 1992).

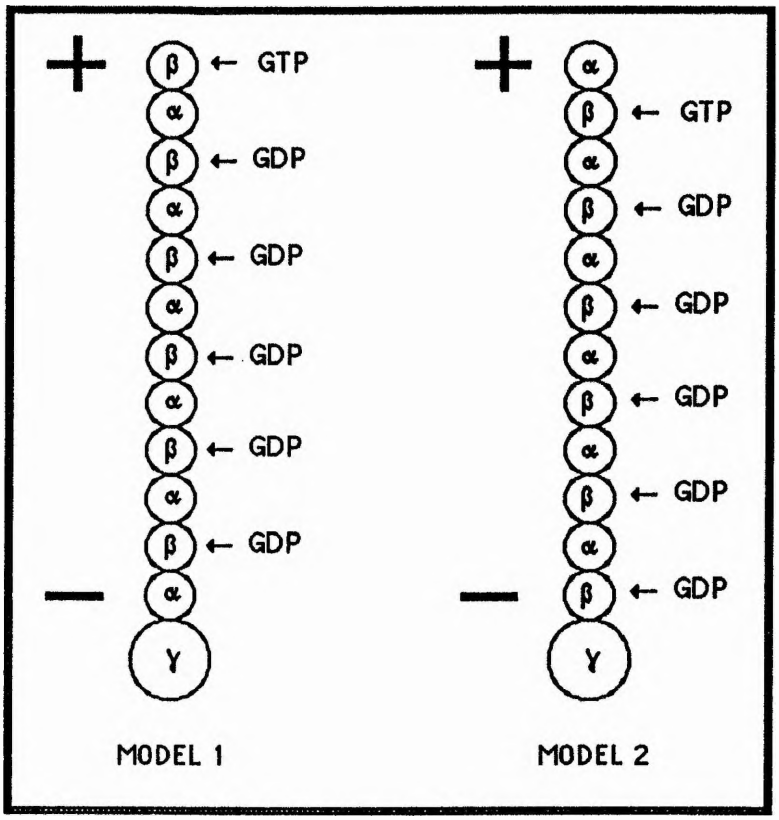

Fig.2 *Models of αβ-heterodimer polarity in a microtubule. Model 1: α-tubulin is associated with γ-tubulin at the MTOC. Model 2: β-tubulin is associated with γ-tubulin at the MTOC.*

1.4 Microtubule-organizing centres

MTOC's can be divided into those which contain centrioles and those which do not. The conventional MTOC is the centriole containing centrosome. In most animal cells microtubules are nucleated by the centrosome. The centrosome consists of a pair of centrioles which are surrounded by a cloud of pericentriolar material (Fig.3). The capacity of the centrosome to nucleate microtubules apparently resides within the pericentriolar material (Gould and Borisy,1977).

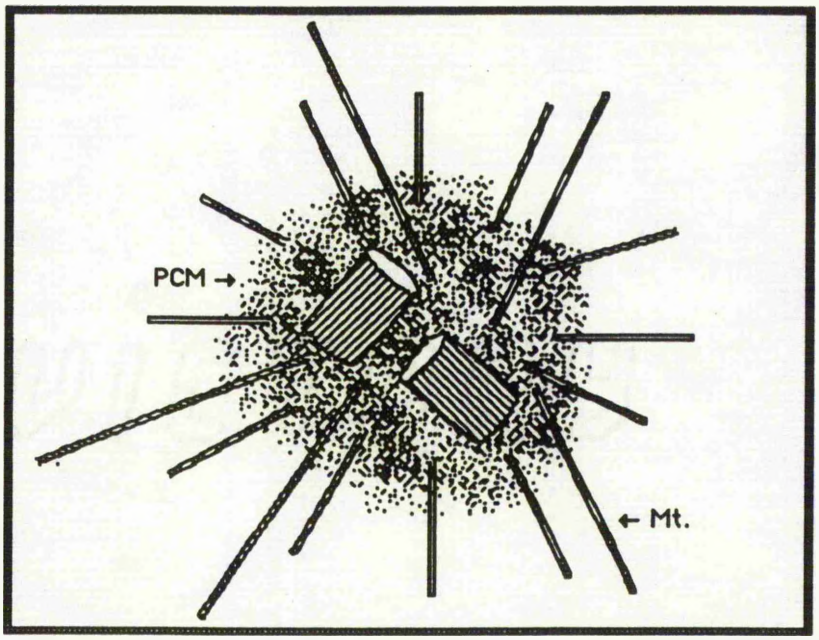

Fig.3 *Centriole-containing centrosome. A pair of centrioles surrounded by peri-centriolar material (PCM). Microtubules are initiated within the PCM.*

Elucidating the molecular nature of pericentriolar material is an area of research that is still in its infancy. The discovery of γ-tubulin (Oakley and Oakley, 1989) appears to be of considerable importance. It is concentrated in the pericentriolar material where microtubule ends are found and appears to be involved in microtubule nucleation (Stearns *et al.*,1991). Many proteins which associate with the centrosome have been identified and in some cases their function determined (Kalt and Schliwa,1993). However, there are probably many other proteins within the centrosome still to be identified. It is not surprising therefore that relatively little is known about how centrosomal proteins interact with each other, and consequently how microtubules are nucleated.

In some cell types, microtubules are nucleated at MTOC's which lack centrioles. For example, plant cells do not contain centrioles. Microtubules are nucleated by dense perinuclear material at the nuclear surface of higher plant cells (Falconer *et al.*,1988; Lambert,1993). Myotubes of developing skeletal muscle lose

their centriole-containing centrosomes and microtubule nucleation switches to dense material at their nuclear surface (Tassin *et al.*,1985). Plasma membrane-associated microtubule-nucleating sites are present in the epithelial cells of the *Drosophila* wing (Mogensen and Tucker,1987). A feature which appears to be common to all MTOC's, including the centrosome, is that microtubules are nucleated in dense material. Microtubules are nucleated in the pericentriolar material of centrosomes; while microtubules are nucleated at pericentriolar-like material at MTOC's which lack centrioles.

Unfortunately, electron microscopy does not provide information about the molecular organization and structure of centrosomal pericentriolar material and non-centrosomal pericentriolar-like material. Therefore whether such materials are a molecular 'soup' devoid of any coherent structure that merely contain the proteins required for microtubule nucleation or whether they are highly ordered molecular structures which contain specific sites for microtubule nucleation has not been resolved. However, it is clear that in some cells which contain non-centrosomal nucleating-sites, that microtubule arrays consist of an exact number of microtubules. For example, there are exactly 9 microtubules in the haptonemata of certain phytoflagellates, 12 rootlet microtubules in *Chlamydomonas,* and 24 cortical microtubules in the sporozoites of *Eimeria* (cited in Tucker,1984). Such observations have contributed to the formulation of a nucleating element hypothesis for the control of microtubule nucleation (Tucker,1982). This hypothesis predicts that discrete nucleating elements are contained within MTOC's, and that each nucleating element can initiate the growth of one microtubule.

Whether the molecular composition of the dense material in acentriolar MTOC's is the same as the pericentriolar material which surrounds centrioles still remains to be established. Early indications are that at least some proteins, as would be anticipated, are found not only at the pericentriolar material of centrosomes but also at acentriolar MTOC's. For example, γ-tubulin is present at the meiotic spindle poles of mouse oocytes, which lack centrioles (Palacios *et al.*,1993). Whether

microtubules at acentriolar MTOC's are nucleated in the same way as those at centrosomes requires further investigation. It is interesting, that the plasma membrane associated MTOC's of *Drosophila* wing epithelial cells nucleate microtubules with predominantly 15 protofilaments (Mogensen and Tucker,1988) instead of the 13 protofilament microtubules that are specified at centrosomes (Tilney *et al.*,1973). This may indicate that differences have evolved between MTOC's which enable them to nucleate the type of microtubule a cell requires.

1.5 Microtubule Dynamics

Under certain conditions purified tubulin can polymerize onto the ends of stable microtubule fragments from the core of a cilium (Walker *et al.*,1988). Microtubule elongation at one end of a microtubule fragment progresses at three times the rate of that at the other end. The fast growing end is called the plus end and the slower growing end is called the minus end. Hook decoration, the addition of tubulin subunits to the walls of existing microtubules, permits assessment of the polarity of microtubules and thereby identifies the plus end of a microtubule from its minus end (McIntosh and Euteneuer,1984). In this way it has been established that the plus end (fast growing end) of a microtubule extends away from MTOC's such as the centrosome.

The nucleotide, GTP, appears to be important for microtubule assembly *in vitro* and *in vivo* (Mitchison and Kirschner,1984; Cassimeris *et al.*,1988). Each tubulin subunit can bind one molecule of GTP. The GTP which is bound to α-tubulin can not be exchanged and thus appears to be a structural component of α-tubulin. In contrast, GTP binds at an exchangeable site on β-tubulin. Tubulin-GTP will polymerise spontaneously into microtubules at 37^0C in the presence of magnesium *in vitro* (Mitchison and Kirschner,1984). The GTP bound to β-tubulin is hydrolysed to GDP shortly after the polymerization of the tubulin heterodimers. Thus, GDP is bound

to the β-tubulin subunits in the interior of a microtubule. Provided a source of GTP is present, microtubules will continue to elongate and reach a steady state. The steady state is an equilibrium that can be established between polymerized tubulin and tubulin free in the cytoplasm. The concentration of tubulin in the cytoplasm at this steady state is called the critical concentration. If the concentration of tubulin falls below the critical concentration the microtubule will begin to disassemble. Microtubules can be assembled from tubulin in the presence of GTP analogues which are only slowly hydrolysed (Carlier *et al.*,1984). This indicates that GTP hydrolysis does not drive microtubule assembly. These microtubules are also very stable and do not depolymerize in the presence of colchicine or when the tubulin concentration is lowered below the critical concentration. This suggests that GTP hydrolysis weakens the bonds between tubulin heterodimers which under certain conditions enables the microtubule to disassemble.

Microtubules do not just elongate or disassemble. They are capable of alternating between these two states in a random fashion. Thus microtubules are described as being dynamically unstable. Dynamic instability is a property of microtubules which enables a microtubule to go through periods of polymerization and periods of depolymerization (Mitchison and Kirschner,1984). The abrupt transition between the period of polymerization and depolymerization is called 'catastrophe' (Walker *et al.*,1988). While the abrupt transition between depolymerization and polymerization is called 'rescue' (Walker *et al.*,1988). It has been proposed that a 'GTP' cap protects the plus end of a microtubule from catastrophe (Carlier and Pantaloni,1981; Erickson and O'Brien,1992). There is apparently a lag in the hydrolysis of GTP after it has been incorporated at the plus end of a microtubule. The hypothesis predicts that as long as tubulin subunits are incorporated at the plus end of a microtubule at a greater rate than the rate of GTP hydrolysis, the microtubule will not disassemble. The evidence for such a cap, however, has not been substantiated. Apparently even if a GTP cap does exist it may be no more than one tubulin subunit deep (Drechsel and Kirschner,1994). The minus

end of a microtubule is also dynamically unstable *in vitro*. However, it is less prone to dynamic instability and thus more stable than the microtubule plus end. The mechanism by which this stability is achieved at the minus end is not known.

Dynamic instability was discovered using pure tubulin *in vitro* (Mitchison and Kirschner,1984). However, it is also exhibited by microtubules *in vivo*. For example, dynamic instability has been observed in individual microtubules of fibroblast cells (Sammak and Borisy,1988) and newt lung epithelial cells (Cassimeris *et al.*, 1988). A feature of dynamic instability which is apparent in interphase cells is the ability of a microtubule to shorten and then to elongate, repeatedly. This occurs at the periphery of many cells and has been called 'tempered dynamic instability' (Sammak *et al.*,1987). In effect microtubules which reach the cell periphery are relatively long and if they begin to depolymerize the probability is that they will be 'rescued' before they are completely depolymerized. It has been demonstrated that the half-life for microtubule replacement is shortest at the leading edge of cells in culture (Sammack *et al.*,1987). 'Tempered dynamic instability' may play an important role in the spatial organization of microtubules in cells.

Dynamic instability has also been observed in mitotic cells. Microtubules of the mitotic spindle are apparently far more dynamic than those of the interphase microtubule array. For example, fluorescence photobleaching recovery indicated that microtubule turnover is approximately 20 times faster in mitotic cells than in interphase cells (Saxton *et al.*, 1984).

A microtubule is much less dynamic if its plus end is capped. In some interphase cells, the plus ends of microtubules may be captured by particular membrane associated proteins which control their stability (Kirschner *et al.*,1986). In mitotic cells, the plus end of some microtubules in the mitotic spindle are associated with the kinetochore (Euteneuer and McIntosh,1981). The kinetochore microtubules are much less dynamic than the astral and interzone microtubules of mitosis. This is apparently because the plus end of kinetochore microtubules are capped by their association with the kinetochore (Mitchison and Kirschner,1985). The minus ends of

most microtubules are apparently associated with a MTOC such as the centrosome or spindle pole body *in vivo*. This association probably caps the minus end which protects it from catastrophe. However, very little is known about dynamic instability at the minus end of microtubules *in vivo*. This is largely due to the difficulties in resolving individual microtubules at nucleating MTOC's by fluorescence microscopy.

1.6 Microtubule-associated proteins

A major characteristic of microtubule associated proteins (MAP's) is that they bind to and enhance the overall assembly of microtubules (Lee,1993). There are many different types of MAP's. Some are widespread while others are only found in certain cell types. Furthermore, some MAP's are only associated with microtubules in specific regions of a cell. For example, some MAP's are present in nerve cell dendrites and the cell body but absent from axons. The functional significance of a differential localization of MAP's has not been resolved. However, it does indicate that compartmentalized differentiation can occur in regions of cytoplasm within the same cell. The MAP's present in neuronal tissues have been extensively studied. Presumably this reflects the large quantities of tubulin that can be purified from animal brains. In addition, the MAP tau has been found to be a major component of one of the neuropathological abnormalities of Alzheimer's disease. There are two major classes of MAP's which can be isolated from brain tubulin (Olmsted,1986). One class are the high molecular weight proteins which include MAP-1 (350Kd) and MAP-2 (280Kd). The other class is the tau protein, the isoforms of which have a diverse range of molecular weights from 55 to 65Kd. Both classes of MAP have two binding domains. One binds to the surface of microtubules while the other probably binds to other cellular components. Therefore MAP's possibly act as 'brackets', linking cellular components to microtubules.

The MAP's appear to increase the stability of microtubules. Video enhanced microscopy indicates that MAP's can increase growth rate and 'rescue frequency' of microtubules (Pryer *et al.*,1992). In effect they may decrease dynamic instability. If MAP's are phosphorylated there is a considerable reduction of their binding to microtubules (Verde *et al.*,1992). This apparently makes the microtubule less stable as it is more prone to catastrophe. It has been proposed that this would be an effective way to disassemble the interphase array when the cell is entering mitosis. However, the extent to which MAP's stabilize microtubules has not been established. Furthermore, other forms of microtubule stabilization have been identified which suggests MAP's may not always be required to stabilize microtubules. For example, three proteins have been identified that are capable of inducing microtubule stability *in vitro*. These include STOP (stable tubule only protein) protein, myelin basic protein (MBP), and histone H1. Evidence indicates that both STOP (Margolis *et al.*,1990) and histone H1 (Multigner *et al.*,1992) may play a role in microtubule stabilization *in vivo*.

1.7 Post-translational modifications

Polymerized tubulin can be covalently modified. There are various covalent modifications of polymerized tubulin. The most widespread are the acetylation on lysine-40 of the β-tubulin subunit (Le Dizet and Piperno,1987), and detyrosination of the carboxy-terminus of the α-tubulin subunit (Thompson,1982). Antibodies raised against acetylated and detyrosinated tubulins stain stable microtubules (Schulze *et al.*, 1987; Piperno and Fuller,1985). However, studies have established that post-translational modifications do not stabilize microtubules but actually occur on microtubules that have already been stabilized *in vivo* (Khawaja et. al.,1988). Furthermore, polymerized tubulin in its detyrosinated state does not effect microtubule stability *in vitro* (Khawaja *et al.*,1988). Therefore the role of post-translational modifications has not been established. The presence or absence of

acetylated and detyrosinated forms of polymerized tubulin gives an indication of the 'age' of microtubules. Both these modifications are slow enzymatically controlled reactions. Therefore in cells where microtubule turnover is rapid there are very few detyrosinated and acetylated microtubules. In contrast, in cells where microtubule turnover is low most microtubules are stable. Therefore the microtubules have existed long enough to be completely acetylated and detyrosinated.

1.8 Microtubule-dependent motor proteins

There are two classes of motor protein. The cytoplasmic dyneins and the kinesins. Microtubule motors can only move in one direction along a microtubule. They either move towards the plus end of a microtubule or towards the minus end. It has been established that cytoplasmic dynein is a minus end-directed microtubule motor (Paschal and Vallee,1987). In contrast, most kinesins are plus end-directed microtubule motors (Vale *et al.*, 1985). Cytoplasmic dyneins are involved in organelle transport and probably in mitosis. For example, they are associated with minus end-directed organelles which include lysosomes and late endosomes (Lin and Collins,1992). Kinesins are more diverse, and are involved in organelle transport, and in the transport of synaptic vesicles along axons. They may also be involved in mitosis and meiosis. For example, anti-kinesin antiserum stains the spindle poles of mammalian and amphibian cells (Neighbors *et al.*,1988); although the possible mitotic function of kinesins remains unresolved.

Cytoplasmic dyneins and kinesins are both composed of two heavy chains and several light chains. The heavy chains are highly conserved throughout each class of motor protein. They form a domain which binds to the microtubule and depend upon ATP hydrolysis to enable the protein to move along the microtubule. Kinesin movement is 'quantized' (Mandlekow and Mandlekow,1994). In effect it 'steps' along the protofilament of a microtubule. Most light chains are structurally similar (e.g. α-

helical coiled coil). However, there is no apparent conservation of amino acid sequence between light chains of different motor proteins. Therefore it has been suggested that the light chains specify the organelles or molecules they can bind (Goldstein,1991).

1.9 Microtubule Severing

Recently a protein which severs microtubules has been discovered and characterized (McNally and Vale,1993). It has been called katanin (named after the Japanese word for samurai sword, katana). An analogue of ATP which can not be hydrolysed can bind to katanin. Katanin bound to this ATP analogue, can not sever microtubules. This indicates that ATP hydrolysis and not just ATP binding, is required in order to sever microtubules. Thus katanin is an ATPase that uses the energy from ATP hydrolysis to break tubulin-tubulin bonds within the interior of a microtubule.

Centrin, a calcium binding protein, appears to play an essential role during flagella excision in *Chlamydomonas reinhardtii* (Sanders and Salisbury,1989). A centrin based stellate array of fibres are located between the flagellar axoneme and its basal body. Contraction of the centrin-based fibres creates a shearing force and torsional load which can sever through the microtubules in this region. A detergent-extracted cell model of *Chlamydomonas* has been used to elucidate the molecular mechanism which controls flagellar excision (Sanders and Salisbury,1994). The addition of calcium above physiological levels results in flagellar excision. In contrast, buffers containing EDTA, which chelate free calcium, result in a complete loss of flagellar excision competence. Furthermore, anti-centrin antibodies block calcium induced flagellar excision. Centrin's molecular structure is highly conserved across species (Errabolu *et al.,* 1994). However, if centrin's function of severing microtubule has also been conserved in higher eukaryotes remains to be established.

Whether more than one form of microtubule severing is widespread throughout different cell types is open to debate. Regardless, the general function of microtubule severing may be to create new free ends which expose tubulin-GDP. These subunits would be subject to catastrophe and consequently would rapidly depolymerize. In this way, microtubule severing may play an important role in the depolymerization of the interphase array during the transition to mitosis (Karsenti,1993). It has also been suggested that microtubules may be severed at the centrosome in order to release microtubules (Sanders and Salisbury,1994).

1.10 Microtubule release from the centrosome

It has not been established whether microtubule release from the centrosome is a widespread phenomenon. However, it has been proposed that microtubules are nucleated at the neuronal centrosome within the cell body and then released for translocation into the nerve axon and dendrites (Bass and Joshi,1992). Indirect evidence indicates that the neuronal centrosome nucleates and releases microtubules which are translocated into the nerve axon. Microtubules in the nerve axon have a uniform polarity. Their plus ends are directed towards the distal end of the axon (Heidemann *et al.*,1981) whereas microtubules in the dendrites have approximately equal proportions of microtubules with opposite polarities (Bass *et al.*,1988). However, very few microtubules are attached to the centrosome. γ-Tubulin is only concentrated at the neuronal centrosome (Bass and Joshi,1992). If γ-tubulin is responsible for microtubule nucleation then it is possible that microtubules are nucleated at and released from the centrosome. Neurons have been incubated in nocodazole (which depolymerizes microtubules). When this drug is removed hundreds of microtubules assemble in the region of the centrosome (Yu *et al.*,1993). Most of these microtubules are attached to the centrosome. However, unattached microtubules are present in the cell body at decreasing levels with increasing distance

from the cell body. These experiments may indicate that the neuronal centrosome nucleates and releases microtubules in order to establish the organized arrays of microtubules in the axons and dendrites.

Dynamic instability at the plus end of a microtubule may only be able to account for the complete disassembly of short microtubules (Cassimeris *et al.*,1988). Apparently, depolymerization of microtubules from their plus end by many short catastrophic events would apparently take too long to account for the complete depolymerization of the majority of microtubules within a cell (McBeath and Fujiwara,1990). Consequently, it has been proposed that microtubules may detach from the centrosome in order that they can completely depolymerize from their minus end as well as their plus end in interphase LT-cells from the goldfish scale (McBeath and Fujiwara,1990). When these cells are rapidly chilled to - 3^0C the average length of microtubules bound to the centrosome does not change. However, free microtubules in close proximity to the centrosome are found which are approximately half the length of microtubules attached to the centrosome.

1.11 The effect of taxol on microtubule organization

Taxol is an anti-mitotic drug isolated from the western yew, *Taxus brevifolia* (Wani *et al.*,1971). It completely inhibits the division of exponentially growing cells. For example, HeLa cells incubated with taxol for 20hrs are blocked in late G_2 and/or mitosis (Schiff *et al.*,1979). Mitotic spindles are not assembled in the presence of taxol. Most cells blocked in mitosis contain several taxol induced microtubule asters (De Brabander *et al.*,1981; Schatten *et al.*,1982; Albertini,1987). Taxol is currently used for the treatment of ovarian cancer, and its potential to treat breast, lung and other cancers is being investigated (Rowinsky and Donehower,1991).

1.11.1 Taxol induced microtubules *in vitro*

In vitro, taxol promotes the assembly of microtubules from purified tubulin (Schiff *et al.*,1979). Apparently, taxol decreases the lag time for microtubule assembly and shifts the equilibrium for assembly in favour of microtubules. Thus taxol decreases the critical concentration of tubulin required for assembly. Microtubules formed in taxol are relatively stable. For example, taxol induced microtubules are resistant to depolymerization by elevated calcium levels (Schiff *et al.*,1979). In the presence of taxol, microtubules will assemble under conditions in which polymerization would not normally occur. For example, taxol induces microtubule assembly at low temperatures (Thompson *et al.*, 1981). Taxol binds to tubulin with a stoichiometry of one (Parness and Horwitz,1981; Manfredi *et al.*, 1982). Taxol binds more strongly to intact microtubules than to unpolymerized tubulin dimers. However, the binding of taxol to tubulin is reversible. Taxol appears to bind to the β-tubulin subunit (Rao and Horwitz,1992). However, taxol does not effect the binding or the hydrolysis of GTP (Carlier and Pantaloni,1981).

1.11.2 Taxol induced microtubules *in vivo*

The effect of taxol on microtubule organization appears to be more complex *in vivo* than *in vitro*. Microtubules in interphase cells are replaced by microtubule bundles upon taxol incubation (De Brabander *et al.*,1981). It has been claimed that the centrosome does not nucleate microtubules in the presence of taxol. Taxol arrests cells in G2 and/or mitosis. A mitotic spindle is not formed. Instead, taxol induces several microtubule asters per cell (De Brabander *et al.*,1981; Schatten *et al.*,1982; Manfredi and Horwitz,1986; Albertini,1987). Only two microtubules asters per cell are associated with centriole containing centrosomes (De Brabander *et al.*,1981). Under normal conditions these would form the spindle poles. Microtubule asters

which do not contain centrioles do, however, contain several proteins which are normally associated with the spindle poles (Stearns and Kirschner,1994; Buendia *et al.*,1990; Verde *et al.*,1991; Sager *et al.*,1986;).

Taxol stabilizes microtubules *in vivo*. However, they are not hyperstable unlike taxol induced microtubules *in vitro*. Taxol induced microtubules *in vivo* are dynamic, albeit at a reduced level compared with normal microtubules. For example, taxol induced microtubule bundles are replaced by microtubule asters during the transition between interphase and mitosis (De Brabander *et al.*,1981). Microtubules induced by 10 or 100μM taxol are resistant to 2μM nocodazole (which induces the loss of microtubules in cells not incubated in taxol). However, microtubule asters induced by a low concentration of taxol (0.1μM) in mitotic extracts (which closely mimic *in vivo* conditions) will depolymerize after approximately 40 minutes incubation in a high concentration (20μM) of nocodazole (Verde *et al.*,1991). In comparison, microtubules in control cells will depolymerize after only 2 minutes in nocodazole. Microtubules depolymerized by nocodazole, repolymerize upon the addition of taxol (De Brabander *et al.*,1981; Verde *et al.*,1991). These experiments indicate that taxol does not hyperstabilize microtubules *in vivo* but instead reduces their dynamic instability and promotes their assembly.

The mechanism of taxol induced microtubule assembly *in vivo* is not clear. Taxol reduces the critical concentration of tubulin required for spontaneous polymerization of microtubules *in vitro* (Schiff *et al.*, 1979). Microtubules may be polymerized simply because the critical concentration for assembly is sufficiently lowered *in vivo* (Verde *et al.*,1991). However, several centrosomal proteins are located at the taxol induced microtubule asters. Therefore the *in vivo* mechanism of microtubule assembly in the presence of taxol, may involve more than simply a reduction in the critical concentration of tubulin.

1.11.3 Microtubule protofilament number of taxol-induced microtubules

Microtubules are composed of thirteen protofilaments in the vast majority of animal and plant cells (Tilney *et al.*,1973). Microtubules with other protofilament numbers are known. For example, most microtubules are composed of 15 protofilaments in epidermal cells of the *Drosophila* wing (Tucker *et al.*,1986) and in certain supporting cells of the mammalian organ of Corti (Saito and Hama,1982).

Depending on the conditions for assembly, microtubules with 12 to 16 protofilaments occur *in vitro* (Wade *et al.*,1990). Microtubule protofilament number is restricted to the normal 13 protofilaments if microtubules are grown from 'seeding structures' such as axonemal fragments and centrosomes *in vitro* (Allen and Borisy,1974; Scheele *et al.*,1982; Evans *et al.*,1985). Purified tubulin in the presence of GTP, magnesium and taxol at 37^0C, polymerizes into microtubules with 12 protofilaments (60%) and 13 protofilaments (40%) (Andreu *et al.*,1992). However, if tubulin and MAP's are incubated in taxol, there are far fewer 12 protofilament microtubules (Andreu *et al.*,1992).

The situation *in vivo* is apparently different. Taxol perturbs microtubule protofilament number in the epidermal cells of the developing *Drosophila* wing (Mogensen and Tucker,1990). Provided taxol is added to these cells prior to the onset of nucleation, the vast majority of microtubules that are subsequently nucleated are composed of 12 rather than the normal 15 protofilaments.

1.12 Centrosomal proteins

Several proteins have been identified which are present at the centrosome (For review see Kalt and Schliwa,1993). The function of most of these proteins has not been determined. Some proteins are only transiently associated with the centrosome during the cell cycle. For example, several proteins have been identified which only

associate with the centrosome during mitosis (Maekawa *et al.*,1991; Todorov *et al.*,1992; Paul and Quaroni,1993). Several proteins have been identified which are present in centrosomes throughout the cell cycle (Moudjou *et al.*,1991; Oakley and Oakley,1989; Clark and Meyer,1992; Doxsey *et al.*,1994). These include, γ-tubulin (Oakley and Oakley,1989) and pericentrin (Doxsey *et al.*,1994). Both of these proteins are of particular interest because of their apparent involvement in microtubule nucleation.

1.12.1 γ-Tubulin

γ-Tubulin was recently discovered in the filamentous fungus *Aspergillus nidulans* (Oakley and Oakley,1989). This was achieved using a genetic approach called suppresser analysis. Basically, the phenotype which results from a mutation in one gene can be reverted by a complementary mutation in another gene. The gene product of the complimentary mutation can directly interact with the gene product of the original mutant gene and consequently suppress the original mutant phenotype. In *Aspergillus nidulans, benA33* is a heat-sensitive β-tubulin mutation. This mutation blocks growth by preventing the disassembly of microtubules (Oakley and Morris,1981). However, it was discovered that this conditionally lethal mutation is suppressed by a mutation in the *mipA* gene (a gene which was previously unidentified) (Weil *et al.*,1986). Furthermore, double mutants constructed from various *mipA* and *benA33* alleles have various phenotypes. This is apparently a good indication that the gene product of *mipA* may directly interact with the β-tubulin encoded by the *benA33* gene. Subsequently the *mipA* gene was isolated and sequenced (Oakley and Oakley,1989). It became evident that a novel tubulin protein had been discovered. This tubulin has been named γ-tubulin.

The isolation and sequencing of *Aspergillus nidulans* γ-tubulin cDNA has enabled the subsequent isolation and sequencing of γ-tubulin cDNA's from several

other species. These include, *Drosophila*, Human, *Xenopus laevis* and *Schizosaccharomyces pombe* (Zheng *et al.*,1991; Stearns *et al.*,1991; Horio *et al.*,1991). It is clear from the amino acid sequences that γ-tubulin is highly conserved. For example, 98% homology exists between *Xenopus laevis* and Human γ-tubulin (Oakley,1994).

Various antibodies have been raised against γ-tubulin to establish its localization. γ-Tubulin is localized at the spindle pole body in *A. nidulans* (Oakley *et al.*,1990). In mammalian cells γ-tubulin is localized at centrosomes at all stages of the cell cycle. However, γ-tubulin antibodies stain the centrosomes with greatest intensity at mitosis (Zheng *et al.*, 1991a; Stearns *et al.*,1991) when the nucleating activity of the centrosome is also highest (Oakley,1994). Furthermore, it has been shown by immuno-electron microscopy that γ-tubulin is localized in the pericentriolar material of centrosomes (Stearns *et al.*,1991). This would be anticipated if γ-tubulin is involved in microtubule nucleation since PCM is responsible for the nucleation of microtubules (Gould and Borisy,1977). γ-Tubulin has also been detected in higher plant cells. For example, γ-tubulin has been found at a suspected acentriolar microtubule nucleating-site in the developing guard cells of *Allium cepa* L. (McDonald *et al.*,1993). Furthermore, two γ-tubulin homologues have been identified in *Arabidopsis* (Liu *et al.*,1994). However, it appears that at least one of these homologues is located not only at the minus ends of microtubules but also along much of the lengths of microtubule arrays. Plant cells do not contain centriole containing centrosomes. Therefore a dispersed distribution of γ-tubulin in plant cells may help explain how microtubules are organized in plants.

What is the function of γ-tubulin? The γ-tubulin genes of *A. nidulans* and *Sch. pombe* have been disrupted by a complex genetic process (Oakley *et al.*,1990; Stearns *et al.*,1991; Horio *et al.*,1991). Examination of the disruptants by immunofluorescence microscopy reveals an almost complete absence of mitotic spindles, and a substantial decrease in the number and lengths of cytoplasmic microtubules (Oakley *et al.*, 1990). Thus, the disruptant experiments indicate that γ-tubulin is essential for microtubule

assembly in these species. Furthermore, a mutation to a γ-tubulin gene also greatly reduces the number of microtubules associated with the centrosome of *Drosophila* neuroblast cells (Sunkel *et al.*,1995).

It also appears that γ-tubulin may be essential for microtubule assembly in mammalian cells. Antibodies raised against γ-tubulin have been microinjected into HeLa, mouse 3T3, and human pancreatic epithelial cells (Joshi *et al.*,1992). This did not affect the microtubules in these cells. However, for the same cells, microtubules have been depolymerized by nocodazole and subsequently microinjected with a γ-tubulin antibody and the nocodazole then removed (Joshi *et al.*,1992). Microtubules do not reassemble under these conditions. If cells are injected with this antibody at G_2 stage in the cell cycle, when cells enter mitosis they do not construct a normal mitotic spindle. The disruptant experiments and the microinjection experiments detailed above, indicate that γ-tubulin is involved in microtubule nucleation

Sperm centrioles are not competent to nucleate microtubules and are not associated with γ-tubulin (Stearns *et al.*1994). However if they are added to a meiotic egg extract a functional centrosome is formed which nucleates microtubules (Stearns *et al.*,1994). Under these conditions γ-tubulin is found to be localized around the centrioles. If such centrioles are added to a meiotic egg extract which has been incubated in nocodazole (which prevents microtubule polymerization), γ-tubulin is still recruited by the centrioles. This indicates that γ-tubulin is recruited by the centrosome independent of microtubules. As well as being associated with the centrosome γ-tubulin is also present in a soluble form in the cytoplasm. It is part of a large protein complex which has been named the γ-some (Stearns and Kirschner, 1994). It has been demonstrated that the γ-some is recruited by the centrosome for microtubule nucleation. Furthermore, there are indications that the γ-some can associate with the minus ends of microtubules which are not associated with the centrosome. For example, γ-tubulin antibody apparently stains the centre of DMSO and taxol induced asters *in vitro* (Stearns and Kirschner, 1994).

γ-Tubulin alone is apparently not sufficient for microtubule nucleation. Activated *S. pombe* spindle pole bodies stain with both γ-tubulin antibody and MPM-2 antibody (which stains phosphorylated antigens at the centrosome throughout the cell cycle but most intensely during mitosis (Vandre *et al.*,1984)). However, inactive spindle pole bodies stain with γ-tubulin antibody but not with MPM-2 antibody (Masuda *et al.*,1992). This may mean that γ-tubulin must be modified before it can nucleate microtubules. Alternatively, an additional protein may be required for microtubule nucleation.

1.12.2 Pericentrin

An autoimmune serum named serum 5051, from a patient with scleroderma, is used as an immunofluorescent marker for centrosomes and non-centrosomal MTOC's (Tuffanelli *et al.*,1983; Calarco *et al.*, 1983; Clayton *et al.*, 1985). It recognizes several proteins on a Western blot (Doxsey *et al.*,1994). This autoimmune serum stains centrosomes in mammals (Tuffanelli *et al.*, 1983) and plants (Clayton *et al.*, 1985) and therefore one of the proteins it recognises may play an important role in the centrosome.

In order to identify the gene which encodes the centrosomal 5051 antigen, a mouse 1 gt11 cDNA expression library was screened with 5051 autoimmune sera (Doxsey *et al.*,1994). Only one cDNA was isolated, indicating that the protein was probably rare. This protein has been called pericentrin. The cDNA was inserted into a vector and over expressed by *E. coli*.. The resulting fusion protein was isolated on a gel and subsequently injected into a rabbit to raise an anti-pericentrin polyclonal antiserum. The affinity purified anti-pericentrin antiserum recognises a 220kd protein in cellular fractions enriched with centrosomes and separated on a western blot. This antiserum does not recognize a 220kd protein from whole cell lysates. Furthermore, two more antisera generated against a different region of pericentrin do not detect a

220kd protein from whole cell lysates. Therefore it appears that pericentrin is quite rare. It has been estimated that there are 540 molecules of pericentrin per centrosome. In contrast, there are 2.7 x 10^4 molecules of tubulin per centrosome. From the amino acid sequence of pericentrin it has been predicted that its structure is a long central coiled-coil which is flanked by non-coiled domains. The long central coiled-coil is a characteristic of some structural proteins such as myosin and keratin (Cohen and Parry, 1990; Lupas *et al.*, 1991).

Pericentrin appears to be highly conserved. The anti-pericentrin antisera stain centrosomes throughout the cell cycle across many different species (Doxsey *et al.*,1994). For example, it stains centrosomes in all mammalian cells tested. These include, rat, mouse, hamster, cow, human, donkey and kangaroo. The antisera also stain the oral apparatus and centrioles of the ciliate *Tetrahymena*, the spindle poles of *Naegleria*, the sperm centrioles of *Xenopus* (at low levels), and the acentriolar microtubule nucleating sites in mammalian muscle. The antisera staining changes with the nucleating capacity of the centrosomes. They stain the centrosome/spindle poles most intensely at metaphase and least intensely at telophase (Doxsey *et al.*,1994).

Pericentrin appears to be an integral component of the centrosome (Doxsey *et al.*,1994). For example, it persists at the centrosome even after cells have been extracted with non-ionic detergents. Furthermore, pericentrin appears to be localized in the pericentriolar material (PCM). For example, PCM of isolated centrosomes, and not centrioles, is immunogold labelled with anti-pericentrin antisera (Doxsey *et al.*,1994). Furthermore, mouse oocytes do not contain centrioles. However, the anti-pericentrin antisera stain PCM like material at their spindle poles (Doxsey *et al.*,1994).

What is the function of pericentrin? If mouse oocytes are microinjected with the anti-pericentrin antisera, the vast majority of meiotic spindles are disrupted and some are even absent (Doxsey *et al.*,1994). A similar result occurs at the mitotic spindles of *Xenopus* embryos. If sperm centrioles are added to Xenopus extracts they will recruit nucleating components and acquire nucleating capacity (Murray and

Kirschner,1989). When the anti-pericentrin antisera are added to the extracts plus centrioles, approximately half the number of microtubules were present at each centriole containing aster compared with the control (Doxsey *et al.*,1994). If the extracts were incubated with the antisera prior to the addition of centrioles, there were only around 10% of the number of microtubules in each aster compared with the controls. These experiments indicate that pericentrin appears to contribute towards the ability of the centrosome to nucleate microtubules. However, *in vitro* these antisera do not affect the nucleation of microtubules at isolated centrosomes incubated in purified tubulin (Doxsey *et al.*,1994). It has been suggested that *in vivo*, pericentrin may block activities which would otherwise block microtubule nucleation. Alternatively, conditions *in vivo* may be very stringent and require a contribution from components regulated by pericentrin in order that microtubules may be nucleated (Doxsey *et al.*,1994).

The relationship, if any, between pericentrin and γ-tubulin with respect to microtubule nucleation has not been resolved. However, perturbation of pericentrin function by the binding of anti-pericentrin antisera, does not effect the recruitment of γ-tubulin at the centrosome. For example, sperm centrioles recruit γ-tubulin from *Xenopus* egg extracts even in the presence of anti-pericentrin antisera (Doxsey *et al.*,1994).

Section B : Construction and function of the microtubule arrays which have been investigated

1.13 The telophase midbody and associated microtubule bundles

At anaphase one bundle of polar microtubules is associated with each spindle pole. The plus end of both microtubule arrays extend from their spindle poles and overlap and interdigitate with each other at the spindle equator. The plus end addition of tubulin to the interdigitated microtubules accompanied by 'antiparallel sliding' apparently contributes towards the elongation of the mitotic spindle (Saxton and McIntosh,1987; Shelden and Wadsworth,1990). This increases the separation between the segregating chromosomes.

At late anaphase a distinct row of 'stem bodies' span the equator (McIntosh and Landis,1971). Each 'stem body' consists of an amorphous clump of dense material. The ends of the two opposing microtubule bundles appear to be associated with each 'stem body'. Some microtubules apparently pass through each stem body, although it is likely that the majority terminate within each 'stem body'. Thus the stem body is a region of microtubule interdigitation.

By telophase the stem bodies have aggregated into a disc of amorphous dense material at the equator which is called the midbody. Two microtubule bundles are associated with the midbody. The majority of their plus ends terminate in the midbody matrix (Euteneuer and McIntosh,1980). Some appear to stop short of the midbody while others pass through the midbody. Therefore, the midbody is a region of microtubule interdigitation.

A degree of inconsistency exists in the literature as to the exact definition of the midbody. Some authors define the midbody as a disc of amorphous dense material with which two microtubule bundles associate (Mullins and Biesele,1973,1977;

Schulze and Blose,1984; Kidder *et al.*,1988; Asano *et al.*,1991; Ratner,1992). Others define the midbody as the region incorporating the entire length of both microtubule bundles and the disc of dense material (Euteneuer and McIntosh,1981; Mullins and McIntosh,1982; Julian *et al.*,1993). It is proposed in this thesis to adopt the former definition of a midbody.

The minus ends of the midbody-associated microtubule bundles are not associated with the centrosomes. These microtubules have the same polarity as the late anaphase polar microtubules. Therefore, it has been suggested that the midbody-associated microtubule bundles are 'remnants' of the polar microtubules of the mitotic spindle (McIntosh and Landis,1971; McIntosh *et al.*, 1975). However, this may not be the case. A recent investigation has found that γ-tubulin is concentrated at the minus ends of each midbody-associated microtubule bundle (Julian *et al.*, 1993). γ-Tubulin antibodies microinjected into anaphase cells prevent the formation of the microtubule bundles between the two incipient daughter cells. Therefore it has been suggested that specialized microtubule-organizing centres are assembled on each side of the division plane between the incipient daughter cells. These would be responsible for the nucleation of the midbody associated microtubules.

The function of the midbody and its associated microtubule bundles has not been established. However, they form in the vast majority of animal cells (Mullins and Biesele,1977; Mullins and McIntosh,1982; Schulze *et al.*, 1984; Kidder *et al.*,1988; Rattner,1992; Julian *et al.*,1993) which indicates that they may have a fundamental role. In most animal cells during cytokinesis the cleavage furrow constricts around the midbody which results in a membrane bound 'bridge' between the incipient daughter cells (Mullins and Biesele,1977). The midbody and its associated microtubule bundles are contained within a relatively long and narrow membrane-bound cytoplasmic strand that is called the intercellular bridge (Fig.4). The intercellular bridge may persist for several hours and consequently into G_1 of interphase before the completion of cytokinesis (Sanger *et al.*,1985). Why this structure should persist for several hours has not been established. It has been hypothesized that the function of the midbody-

associated microtubule bundles is to provide support to the intercellular bridge and to resist the cytokinetic forces (Mullins and Biesele,1977). This appears possible since these microtubule bundles are not dynamic. For instance, midbody-associated microtubule bundles are extremely stable to cold (Brinkley,1975; Margolis *et al.*,1990), high pressure (Salmon *et al.*, 1976) and colchicine (Oppenheim *et al.*,1973). They also exhibit a slow turnover of tubulin subunits (Gorbsky *et al.*,1990). However, why the cell should require the cytokinetic forces to be resisted for several hours is not clear.

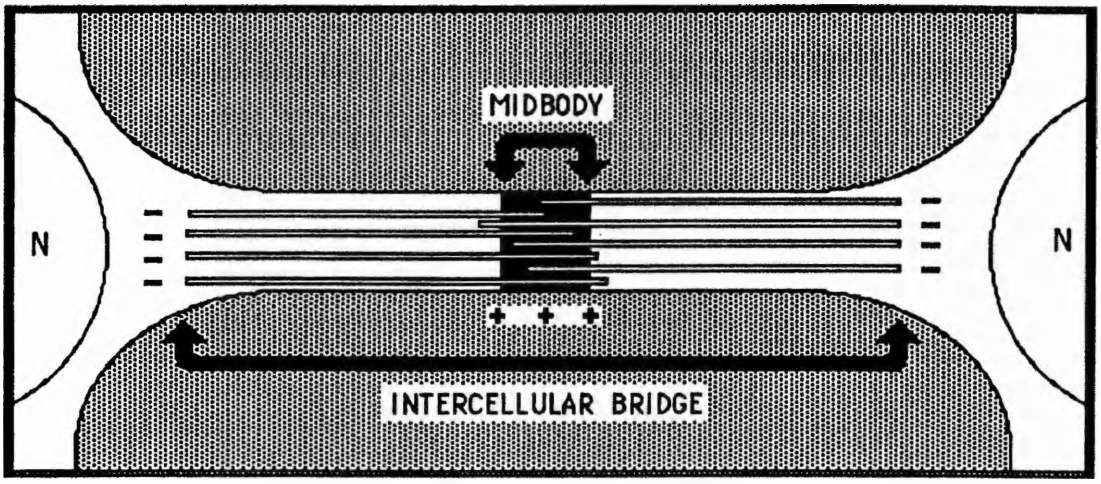

Fig.4 *Schematic diagram of a typical mammalian intercellular bridge. The midbody and two midbody-associated microtubule bundles are contained within the intercellular bridge. The plus ends of the two microtubule bundles overlap and interdigitate at the midbody.*

It has been suggested that the midbody functions as a 'plug' to prevent the passage of molecules between the incipient daughter cells (Allenspach and Roth,1967; Mullins and Biesele,1977). However, microinjected fluorescent molecules can pass through the midbody of HeLa cells (Schulze and Blose,1984).

A 'cocktail' of proteins, which associate with the mitotic spindle, subsequently concentrate at the midbody (Davis *et al.*,1983; DeMay *et al.*,1984; Vandre *et al.*,1984; Sellitto and Kuriyama,1987; Bastmeyer and Russel,1987; Cooke *et al.*,1987; Williams

et al.,1988; Andreassen *et al.*,1991; Todorov *et al.*,1992). The midbody is discarded by the cell when the daughter cells finally separate. Therefore it has been suggested that the midbody may function as a 'waste disposal unit' for mitotic proteins.

An antigen (CHO1) exclusively localized in the stem bodies and the midbody has been characterized (Sellitto and Kuriyamam,1988). It has been suggested that this antigen and other components of the stem body, may be involved in the generation of forces for 'antiparallel sliding' of microtubules. Therefore it may be the function of the stem bodies rather than that of the midbody which is of particular importance to cells (Sellitto and Kuriyamam,1988). The number of different suggestions regarding the function of the midbody and the stem bodies, and their associated microtubule bundles, appears to reflect how little is really understood about their function.

Of particular interest is the identification of an antigen, TD-60, which is localized at both sides of each stem body and subsequently at both sides of the midbody (Andreassen *et al.*,1991). This antigen is resistant to disruption when the microtubule bundles are destroyed or when the cell is lysed. Therefore, it is considered to be a component of a mitotic organelle. This mitotic organelle has been called the telophase disc. A hypothesis for the function of a recently identified component called the telophase disc has been proposed based on its location. The telophase disc may provide a mechanism for aligning actin and myosin to ensure cleavage occurs at the midpoint of the mitotic spindle (Margolis and Andreassen, 1993). However, at present it has not been reported whether disruption of the telophase disc can affect cytokinesis.

1.14 Daughter Cell Separation

The termination of daughter cell separation has only been investigated in detail in two cell types. These are HeLa cells (Byers and Abramson,1968), which were derived from malignant tissue, and D-98S cells (Mullins and Biesele,1972,1977),

which are derived from human sternal bone marrow (Berman and Stulberg,1956). In HeLa cells during the latter stages of cytokinesis, the intercellular bridge apparently elongates (Byers and Abramson,1968). 'Waves' of cytoplasmic swelling which appear to originate at the midbody move along one half of the intercellular bridge towards the juncture between the bridge and an incipient daughter cell body (Fig.5). It has been suggested that these 'waves' are responsible for the separation of the bridge from one incipient daughter cell. The separation apparently occurs at the juncture between one end of the bridge and one of the cell bodies (Fig.5).

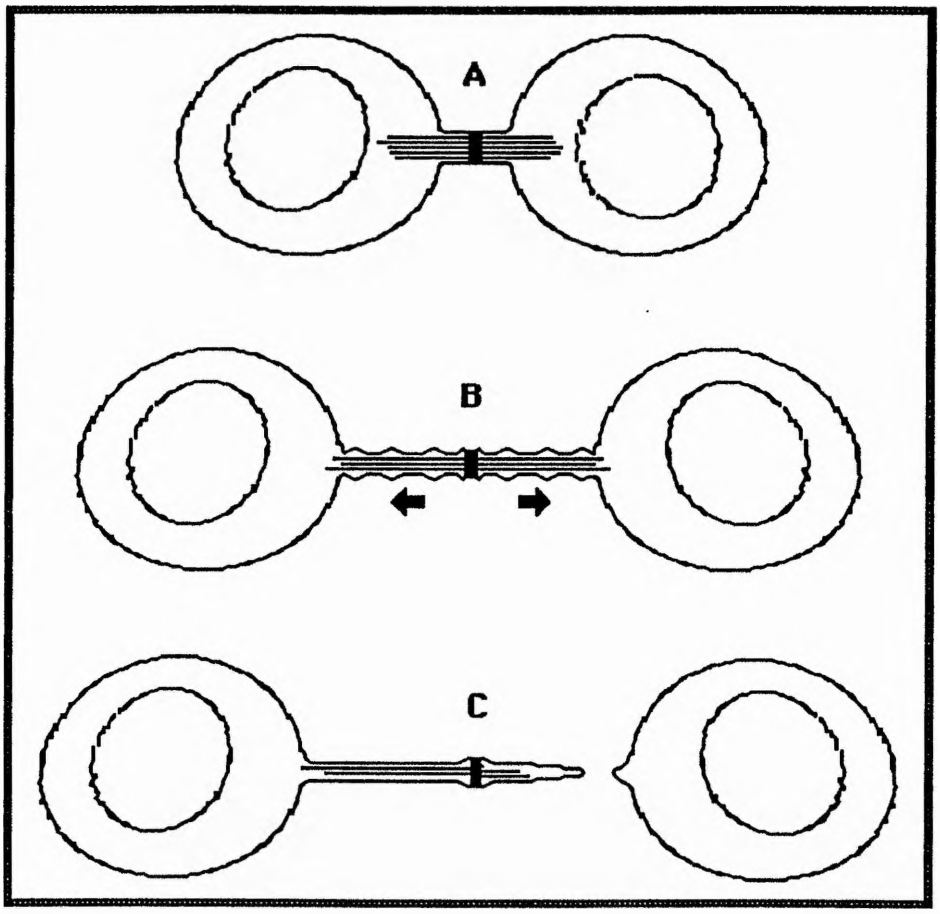

Fig.5 *Schematic diagram which summarises daughter cell separation in HeLa cells.* **(a)** *Formation of the intercellular bridge.* **(b)** *The intercellular bridge lengthens and a series of cytoplasmic 'waves' which originate at the midbody pass along the intercellular bridge.* **(c)** *Daughter cell separation is completed when the intercellular bridge breaks at the junction with one cell body.*

A more extensive investigation of daughter cell separation in D-98S cells has been carried out (Mullins and Biesele,1973,1977). This involved time lapse photography and an ultrastructural study. The diameter of the intercellular bridge decreases from approximately 1.5μm to less than 0.5μm. Time lapse photography reveals that an overall reduction in bridge diameter occurs, except at the midbody. Therefore, as bridge diameter decreases the midbody progressively projects further beyond the width of the bridge. This protruding portion of the midbody is actually a ridge which completely encircles the remainder of the midbody. No microtubules are present in this protruding portion. The significance of ridge development has not been established.

A further reduction in bridge diameter occurs in a portion of the bridge on both sides of the midbody. This has been called 'narrowing' (Mullins and Biesele,1977). A series of 'waves', similar to those reported in the intercellular bridge of HeLa cells, move along the 'narrowing' portions of the bridge in D-98S cells. This may represent the retraction of cytoplasm into an incipient daughter cell body. The microtubules in the 'narrowing' portions become more compact. In addition a number of microtubules appear to be lost as each 'narrowing' portion becomes narrower. It has been suggested that the rate of microtubule loss may control the rate of 'narrowing'. Subsequently one half of the intercellular bridge appears to stretch and its connection with one of the cell bodies is broken. It has been suggested that the considerable reduction in bridge diameter and increase in length that occurs prior to daughter cell separation is required in order that it can be 'snapped' by the movement of the daughter cells (Mullins and Biesele,1977). The events which result in daughter cell separation in D-98S cells are summarized in Fig. 6.

The remnant of the intercellular bridge apparently loses contact with the daughter cell body to which it is still attached. However, the evidence for this is not conclusive. Apparently the constant random motion of the bridge in and out of the plane of focus made it difficult to follow its eventual fate (Mullins and Biesele,1977). Ultrastructural serial sections of the midbody after the completion of daughter cell

separation indicate that it is discarded by the daughter cells. At this stage it is called a remnant midbody. It has lost most of its dense matrix and apparently in some cases the midbody does not contain any microtubules (Mullins and Biesele,1977).

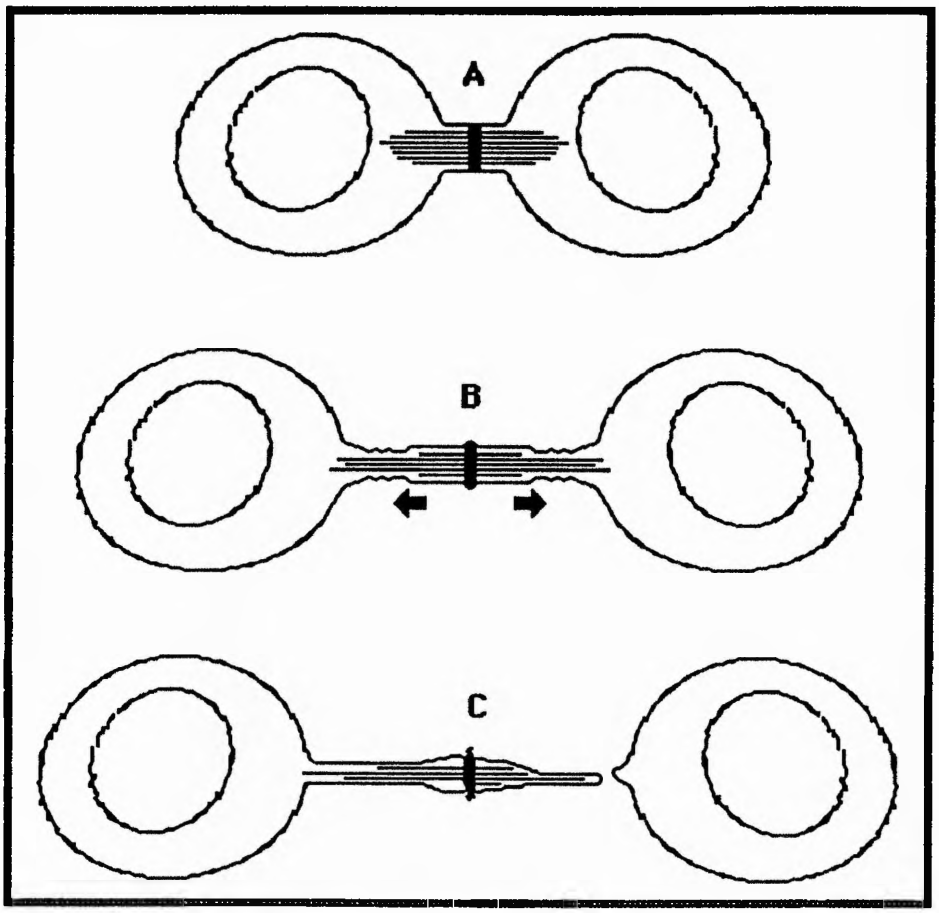

Fig.6 *Schematic diagram which summarises daughter cell separation in D-98S cells.* **(a)** *Formation of the intercellular bridge.* **(b)** *The intercellular bridge lengthens and decreases in diameter. 'Narrowing' further reduces the diameter of two portions of the intercellular bridge, one on either side of the midbody. A series of 'waves' pass along the 'narrowed' portions. The number of microtubules within these portions decreases.* **(c)** *Movements of the incipient daughter cells further stretch and snap one half of the intercellular bridge.*

1.15 *Drosophila* embryos

1.15.1 Development of the pre-gastrulation embryo

After fertilization, the *Drosophila* embryo undergoes thirteen consecutive rounds of nuclear division as a syncitium. Consequently, initial development has been conveniently separated into thirteen stages (Foe and Alberts,1983). Each stage corresponds to one round of nuclear division. During the first few stages all the dividing nuclei are located in the interior of the fertilized egg. Most nuclei begin migrating towards the inner surface of the fertilized egg during late stage 7 and early interphase of stage 8 (Foe and Alberts,1983). A small number of nuclei, known as the 'yolk nuclei' remain in the interior of the embryo. The nuclei which have been migrating reach the inner fertilized egg surface by stage 10. They become evenly distributed in a monolayer just under the egg surface. At this stage, nuclei located at the posterior pole cellularize, forming the 'pole cells'. These are the potential germ cell progenitors. The nuclei at the inner surface of the fertilized egg undergo four nearly synchronous divisions as a syncytium (stages 10 to 13). Cellularization of these nuclei occurs during the first half of interphase 14 and subsequently gastrulation proceeds (Foe and Alberts,1983).

1.15.2 The centriole cycle in the syncitial blastoderm

The nuclear divisions in the early embryo consist of M and S phases with no discernible G_1 and G_2 phases (Glover,1989). There is no G_2 phase until stage 14 and no G_1 phase until the interphase of stage 17 (Edgar and O'Farrell,1990). Consequently, the centriole cycle in the syncitial blastoderm is different from that in most animal cells. In the early *Drosophila* embryo, the pair of centrioles in each

centrosome lose their orthogonal alignment during metaphase (Callaini and Riparbelli,1990). By telophase each centrosome has split into two (Warn and Warn,1986; Warn *et al.*,1987; Kellogg *et al.*,1988). Centriole replication within each centrosome has apparently begun by telophase so that a new procentriole grows near, and perpendicular to, the base of each old centriole. Elongation of this procentriole is completed during S phase. In contrast, in most animal cells the pair of centrioles move slightly apart during G_1, centriole replication begins during S phase and elongation of the new procentriole is completed during G_2.

1.15.3 Microtubule organization in the syncitial blastoderm of the embryo

The embryo possesses a syncitial blastoderm from stage 10 to stage 13. Each nucleus is located within a highly organized region of the cytoplasm which is called a surface cap (Warn and Warn,1986) or cytoplasmic bud (Foe and Alberts,1983). A network of F-actin outlines the surface of each cap (Warn *et al.*,1984). A pair of centrosomes is positioned between the apical surface of each nucleus and the surface of each cap (Warn and Warn,1986; Callaini and Riparbelli,1990). In methanol fixed embryos, microtubules appear to be concentrated around the centrosomes. A substantial array does not appear to extend from the centrosomes (Warn and Warn, 1986). However, microtubule arrays which extend inward from these centrosomes are apparently preserved if embryos are incubated in a low concentration of taxol for 30 seconds prior to fixation (Karr and Alberts,1986). Apparently in this instance, taxol stabilizes the existing microtubules rather than inducing polymerization.

During cellularization at stage 14, the plasma membrane elongates down between the base of adjacent surface caps. 'Furrow canals' which represent bulbous leading edges of elongating plasma membrane, eventually undercut the elongating nuclei to establish a monolayer of cells. Prior to the completion of cellularization, microtubules elongate from a pair of closely associated centrosomes (3-4μm apart).

These are located between the apical surface of the nucleus and the surface of the embryo. Microtubules extend down past the nuclei and extend into a layer of yolk free cytoplasm (Foe *et al.*,1993). Microtubule preservation was achieved using formalin fixative but not taxol. Many previous investigations have reported that microtubules extend to the base of the nuclei at stage 14 (Fullilove and Jacobsen,1971; Warn and Warn,1986; Katoh and Ishikawa,1989). It is possible that a more vigorous fixation (e.g. methanol), does not preserve the microtubules which apparently extend into the yolk free cytoplasm. Microtubule acetylation, which stabilizes microtubules, occurs during stage 14 (Wolf *et al.*,1988). This may explain why microtubules around the nuclei are preserved. These microtubules may be acetylated portions of microtubule arrays which less rigorous fixation methods have preserved.

1.16 *Drosophila* indirect fibrillar flight muscles (IFMs)

1.16.1 Function of IFMs

The adult thorax contains two groups of fibrillar indirect flight muscles (IFMs). These are the dorsal longitudinal muscles (DLMs) and dorsal ventral muscles (DVMs) (Fig.7), (Crossley,1978). The IFMs, as their name suggests, are not directly associated with the bases of wing blades. They are, however, associated with the thoracic cuticle. The thorax oscillates like a tuning fork due to the antagonistic action of the two sets of IFMs. The change in thorax shape controls the up and down strokes of the insect wing-beat. The wing-beat frequency is far higher than can be achieved by the innervation of IFMs by neuronal action potentials. The IFMs are asynchronous since their contractions are not synchronized with the arrival of action potentials. In essence, action potentials serve as the 'ignition' and 'fuel' for insect IFM contraction.

Action potentials initiate and sustain contraction, but do not control the frequency of contraction of IFMs.

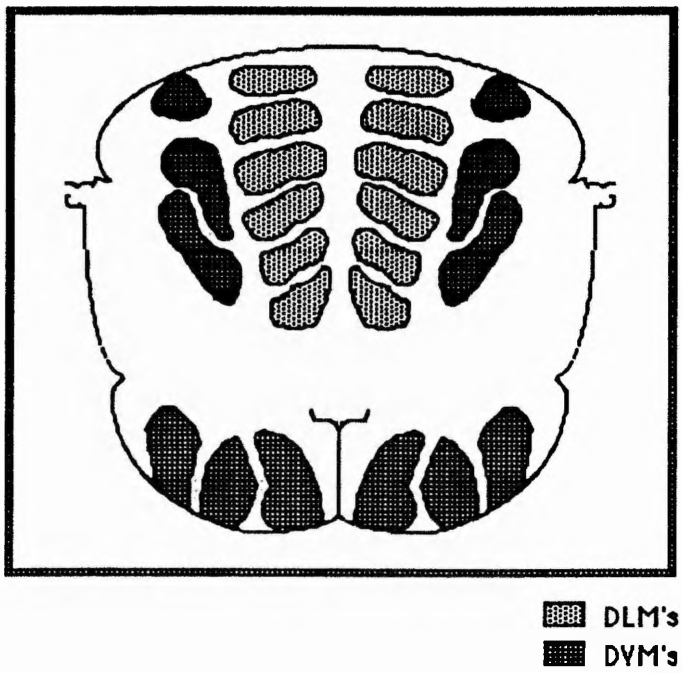

Fig.7 *Schematic diagram of a cross-section through the thorax of Drosophila which shows the location of the indirect fibrillar flight muscles. DLM - Dorsal longitudinal muscle. DVM - Dorsal ventral muscle.*

1.16.2 Early development of IFMs

During metamorphosis most larval muscles are destroyed by histolysis. However, some larval muscles persist during metamorphosis. This has been demonstrated using a transformant line which expresses the enzyme, β-galactosidase, under the control of the gene promoter (MHC-lacZ) for the myosin heavy-chain gene (Fernandes *et al.*, 1991). The enzyme is expressed in all muscles of the embryo, larva and the adult of the transformant line. Thus, the addition of the β-galactosidase substrate enables the detection of any persistent larval muscles during metamorphosis. In this way three pairs of larval oblique muscles have been found to persist into

metamorphosis. It has been determined that these muscles are the precursors for adult DLMs.

The larval oblique muscles begin to degenerate by 8 hours after the start of pupariation (a.s.p.). By 12hrs a.s.p., myoblasts accumulate around the surface of the three pairs of persistent larval oblique muscles which are the 'pretemplates' for DLMs (Fernandes *et al.*, 1991). The origin of these myoblasts has not been ascertained. They are possibly derived from adepithelial cells which are associated with the wing imaginal disc (Poodry and Schneiderman,1970; Lawrence,1982; Fernandes *et al.*,1991). The 3 pairs of 'pretemplates' begin to split at 14hrs a.s.p. and are completely surrounded by myoblasts. The myoblasts apparently begin to fuse with the 'pretemplates' at 16hrs a.s.p. (Fernandes *et al.*,1991). By 20hrs a.s.p the 'pretemplates' have completely split to form the six pairs of 'templates' for the DLMs.

Although structurally mature DLMs and DVMs are indistinguishable their initial development is quite different. The DLMs are derived from larval muscle precursors. In contrast the DVMs arise *de novo*. The myoblasts migrate to the site where these muscles will develop. This has been demonstrated by using a transformant line which expresses the enzyme, β-galactosidase, under the control of the actin-lacZ promoter (Fernandes *et al.*, 1991). This promoter only allows the expression of β-galactosidase in adult muscle. This enzyme can be detected at the site of the developing DVMs at a time (16-24hrs a.s.p) when the enzyme controlled by the MHC-lacZ promoter can not be detected. The MHC-lacZ promoter does not express the enzyme in the DVMs until later in development, indicating that this is adult-specific promoter activity. Therefore, the DVMs do not develop from a larval template.

1.16.3 Myofibrillogenesis

Mature myofibrils span the entire lengths of IFMs (Fig.8). They are similar to those of vertebrate skeletal muscle since they are composed of thick and thin filaments organized into sarcomeres, the basic repeating unit. Z-discs mark the boundary between the ends of adjoining sarcomeres. These are responsible for the characteristic striated appearance of the IFMs.

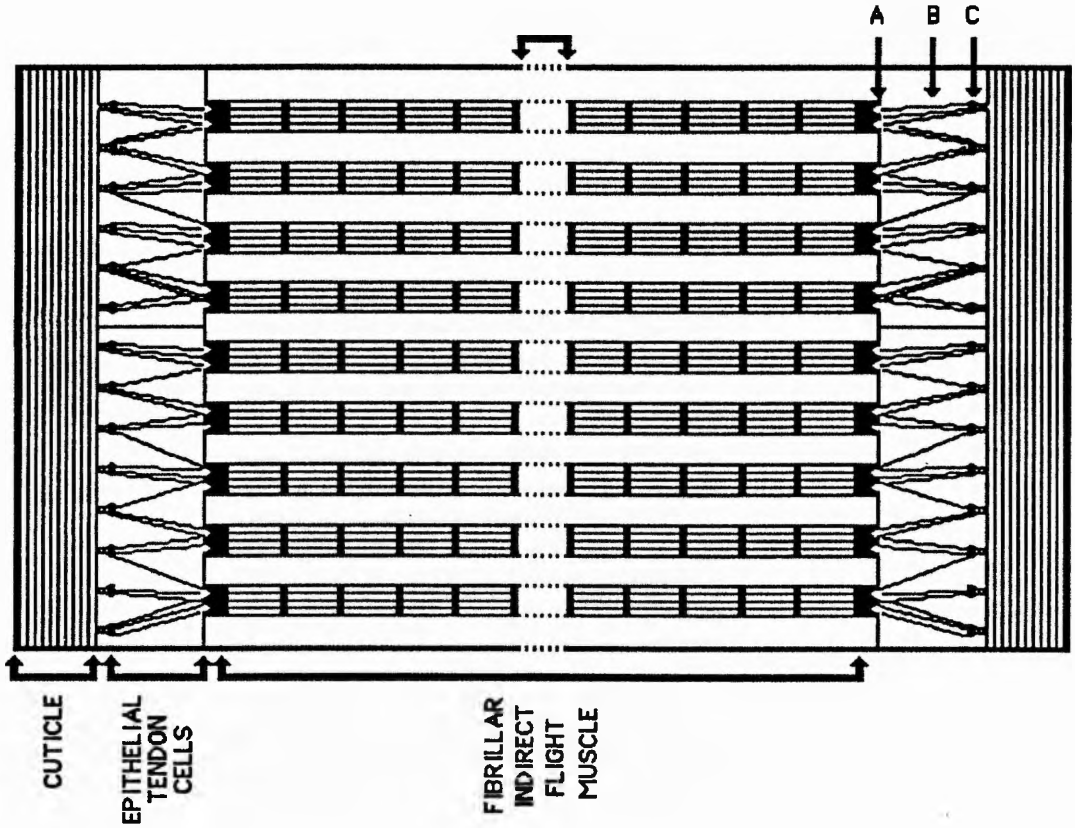

Fig.8 *Schematic diagram of a mature fibrillar muscle cell, epithelial tendon cells and cuticle. Each myofibril is associated at its ends with a myotendon junction (A). Microtubule arrays (B) form a 'link' between the mytotendon junctions and regions of invaginated cuticle (C) in the epithelial tendon cells.*

The myosin of IFMs is hollow, unlike that of vertebrate skeletal muscle. Each thick filament is surrounded by only six thin filaments. In contrast, twelve thin filaments surround each thick filament in vertebrate skeletal muscle.

Relatively little is known about the development of myofibrils of IFMs. It has not been resolved whether the myofibrils are initiated at sites on the inner surface of the muscle or within the interior of the muscle (Shafiq,1963; Auber,1969; Peristianis and Gregory,1971; Cifuentes-Diaz,1989). During myofibrillogenesis a 'sheath' of microtubules surround each developing myofibril (Auber,1969). Microtubule 'sheaths' may function as scaffolds to aid the alignment of thick and thin filaments.

1.16.4 Muscle insertion sites of IFMs

The ends of myofibrils in insects are anchored to the surface of myotendon junctions which are located at the ends of IFMs (Lai-Fook,1967; Reedy and Beall,1993a). Each myotendon junction has an undulating topography which increases its surface area. The ends of IFMs are associated with a cellular tendon (instead of an extracellular collagenous tendon which is associated with the ends of vertebrate skeletal muscle). The cellular tendons (epithelial tendon cells) (Fig.8) serve as a physical link between the cuticle and the IFMs (Auber,1963; Reedy and Beall,1993b). Arrays of microtubules span from the apical to the basal surface of each epithelial tendon cell (Fig.8). One end of these arrays associate with the surface of the myotendon junctions in the epithelial tendon cells (Fig.8). These microtubule arrays enable the force generated by the contraction of myofibrils to be exerted on the cuticle (Auber,1963; Reedy and Beall,1993b).

The myotendon junction surface, on the muscle side, is associated with a dense cap of amorphous material (Fig. 8). This dense cap is itself associated with the end of a myofibril. It has been suggested that the dense caps are actually modified terminal Z-discs (Reedy *et al.*,1993). This is possible since mutant alleles of α-actinin, a

protein located at the Z-discs of myofibrils, disrupt the integration of the terminal sarcomere with the plasma membrane in *Drosophila* (Fyrberg *et al.*,1990).

1.17 *Drosophila* larval neuroblasts

The larval central nervous system (CNS) consists of two brain hemispheres which include the optic lobes and a ventral ganglion. Unlike most larval organs the CNS persists into the adult stage. A large number of neurons are added to CNS during the larval stages. Neuroblast cells are responsible for the generation of these postembryonic neurons (Prokop and Technau,1991). Neuroblasts are stem cells and each neuroblast lineage generates a characteristic set of neurons. Neuroblasts divide asymmetrically to yield a second neuroblast and a ganglion mother cell. The ganglion mother cell divides yielding two ganglion cells. The neuroblasts can be identified by their size. They have a diameter of 10μm and are the largest cells in the CNS of *Drosophila* (Truman *et al.*, 1993). Neuroblasts are present throughout the larval CNS. All the different neuroblast lineages are rapidly dividing during the third instar larval stage. For example, the number of neuroblasts in the optic lobes peak at the third instar larval stage (Hofbauer and Campos-Ortega,1990)

1.18 Microtubule-organization in MDCK cells

MDCK cells establish cellular polarity upon forming a confluent monolayer when grown on filter supports (Bacallao *et al.*,1989). They also establish partial cellular polarity upon forming a confluent monolayer when grown on glass coverslips (Buendia *et al.*,1990; Peppercok *et al.*,1990). Cellular polarity can be determined by the position of the MTOC since it nucleates microtubules which are polar structures. For example, motor proteins, which appear to be responsible for the transport of cellular components, can only travel in one direction along a microtubule (Vale *et*

al.,1985). It appears that microtubules are responsible for the movement of certain cellular organelles such as the Golgi apparatus (Thyberg and Moskalewski,1985; Vale,1987). The control of Golgi apparatus position by microtubule polarity determines the initial localization of specific proteins. In this way it appears that the MTOC may establish the cells' polarity.

In an isolated MDCK cell a pair of centrioles are closely associated and located in the medial region of the cell (Buendia *et al.*,1990). However, upon the formation of cell to cell contacts the pair of centrioles move apart and may be separated by up to 13μm. Only when the cell is part of a confluent monolayer do the centriole pair become closely associated once again. However, they are now located above the apical surface of the nuclear membrane once a cell has established its polarity.

The formation of cell junctions, upon cell to cell contact, causes a reorganization of the actin network in sub-confluent cells (Buendia *et al.*,1990). If filamentous actin is depolymerized in sub-confluent cells the centrioles move back together. However, if the microtubules are depolymerized the centrioles move further apart. Therefore, it has been suggested that actin pulls centrioles apart while microtubules resist this movement. This is possibly the mechanism which controls the precise positioning of the centrioles during polarization (Buendia *et al.*,1990).

The centrioles move at the correct time to the correct place to establish apical to basal cell polarity. However, this is tempered by the fact that very few microtubules are nucleated in the immediate vicinity of the centrioles in isolated, sub-confluent or confluent MDCK cells (Bre *et al.*,1987; Bacallao *et al.*,1989; Buendia *et al.*,1990; Peppercock *et al.*,1990). Paramecium axonemal tubulin has been microinjected into isolated MDCK cells (Bre *et al.*,1990). This tubulin appears to assemble in a broad region close to the nucleus which probably encompasses the centrioles. However, it is not clear how these microtubules are nucleated. Where and how microtubules are nucleated in sub-confluent cells is also not clear. An extensive microtubule network exists in sub-confluent cells. However, they have no focal point. Therefore, it has been

suggested that microtubule nucleating material (which appears to be loosely associated with the centrioles of isolated interphase cells), becomes more dispersed upon the establishment of cell to cell contacts (Pepercok *et al.*,1990).

MDCK cells which are grown to confluence on filter supports become fully polarized (Bacallao *et al.*,1989). A pair of centrioles are located just below the apical surface of the cell and the Golgi apparatus is located above the apical surface of the nucleus. There is an apical network of microtubules and a microtubule bundle oriented from the apex to the base of the cell. Very few microtubule ends are located in the immediate vicinity of the centrioles. However, the minus ends of microtubules in the apical to basal oriented bundle are located in the apical region of the cell. It has been suggested that in addition to the pair of centrioles, microtubule nucleating material is also relocated to an apical region of the cell during the establishment of cell polarity (Pepercok *et al.*,1990a). It is not clear whether these microtubules are nucleated by material which may have become relocated at the cell apex. It is apparent that these microtubules are extremely stable and require cold in addition to nacodazole to be depolymerized (Bacallao *et al.*,1989). This stability appears to occur upon the establishment of a confluent monolayer (Pepercok *et al.*,1990b). It is not clear how this stability is achieved although it has been suggested that increased stability is possibly the result of microtubule plus end capping or the binding of MAP's (Pepercok *et al.*,1990b).

Chapter 2

Materials and Methods

The accounts of techniques and procedures are grouped together in terms of the Thesis Chapters to which they have most relevance.

2.1 Chapter 3: Pericentrin, or a homologue, is localized at myotendon junctions between fibrillar indirect flight muscle cells and epithelial tendon cells in *Drosophila*

2.1.1 Staging of *Drosophila* pupae

Immobile, white prepupae (*Drosophila melanogaster*, Oregon strain S) with everted spiracles were selected. These turn a tan colour within 60mins at 25^{0}C. For the purpose of this study the white prepupae were considered to be at 0 hrs after the start of pupariation (a.s.p.). These were incubated in a Petri-dish with moist filter paper at 25^{0}C. Thus various developmental stages at a specific time after the start of pupariation could be used for experimental purposes.

2.1.2 Removal of the pupal case

In order to remove the pupal case without damaging the pupa it was essential to adhere the ventral surface of the pupal case to double sided sticky tape attached to a

glass slide. Dissections were performed using a Zeiss Stereozoan IV dissecting binocular microscope. The tip of a tungsten needle was used to pry open the operculum. The tip was carefully inserted through the pupal case just above the proximal end of one developing wing. A gap between the pupal case and surface of the pupa exists in this region. Small lateral movements of the tungsten needle tip towards the anterior end of the pupa were made to gradually sever the annular sclerites of the pupal case. A fine tipped pair of forceps were used to peel the severed sclerites away from the surface of the pupa. Further lateral movements of the tungsten needle tip, towards the posterior end of the pupa, were made to gradually sever more sclerites just above one wing. These severed sclerites were peeled off the surface of the pupa. The hooked tip of a tungsten needle was carefully inserted under the first sclerite of the abdomen. This was gently scraped backwards and outwards away from the surface of the pupa. This severed the sclerite without puncturing the surface of the pupa. Only a couple of abdomen sclerites had to be removed in this fashion since the pupa could be gently pried from the remaining intact sclerites. The completely intact pupa could then be lifted clear from the dissected pupal case by positioning the shaft of a tungsten needle at the joint between a wing and thorax, and then transferred onto a clean glass slide.

2.1.3 Dissection of pupae for transmission electron microscopy

Two different dissection techniques were employed in order to facilitate the subsequent entry of fixatives. Either the abdomen was removed (dissection technique 1) or alternatively both the abdomen and head were removed (dissection technique 2) from pupae. The latter procedure was employed for the early developmental stages.

Dissection technique 1

The adult cuticle prevents entry of fixatives into the intact pupae. Therefore it was necessary to remove the abdomen. This was performed using a binocular microscope. Pupae, each previously removed from its pupal case (see section 2.1.2), were placed in dissecting medium. The posterior end of each abdomen was pierced and held in place with the tip of a tungsten needle. The tip of a second tungsten needle was used to gently tear open the proximal end of the abdomen. As much of the abdomen was removed as possible without disturbing the contents of the thorax. The tip of a tungsten needle was also used to puncture small holes in the developing head of a pupa. Dissected pupae were immediately transferred to 2.5% glutaraldehyde fixative in phosphate buffer (see section 2.1.4).

Dissection technique 2

The method of dissection outlined above proved unsatisfactory for early developmental stages. The internal pressure of the pupae resulted in their entire contents being devastatingly disrupted upon the insertion of a tungsten needle into the abdomen. An alternative method of dissection was devised. Half the surface of a glass slide was covered with double sided sticky tape. The ventral surface of a pupae, previously removed from its pupal case (see section 2.1.2), was precisely placed at the interface between the glass surface and sticky tape surface. The ventral surface of the abdomen was attached to the sticky tape surface while the thorax and head were positioned on the glass surface. The fine tip of a red hot iron needle was used to cauterise the posterior end of the abdomen. This completely coagulated most of the material in the posterior portion of the abdomen. This was scraped out with the tip of a tungsten needle. The anterior end of the abdomen was not cauterised to ensure that the thorax was not effected. The anterior end of the head was also cauterised. This was

sufficient to allow entry of fixatives into the thorax. The intact thorax and remnants of the head and abdomen were immediately transferred to 2.5% glutaraldehyde in phosphate buffer (see section 2.1.4).

2.1.4 Preparation of *Drosophila* pupae for transmission electron microscopy

After dissection, pupae were immediately fixed in 2.5% glutaraldehyde (Emscope) in phosphate buffer (0.05M, pH 7.6) for approximately 30 minutes and subsequently rinsed in the phosphate buffer for 2 minutes. They were post-fixed in 1% osmium tetroxide (Emscope) in the same buffer for 30 minutes and subsequently rinsed in phosphate buffer. After fixation, the pupal tissue was *en bloc* stained with 1% aqueous uranyl acetate solution overnight at room temperature. Pupal tissue was then dehydrated using a graded ethanol series, and transferred to 100% propylene oxide. The specimens were then passed through a graded series of propylene oxide/araldite resin mixtures, to allow adequate penetration of resin, before being flat embedded in araldite epoxy resin (Emscope). The resin with embedded tissue was left to harden for 48hrs at 60^0C.

2.1.5 Transmission electron microscopy

Glass knives (made with an LKB Knifemaker, LKB, Stolkholm) were used to cut thick (1μm) sections which were subsequently stained using 1% methylene blue dissolved in aqueous borax (1%) solution. Bright field microscopy (Zeiss Universal Microscope) was used to examine these sections.

A diamond knife (Deleware Diamond Knife) was used to cut ultra-thin sections with thickness of 75-90nm (silver and gold interference colours). Copper grids were coated with a solution of 1% chloroform, allowed to dry and coated with carbon. Ultra-

thin sections were mounted on the carbon coated copper grids. The sections were then stained with 2% uranyl acetate in 70% ethanol for 20 minutes followed by lead citrate (Reynolds, 1963) for 5 minutes. Both thick and ultra-thin sections were cut with a Reichert Om-U3 ultramicrotome or a Reichert Ultracut-S ultramicrotome.

Electron microscopy was carried out using a Philips 301 electron microscope operated at 60 kV. Micrographs were taken using 'Ilford technical (electron microscope) film' which was developed in Kodak D-19. Prints were prepared using 'Ilford multigrade' photographic paper and developed in Ilford Multigrade rapid developer.

2.1.6 Cryostat microtomy of *Drosophila* pupae

Whole pupae (after pupal case removal, see section 2.1.2) were placed into to a drop of 'Reichert-Jung Tissue Freezing Medium'. Pupae in 'Tissue Freezing Medium' were then placed on a cryostat chuck and frozen in isopentane cooled to -160^{0}C by liquid nitrogen. The frozen chuck with specimens was placed in a cryostat chamber (Reichert-Jung Frigocut 2800E) at - 20^{0}C and allowed to equilibrate prior to sectioning. Frozen sections, 6-10µm thick, were cut using a tungsten steel knife (Leica). Initial sections were stained using a diluted solution of 1% methylene blue dissolved in aqueous borax (1%) solution and examined with a bright field microscope (Zeiss Universal Microscope). This was performed until fibrillar muscle was clearly present. Subsequently, sections were transferred to gelatine-coated slides (the gelatine increases the adhesiveness of section to slide).

2.1.7 Immunolabelling of cryostat tissue sections of *Drosophila* pupae

Tissue sections (6-10μm thick) were fixed in 100% methanol at -20^{0}C for 5 mins, followed by 5 mins in 100% acetone. Sections were detergent extracted in 0.1 % Triton-X-100 in phosphate-buffered saline (PBS) for 15mins, briefly rinsed in PBS and subsequently incubated in 10% goat serum for 60mins. Tissue sections were incubated in primary antibodies in a moist chamber at 4^{0}C for 15 hours. They were then rinsed extensively (60mins) in PBS, followed by a 60min incubation in 10% goat serum for 60mins, and subsequently incubated with the appropriate secondary antibodies. Tissue sections were then rinsed extensively in PBS (2hrs), briefly rinsed in distilled water, and subsequently mounted with N-propyl gallate/glycerol in PBS to reduce photobleaching.

2.1.8 Antibodies

Tissue sections of *Drosophila* pupae were stained with three different affinity purified anti-pericentrin antisera, M1, M8 or 4b5MA-1 (supplied by S.J. Doxsey, Dep. of Cell Biology, University of Massachusetts Medical School, Worcester, MA). The stock antibody concentration was 5 mg/ml and was diluted to 1:500. Anti-α-tubulin monoclonal antibody (Amersham Life Sciences) was diluted to 1:500. Tissue sections were also stained with three different rabbit pre-immune sera (diluted to 1:500). The pre-immune sera used were from rabbits prior to their inoculation with pericentrin fusion proteins. Both secondary antibodies, DTAF conjugated goat anti-rabbit IgG (H+L) and Texas Red conjugated goat anti-mouse Ig G(H+L) (Jackson Immuno Research laboratories) were diluted to 1:500.

2.1.9 Phase contrast, Immunofluorescent and laser scanning confocal microscopy

Phase contrast and immunofluorescent images of cells were observed using a Nikon inverted microscope (Diaphot model TMD) with epi-fluorescence attachments. A Bio-Rad MRC-600 series laser scanning confocal imaging system with a krypton/argon laser was also employed to generate phase contrast images of cells and confocal images of antisera localization within cells. These images were recorded and stored on an optical disc. Images could be subsequently relayed to a colour video monitor (Sony Trinitron, PYM-1444QM) and printed onto Sony UPC-5010P paper using a colour video printer (Sony Mavigraph UP-5000P).

The Bio-Rad MRC-600 series laser scanning confocal imaging system enabled serial optical sections (of any predetermined increment) to be taken through a specimen and recorded. This is called a Z-series. Using Comos 603 software these images were subsequently superimposed upon each other. This results in a 2 dimensional image which is a record of the 3 dimensional localization of the antiserum. In this thesis, such images are referred to as a 'projected Z-series'.

The imaging system can also simultaneously record (within the exact same region of a specimen) the localization of two different antisera or alternatively the localization of one antiserum plus the phase contrast image. In this thesis, such images are referred to as 'dual images'. Simultaneously recorded images can subsequently be merged. This facilitates the visualization of the spatial localization of two different antisera with respect to each other. The localization of two different antisera is obvious in such images since each is given a different pseudocolour. In this thesis, these will be referred to as 'merged images'.

2.2 Chapter 4: anti-pericentrin antisera stain *Drosophila* centrosomes

2.2.1 Preparation of fixed whole *Drosophila* embryos

Embryos between developmental stages 10 and 14 (Foe and Alberts,1983) were obtained using the following method. A pre-egg collection was taken to eliminate any fertilized eggs which were stored in the uterus of females. Fresh agar plates, smeared with yeast, were added to bottles containing flies. The fly bottles were returned to the incubator at 25^0C for 2hrs. This results in a broad range of developmental stages. All embryos were removed from the agar plates using a fine tipped brush and a saturated sugar solution. These were then decanted into a steel mesh basket (as described in Wieschaus and Nusslein,1986) and rinsed several times in distilled water.

The procedure for the dechorionation and removal of vitelline membranes from syncitial blastoderm embryos was a modified version of that described previously (Mitchison and Sedat, 1983; Foe and Alberts, 1983). Dechorionation was performed by immersing the embryos, (contained in a steel mesh basket), in a 50% commercial bleach solution for 90 seconds. This was followed by several rinses in distilled water. Embryos were transferred, with a fine tipped brush, from the steel mesh basket to a heptane/methanol bilayer at -20^0C (10ml of heptane, 9ml 90% methanol, 1ml 0.5M EGTA, pH 6.0). The bilayer was swirled for 10 minutes or until the majority of embryos were free of their ruptured vitelline membranes. Embryos free of their vitelline membranes sink from the heptane/methanol interphase to the lower methanol phase. Fixation was allowed to occur for approximately 10 minutes. The fixed embryos are hydrated through two changes each of 70, 50, and 25% methanol/0.5M EGTA solution (where the aqueous component is PBS). All embryos were then processed for immunocytochemistry.

2.2.2 Immunolabelling of devitellinized *Drosophila* embryos

The devitellinized embryos, (contained in a steel mesh basket), were rinsed in PBS (4 x 15mins) and subsequently extracted with 0.1% Triton-X-100 (2 x 30mins). Non-specific protein binding sites were blocked by incubating in 10% goat serum (2 x 30mins). Embryos were incubated with primary antibodies (see section 2.2.3), in a moist chamber at 25^0C overnight. This was followed by extensive rinsing in PBS (5 x 25mins) and then incubation in 10% goat serum (2 x 30mins). Embryos were incubated with appropriate secondary antibodies (see section 2.2.3) for 3hrs at room temperature. They were then rinsed extensively in PBS (5 x 25mins), before being transferred to mountant in a watch glass. A drop of mountant (N-propyl galate/glycerol in PBS) containing embryos was placed on the surface of a glass slide between two broken halves of a coverslip, (which functions as spacers). A whole coverslip was placed on top of the spacers. Dental wax was used to seal the coverslip to the glass slide. Embryos were screened by phase contrast microscopy for syncitial blastoderm embryos (stage10-13) and embryos during cellularization (stage 14). The cells were subsequently examined (see section 2.1.9).

2.2.3 Antibodies tested with *Drosophila* embryos

Drosophila embryos were stained with one of three different affinity purified anti-pericentrin antisera, M1, M8 or 4b5MA-1. (supplied by S.J. Doxsey, Dep. of Cell Biology, University of Massachusetts Medical School, Worcester, MA). The stock antibody concentration was 0.5 mg/ml and was diluted to 1:500. Anti-alpha tubulin monoclonal antibody (Amersham Life Sciences) was diluted to 1:500. Embryos were either stained with one of the anti-pericentrin antisera or double stained with an anti-pericentrin antiserum and anti-alpha tubulin monoclonal antibody. Both secondary

antibodies, fluorescein DTAF conjugated goat anti-rabbit IgG (H+L) and Texas Red conjugated goat anti-mouse IgG (H+L) (Jackson Immuno Research laboratories), were diluted to 1:500.

2.2.4 Culture of *Drosophila* epithelial cells

Clone 9, a cloned epithelial cell line derived from a *Drosophila* wing imaginal disc cell line, CME W1, was passaged and plated *in vitro* as described previously (Currie *et al.*, 1988). The culture medium used is described in detail in Cullen and Milner (1991) and is a modified version of Shields and Sang's M3 culture medium. For experimental purposes cells were plated directly onto glass coverslips contained in 60mm Petri dishes at approximately 375 000 cells per slide. These were incubated at 25^0C for 48 hours.

2.2.5 Immunolabelling of *Drosophila* epithelial cells

Cell monolayers adhered to glass coverslips were rinsed for 5 seconds in PBS at room temperature. They were then fixed in 100% methanol at -20^0C for 5 minutes. Cells were hydrated and their non-specific protein binding sites blocked by treating with 10% goat serum in PBS for 30 minutes. They were then incubated in primary antibodies in a moist chamber at 4^0C overnight. This was followed by an extensive rinse in PBS for two hours while being gently agitated to enhance the rinsing out of excess antibody from the cells. They were next incubated in 10% goat serum in PBS for 30mins. Cells were incubated in appropriate secondary antibodies for 3hrs at room temperature. This was followed by rinsing extensively in PBS for 2hrs as described above. Finally, cells were rinsed briefly in distilled water and subsequently mounted in propyl-gallate mountant on glass slides and cover slips were sealed with dental wax.

2.2.6 Antibodies tested with *Drosophila* epithelial cells

Drosophila C9 epithelial cells were stained with three different affinity purified anti-pericentrin antisera, M1, M8 or 4b5MA-1 (supplied by S.J. Doxsey, Dep. of Cell Biology, University of Massachusetts Medical School, Worcester, MA). The stock antibody concentration was 5 mg/ml and was diluted to 1: 500. Anti-alpha tubulin monoclonal antibody (Amersham Life Sciences) was diluted to 1:500. Cells were either stained with one of the anti-pericentrin antisera or double stained with an anti-pericentrin antiserum and anti-α-tubulin monoclonal antibody. Both secondary antibodies, fluorescein DTAF conjugated goat anti-rabbit IgG (H+L) and Texas Red conjugated goat anti-mouse Ig G(H+L) (Jackson Immuno Research laboratories), were diluted to 1:500.

2.2.7 SDS-Polyacrylamide gel electrophoresis, Western blotting and Immunoblotting

Protein sample preparation

Whole cell lysates were prepared by a method described previously (Stearns *et al.*,1991). Cells were rinsed twice in PBS to remove traces of medium. Sample buffer (tris/glycerol, b-mercaptoethanol, and the detergent sodium dodecyl sulphate) was added to the cells (200ml/petri-dish) and mixed to lyse the cells. The resulting viscous solution (due to chromatin release), was immediately transferred to an eppindorf tube and boiled for three minutes. This denatured the proteins and deactivated protease enzymes. The sample was sonicated (Sonifier cell disrupter, Ultrasonics, Inc.) several times to break up the chromatin which results in a less viscous solution. The sample containing the whole cell lysate could be stored at -70^{0}C for two weeks.

times to break up the chromatin which results in a less viscous solution. The sample containing the whole cell lysate could be stored at -70^{0}C for two weeks.

SDS-Polyacrylamide gel electrophoresis

The whole cell lysate samples were separated according to their molecular weight by SDS-polyacrylamide gel electrophoresis (SDS-PAGE) using a Bio-Rad Mini Protean II Dual Slab Cell. The protocol adopted was that detailed in the accompanying instruction manual, and which is based on the Laemmli buffer system (Laemmli,1970). Both 7% and 12% polyacrylamide gels were cast depending on which protein would eventually be assayed for in the immunoblot. To enhance the chances of detecting pericentrin (200-220Kd), the protein samples were separated on 7% polyacrylamide gels. To detect γ-tubulin (~ 50Kd) and acetylated-tubulin (~ 53Kd), proteins were separated on a 12% polyacrylamide gel. The mobility of proteins is inversely proportional to the concentration of acrylamide used to construct the gels. Therefore high molecular weight proteins are more mobile, and thus better separated from other proteins, in 7% rather than in 12% polyacrylamide gels. After the 'running' and 'stacking' polyacrylamide gels had completely polymerized, 10ul of 'total cell protein'/sample buffer was loaded into each well of the stacking gel except one. This well was loaded with sample buffer containing molecular weight markers (MW-SDS-200, Sigma). Gels were run at 200V for approximately 55 mins in a BioRad vertical minigel format using tris/glycine/SDS running buffer in the upper and lower buffer chambers. Proteins were separated along the length of the gel in discrete bands according to their molecular weight. Two lanes from the gel were removed, one which contained the separated proteins of the cell sample, the other the separated molecular weight markers. These were stained in Coomassie Blue R-250 in fixative (40% methanol, 10% acetic acid) and then destained for 3hrs in fixative (40% methanol/10% acetic acid), to remove background staining. This effectively revealed the protein bands.

Western Blotting

Proteins within the remaining portion of the SDS-PAGE gels were transferred onto Bio-Rad nitro-cellulose paper using a Bio-Rad mini trans-blot electrophoretic transfer cell. The protocol adopted for this procedure is detailed in the accompanying instruction manual for this apparatus. Briefly : gels were equilibrated in transfer buffer (tris and glycine with 20% methanol) for 15 mins. Prior to being loaded into a 'gel cassette' each gel was first incorporated into a fibre pad/filter paper/nitro-cellulose paper 'sandwich', (all of which were pre-soaked in transfer buffer). The cassette was then placed into a buffer tank to which a power source was attached. Western blot transfers were carried out at 100 volts for 1 hour. The nitro-cellulose sheets containing the transferred proteins were stored in tris buffered saline at 4^0C overnight.

Immunoblotting

The nitro-cellulose paper which contains the transferred proteins was cut into 0.5cm strips, parallel to the separated proteins, and incubated in 1% goat serum in PBT (PBS + 0.05% Tween) for 60mins, in order to block non-specific protein binding sights. Nitro-cellulose strips were then incubated in a primary antibody for two hours and subsequently rinsed in PBT (4 x 10mins). Nitro-cellulose strips were blocked for a further 30mins in 1% goat serum in PBT before being incubated in the appropriate secondary antibody (goat anti-rabbit IgG(H+L) or goat anti-mouse IgG(H+L), conjugated with horse-radish peroxidase) for 1 hour. They were next rinsed in PBT (3 x 10mins). Nitro-cellulose strips were then incubated with a DAB substrate/30% H_2O_2 in PBS, until protein band(s) appeared. Each developed nitro-cellulose strip was rinsed and stored in distilled water in the dark until photographed. Controls included omitting primary antibodies and omitting secondary antibodies.

2.3 Chapter 5: Daughter cell separation in MDCK cells

2.3.1 Cell culture

MDCK cells were cultured in MEM, complete minimum essential medium (500ml minimum essential medium, 5ml non-essential amino acid solution, 5ml L-glutamine, 2.5ml karamycin solution, 25ml foetal calf serum and 25ml horse serum), at 37^0C in a 5% CO_2 atmosphere. Cells were passaged weekly using 0.25% trypsin solution in Earls balanced salt solution with 2mM EDTA, counted using a Coulter Counter, and seeded at a density of 1 x 10^6 cells per 75cm^2 roux flask. Cells for immunofluorescence experiments were seeded on sterile 12mm glass coverslips, each contained within a 60mm sterile Petri-dish. Cells were seeded at a density of 0.25 x 10^6 per 5ml of cMEME and incubated at 37^0C in a 5% CO_2 atmosphere for 48hrs prior to each experiment. This resulted in sub-confluent populations of MDCK cells.

2.3.2 Preparation of MDCK cells for transmission electron microscopy

Cells were prepared for transmission electron microscopy as described for *Drosophila* pupae (see section 2.1.4), but with the following modifications. Cacodylate buffer, pH 7.3, was used in place of phosphate buffer. At no stage during the preparation were cells exposed to air as this results in severe shrinkage of cells. In order that the cells were retained below a liquid meniscus at all times, each subsequent solution was flushed through the previous solution, several times. This procedure effectively changed the solution covering the cells. Furthermore, cells were embedded in the surface of resin filled gelatine capsules, (six resin filled gelatine capsules per coverslip). Sections were cut, stained, photographed and developed as described previously (see section 2.1.5)

2.3.3 Immunolabelling of MDCK cells

The cells were processed for immunofluorescence as described previously for *Drosophila* epithelial cells (see section 2.2.5). The cells were examined as described previously (see section 2.1.9).

2.3.4 Antibodies

Anti-α-tubulin monoclonal antibody (Amersham Life Science) was diluted to 1:500. The secondary antibody, Texas Red conjugated goat anti-mouse Ig G(H+L) (Jackson Immuno Research laboratories), was diluted to 1:500.

2.4 Chapter 6: Spatial and temporal localization of an antigen closely associated with the midbody of MDCK cells

2.4.1 Cell culture

MDCK cells were cultured as described previously (see section 2.3.1)

2.4.2 Immunolabelling of MDCK Cells

The cells were processed for immunofluorescence as described previously for *Drosophila* epithelial cells (see section 2.2.5). The cells were examined as described previously (see section 2.1.9).

2.4.3 Primary Antibodies

(1) Non-affinity purified XGC anti-γ-tubulin antiserum; raised in a rabbit against a synthesised peptide of the carboxyl terminus of *Xenopus* γ-tubulin, coupled to a carrier protein (supplied by T. Stearns, Department of Biological Sciences, Stanford University, Stanford, California). Dilution 1:500.

(2) Affinity purified XGC anti-γ-tubulin antiserum, (Supplied by T. Stearns, Address as above). Dilution 1:500.

(3) Human anti-γ-tubulin antiserum; raised in a rabbit against a synthesised peptide of the carboxyl terminus of human γ-tubulin, coupled to a carrier protein (supplied by M. Wright, Laboratoire de Pharmacologie et de Toxicologie Fondamentales, Toulouse, France). Dilution 1:500.

(4) Affinity purified *Drosophila* anti-γ-tubulin antiserum (supplied by W. Whitfield, Dept. of Biochemistry, University of Dundee). Dilution 1:500

(5) Anti-α-tubulin monoclonal antibody (Amersham Life Science). Dilution 1:500.

MDCK cells were stained with all the above antisera. In some cases double staining effected by using these sera in conjunction with anti-α-tubulin monoclonal antibody (1 to 4).

2.4.4 Secondary Antibodies

Both secondary antibodies, Fluorescein DTAF conjugated goat anti-rabbit IgG (H+L) and Texas Red conjugated goat anti-mouse Ig G(H+L) (Jackson Immuno Research laboratories), were diluted 1:500.

2.4.5 Extraction of MDCK cells prior to fixation

In some experiments MDCK cells were extracted prior to fixation to depolymerize microtubules. Cells were extracted with 0.5% triton-X-100 in PBS for 2mins and subsequently fixed in 100% methanol. Cells were then processed for immunofluorescence as previously described for *Drosophila* epithelial cells (see section 2.2.5). They were subsequently double stained with non-affinity purified XGC gamma tubulin antiserum (1:500) and anti-alpha tubulin monoclonal antibody (1:500). The cells were subsequently examined (see section 2.1.9).

2.4.6 SDS-Polyacrylamide gel electrophoresis, Western blotting and Immunoblotting

As described previously (see section 2.2.7)

Third instar larvae were placed in a modified version of Shield and Sang's M3 culture medium (Cullen and Milner,1991) and dissections were performed under a binocular microscope. A pair of fine forceps held the posterior end of a larval abdomen while another pair were used to grasp the anterior end of the larval head. The forceps were gently pulled in opposite directions to reveal the internal structures of the larva. The brain and thoracic ganglion were separated from the imaginal discs and other tissues using a pair of tungsten needles.

2.5.2 Taxol incubation of third instar *Drosophila* larval CNS

When larval brains and thoracic ganglia were incubated in the presence of taxol for 18hrs, taxol and DMSO were present in the culture medium at final concentrations of 10mM and 0.1% respectively. Some larval brains and thoracic ganglia were incubated in 0.1% DMSO. Other were not incubated in taxol or DMSO and fixed immediately after dissection.

2.5.3 Immunolabelling of *Drosophila* third instar larval CNS

The cells were processed for immunofluorescence as described previously for *Drosophila* epithelial cells (see section 2.2.5), except for the following modifications. Larval brains and thoracic ganglia were fixed in 4% paraformaldehyde in PBS, pH 7.2, for 30 minutes and subsequently extracted in 0.3% Triton X-100 for 60 minutes. These were mounted with their ventral sides upwards in order that neuroblasts were in close proximity to the microscope objective (personal communication: Cayetano Gonzalez, European Molecular Biology laboratory, Heidleberg, Germany). The larval brains and thoracic ganglia were examined as described previously (see section 2.1.9).

2.5.4 Antibodies

Larval brains and thoracic ganglia were stained with anti-α-tubulin monoclonal antibody (Amersham Life Science) diluted 1:500. The secondary antibody, Texas Red conjugated goat anti-mouse Ig G(H+L) (Jackson Immuno Research laboratories), was diluted 1:500.

2.5.5 Preparation of third instar *Drosophila* larval CNS for transmission electron microscopy

Control and 18hr taxol incubated brains and thoracic ganglia were processed for transmission electron microscopy as described previously (see section 2.1.4). Sections were cut, stained, and photographed as described previously (see section 2.1.5)

2.6 Chapter 8: The effect of taxol on centrosomal activity and protofilament number in MDCK cells.

2.6.1 Cell culture

MDCK cells were cultured as described previously (see section 2.3.1).

2.6.2 Taxol incubation

When MDCK cells were incubated in the presence of taxol, taxol and DMSO were present in cMEME at final concentrations of 10μM and 0.1% respectively. Some MDCK cells were incubated in 0.1% DMSO. Other cells were not incubated in taxol or

2.6.2 Taxol incubation

When MDCK cells were incubated in the presence of taxol, taxol and DMSO were present in cMEME at final concentrations of 10μM and 0.1% respectively. Some MDCK cells were incubated in 0.1% DMSO. Other cells were not incubated in taxol or DMSO. The 10 μM taxol / 0.1% DMSO in cMEME was filter sterilised prior to its use to minimise the chances of bacterial infection. MDCK cells grown on sterile coverslips, were incubated in 10μM taxol / 0.1% DMSO in cMEME for specific lengths of time prior to fixation for either immunofluorescence or electron microscopy. Cells processed for immunofluorescence were incubated in 10μM taxol/0.1%DMSO or 0.1% DMSO or cMEME only for 30mins, 2hrs, 4hrs or 18hrs. Cells processed for electron microscopy were incubated in cMEME or 10μM taxol / 0.1% DMSO for 18hrs.

2.6.3 Immunolabelling of taxol incubated MDCK cells

Taxol incubated, DMSO incubated, and cMEME only incubated cells were processed for immunofluorescence as described previously for *Drosophila* epithelial cells (see section 2.2.5). The cells were examined as described previously (see section 2.1.9).

2.6.4 Antibodies

(1) Affinity purified XGC anti-γ-tubulin antiserum (supplied by T. Stearns, Department of Biological Sciences, Stanford University, Stanford, California). Dilution 1:500.

(2) Affinity purified M8 anti-pericentrin antiserum (supplied by S.J Doxsey, Address as above). Dilution 1:500.

(3) Anti-α-tubulin monoclonal antibody (Amersham Life Sciences). Dilution 1:500.

Taxol incubated, DMSO incubated, and cMEME only incubated cells were stained with all of the above antisera. Taxol incubated and cMEME only incubated cells were also double stained with anti-α-tubulin monoclonal antibody in conjunction with each of the other two antisera.

2.6.5 Preparation of taxol incubated MDCK cells for transmission electron microscopy

Taxol incubated and cMEME only incubated cells were processed for transmission electron microscopy as described previously (see section 2.3.2). Sections were cut, stained, and photographed as described previously (see section 2.1.5)

2.6.6 Preparation of MDCK cells for assessment of microtubule protofilament number

MDCK cells were incubated in 10mM taxol, 0.1% DMSO and cMEME as described previously (see section 2.6.2). MDCK cells were processed in order to reveal microtubule protofilament number using transmission electron microscopy. The procedure adopted was a modified version of that used to determine microtubule polarity by hook decoration in polarised MDCK cells (Bacallao *et al.*, 1989). The initial steps prior to fixation, were all performed at 37^0C. This was critical to avoid

microtubule depolymerization. Furthermore, all buffers and glassware were maintained at 37^{0}C prior to their use by storing in heating blocs (Techne DRI-Block DB.2A.). Cells were rinsed briefly in 'rinsing buffer' (0.5M K-PIPES, pH 6.8, 10mM $MgCl_2$, 20mM EGTA, 25% glycerol). Cells were then lysed with 'lysing buffer' (same as rinsing buffer but with addition of 0.15% Triton-X-100) for 5mins at 37^{0}C. They were next rinsed in 'rinsing buffer', before being fixed in 4% glutaraldehyde, 2% tannic acid in 100mM cacodylate buffer for 3mins at 37^{0}C. Tannic acid binds to the surface of microtubule protofilaments thereby increasing the contrast of a microtubule profile. Cells were fixed for a further 30mins in 2% glutaraldehyde, 2% tannic acid in 100mM cacodylate buffer at room temperature and then rinsed extensively to remove excess fixative in cacodylate buffer. This was followed by post fixation in 2% osmium tetroxide in 100μM cacodylate buffer for 2hrs. Cells were then rinsed in double distilled water before being stained *en bloc* in 1% uranyl acetate overnight at room temperature. Cells to be embedded in araldite were subsequently processed as described for non taxol incubated MDCK cells (see section 2.3.2). However some cells were embedded in water soluble nanoplast resin (Nanoplast-Melamine Embedding Kit A2045, Polaron equipment Ltd.). This permits the infiltration, drying and hardening of cells and tissues without the need of dehydration by organic solvents. It has been reported that it enhances section contrast (Westphal and Frosch, 1984; Mogensen and Tucker,1988) and consequently improves the contrast of microtubule protofilaments. Sections were cut, stained, and photographed as described previously (see section 2.1.5)

Chapter 3

Pericentrin, or a homologue, is localized at myotendon junctions between fibrillar flight muscle cells and epithelial tendon cells in *Drosophila*

3.1 Introduction

Most animal cells possess a centriole-containing centrosomal microtubule organizing centre. However, wing epidermal cells and ommatidial cone cells of *Drosophila* lose their centrioles and centrosomes prior to assembly of certain microtubule arrays (Tucker *et al.*,1986; Mogensen and Tucker,1987; Mogensen *et al.*,1989; Mogensen *et al.*,1993).

Insect myogenesis includes some features which are common to muscle development in general. Arrays of aligned microtubules assemble parallel to the longitudinal axes of large elongate syncytial muscle cells (Finlayson,1975; Crossley,1978). During *in vitro* vertebrate myogenesis, centriole-containing centrosomes are lost at an early stage in the assembly of such microtubule arrays (Tassin *et al.*,1985). Microtubule assembly is apparently nucleated by material close, or attached, to the outer surfaces of nuclear envelopes in such cells (Tassin *et al.*,1985; Kronebusch and Singer,1987).

Are centrosomes also lost during *Drosophila* myogenesis? If so, are they replaced by a peri-nuclear nucleating system as in vertebrate muscle cells, or do they rely on cell surface-associated MTOC's as in wing epidermal and ommatidial cone cells? These

questions have been explored by ultrastructural analysis and immunocytochemistry at several stages of fibrillar flight muscle myogenesis.

Pericentrin and γ-tubulin both associate with centrosomes. Evidence indicates that both are involved in microtubule nucleation (Stearns *et al.*,1991; Doxsey *et al.*,1994). Therefore, antisera against both proteins have been employed in an attempt to identify the MTOC in fibrillar muscle.

The ends of fibrillar muscle cells are attached to epithelial tendon cells. In the mature fly, large transcellular bundles of microtubules are present in epithelial tendon cells (Auber,1963). Microtubules span each epithelial tendon cell; they run between the apical surface (which is associated with the cuticle) and the basal surface of each cell. Microtubule ends are closely associated with the surface of each myotendon junction at the bases of epithelial tendon cells. It has been suggested that these microtubules are most likely responsible for the transmission of tension from the muscle cells to the cuticle (Brown,1993). Thus microtubule organization has also been investigated in these cells using the procedures outlined above for muscle cells.

Cells have been examined at several stages after the start of pupariation (a.s.p.).

3.2 Results

3.2.1 Ultrastructure of myotendon junctions at 40 hours a.s.p.

There are usually between 4 to 6 microtubule profiles grouped around each cross-sectional profile of a myofibril (Fig.1). The terminal sarcomere of a myofibril is anchored to a structure which has been called a modified Z-disc (Reedy and Beall,1993a,b) (Fig.2). The modified Z-disc is associated with the inner surface of the plasma membrane at a junction which has been called a myotendon junction (Reedy and Beall,1993a,b) (Fig.2). Myotendon junctions are located between the ends of the fibrillar muscle cells

and the adjoining epithelial tendon cells. The area of contact between the end of a modified Z-disc and the surface of a myotendon junction in a muscle cell is marked by a thin layer of very dense material (Fig.3). This dense layer protrudes beyond the width of the modified Z-disc and in fact constitutes the surface of a myotendon junction in the muscle cells. This dense layer will be referred to as dense belt one (DB1). There is no dense belt at the surface of a myotendon junction in the epithelial cell at this stage (Fig.3).

In the muscle cells microtubules run closely alongside modified Z-discs (Fig. 3,4). The ends of these microtubules appear to be closely associated with each DB1 (Fig.4).

No centrioles or centrosomes were detected in sequential serial sections of muscle cells at this stage. Sequential sections reveal centrioles in epidermal cells at earlier pupal stages (Tucker *et al.*, 1986).

3.2.2 Ultrastructure of myotendon junctions at 55 hrs a.s.p

There are usually between 12 to 15 microtubules grouped around a myofibril at 55hrs a.s.p. (Fig.5). Each DB1 is very pronounced at 55 hrs a.s.p. (Fig.6). Cross sections through modified Z-discs reveal microtubule profiles organized around their periphery (Fig.7). These microtubules do not appear to make contact with the modified Z-discs. Microtubule ends appear to make contact with each DB1 (Fig.6).

A few microtubules are present in the vicinity of the myotendon junction surface in the epithelial tendon cells (Fig.6). There is no dense belt at the surface of the myotendon junction in the epithelial tendon cells (Fig.6).

No centrioles or centrosomes have been found in sequential serial sections of muscle cells at this stage.

3.2.3 Ultrastructure of myotendon junctions at 86hrs a.s.p.

Fibrillar muscle is mature, or nearly mature, just prior to eclosion, at 86hrs a.s.p. There are no microtubule profiles around each cross-sectional profile of a myofibril at this stage (Fig.8). The area of contact between the end of a modified Z-disc and a myotendon junction is convoluted (Fig.9). A DB1 is present at the surface of each myotendon junction in the muscle cells (Fig.9). Very few microtubules are present in the mature muscle cells. Unlike the situation at earlier developmental stages, microtubules do not appear to associate with each DB1 of the myotendon junction in the mature muscle cells (Fig.9). Several transcellular bundles of microtubules span each epithelial tendon cell; they run between the apical surface (which is associated with the cuticle) and the basal surface of each cell (Fig.10). A layer of dense material is present at the surface of each myotendon junction in the epithelial cells (Fig.11 and Fig.12). This dense layer will be referred to as dense belt 2 (DB2). The ends of microtubules in the basal region of each epithelial tendon cell are closely associated with each DB2 (Fig.9,11). No centrioles or centrosomes have been found in sequential serial sections of mature fibrillar muscle cells.

3.2.4 Pericentrin localization in fibrillar muscle and epithelial tendon cells

Sections of thoraces were stained with three different affinity purified anti-pericentrin antisera (AP pericentrin antisera) at several stages of muscle development (40, 65, 89hrs a.s.p.). Images of fluorescently stained regions obtained by confocal laser scanning microscopy (Fig.13) have been superimposed with phase contrast images (Fig.14) obtained by non-confocal laser scanning microscopy of the same regions of the sections (Fig.15). This was performed by using two different optical channels. One optical channel excites fluorescein while the other excites Texas red. Images of the exact same region are merged in exact spatial register using Comos 600 software (see material

and methods, section 2.1.9). The AP pericentrin antisera stained sites are located at the interface between the ends of muscle cells and the epithelial tendon cells at all the different stages investigated. The location of these stained sites corresponds to the location of myotendon junctions. The AP pericentrin antisera do not stain any other cytoplasmic regions in muscle or epidermal cells or any components that might represent centrosomes or the surfaces of nuclear envelopes. Rabbit pre-immune sera, (one from each rabbit subsequently responsible for the production of each different pericentrin antisera), do not stain the sites which correspond to where myotendon junctions are located. Hence, antibodies present in the host, prior to inoculation with a fusion protein (which may not have been removed by affinity purification) can not account for the staining obtained with the AP antisera. These sites do not stain, when thoracic sections are incubated with the fluorescently conjugated secondary antibody but without the primary antibody. Hence, staining is not a result of non-specific binding of the secondary antibody.

3.2.5 γ-Tubulin localization in fibrillar muscle

Numerous attempts to determine the localization of γ-tubulin in cryostat sections of *Drosophila* fibrillar muscle and epithelial tendon cells, from 65 hours to 89 hours a.s.p., have proved inconclusive. The affinity purified *Xenopus*/gamma/C-terminus anti-γ-tubulin antiserum (AP XGC γ-tubulin antiserum) does not stain sites which correspond to the location of the myotendon junctions. An affinity purified *Drosophila* γ-tubulin antiserum has also been used. It neither convincingly, nor consistently, stains sites which correspond to the location of the myotendon junctions. Occasionally, stained sites can be detected at the interface between the ends of muscle cells and epithelial tendon cells (Fig.16). However, these do not resemble the AP pericentrin antisera stained sites, as would be anticipated (cf. Fig.'s 15 and 16). There is no detectable staining elsewhere in the muscle cells or epithelial tendon cells.

3.3 Discussion

3.3.1 Does the surfaces of each myotendon junction in fibrillar muscle cells function as an MTOC?

A dense belt 1 (DB1) is present at the surface of each myotendon junction in muscle cells throughout myofibrillogenesis and at maturity. During myofibrillogenesis the ends of microtubules associate with each DB1. A recent publication has also reported the close association of microtubule ends with the surface of myotendon junctions in *Drosophila* fibrillar muscle during myofibrillogenesis (Reedy and Beall,1993 a,b). The results presented here confirm the recently published data. They also extend them. This investigation provides evidence that the surface of each myotendon junction in muscle cells may function as a MTOC. Furthermore, there is also evidence that the surface on the opposite side of each myotendon junction in the epithelial cells may also operate as a MTOC.

Microtubules surround, but do not appear to make contact with, the terminal modified Z-discs in *Drosophila* fibrillar muscle cells during myofibrillogenesis. Throughout myofibrillogenesis the ends of microtubules appear to make contact with the peripheral region of the DB1 of each myotendon junction in muscle cells. Furthermore, microtubule ends associate with the surface of each myotendon junction at 35 hrs a.s.p. (Reedy and Beall,1993a). This is prior to the association of each myotendon junction with a terminal modified Z-disc. The ultrastructural evidence presented here and in the Reedy publication, indicates that the dense belt or component/s of its structure may function as a MTOC.

Sites which correspond to the location of myotendon junctions, stain with three different AP pericentrin antisera throughout myofibrillogenesis. Western blots and immunoblots were not performed as isolation of the fibrillar muscle proved impossible. Furthermore, identification of pericentrin on Western blots has only been achieved

previously by isolating and concentrating centrosomes (Doxsey *et al.*, 1994). No further means of determining the specificity of staining are as yet available.

In summary, microtubule ends associate with the DB1 of each myotendon junction in muscle cells. Furthermore, pericentrin or a homologue is present at myotendon junctions during myofibrillogenesis. Thus the DB1 of each myotendon junction in muscle cells may function as an MTOC during myofibrillogenesis. Ultrastructural localization of AP pericentrin antisera using immunogold labelling could resolve the precise location of pericentrin or its homologue. This would confirm whether or not the DB1 of each myotendon junction in muscle cells, contains component/s which function as a MTOC.

3.3.2 Why does the myotendon junction stain with AP pericentrin antisera at 86hrs a.s.p. ?

In cultured mammalian cells, the amount of pericentrin at the centrosome is greater during mitosis than during interphase. Thus the amount of pericentrin associated with the centrosome appears to correlate with the nucleating activity of the centrosome (Doxsey, 1994). It would be anticipated that the function of pericentrin in *Drosophila* would be similar to its function in mammalian cells. At 86 hrs a.s.p. the ends of microtubules do not associate with the DB1 of each myotendon junction in muscle cells. Therefore, pericentrin would either (1) not be expected at this location or (2) be expected to be considerably less abundant than during myofibrillogenesis. However, there is no detectable difference in the intensity with which AP pericentrin antisera stains sites which correspond to the location of myotendon junctions from 40hrs to 86hrs a.s.p.

At 86hrs a.s.p. a dense belt 2 (DB2) is present at the surface of each myotendon junction in the epithelial cells. At this stage, microtubule ends are closely associated with each DB2. This dense belt is not present from 40 to 55hrs a.s.p. Microtubule ends do not appear to associate with the surface of each myotendon junction in the epithelial cells,

from 40 to 55hrs. Therefore, the occurrence of a DB2 and the association of microtubule ends with each myotendon junction surface in epithelial cells may temporally coincide. This could explain why the AP pericentrin antisera stain sites which correspond to the myotendon junctions at 86hrs a.s.p. Pericentrin may be a component of the DB2 which forms after 55 hours but prior to 86 hours a.s.p. It is possible that at 86hrs a.s.p., pericentrin is present at the DB2 but is no longer present at the DB1 of each myotendon junction. Immunogold labelling could be employed to resolve whether or not pericentrin is spatially and temporally associated with both the DB1 and DB2 of each myotendon junction.

3.3.3 Do myotendon junctions nucleate or capture microtubules?

Microtubule ends associate with the dense belts, DB1 and DB2, of each myotendon junction in a temporal manner. Do both DB1 and DB2 capture microtubules or do they both nucleate microtubules? Alternatively, does DB1 capture microtubules and DB2 nucleate microtubules, or vice versa? There is no evidence to rule out microtubule nucleation on one surface and microtubule capture on the opposite surface of each myotendon junction. However, microtubules are captured by both surfaces of similar cell junctions located between epithelial cells in *Drosophila* wings (Mogensen *et al.*,1989). This suggests that in *Drosophila*, both surfaces of such cell junctions may organize microtubules in the same manner. This does not imply that the myotendon junction must also capture microtubules on both of its surfaces. In fact, the presence of pericentrin at myotendon junctions, and its apparent absence at wing epithelial cell junctions, (personal communication, Dr. M.M. Mogensen, School of Biological and Medical Sciences, University of St.Andrews) suggests that at least one surface of each myotendon junction may nucleate microtubules.

Currently, pericentrin has only been detected at sites which nucleate microtubules (predominantly mammalian centrosomes). Pericentrin is present at myotendon junctions

during myofibrillogenesis. From 35 to 55hrs a.s.p. microtubule ends associate with each DB1. Between these stages of development each DB2 is not apparent and microtubules do not appear to associate with the surface of each myotendon junction in the epithelial tendon cells. This suggests that the DB1 dense belts are solely responsible for the AP pericentrin antisera staining at myotendon junctions during most of myofibrillogenesis. The evidence for localization of pericentrin at each DB1 suggests that each DB1 is responsible for microtubule nucleation in muscle cells during myofibrillogenesis.

At maturity microtubule ends are closely associated with the DB2 dense belts but not with the DB1 dense belts. This suggests that the DB2 dense belts are more likely to be responsible for the AP pericentrin antisera staining at myotendon junctions at maturity. The possible localization of pericentrin at DB2 dense belts suggests that they may be responsible for microtubule nucleation in epithelial tendon cells at 86hrs a.s.p. It has been proposed previously that the surface of each myotendon junction in epithelial cells may be to function as a site which nucleates microtubules (Reedy and Beall,1993b). Ultrastructural evidence apparently indicates that microtubules may be captured at the other (apical) ends of the epithelial tendon cells (Reedy and Beall,1993b).

Current evidence indicates that γ-tubulin may play a role in microtubule nucleation and that it is concentrated at microtubule nucleating sites (Stearns *et al.*,1991). However, numerous attempts to establish whether or not γ-tubulin is present at myotendon junctions has proved inconclusive. The AP XGC γ-tubulin antiserum does not stain the myotendon junctions. Furthermore, an AP *Drosophila* γ-tubulin antiserum did not convincingly nor consistently stain sites at the interface between the muscle and epithelial tendon cells. It is possible that γ-tubulin is present at the myotendon junction but that the antigen is destroyed during the preparation of the material (see material and methods, sections 2.1.6, 2.1.7).

The evidence outlined above appears to suggest that both surfaces of a myotendon junction may nucleate microtubules. The surface of the myotendon junctions in the muscle cells may nucleate microtubules throughout myofibrillogenesis. While the surface of the myotendon junctions in the epithelial cells may nucleate microtubules towards the

end of myofibrillogenesis and just prior to eclosion. However several issues must be resolved in order to establish this conclusively. Immunogold labelling should be employed to establish the spatial and temporal localization of pericentrin at myotendon junctions during myofibrillogenesis and at maturity. Although pericentrin has been implicated as an important protein for microtubule nucleation, until more is known about its precise function, its presence at myotendon junctions can not be considered as conclusive evidence of microtubule nucleating-sites. Further attempts to establish whether or not γ-tubulin is present at the myotendon junctions may be of value. However, it is likely that a protocol, modified with respect to the one used here (see material and methods, section 2.1.7) may be required.

3.3.4 Alternative microtubule-nucleating sites?

Neither ultrastructural analysis nor immunocytochemistry have provided any evidence to indicate an alternative site for microtubule nucleation in the muscle or epithelial tendon cells. No centrioles or centrosomes were detected in sequential serial sections of muscle cells during myofibrillogenesis or at maturity. AP pericentrin antisera do not localize at any sites in muscle cells or epithelial tendon cells other than those which correspond to the location of myotendon junctions. No evidence of γ-tubulin within the interior of these cells has been detected. However, γ-tubulin is expressed in *Drosophila* (Zheng *et al.*, 1991a,b, Sunkel *et al.*, 1995). Therefore, the possibility that the antigen is masked or destroyed can not be ruled out.

Fig.1 Cross sectional profile of a developing myofibril surrounded by microtubules (arrow). 40hrs a.s.p. Scale bar, 0.2μm.

Fig.2 Longitudinal section of the end of a developing myofibril. The modified Z disc (large arrow) of a terminal sarcomere is associated with a myotendon junction (small arrow). 40hrs a.s.p. Scale bar, 0.5μm.

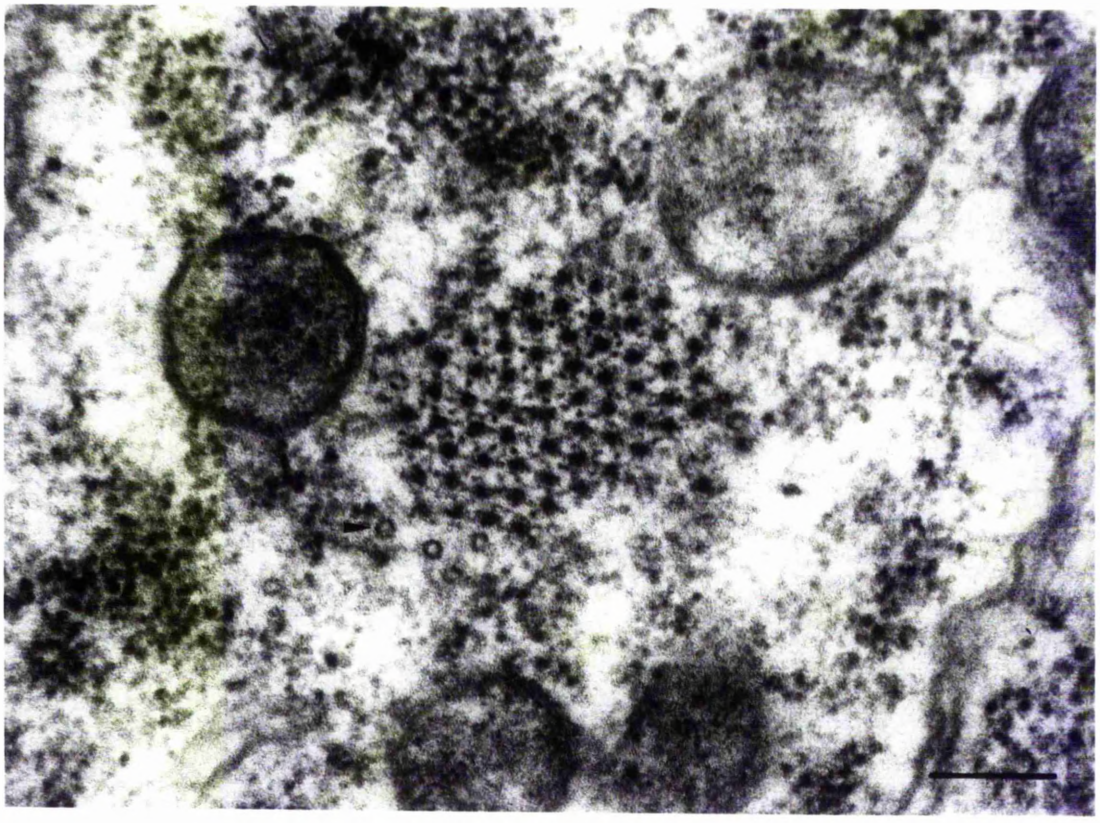

Fig.3 Longitudinal section of the end of a developing myofibril. The surface of the myotendon junction in the muscle cell is marked by a thin layer of dense material (small arrow). There is no dense layer of material at the surface of the myotendon junction in the epithelial tendon cell. Microtubule ends are closely associated with the surface of the myotendon junction in the muscle cell (large arrow). 40hrs a.s.p. Scale bar, 0.2μm.

Fig.4 Longitudinal section of the end of a developing myofibril. The ends of microtubules are closely associated with the surface of the myotendon junctions in the muscle cells (arrows). 40hrs a.s.p. Scale bar, 0.5μm.

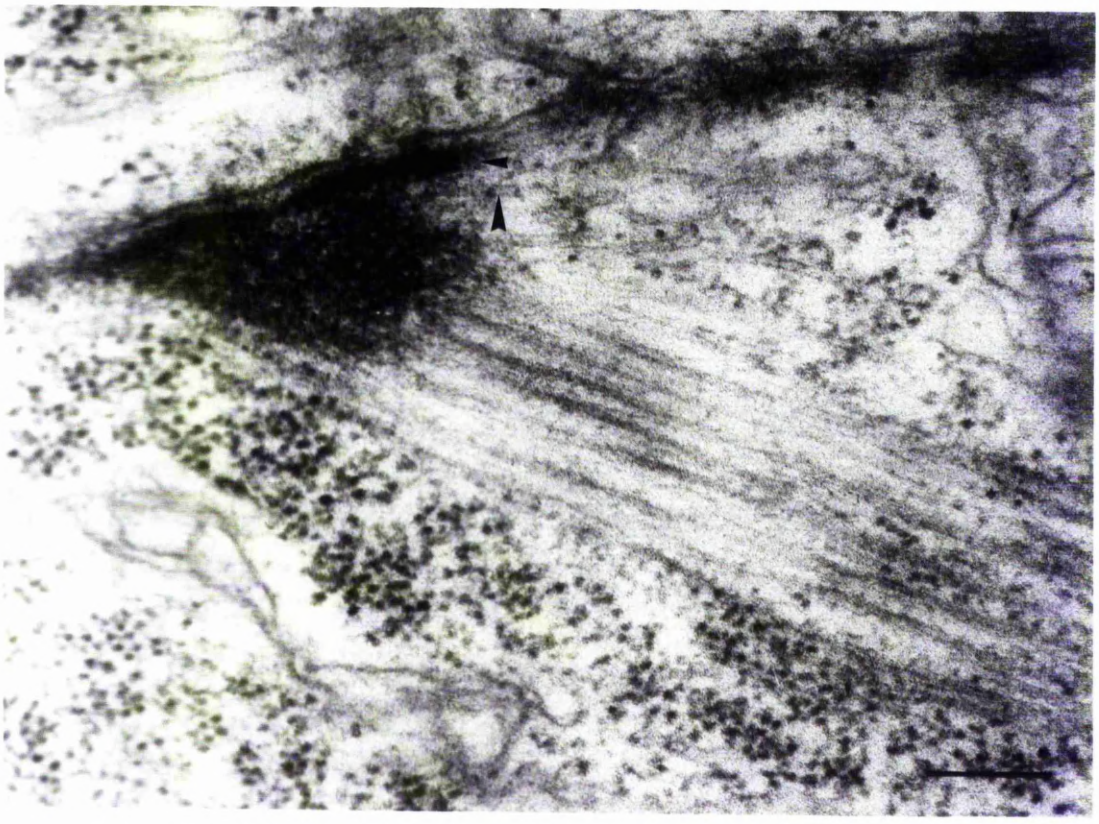

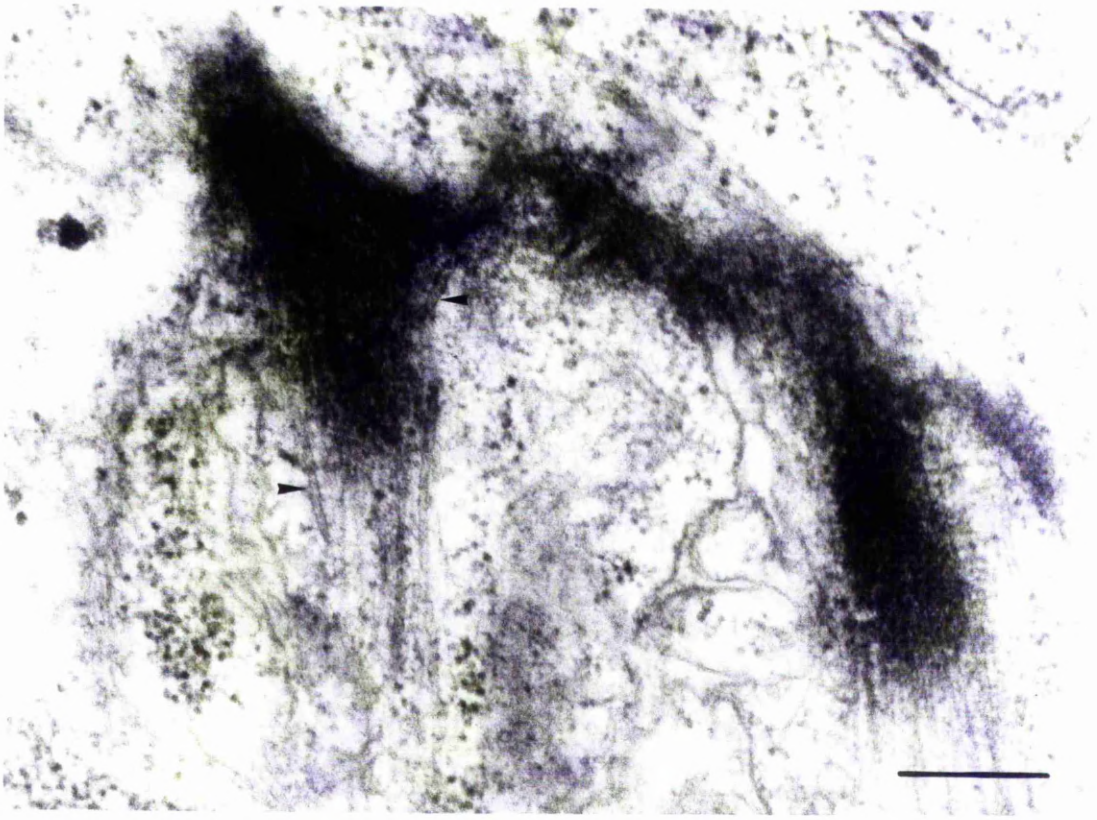

Fig.5 Cross sectional profile of a developing myofibril surrounded by microtubules (arrow). 55hrs a.s.p. Scale bar, 0.2μm.

Fig.6 Longitudinal section through the end of three developing myofibrils. The surface of each myotendon junction in the muscle cell (DB1) is very pronounced. There is no dense belt on the surface of each myotendon junction in the epithelial tendon cells. Microtubule ends appear to make contact with DB1 (arrow). A few microtubules are present in the vicinity of each myotendon junction surface in the epithelial tendon cells. 55hrs a.s.p. Scale bar, 0.3μm.

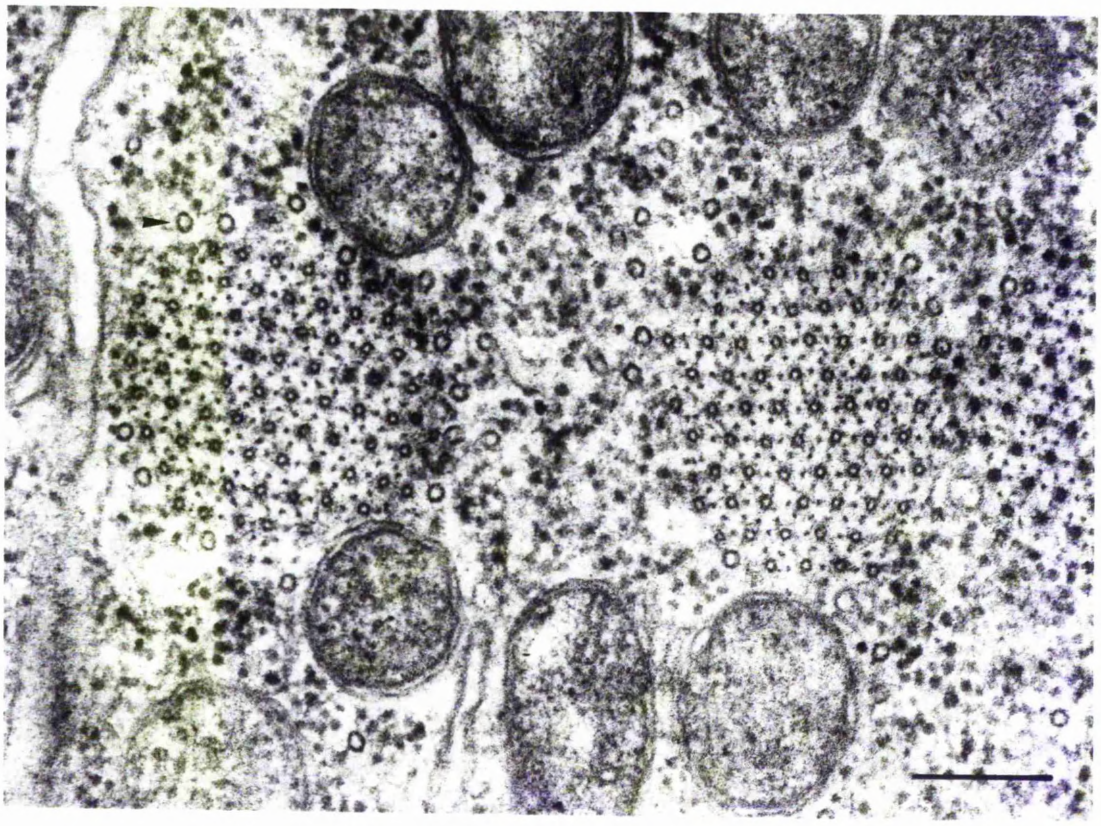

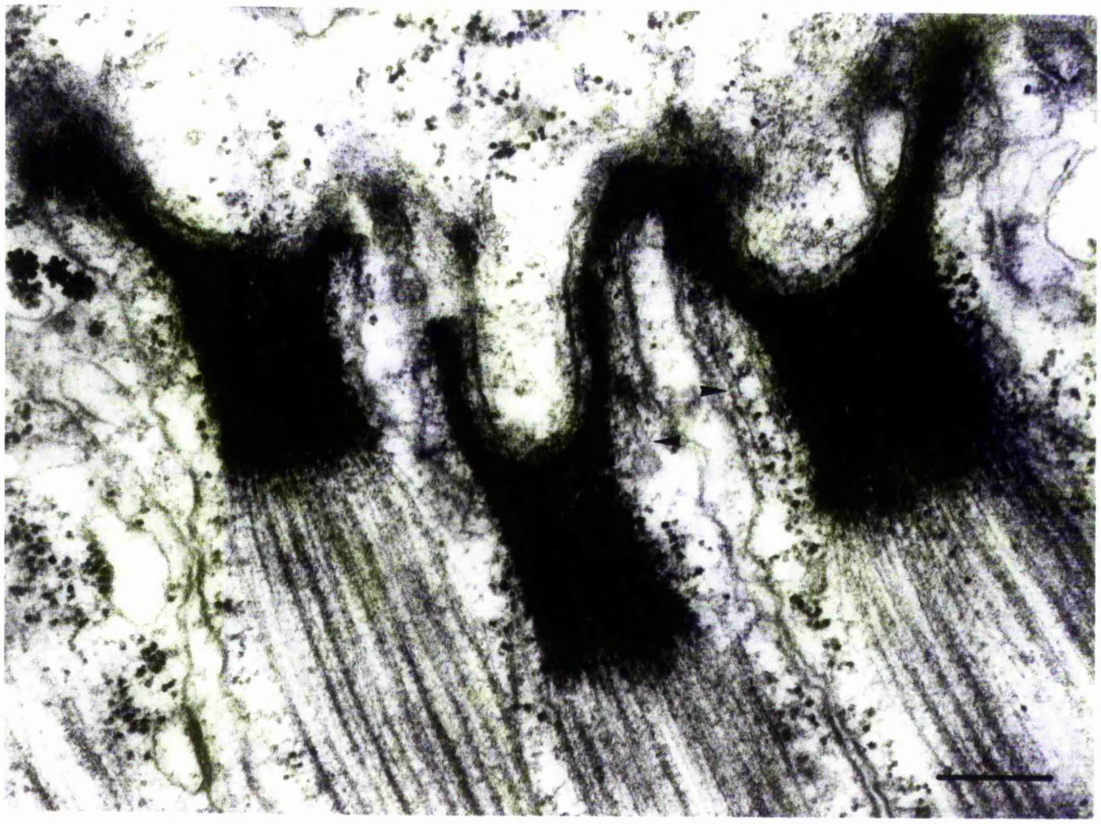

Fig.7 Cross sectional profiles of two modified terminal Z-discs at 55hrs a.s.p. surrounded by microtubules (arrow). The microtubules do not appear to make contact with the modified Z-discs. Scale bar, 0.2μm.

Fig.8 Cross sectional profile of a myofibril at 86hrs a.s.p. Scale bar, 0.2μm.

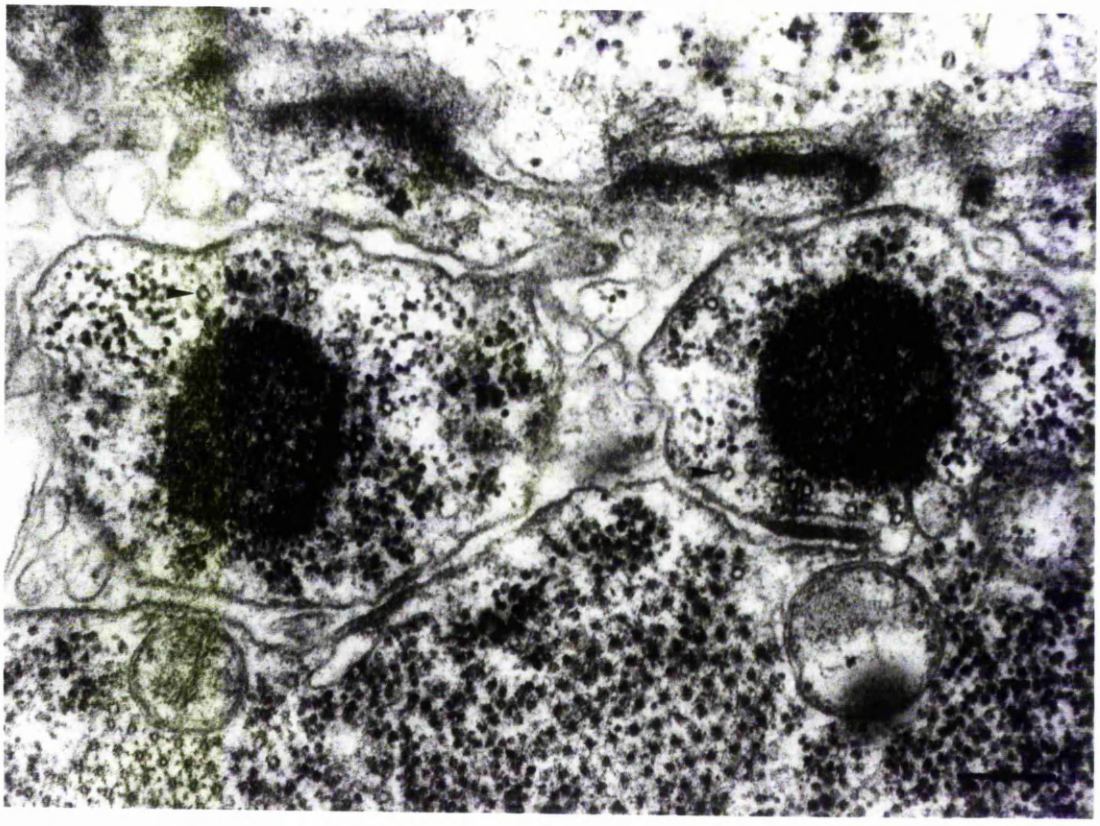

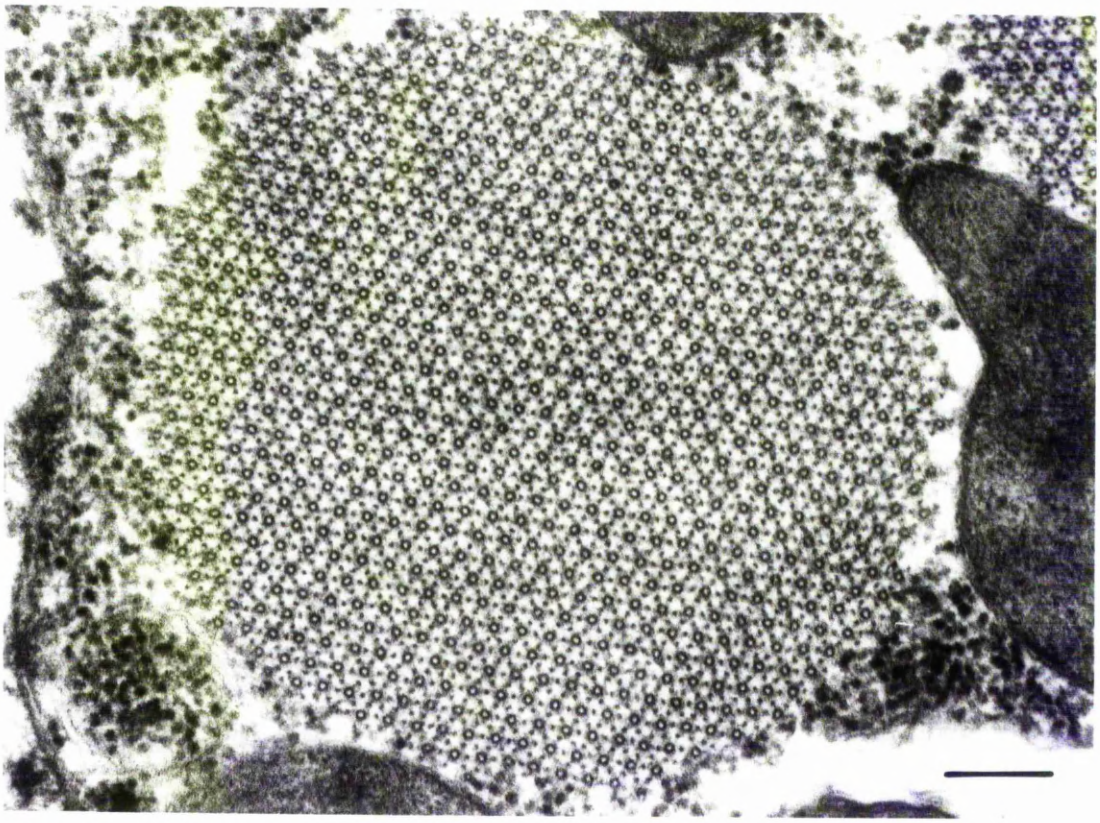

Fig.9 Longitudinal section through the end of a myofibril at 86hrs a.s.p. The myotendon junction, to which a modified Z-disc is associated, is convoluted. A DB1 forms the surface of each myotendon junction in the muscle cell. Microtubule ends are associated with the surface of the myotendon junction in the epithelial tendon cell. Scale bar, 0.3μm.

Fig.10 Several transcellular bundles of microtubules are present in the epithelial tendon cells (arrow). One end of each transcellular bundle is associated with the apical surface of the cell. The other end of each transcellular bundle is associated with the surface of the myotendon junction in the epithelial tendon cells. Scale bar, 0.5μm.

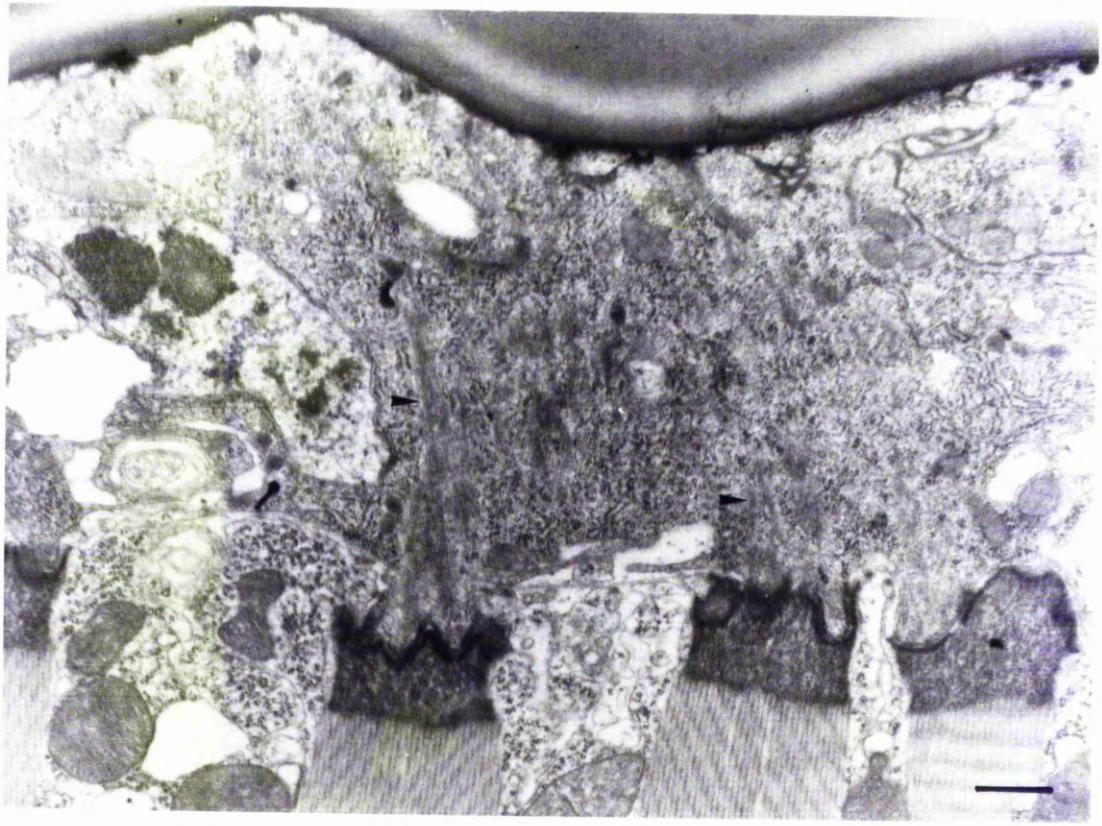

Fig.11 Oblique section through a myotendon junction at 86hrs a.s.p. A dense belt is present at both surfaces of the myotendon junction. A DB1 is associated with the end of a modified Z-disc in the muscle cell (small arrow). Microtubule ends are associated with the DB2 of the myotendon junction in the epithelial tendon cell (large arrow). Scale bar, 0.1μm.

Fig.12 Cross section through a myotendon junction and modified Z-disc at 86hrs a.s.p. A dense belt is present at both surfaces of the myotendon junction. A DB1 is associated with the end of a modified Z-disc in the muscle cell (small arrow). A DB2 is present at the surface of the myotendon junction in the epithelial tendon cell (large arrow). Scale bar, 0.2μm.

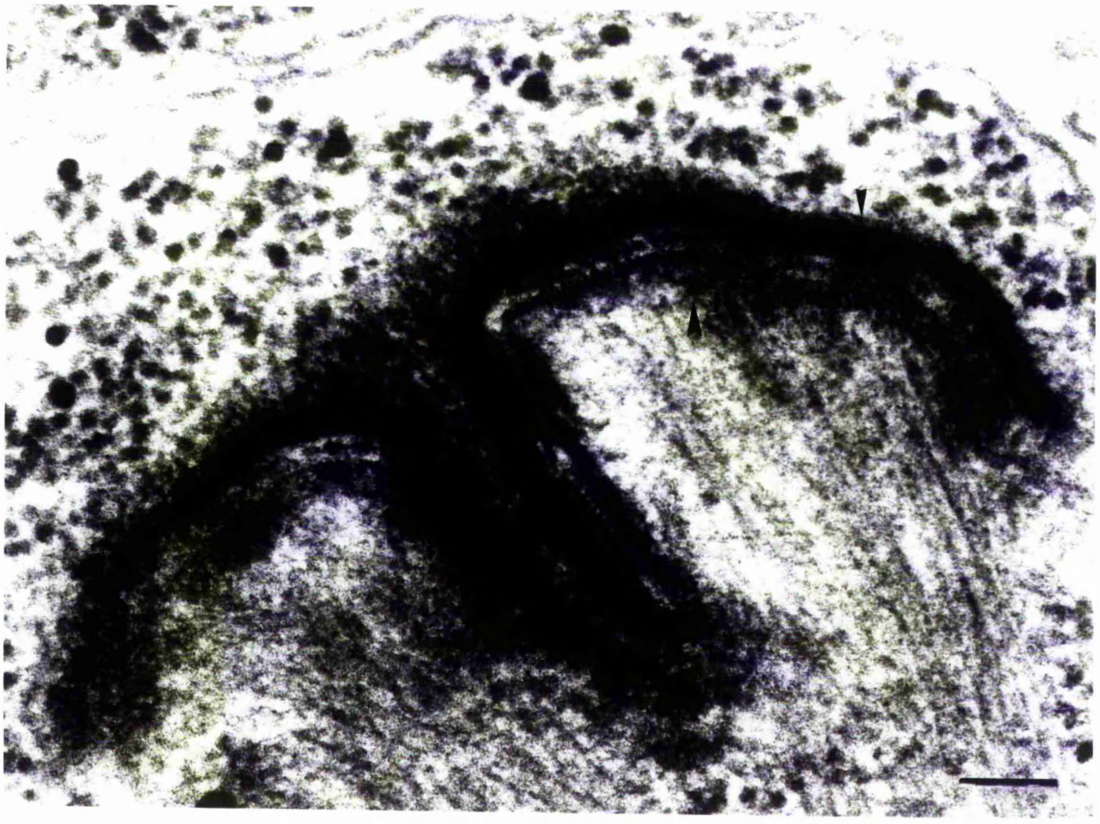

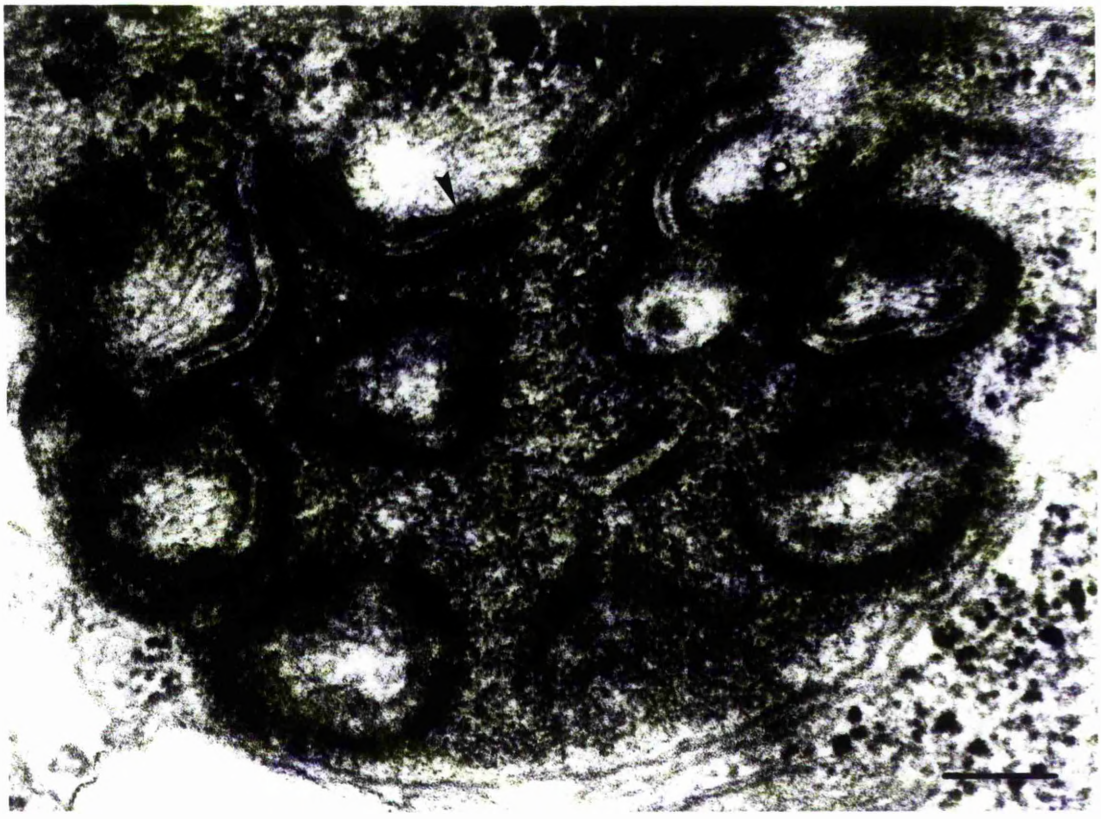

Fig.13 'Projected z-series' of AP M8 anti-pericentrin antiserum localization in fibrillar muscle and epithelial tendon cells (65 hrs a.s.p). The antiserum localizes at the interface between the end of a fibrillar muscle cell and epithelial tendon cells. Confocal laser scanning microscopy. Scale bar, 10μm.

Fig.14 Phase contrast image of the end of a fibrillar muscle cell, myotendon epithelial cell and cuticle (65 hrs a.s.p). An arrow indicates the border between the end of the muscle cell and the epithelial tendon cells. Scale bar, 10μm.

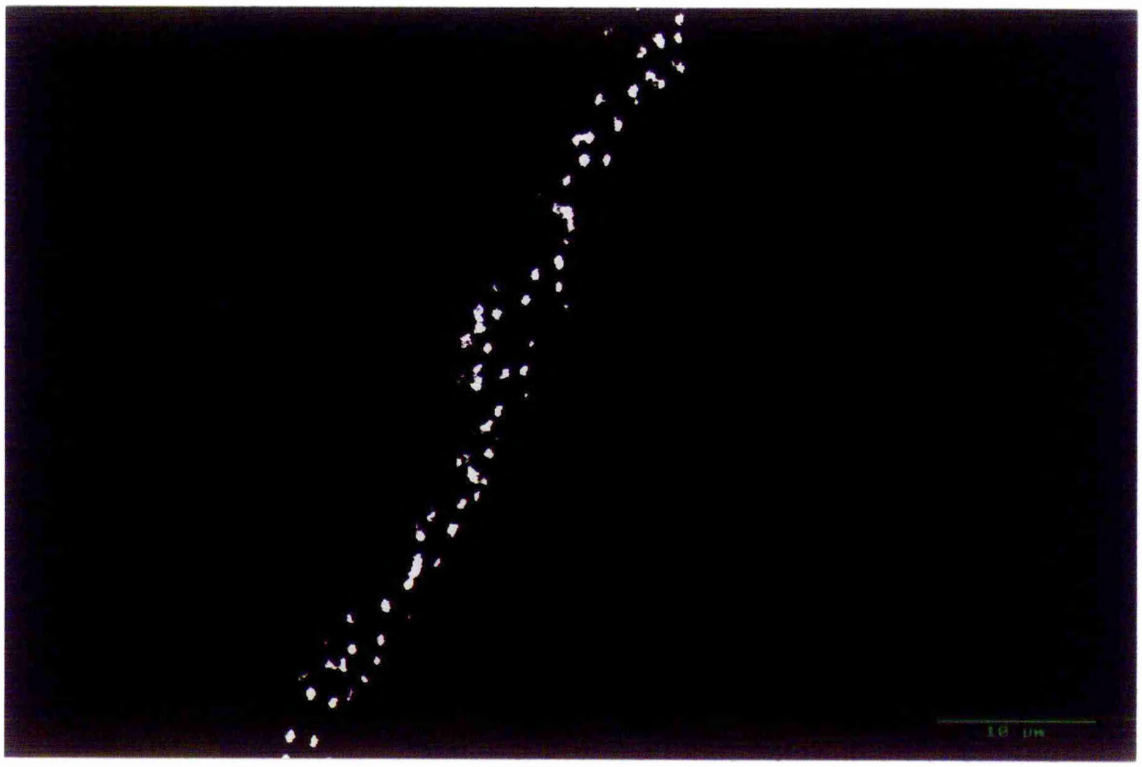
10 µm

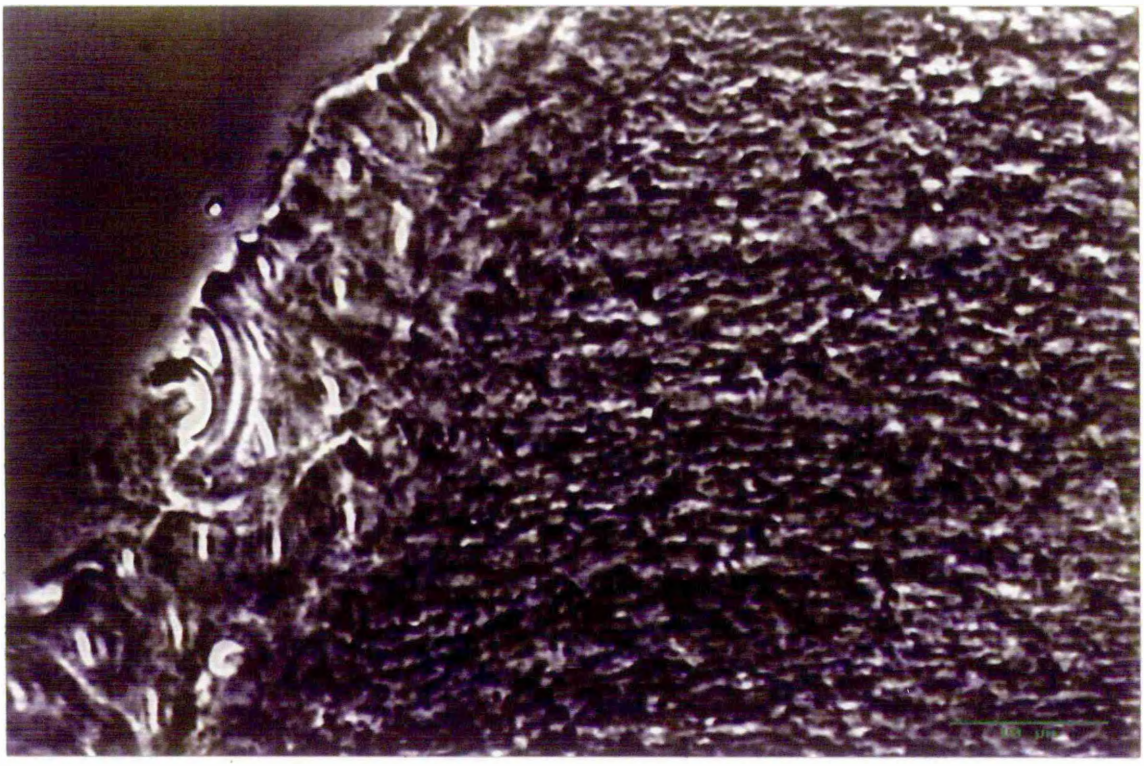

Fig.15 'Merged image'. Confocal image of AP M8 anti-pericentrin antiserum localization (yellow) superimposed with the phase contrast image of exactly the same region of the thoracic section (blue). The anti-pericentrin antiserum is localized at discrete sites at the interface between the end of the fibrillar muscle cell and the epithelial tendon cells (65 hrs a.s.p). The location of the stained sites correspond to the location of myotendon junctions. Scale bar, 10μm.

Fig.16 'Merged image'. Confocal image of AP *Drosophila* anti-γ-tubulin antiserum localization (yellow) superimposed with the phase contrast image of exactly the same region of the thoracic section (blue). The stained regions are located at the interface between the end of the fibrillar muscle cell and the epithelial tendon cells (65 hrs a.s.p). Scale bar, 10μm.

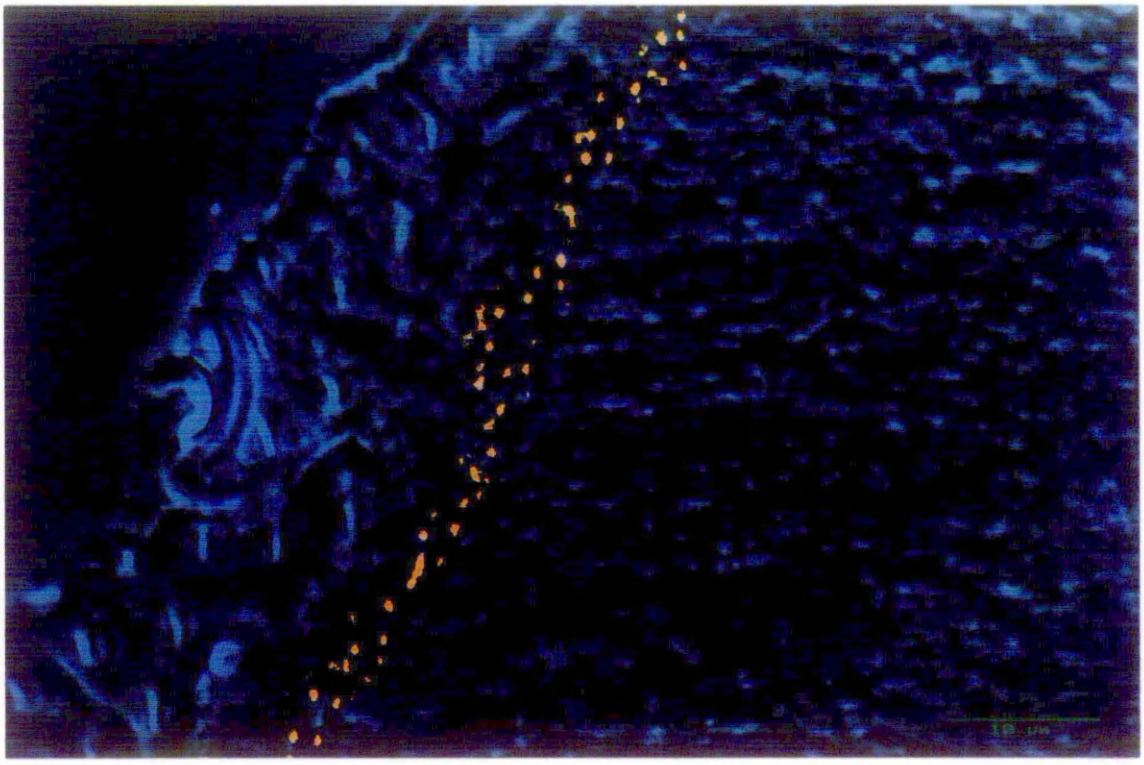

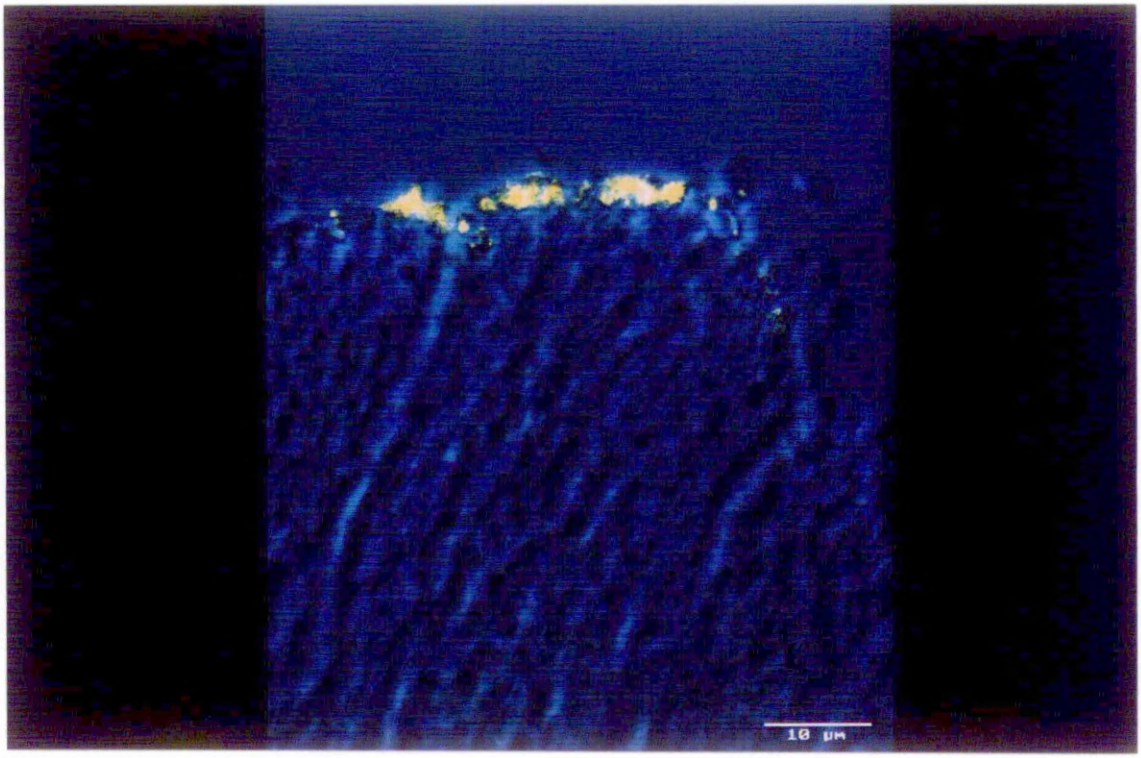
10 µm

Chapter 4

Pericentrin antisera stain *Drosophila* centrosomes

4.1 Introduction

Affinity-purified anti-pericentrin antisera (AP pericentrin antisera) stain *Drosophila* myotendon junctions throughout myofibrillogenesis and in the mature adult. Consequently, the myotendon junctions may be MTOC's. Pericentrin is a structural protein that is apparently involved in microtubule nucleation (Doxsey *et al.*,1994). It has been demonstrated that pericentrin is located in the pericentriolar material of mammalian centrosomes. It is also located around basal bodies and in the oral apparatus (predominantly constructed from microtubules) of the ciliate *Tetrahymena* (Doxsey *et al.*,1994).

It is necessary to test the validity of the localization of the AP pericentrin antisera to myotendon junctions. Therefore, this investigation deals with the question of whether these antisera localize at *Drosophila* centrosomes. Three different AP pericentrin antisera have been tested on *Drosophila* embryos at the syncitial blastoderm stage and at the stage of cellularization (see material and methods for staging procedure). The AP pericentrin antisera have also been tested on *Drosophila* wing imaginal disc derived clone 9 cells (c9 cells).

An affinity purified XGC anti-γ-tubulin antiserum (AP XGC γ-tubulin) did not stain the myotendon junctions. This has been tested on the *Drosophila* c9 cells to establish whether it stains the spindle poles.

4.2 Results

4.2.1 *Drosophila* Embryos

In some embryos at the syncitial blastoderm stage, the pericentrin antisera stain discrete spheres just below the surface of the plasma membrane. The pericentrin antisera stains spheres that are grouped in pairs. The two stained spheres in a pair are approximately 10μm apart. These presumably represent the poles of mitotic spindles (Fig.1). This is the pole to pole distance for mitotic spindles in *Drosophila* embryo at the syncitial blastoderm stage (Callaini and Riparbelli,1990).

Centrosomes in *Drosophila* embryos separate into two very shortly after the end of telophase and thus a pair of centrosomes are present just above the apical surface of each interphase nucleus (Warn and Warn,1986). During nuclear elongation and the cellularization of the blastoderm, microtubules extend downwards from each centrosome. These microtubules are perpendicular to the surface of the embryo and form a microtubule 'basket' around each nucleus (Warn and Warn,1986). None of the AP pericentrin antisera stain the centrosomal pairs which are located just above the apical surface of interphase nuclei during embryo cellularization (Fig.2).

4.2.2 *Drosophila* c9 cell line

4.2.2.1 AP pericentrin antisera localization

Anti-α-tubulin monoclonal antibody (anti-α-tubulin) stains a network of microtubules. Microtubules do not radiate from a discrete spot in interphase*Drosophila* c9 cells (Fig.3). The AP pericentrin antisera do not stain any region of these interphase

cells (Fig.4). However, all three AP pericentrin antisera stain the centrosome/spindle poles from metaphase to telophase (Fig.5,6). The AP pericentrin antisera stain the metaphase centrosome/spindle poles with either high or low intensity. The AP pericentrin antisera always stain the telophase centrosomes. The antisera stain the telophase centrosomes with greatest intensity. No AP pericentrin antisera staining of the mitotic poles of *Drosophila* c9 cells prior to metaphase has been detected.

4.2.2.2 AP XGC γ-tubulin antiserum

The spindle poles of mitotic *Drosophila* wing imaginal disc derived *Drosophila* c9 cells do not stain with the AP XGC γ-tubulin antiserum (Fig.7). There is also no indication that this antiserum stains the centrosomes during interphase.

4.2.3 Specificity of antibody staining

4.2.3.1 Rabbit pre-immune sera

It is important to eliminate the small possibility that antibodies against antigens other than pericentrin were not removed during affinity purification. Each AP pericentrin antiserum has a complimentary rabbit pre-immune serum. Thus, a rabbit pre-immune serum has been used in conjunction with each AP pericentrin antiserum. None of the rabbit pre-immune sera stain centrosomes of *Drosophila* embryos or *Drosophila* wing imaginal disc derived *Drosophila* c9 cells.

4.2.3.2 Immunoblots

The total protein content of *Drosophila* embryos has been separated by Western blotting and subsequently transferred onto nitro-cellulose paper. Some 'lanes' have been immunoblotted with non-affinity purified pericentrin antisera (NA pericentrin antisera) and some with the AP pericentrin antisera. The NA pericentrin antisera stains numerous protein bands (Fig.8). There is a band at 220Kd (the approximate molecular weight of pericentrin) but this is almost certainly not pericentrin. The AP pericentrin antisera do not stain any protein bands. The same procedure was performed and the same results obtained for *Drosophila* c9 cells.

4.2.3.3 Secondary Antibody

Both *Drosophila* embryos and *Drosophila* c9 cells have been incubated with the secondary antibodies but without the primary antibodies. These procedures do not result in any detectable staining.

4.3 Discussion

Three AP pericentrin antisera, each raised against a different region of the pericentrin protein, stain the centrosome/spindle poles in *Drosophila* embryos and c9 cells. Total protein preparations, of either *Drosophila* embryos or c9 cells, separated by SDS-gel electrophoresis, transferred by Western blotting and subsequently assayed for pericentrin with the AP pericentrin antisera do not result in a stained protein band at 220Kd (the approximate molecular weight of pericentrin). Apparently, the scarcity of pericentrin requires the isolation and concentration of centrosomes in order to detect it successfully by an immunoblot (Doxsey *et al.*,1994). An encouraging result was the

absence of any stained protein bands at other molecular weights. The complete absence of stained protein bands indicates that the AP pericentrin antisera do not appear to cross react with any other polypeptides transferred by Western blotting. This result supports the argument that centrosomal/spindle pole staining with the AP pericentrin antisera in *Drosophila* is due to specific antibody binding. Consequently, this increases the likelihood that pericentrin or a homologue is located at the myotendon junctions between fibrillar muscle cells and epithelial tendon cells.

The spatial localization of AP pericentrin antisera is the same as that in mammalian cells (i.e. it is restricted to the centrosome/spindle poles). The temporal localization of the AP pericentrin antisera in *Drosophila* appears to be quite different from that in mammalian cells. The AP pericentrin antisera stain the centrosome/spindle poles from metaphase through to telophase in *Drosophila* c9 cells. No evidence of spindle poles stained with AP pericentrin antisera prior to metaphase has been obtained. Furthermore, during interphase centrosomes do not stain with the AP pericentrin antisera in either *Drosophila* embryos or c9 cells. In contrast, in mammalian cells, pericentrin is localized at the centrosome throughout the cell cycle (Doxsey *et al.*,1994).

Why is pericentrin apparently not associated with the centrosome during interphase, or with the centrosome/spindle poles during the early stages of mitosis? It is possible that the epitopes recognized by the AP pericentrin antisera are masked during interphase and during the early stages of mitosis. However, pericentrin is not masked at the centrosome/spindle poles in mammalian cells at any stage in the cell cycle. If the pericentrin epitopes recognised by the AP pericentrin antisera are not masked during interphase and the early stages of mitosis, then the results in this study indicate that pericentrin is only present at the centrosome/spindle poles from metaphase to telophase.

In mammalian cells pericentrin is most abundant at the centrosome/spindle poles during metaphase (Doxsey *et al.*,1994). The nucleating activity of the centrosome/spindle pole is greatest at metaphase and decreases thereafter (Oakley,1994). Thus the abundance of pericentrin at the centrosome/spindle pole during metaphase in mammalian cells is consistent with its possible involvement in microtubule nucleation (Doxsey *et al.*,1994).

Therefore, it is surprising and also unclear why the AP pericentrin antisera do not intensely stain the spindle poles of metaphase spindles in *Drosophila* c9 cells more frequently. Furthermore, it is also puzzling that the AP pericentrin antisera stain the centrosome/spindle poles during telophase with greatest intensity.

In conclusion, pericentrin, or a homologue, appears to be expressed in *Drosophila* and associates with the centrosome/spindle poles in a cell cycle dependent manner. Until more is known about the precise function of pericentrin the significance of its temporal localization in the centrosomes/spindle poles of *Drosophila* will not become clear. The apparent absence of pericentrin at the spindle poles prior to metaphase does however suggest that the predominant role of pericentrin in *Drosophila* is not to initiate the construction of the mitotic spindle as has been suggested may be its role in mammalian cells (Doxsey *et al.*,1994).

The affinity purified XGC anti-γ-tubulin antiserum does not stain the centrosome/spindle poles of *Drosophila* c9 cells. However, γ-tubulin is expressed in *Drosophila* (Zheng *et al.*,1991a,b; Sunkel *et al.*,1995). Therefore, it appears that this antiserum may not recognize γ-tubulin in *Drosophila*.. This might also account for the complete lack of staining at the myotendon junctions with this antiserum.

Fig.1 Confocal image of AP M1 pericentrin antiserum localization in a whole-mount *Drosophila* syncitial blastoderm embryo. The antiserum stains discrete sites which are grouped into pairs. These sites presumably represent the mitotic spindle poles. Confocal laser scanning microscopy. Scale bar, 10μm.

Fig.2 'Dual image' of AP M1 pericentrin antiserum localization (left hand side - LHS) and anti-α-tubulin localization (right hand side - RHS) in a whole-mount *Drosophila* embryo during cellularization of the blastoderm. Microtubules radiate from a discrete region above the apical surface of each nucleus which corresponds to the location of a pair of centrosomes. The AP M1 pericentrin antiserum does not stain a region above the apical surface of each nucleus. Confocal laser scanning microscopy. Scale bar, 20μm.

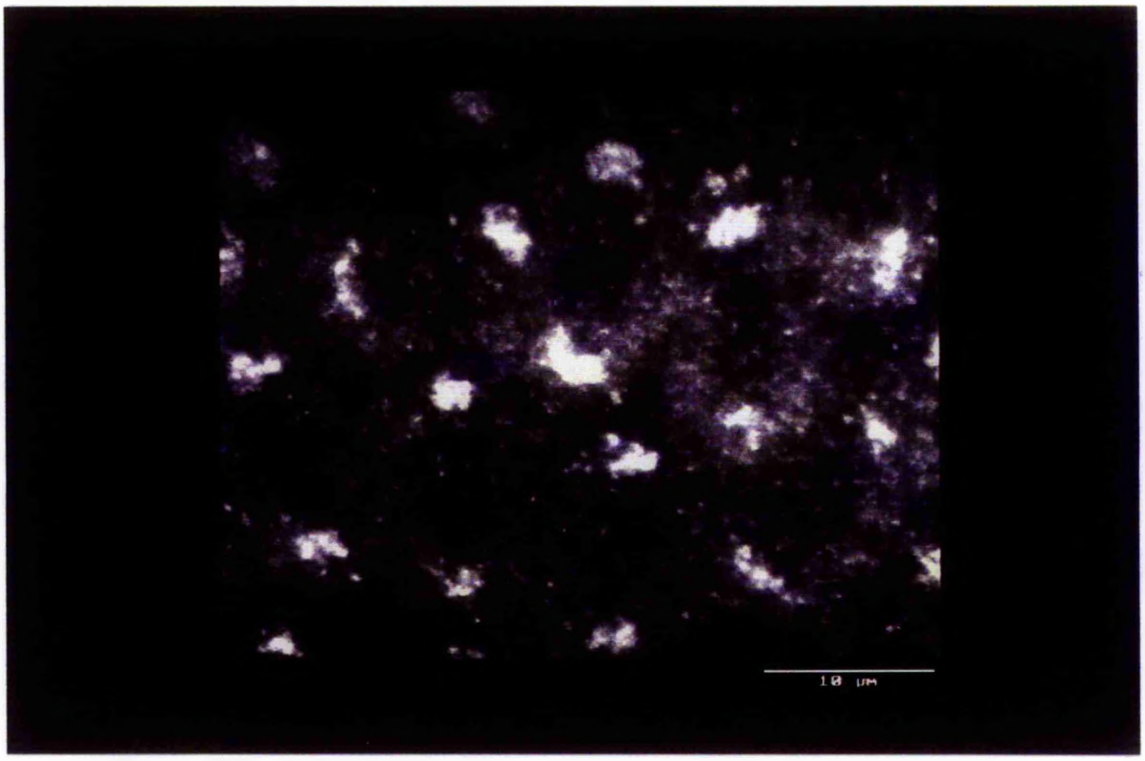
10 µm

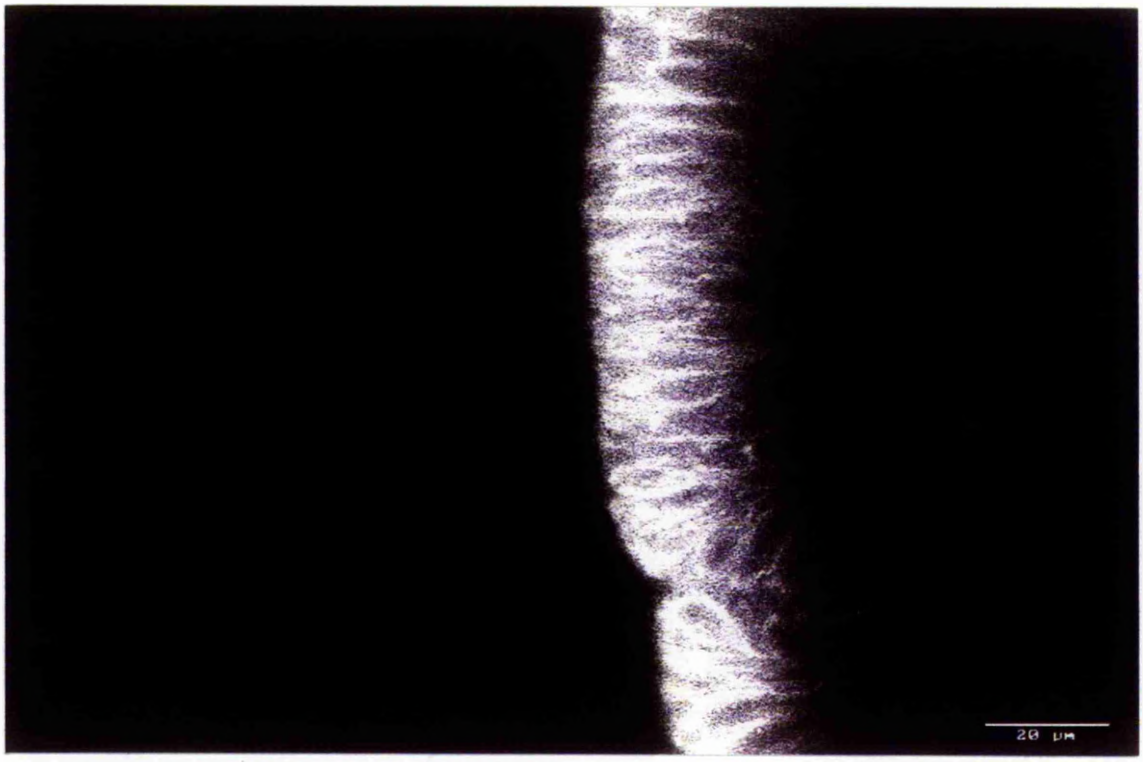
20 µm

Fig.3 Confocal image of anti-α-tubulin localization in interphase *Drosophila* c9 cells. Microtubules do not radiate from a discrete site in interphase cells. Microtubules are organized into a non-focused array. Confocal laser scanning microscopy. Scale bar, 10μm.

Fig.4 'Dual image' of AP M1 pericentrin antiserum localization (LHS) and anti-α-tubulin localization (RHS) in interphase *Drosophila* c9 cells. The AP M1 pericentrin antiserum does not stain any region of the interphase cells. Confocal laser scanning microscopy. Scale bar, 10μm.

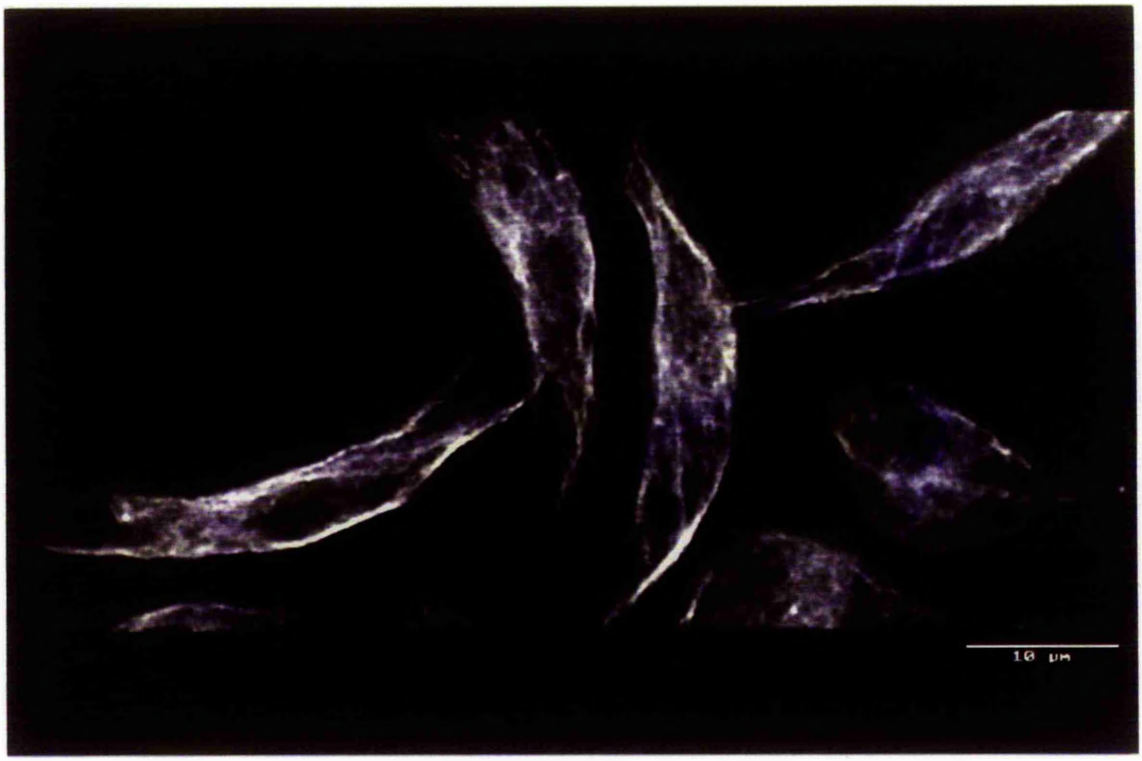
10 µm

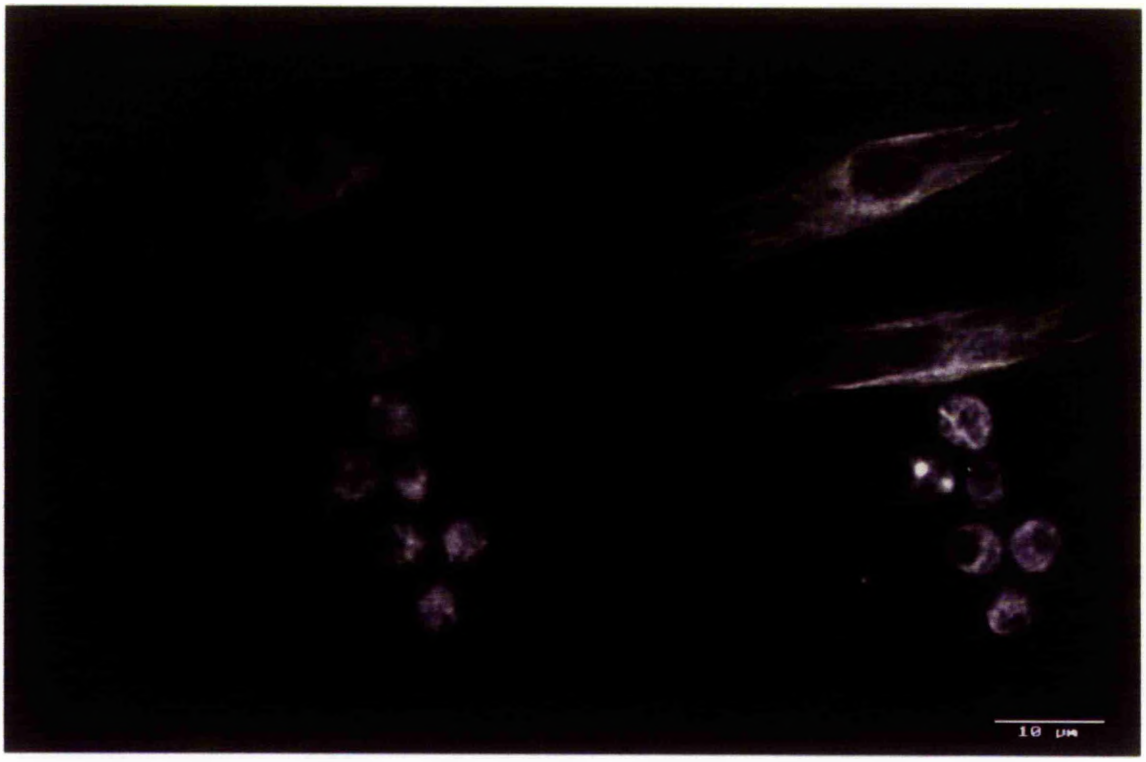
10 µm

Fig.5 'Dual image' of AP M8 pericentrin antiserum localization (LHS) and anti-α-tubulin localization (RHS) in a metaphase *Drosophila* c9 cell. The AP M8 pericentrin antiserum stains the metaphase spindle poles. Confocal laser scanning microscopy. Scale bar, 2μm.

Fig.6 'Dual image' of AP M8 pericentrin antiserum localization (LHS) and anti-α-tubulin localization (RHS) in a telophase *Drosophila* c9 cell. The AP M8 pericentrin antiserum stains the telophase centrosome in each incipient daughter cell. Confocal laser scanning microscopy. Scale bar, 5μm.


2 µm

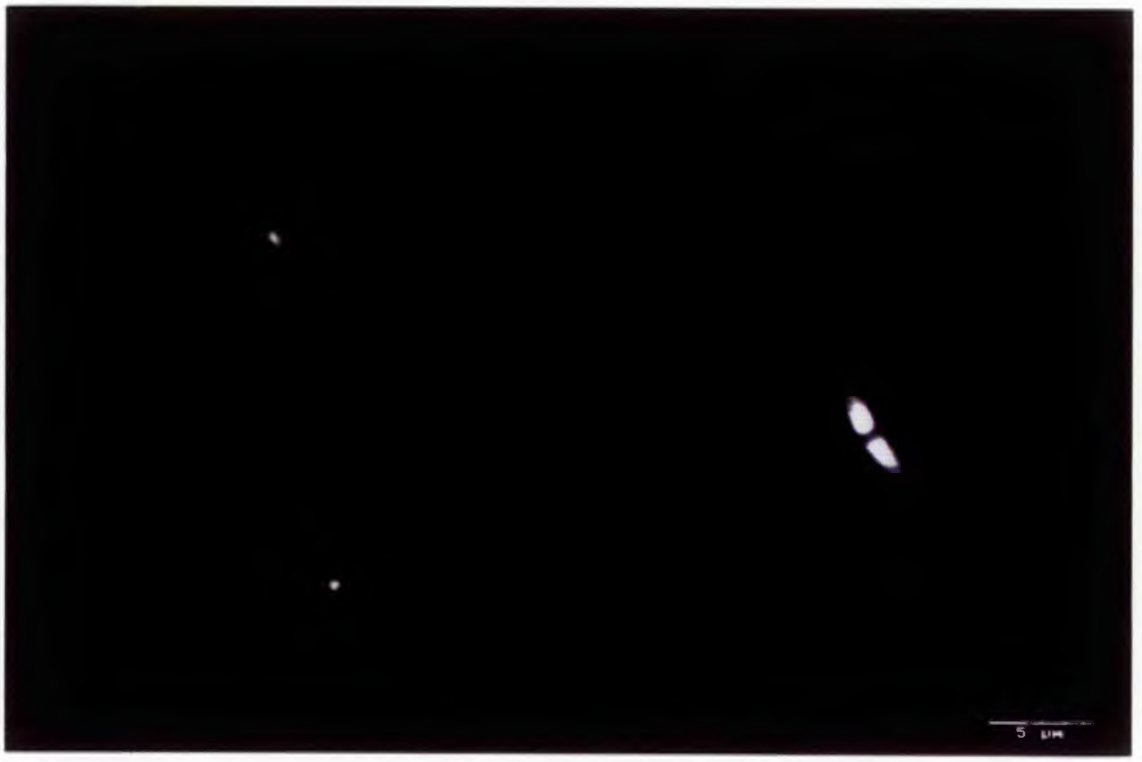
5 µm

Fig.7 'Dual image' of AP XGC γ-tubulin antiserum localization (LHS) and anti-α-tubulin localization (RHS) in a mitotic *Drosophila* c9 cell. The AP XGC γ-tubulin antiserum does not stain the mitotic spindle poles. Confocal laser scanning microscopy. Scale bar, 5μm.

Fig.8 Immunoblots of total protein content of *Drosophila* embryos assayed for pericentrin with non-affinity purified pericentrin antisera. **(a)** NA M1 pericentrin antiserum **(b)** NA M8 pericentrin antiserum **(c)** NA 4b5MA-1 pericentrin antiserum. Each antiserum stains numerous protein bands.

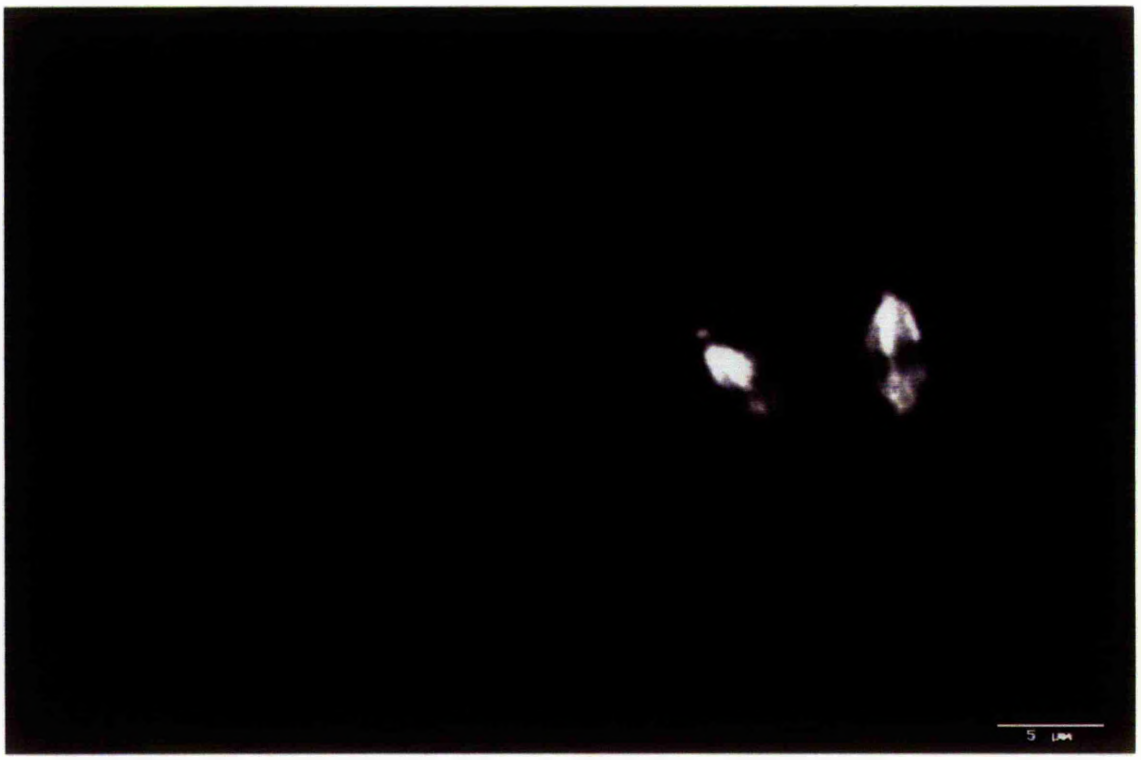
5 μm

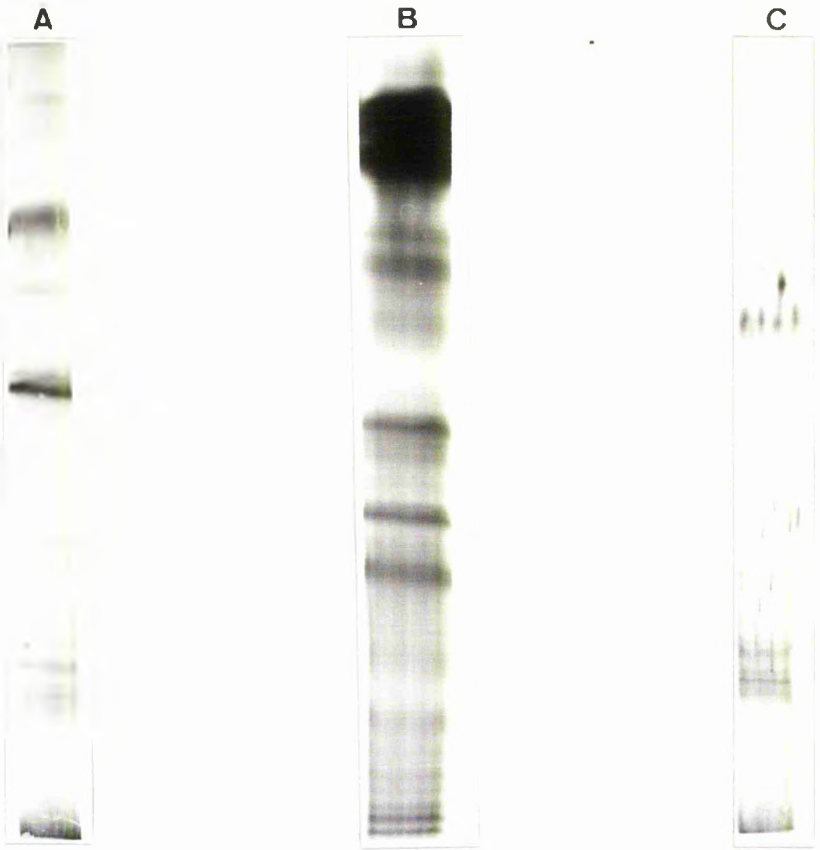
A
B
C

Chapter 5

Midbody-associated microtubule bundles and daughter cell separation in MDCK cells

5.1 Introduction

The intercellular bridge is a membrane-bound cytoplasmic strand which connects two incipient daughter cells. It contains the midbody, a dense matrix of amorphous material, and two midbody-associated microtubule bundles. The intercellular bridge begins to form during telophase and may persist into the following interphase (McIntosh and Landis,1971).

During the terminal stages of daughter cell separation in HeLa cells (derived from malignant tissue) and D-98S cells (derived from human sternal bone marrow) their intercellular bridges lengthen and decrease in diameter (Byers and Abramson,1968; Mullins and Biesele, 1973, 1977). This is apparently promoted by incipient daughter cell movements (Mullins and Biesele,1973). In HeLa cells the intercellular bridge apparently breaks at the region where it makes contact with one of the incipient daughter cells (Byers and Abramson,1968). In D-98S cells a portion of the intercellular bridge located between the midbody and the cell body reduces further in diameter. This has been called 'narrowing' (Mullins and Biesele,1977). Movements of the incipient daughter cells are apparently responsible for the further stretching of the 'narrowed' portion of the intercellular bridge which consequently breaks in D-98S cells (Mullins and Biesele,1977).

The motility of HeLa and D-98S cells is apparently responsible for the substantial lengthening and narrowing of the intercellular bridge (Mullins and Biesele,1977). Lengthening and narrowing of the intercellular bridge is apparently important for the

completion of daughter cell separation. In contrast, epithelial cells are subject to stringent spatial constraints since they are tightly packed into epithelial sheets (see Albert *et al*, 1989). Therefore, can daughter cell separation in epithelial cells occur in the same manner as in HeLa and D-98S cells? MDCK cells have been investigated since they are a highly differentiated epithelial cell line which form cellular junctions and upon reaching confluence establish cellular polarity (Bacallao *et al.*,1989; Buendia *et al.*,1990b; Peppercok *et al.*,1990). Therefore, the mechanism of daughter cell separation in MDCK cells may closely represent that which occurs in the epithelia of mammals.

The two midbody-associated microtubule bundles may be involved in the terminal stages of daughter cell separation. It has been suggested that the rate of microtubule loss from the two microtubule bundles controls the rate at which the intercellular bridge narrows. The two microtubule bundles become more compact from telophase onwards and the number of microtubules in each microtubule bundle decreases as the intercellular bridge becomes narrower in D-98S cells (McIntosh and Landis,1971; Mullins and Biesele,1977). Microtubule organization in the two midbody associated microtubule bundles has been investigated during the terminal stages of daughter cell separation in MDCK cells. This study has distinguished several stages during cytokinesis based on changes in the organisation of the two midbody-associated microtubule bundles. This has enabled the predominant method of daughter cell separation in MDCK cells to be characterized. The results also appear to indicate that midbody-associated microtubule bundles may be severed.

5.2 Results

Approximately 80% of mitotic MDCK cells appear to accomplish daughter cell separation in a different manner from that previously reported for HeLa and D98-S cells. This predominant form of daughter cell separation in MDCK cells has been investigated.

Stage 1

Several stem-bodies, clumps of dense material which align across the former spindle equator by late anaphase, are associated with the ends of microtubules (McIntosh and Landis,1971). Anti-α-tubulin monoclonal antibody stains the stem-body-associated microtubules which span from the nuclear region of one incipient daughter cell to that of the other (Fig.1). During the onset of cytokinesis, furrowing results in the aggregation of the stem-bodies (Fig.2,3) to form the midbody (McIntosh and Landis,1971).

Stage 2

Furrowing appears to arrest when the cleavage constriction has a diameter of approximately 1μm and is occupied by the midbody (Fig.4). This stage is the most abundant in an asynchronous population of MDCK cells. Hence, the length of time spent at this stage is greater than for any other cytokinetic stage.

A relatively long intercellular bridge is a feature of most telophase cells (Buck and Tisdale,1962; Byers and Abramson,1968; Fawcett,1961; Fiil,1978; Mullins and Biesele,1977) and apparently plays a fundamental role in daughter cell separation (Byers and Abramson,1968; Mullins and Biesele,1973,1977). In contrast, it is evident that an extremely short intercellular bridge (approximately 0.5μm) is formed in the vast majority of MDCK cells (Fig.4,5). This intercellular bridge is confined to the midbody. Consequently it only contains the ends of the midbody-associated microtubule bundles (Fig. 4). Anti-α-tubulin does not stain the midbody. It has been suggested previously that the dense matrix of the midbody masks the tubulin antigen (Weber *et al.*,1975; Cande *et al.*,1977; DeBrabander *et al.*,1979).

The incipient daughter cells form cell junctions between each other prior to the completion of their separation (Fig.6). A monoclonal antibody raised against

desmoplakin, a desmosomal protein, stains discrete sites at regions of contact between incipient daughter cell bodies (Fig.7).

In some cases the furrow base of the cleavage constriction appears to have spread a short distance around one side of the midbody (Fig.8). This is correlated with a localized reduction in the diameter of the microtubule bundle in this region.

Stage 3

The diameter of the midbody-associated microtubule bundles has decreased relative to diameters at earlier stages. Furthermore, the entire midbody stains with anti-α-tubulin (Fig.9).

Stage 4

One of the two microtubule bundles loses contact with the midbody (Fig.10). One microtubule bundle remains associated with the midbody even after the other bundle has apparently disassembled (Fig.11). Subsequently, the second microtubule bundle loses contact with the midbody (Fig.12).

Stage 5

Anti-α-tubulin still stains the midbody. However, the midbody is no longer associated with a microtubule bundle (Fig.13). Both microtubule bundles have apparently been completely disassembled. The midbody appears to be in the process of being expelled, or has been expelled, from both daughter cells (Fig.13). There is a marked change in the ultrastructure of the midbody at this stage, compared with earlier stages

(Fig.14). Its fabric is degraded compared with earlier stages and therefore it has been called a remnant midbody (Mullins and Biesele,1977). A membrane envelopes the remnant midbody which is largely composed of short microtubules (that span its entire length) and intermicrotubular material.

A previous ultrastructural investigation has led to the conclusion that the remnant midbody exists in various states of deterioration. Some of the remnant midbodies apparently do not contain any microtubules (Mullins and Biesele, 1977). These findings were based on a small sample of remnant midbodies (approximately 20). Remnant midbodies in MDCK cells were regularly identified by phase contrast microscopy and immunofluorescence (over 100). Anti-α-tubulin consistently stains the remnant midbody even after it has become isolated from both daughter cells (Fig.13). Furthermore, anti-acetylated tubulin monoclonal antibody also consistently stains the remnant midbody (Fig.15).

Specificity of antibody staining

MDCK cells do not stain when incubated with the fluorescently conjugated secondary antibody but without either anti-α-tubulin or anti-acetylated tubulin. Immunoblots of MDCK whole cell lysate assayed for acetylated tubulin with anti-acetylated tubulin monoclonal antibody exhibit a single protein band with a molecular weight (approximately 53Kd) which is the same as that reported for acetylated tubulin (Fig.16)

5.3 Discussion

5.3.1 What is the function of midbody-associated microtubule bundles?

The intercellular bridge which forms in MDCK cells is extremely short. It contains the midbody and only the ends of the two microtubule bundles which are associated with the midbody. Therefore, it is unlikely that the primary role of the midbody associated microtubule bundles is to provide cytoskeletal support for the intercellular bridge as suggested previously (Mullins and Biesele,1977). Furrowing appears to arrest for a period of time when the cleavage constriction has a diameter of approximately 1μm in MDCK cells. Why this should occur is not apparent. Therefore, a hypothesis is proposed which may account for the function of the midbody-associated microtubule bundles and the delay in the completion of daughter cell separation.

The midbody-associated microtubule bundles could operate as the backbone of an intercellular 'highway' between each incipient daughter cell. Incipient daughter cells could communicate rapidly with each other by utilising the microtubule bundles to shuttle 'messages' back and forth between each other i.e. a reciprocal feedback mechanism. This could be achieved by specific microtubule motor proteins carrying specific 'messages' along microtubules. A rapid form of communication between daughter cells may be required to co-ordinate the rate of daughter cell development after the completion of karyokinesis. A 'pacemaker' communication system would insure that both daughter cells are ready for completion of cell separation at the same time. This would insure that when both daughter cells become independent from one another they are both fully capable of integrating into their environment immediately.

5.3.2 Daughter cell separation in MDCK cells

Intercellular bridges which have been reported previously are several micrometers long (Fawcett,1961; Buck and Tisdale,1962; McQuilkin and Earle,1962; Byers and Abramson,1968; Fiil,1978; Mullins and Bieselle,1977). For example, the intercellular bridge is 3μm to 21μm long in D-98S cells (Mullins and Bieselle,1977) and intercellular bridges as long as 125μm occur in L-929 fibroblast cells (McQuilkin and Earle,1962). These intercellular bridges contain a midbody and two midbody-associated microtubule bundles. Furthermore, the intercellular bridges of HeLa and D-98S cells lengthen substantially during the terminal stages of daughter cell separation (Byers and Abramson,1968; Mullins and Bieselle, 1973,1977). In contrast, MDCK cells form an extremely short intercellular bridge (approximately 0.5μm long) which contains the midbody and only the ends of the two microtubule bundles associated with the midbody. Furthermore, it does not elongate during the terminal stages of daughter cell separation.

The midbody-associated microtubule bundles decrease in diameter from telophase to a stage just prior to the termination of daughter cell separation in MDCK cells. This most likely represents a reduction in the number of microtubules in addition to the microtubule bundle becoming more compact. The number of microtubules in midbody-associated microtubule bundles decrease gradually from early telophase to a stage just prior to the termination of daughter cell separation in HeLa and WI-38 human lung derived fibroblastic cells (McIntosh and Landis,1971).

It is apparent that one microtubule bundle completely loses contact with the midbody just prior to the completion of daughter cell separation in MDCK cells. Furthermore, prior to this event the furrow base of the cleavage constriction appears to spread a short distance around one side of the midbody. This may be responsible for a localized reduction in the diameter of the microtubule bundle in this region. It can be postulated that it is this microtubule bundle which is the first to lose contact with the midbody. This would permit the furrow base to completely constrict around one side of the midbody and consequently complete daughter cell separation (Fig.17).

One microtubule bundle remains associated with the midbody even after the other bundle has completely disassembled. This persistent microtubule bundle also appears to eventually lose contact with the midbody. Once this bundle has completely disassembled it is likely that the furrow base completes its constriction around the entire remnant midbody. This procedure would effectively expel the membrane bound remnant midbody from the daughter cell.

Many similarities exist between daughter cell separation in MDCK cells and those reported previously. Indeed the underlying mechanism may be the same. However, this investigation may have helped to pinpoint those events which are, and those which are not, fundamental to daughter cell separation:

(1) It appears that it is not essential for the intercellular bridge to elongate in order to complete daughter cell separation.

(2) It is unlikely that a series of 'cytoplasmic waves' occurs in the intercellular bridges of MDCK cells. The intercellular bridges are too short to accommodate them. These 'waves' have been reported in HeLa and D-98S cells (Byers and Abramson,1968; Mullins and Bieselle, 1973,1977). The 'waves' may retract the cytoplasm from the intercellular bridge into the cell bodies of incipient daughter cells.

(3) Progressively closer apposition of the plasma membrane in the intercellular bridge is essential in order that cytokinesis can be completed. The furrow base probably completely constricts around one side of the midbody in order that daughter cell separation can be completed in MDCK cells. However, midbody-associated microtubule bundles most likely initially act as an obstruction and prevent this from occuring. This obstruction appears to be overcome when one microtubule bundle completely loses contact with the midbody in MDCK cells. The gradual loss of midbody-associated microtubules may be sufficient to permit the plasma membrane in the intercellular bridge region to complete constriction in cell types which stretch their long intercellular bridges.

(4) Locomotary movements of the incipient daughter cells may not be required in order to break the intercellular bridge in MDCK cells. The motility of MDCK cells is restricted since they are connected by cell junctions.

(5) The remnant midbody appears to be expelled from incipient daughter cells in both MDCK cells and other cells which have been investigated.

A fundamental feature of daughter cell separation appears to be the necessity to bring the plasma membrane of the intercellular bridge into closer apposition. Furthermore, it appears that the microtubule bundles prevent the completion of cytokinesis by obstructing the constriction of the furrow base. Therefore, the incipient daughter cells must overcome this obstruction to complete cytokinesis. In MDCK cells it appears that this achieved when one microtubule bundle suddenly loses contact with the midbody. In other cell types investigated the intercellular bridge lengthens and narrows as the number of microtubules within the bridge gradually decreases. Therefore, are the midbody-associated microtubules in MDCK cells and those in cell types which form a long intercellular bridge lost in the same manner? It is highly unlikely that different methods of microtubule loss from the midbody have evolved. However, it is possible that a quantitative difference in microtubule loss from the midbody could occur between different cell types. Consequently, is the manner in which microtubules are lost from the midbody more pronounced in MDCK cells than occurs at the midbody of cells generally? How microtubule bundles may lose contact with the midbody in MDCK cells is discussed in the following section.

5.3.3 Are microtubules severed at the sides of the midbody?

It is proposed that the two midbody-associated microtubule bundles are severed. Each bundle may be severed at its point of entry into the side of the midbody. The plus ends of microtubules are embedded in the midbody (Euteneuer and McIntosh,1980). If microtubule bundles lose contact with the midbody by plus end depolymerization then it would be anticipated that the remnant midbody would not contain any microtubules. However, immunofluorescence has unequivocally established that the remnant midbody does contain microtubules. Furthermore, anti-acetylated-tubulin stains the remnant

midbody. This indicates that microtubules within the remnant midbody are relatively old. Consequently, they are most likely remnants of the midbody-associated microtubules. In addition, it is very unlikely that microtubule polymerization has occurred within the remnant midbody. Thus, it is most likely that at least one and possibly even both midbody-associated microtubule bundles are severed.

The number of microtubules in each midbody-associated microtubule bundle decreases gradually from early telophase to a stage during the termination of daughter cell separation in HeLa and WI-38 human lung derived fibroblastic cells (McIntosh and Landis,1971). However, during this period the ratio of the number of midbody-associated microtubules within the midbody to the number on either side of the midbody increases. McIntosh and Landis described this as an 'unexplained phenomenon'. However, this increase in ratio could be explained by microtubule severing. The two microtubule bundles could be gradually severed at their point of entry to the midbody. This would result in newly exposed microtubule plus ends composed of tubulin-GDP. Therefore, these newly exposed microtubule plus ends will be subject to catastrophe and subsequently would rapidly depolymerize. It is most likely that the severed portion of the microtubules within the midbody would depolymerize at a much slower rate. These severed microtubule portions are probably stabilized by the intermicrotubular material of the midbody. Thus microtubule severing could increase the ratio of microtubules within the midbody compared with the number on either side even though the total number of microtubules is decreasing.

In MDCK cells it is possible that microtubule severing of midbody-associated microtubule bundles is more pronounced than that which may occur at the midbody of other cell types. A sudden increase in the rate of microtubule severing may be required in one incipient MDCK daughter cell. This would enable one microtubule bundle to be rapidly and completely severed and consequently depolymerize quickly. Thus daughter cell separation could be completed. This is because the furrow base would no longer be obstructed from completely constricting around one side of the midbody in MDCK cells. A pronounced increase in the rate of microtubule severing may be an adaptation to

spatially restricted cells which do not have the room to stretch and break their intercellular bridge. Subsequently, an increase in the rate of microtubule-severing may occur in the other daughter cell. in order that the second microtubule bundle is completely severed at the side of the midbody. This would enable the furrow base to complete its constriction around the entire midbody. This would isolate the remnant midbody from both daughter cells. A model for daughter cell separation in MDCK cells based on microtubule severing is proposed in Fig. 18.

Midbody-associated microtubule bundles are hyper-stable. They are resistant to cold (Brinkley,1975; Margolis *et al.*,1990), high pressure (Salmon *et al.*,1976) and colchicine (Oppenheim *et al.*,1973). It seems likely that this stability is due to the microtubule plus end association with the midbody. Intermicrotubular material of the midbody probably caps and stabilizes the microtubules. Therefore, the most effective way to depolymerize hyper-stable microtubules associated with the midbody may be to sever them. The newly exposed dynamically unstable microtubule plus ends would rapidly depolymerize.

It would be of interest to determine whether the recently discovered microtubule severing protein katanin (McNally and Vale,1993) concentrates at the midbody. Centrin, a calcium binding protein, also appears to be involved in microtubule severing. It is involved in the flagella excision of *Chlamydomonas* (Sanders and Salisbury,1994). It would be extremely interesting to establish whether centrin concentrates at the midbody during the terminal stages of daughter cell separation in MDCK cells. Especially since centrin is present at centrosomes throughout the cell cycle (Moudjou *et al.*,1991). If centrin concentrates at the midbody during the terminal stages of daughter cell separation it may be involved in the severing of midbody-associated microtubules. Centrin concentration at the midbody during the terminal stages of daughter cell separation would potentially have an important implication. It would imply that centrin may also be involved in microtubule severing at the centrosome.

Fig.1 'Projected Z-series' of anti-α-tubulin localization in an early telophase MDCK cell. Stem-body associated microtubules span from the nuclear region of one incipient daughter cell to that of the other. Confocal laser scanning microscopy. Scale bar, 5μm.

Fig.2 'Dual image' of a telophase MDCK cell during early cytokinesis. Phase contrast image (LHS) and confocal image of anti-alpha tubulin localization (RHS) of the same telophase MDCK cell. The stem-body associated microtubules have become more compact as the stem-bodies aggregate together. Scale bar, 5μm.

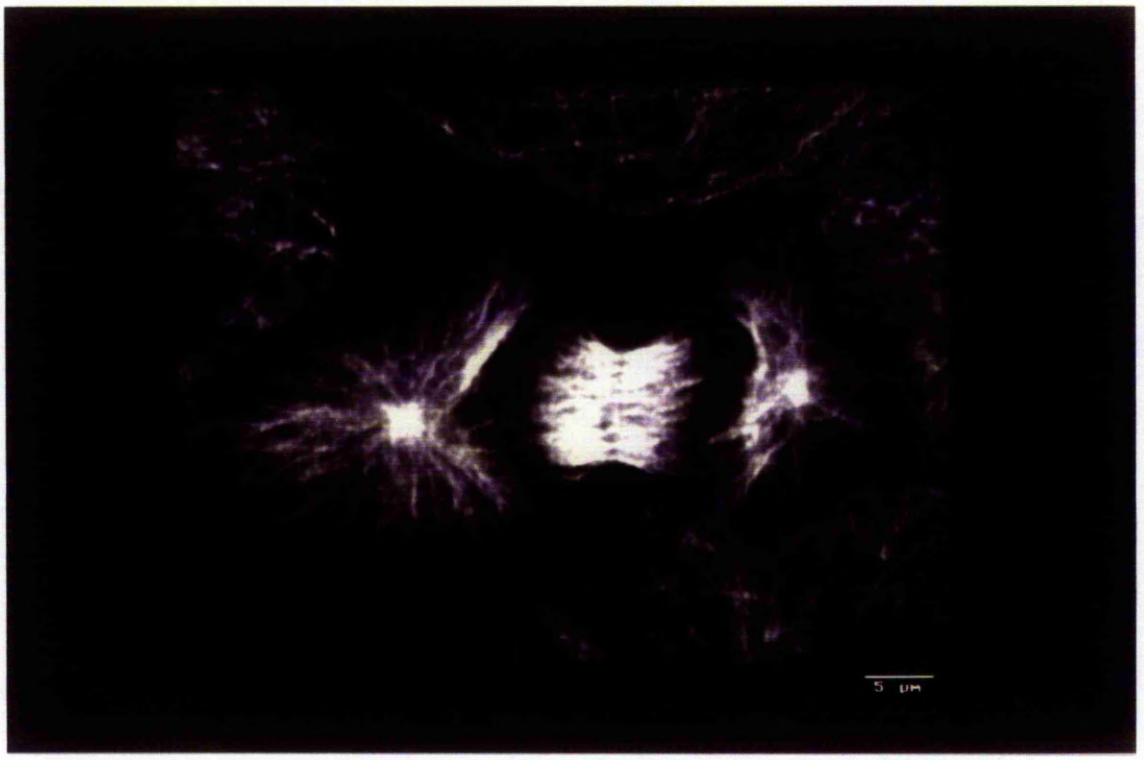
5 µm

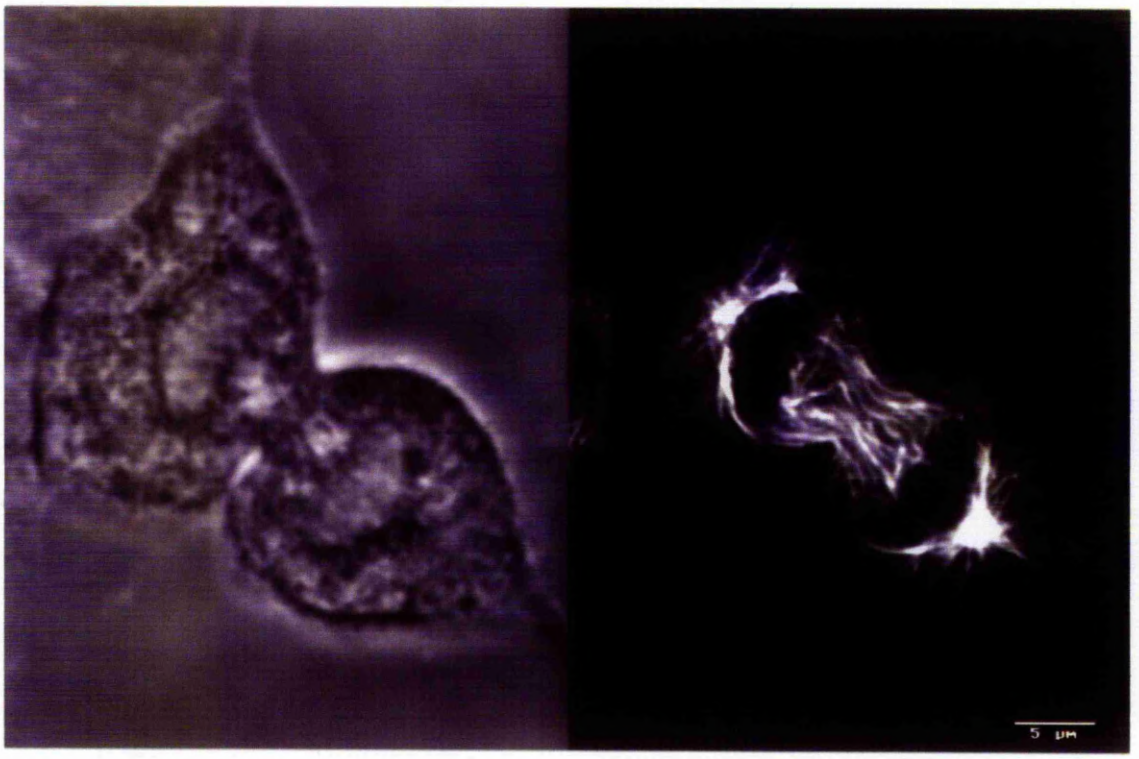
5 µm

Fig.3 Telophase MDCK cell during cytokinesis. Stem-bodies (clumps of dense material aligned across the former spindle equator) are aggregating together to form the midbody. Scale bar, 0.5μm

Fig.4 Cleavage constriction between a pair of incipient MDCK daughter cells which has a diameter of 1μm and is occupied by a midbody. Two microtubule bundles are associated with the midbody. Each microtubule bundle enters one side of the midbody. Consequently, the midbody is a region of microtubule interdigitation. The MDCK cell intercellular bridge is confined to the midbody and therefore is extremely short (approx. 0.5μm). Scale bar, 0.2μm

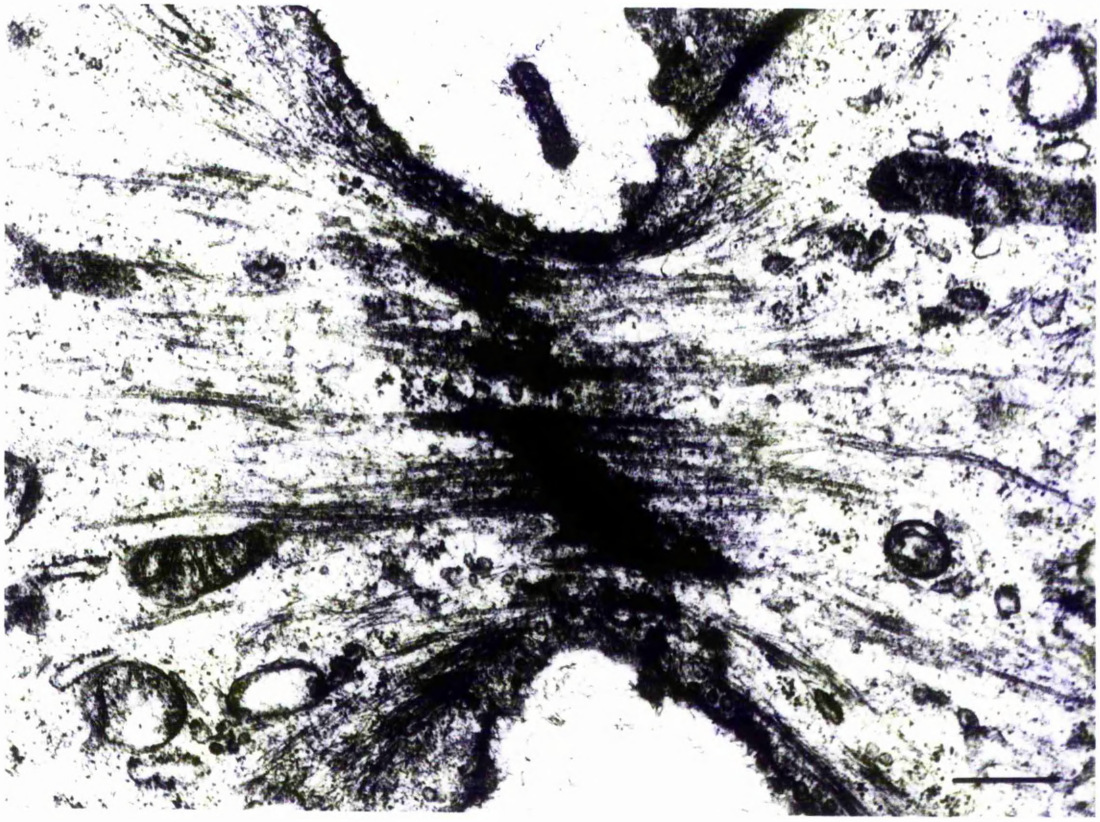

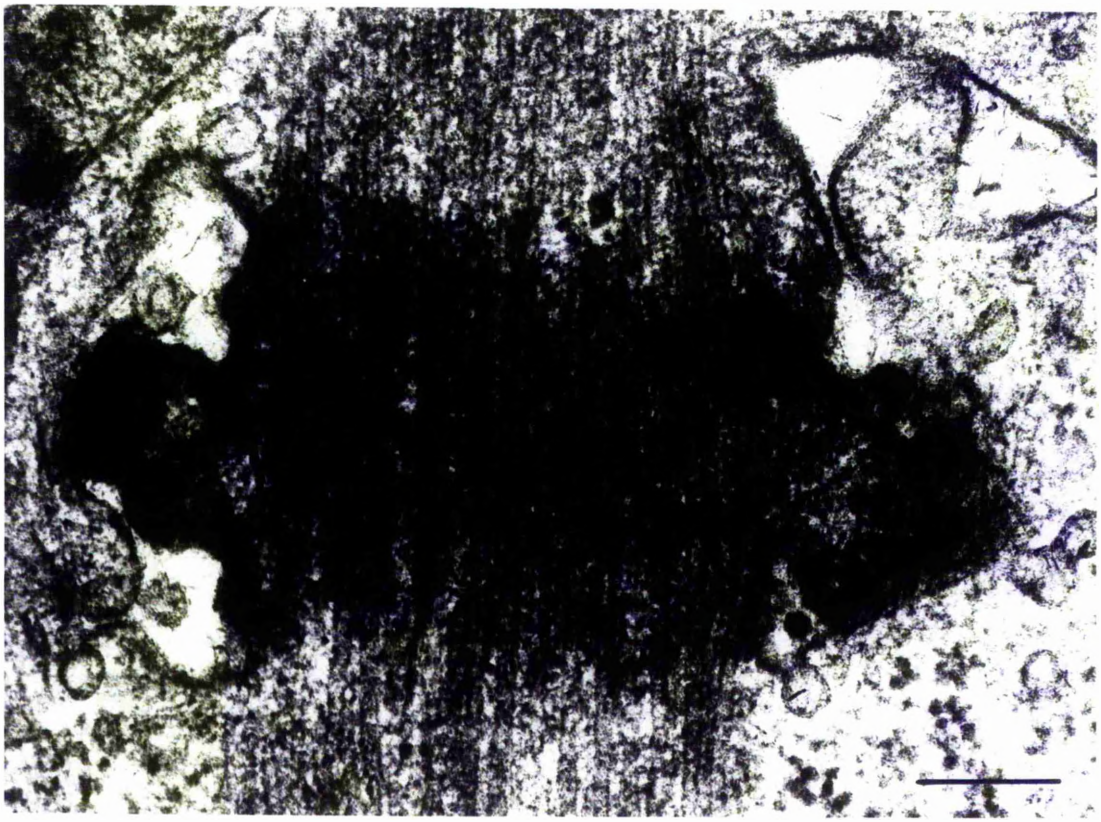

Fig.5 (a) 'Dual image' of a pair of incipient MDCK daughter cells. Phase contrast image (LHS) and confocal image of anti-α-tubulin localization (RHS) of the same telophase MDCK cell. Scale bar, 10μm

Fig.5 (b) 'Merged image' of Fig.5a. The intercellular bridge is confined to the length of the midbody (approximately 0.5μm). Consequently, only the ends of the microtubule bundles (red), which are within the midbody, are contained within the intercellular bridge. Scale bar, 10μm.

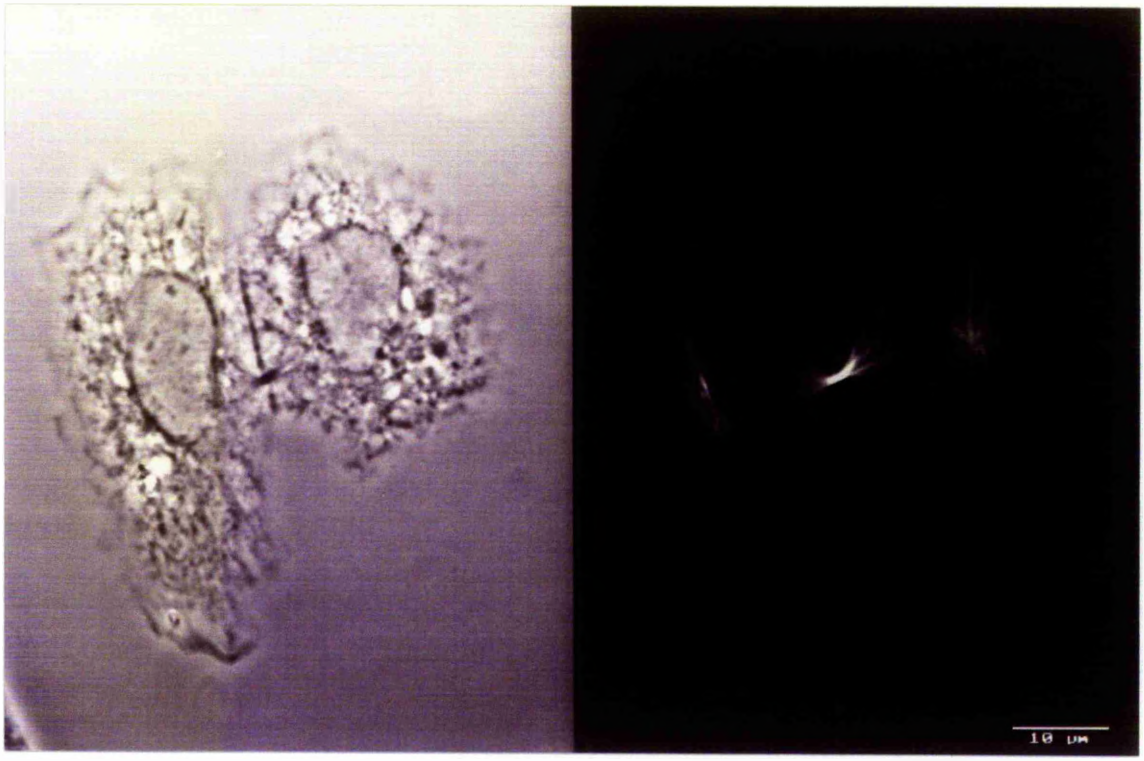
10 µm

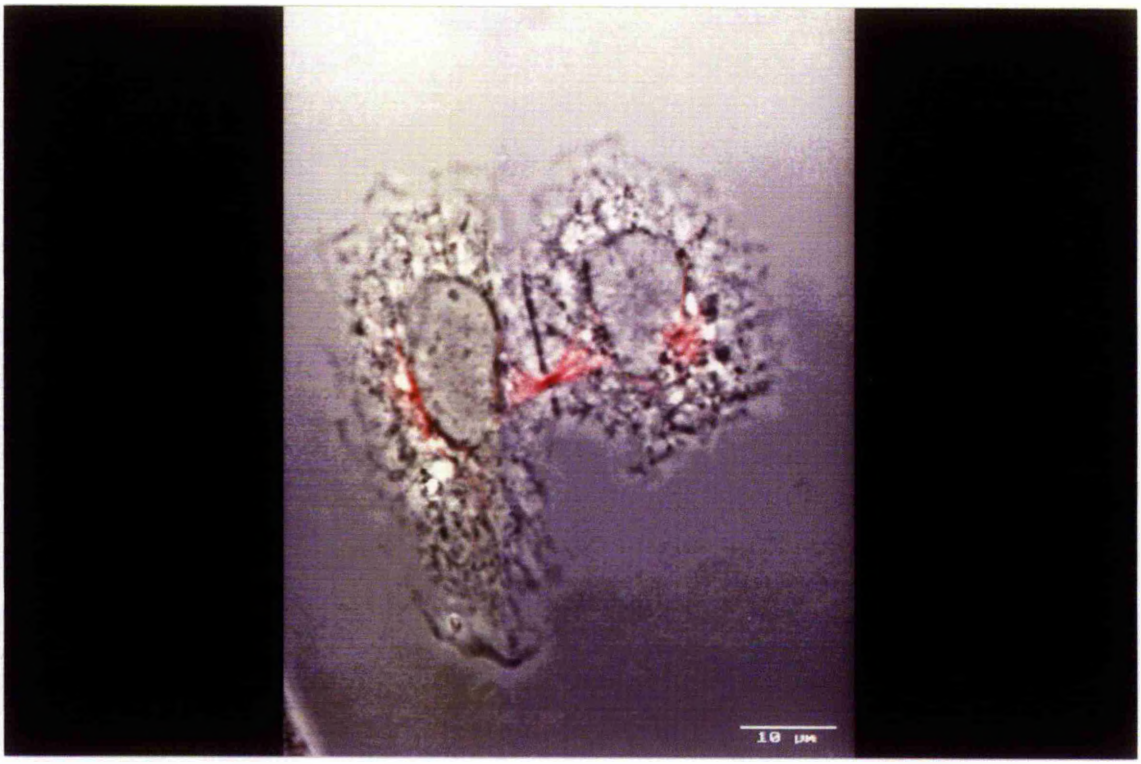
10 µm

Fig.6 Pair of incipient MDCK daughter cells. Cell junctions (arrow) are present between the pair of incipient daughter cells even though they have not completed their separation. Scale bar, 0.5μm.

Fig. 7 'Merged image' of a pair of incipient MDCK daughter cells. Confocal image of anti-desmoplakin monoclonal antibody localization superimposed upon the phase contrast image of the same pair of incipient daughter cells. The antibody is localized at the interface between the two incipient daughter cells. Scale bar, 5μm.

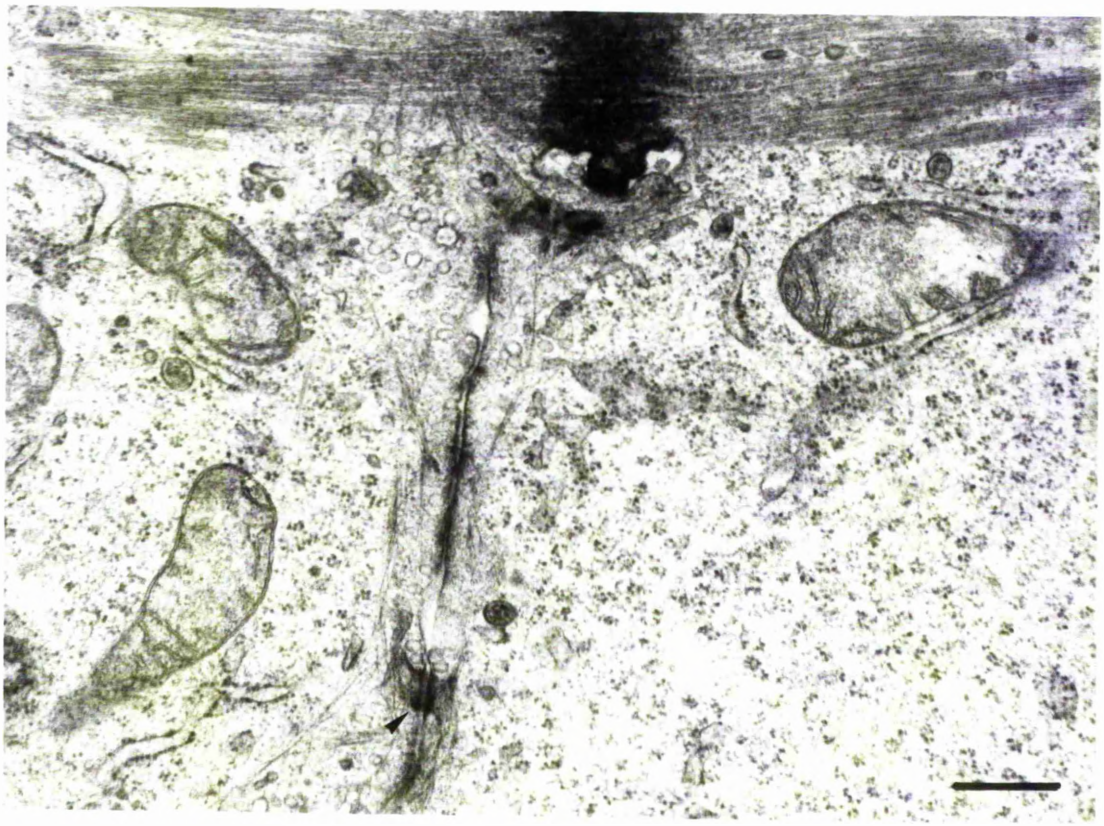

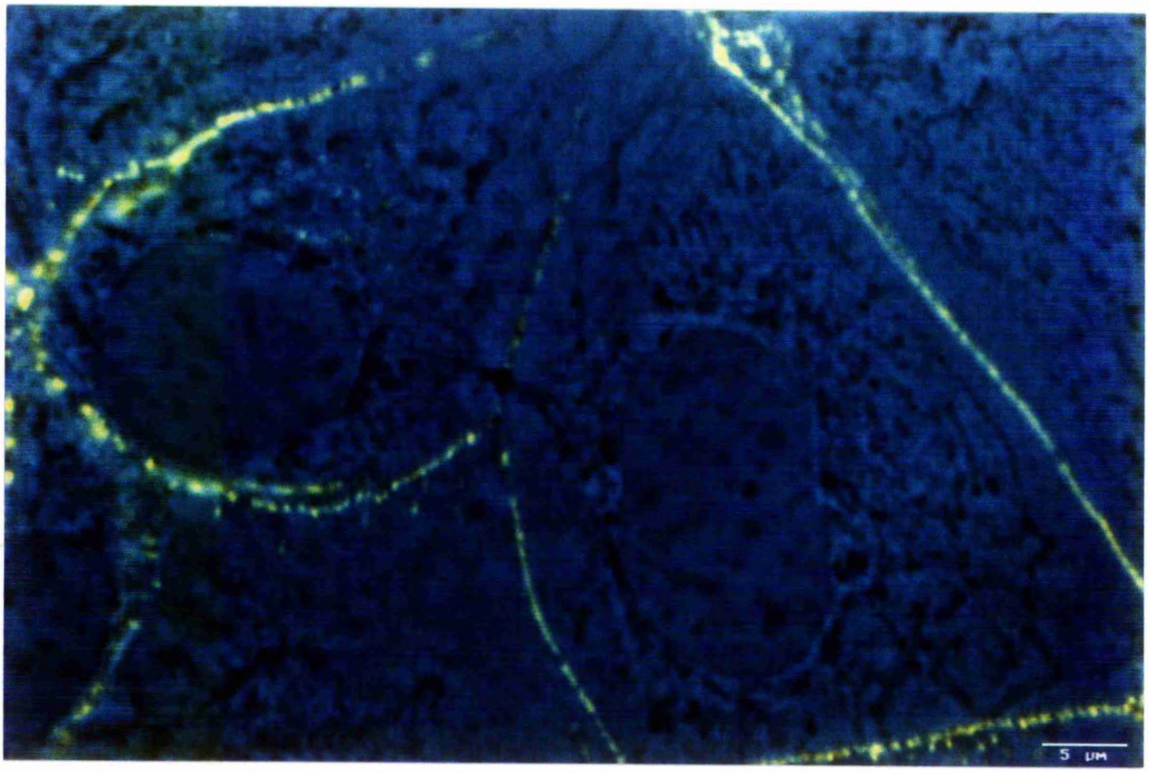
5 µm

Fig.8 (a) Pair of incipient MDCK daughter cells. The furrow base of the cleavage constriction has spread a short distance around one side of the midbody (arrow). Scale bar, 0.2μm.

Fig.8 (b) Pair of incipient MDCK daughter cells. The furrow base of the cleavage constriction appears to have spread further around one side of the midbody (arrow) than that in Fig.8a. The microtubule bundle appears to be more compact where it passes through the cleavage constriction which has spread around one side of the midbody. Scale bar, 0.2μm

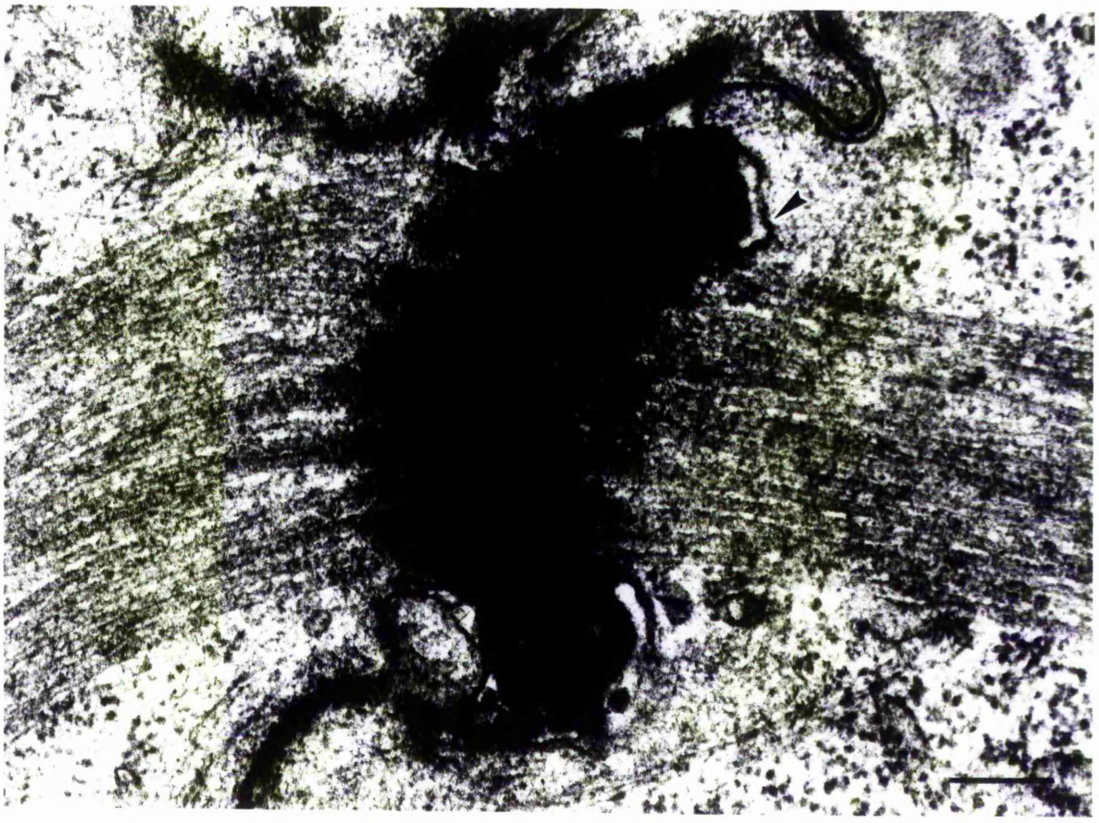

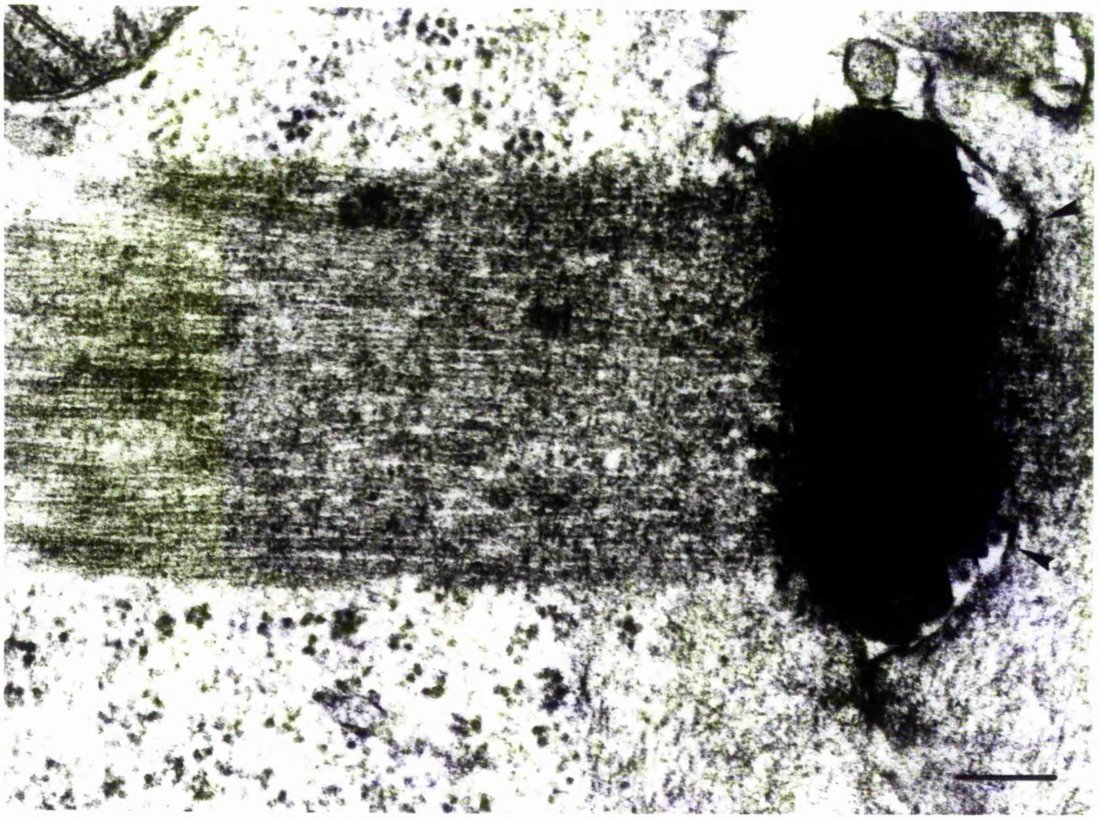

Fig.9 'Projected Z-series' of an anti-α-tubulin stained region which contains an MDCK cell midbody and its associated microtubule bundles. The entire midbody stains with anti-α-tubulin. Furthermore, the two midbody-associated microtubule bundles have decreased in diameter compared with previous stages. Confocal laser scanning microscopy. Scale bar, 5μm.

Fig.10 (a) 'Projected Z-series' of an anti-α-tubulin stained region which contains an MDCK cell midbody. One of the two microtubule bundles has lost contact with the midbody. Scale bar, 5μm.


5 µm

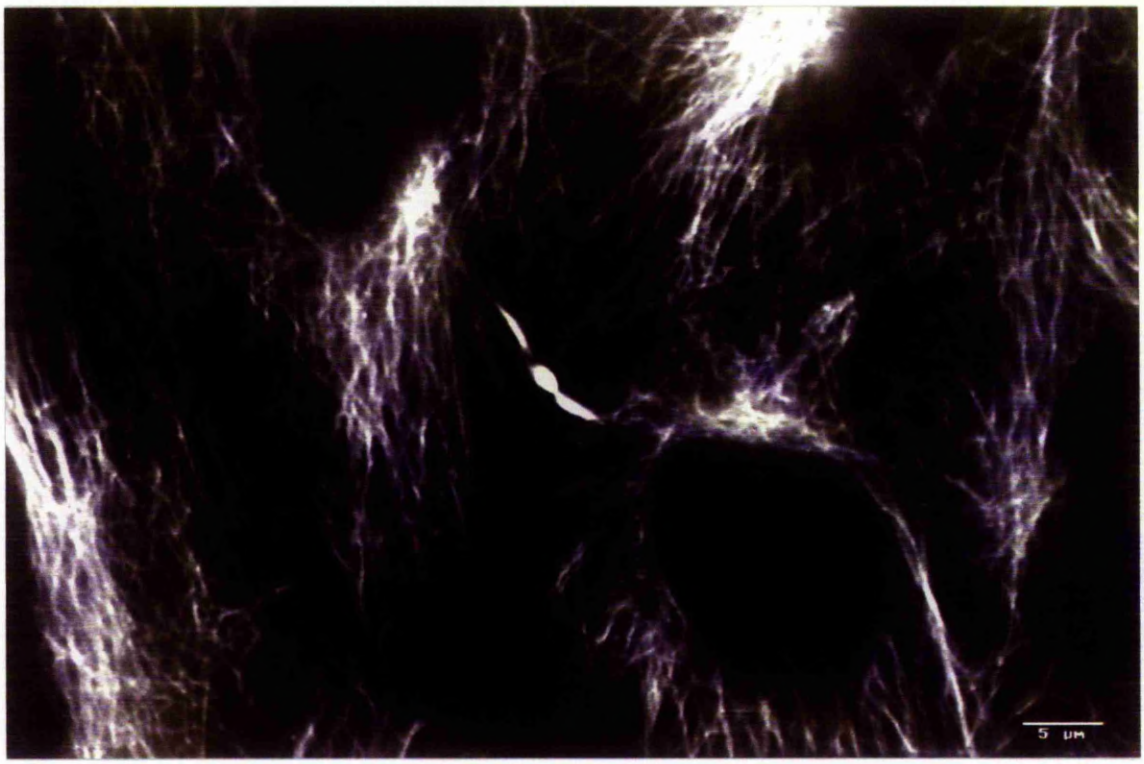
5 µm

Fig.10 **(b)** 'Projected Z-series' of an anti-α-tubulin stained region which contains an MDCK cell midbody. The microtubule bundle which has lost contact with the midbody has a much smaller diameter than the equivalent bundle in Fig.10a. Consequently, the detached microtubule bundle in this figure may have been separated from the midbody longer than the equivalent bundle in Fig.10a. Confocal laser scanning microscopy. Scale bar, 5μm.

Fig.11 'Dual image' of an MDCK cell midbody. Phase contrast image (LHS) and confocal image of anti-α-tubulin localization (RHS) of the same midbody. Only one microtubule bundle is associated with the midbody and the opposing bundle has been completely disassembled. Scale bar, 5μm.

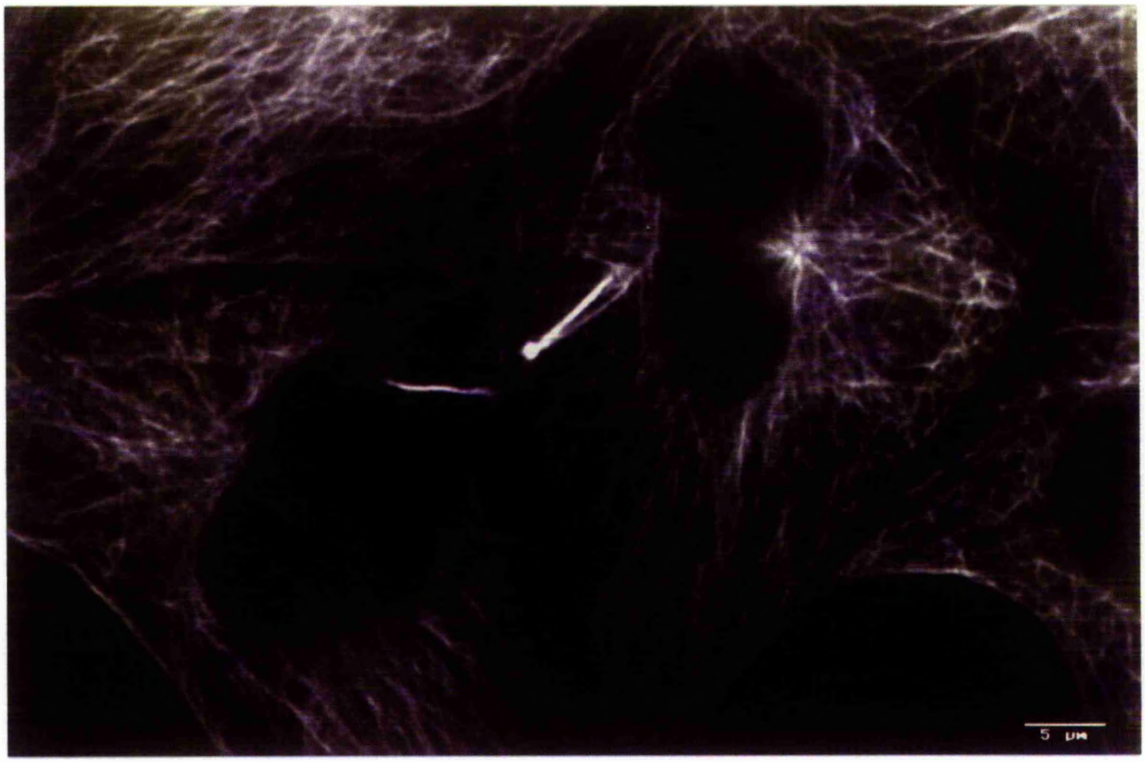
5 µm

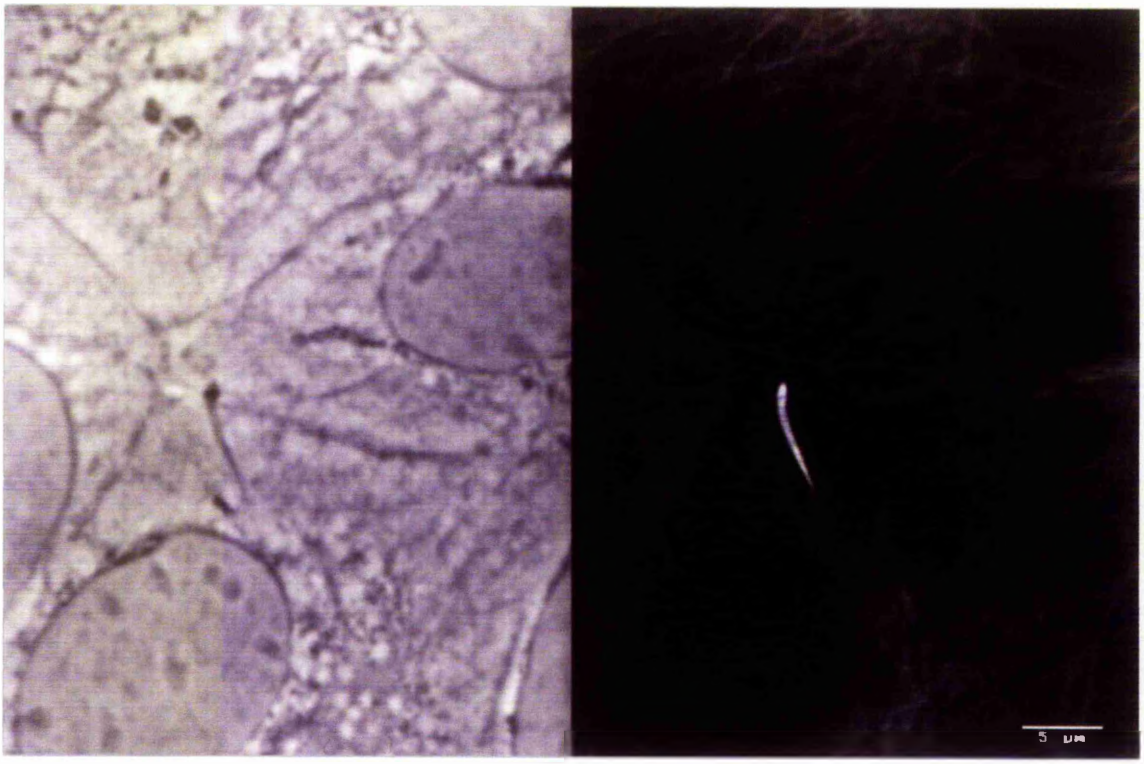
5 µm

Fig.12 'Projected Z-series' of an anti-α-tubulin stained region which contains an MDCK cell midbody. The second microtubule bundle has lost contact with the midbody. Confocal laser scanning microscopy. Scale bar, 5μm.

Fig.13 'Dual image' of an MDCK cell midbody. Phase contrast image (LHS) and confocal image of anti-α-tubulin localization (RHS) of the same midbody. The midbody is not associated with a microtubule bundle. However, it still stains with anti-α-tubulin. Furthermore, both microtubule bundles appear to have been completely disassembled. Scale bar, 5μm.

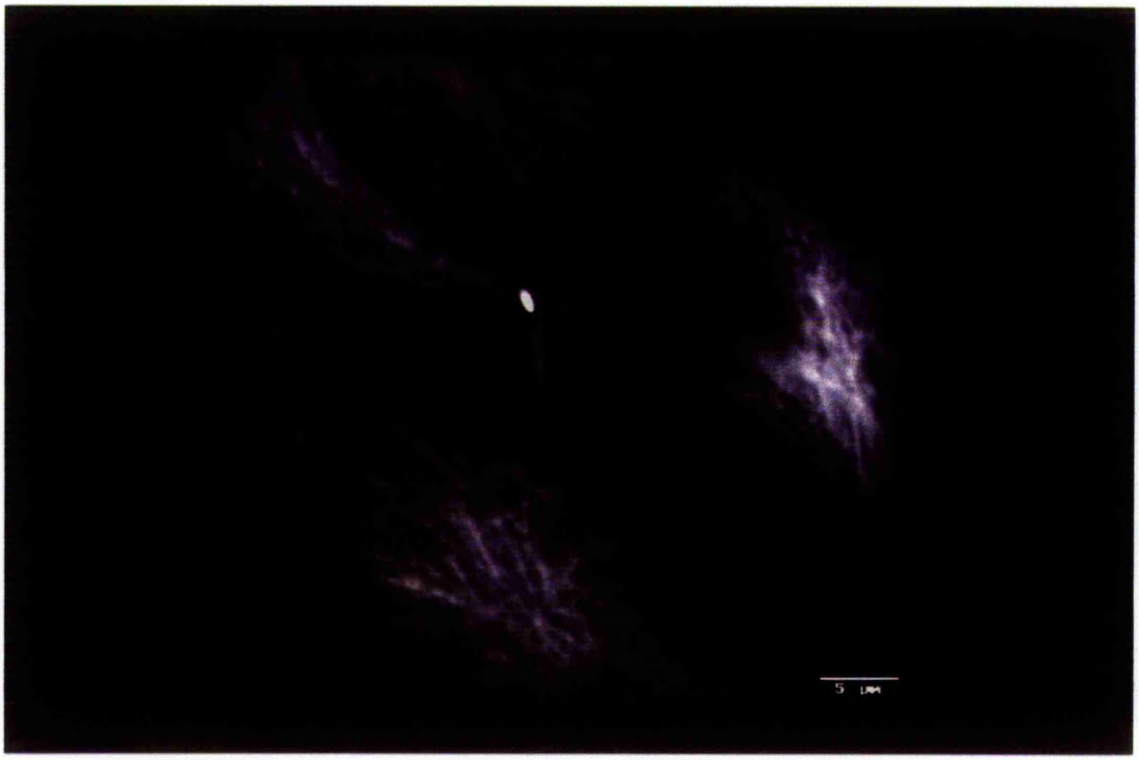
5 µm

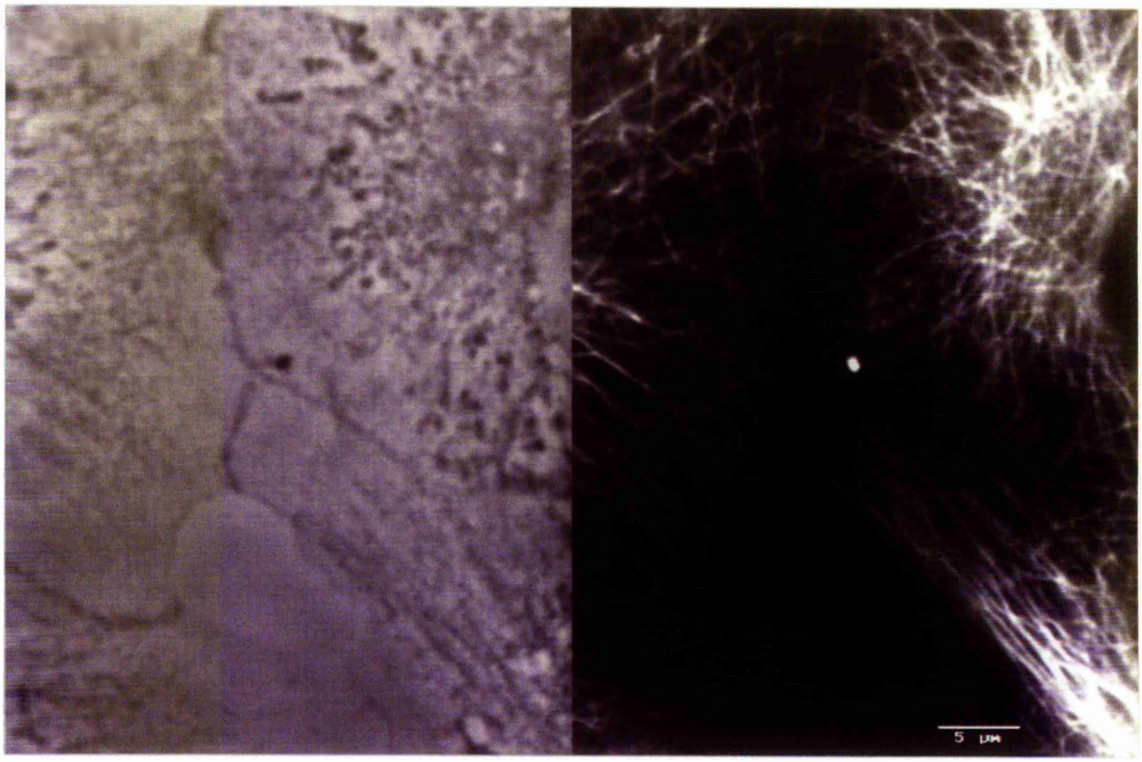
5 µm

Fig.14 Remnant midbody located between two MDCK daughter cells. The midbody appears to be almost completely enveloped by a plasma membrane. Its fabric is degraded and consequently is considerably less dense than at earlier stages. Short microtubules span the entire length of the remnant midbody. Scale bar, 0.2μm.

Fig.15 'Dual image' of an MDCK cell remnant midbody. Phase contrast image (LHS) and confocal image of anti-acetylated-tubulin monoclonal antibody localization (RHS) of the same midbody. The remnant midbody stains with an anti-acetylated monoclonal antibody. Scale bar, 5μm.

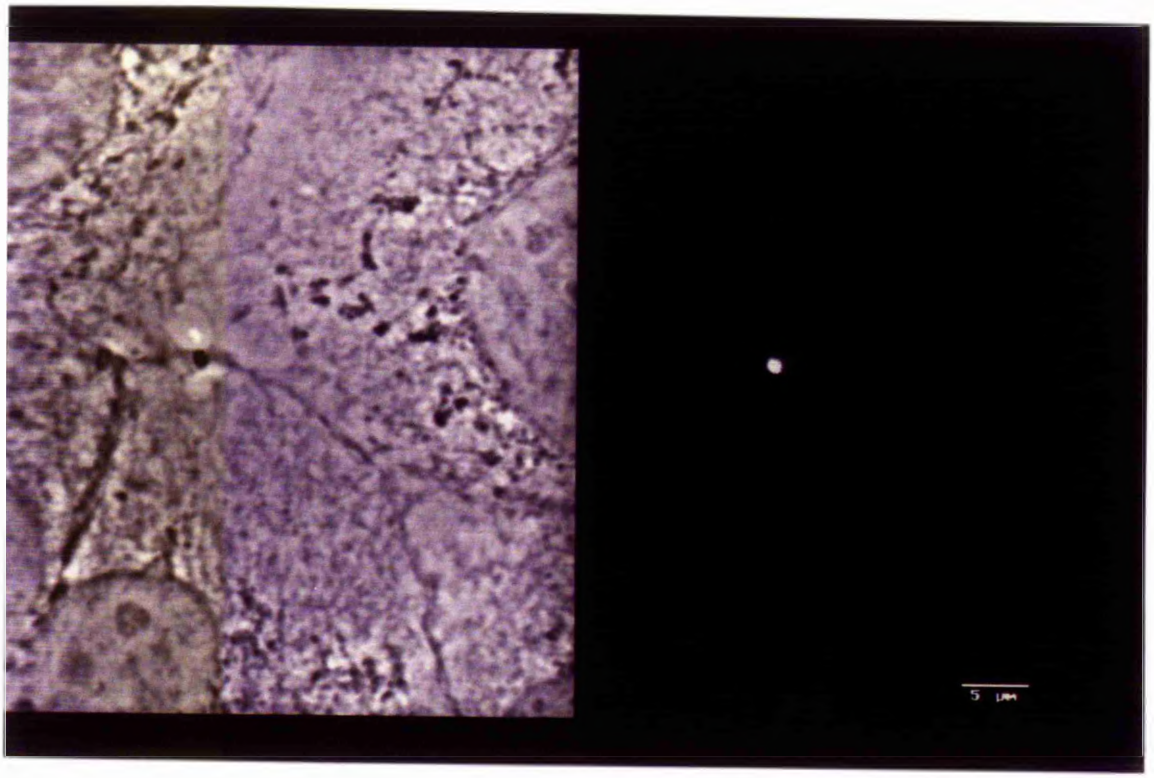
5 µm

Fig.16 Immunoblot of MDCK whole cell lysate assayed for acetylated tubulin with anti-acetylated-tubulin monoclonal antibody. A single protein band is present at approx. 53Kd. which is the same as that reported for acetylated tubulin.

Fig.17 The role of the cleavage constriction in the completion of daughter cell separation in MDCK cells - a model. **(a)** The cleavage constriction is occupied by the midbody. **(b)** The furrow base of the cleavage constriction spreads around one side of the midbody. **(c)** Daughter cell separation is achieved when the furrow base completely constricts around one side of the midbody.

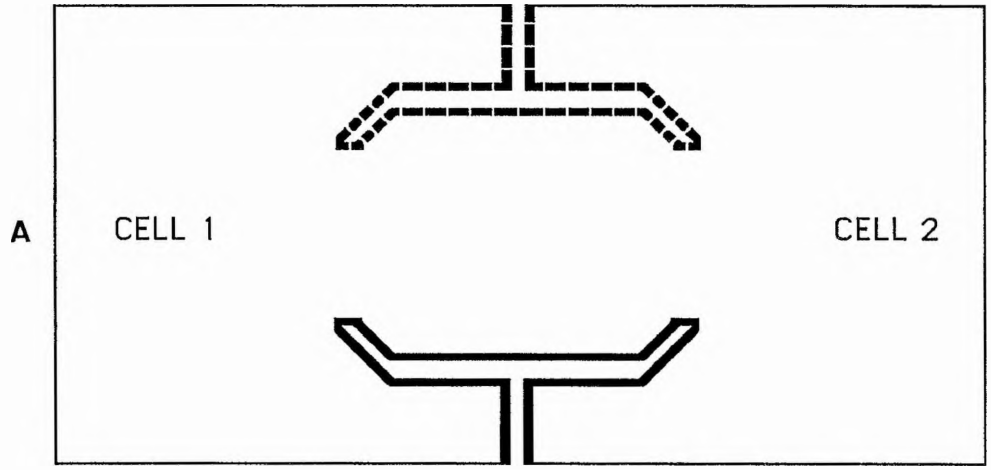
A
CELL 1
CELL 2

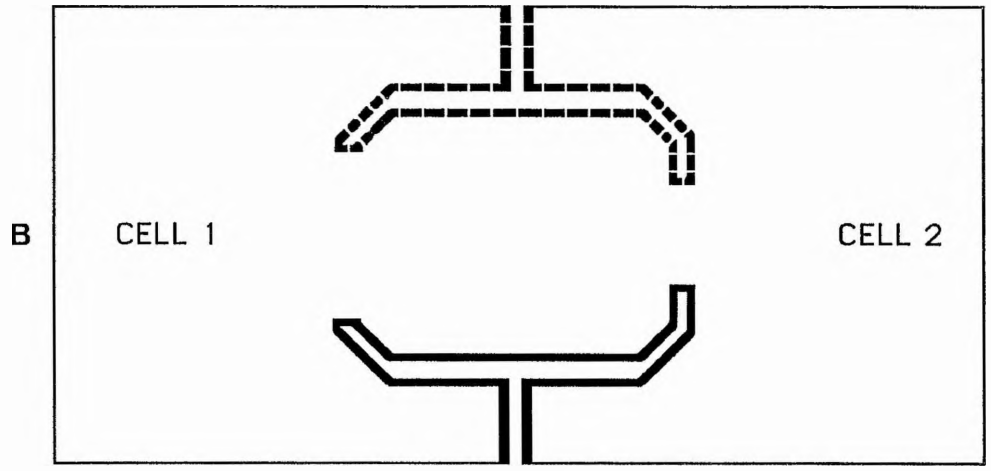
B
CELL 1
CELL 2

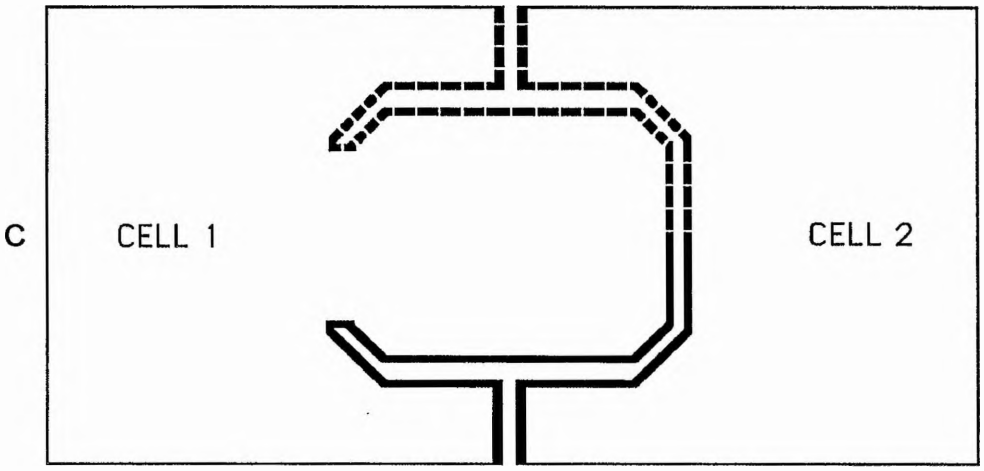
C
CELL 1
CELL 2

Fig.18 Daughter cell separation in MDCK cells - a model. **(a)** Furrowing arrests when the cleavage constriction has a diameter of approximately 1μm. **(b)** The furrow base of the cleavage constriction begins to spread around one side of the midbody **(c)** The microtubule bundle which is associated with the same side of the midbody as the spreading furrow base, is completely and rapidly severed at the side of the midbody. This allows the furrow base to complete its constriction around one side of the midbody and as a result complete daughter cell separation. The severed microtubule bundle rapidly depolymerizes **(d)** The second microtubule bundle is completely severed at the side of the midbody and rapidly disassembles. Consequently, the furrow base is free to complete its constriction around the entire midbody. As a result the midbody is completely isolated from both daughter cells. The remnant midbody contains short microtubules which are the remaining portions of the two severed microtubule bundles. These persist as they are stabilized by the intermicrotubular material of the midbody.

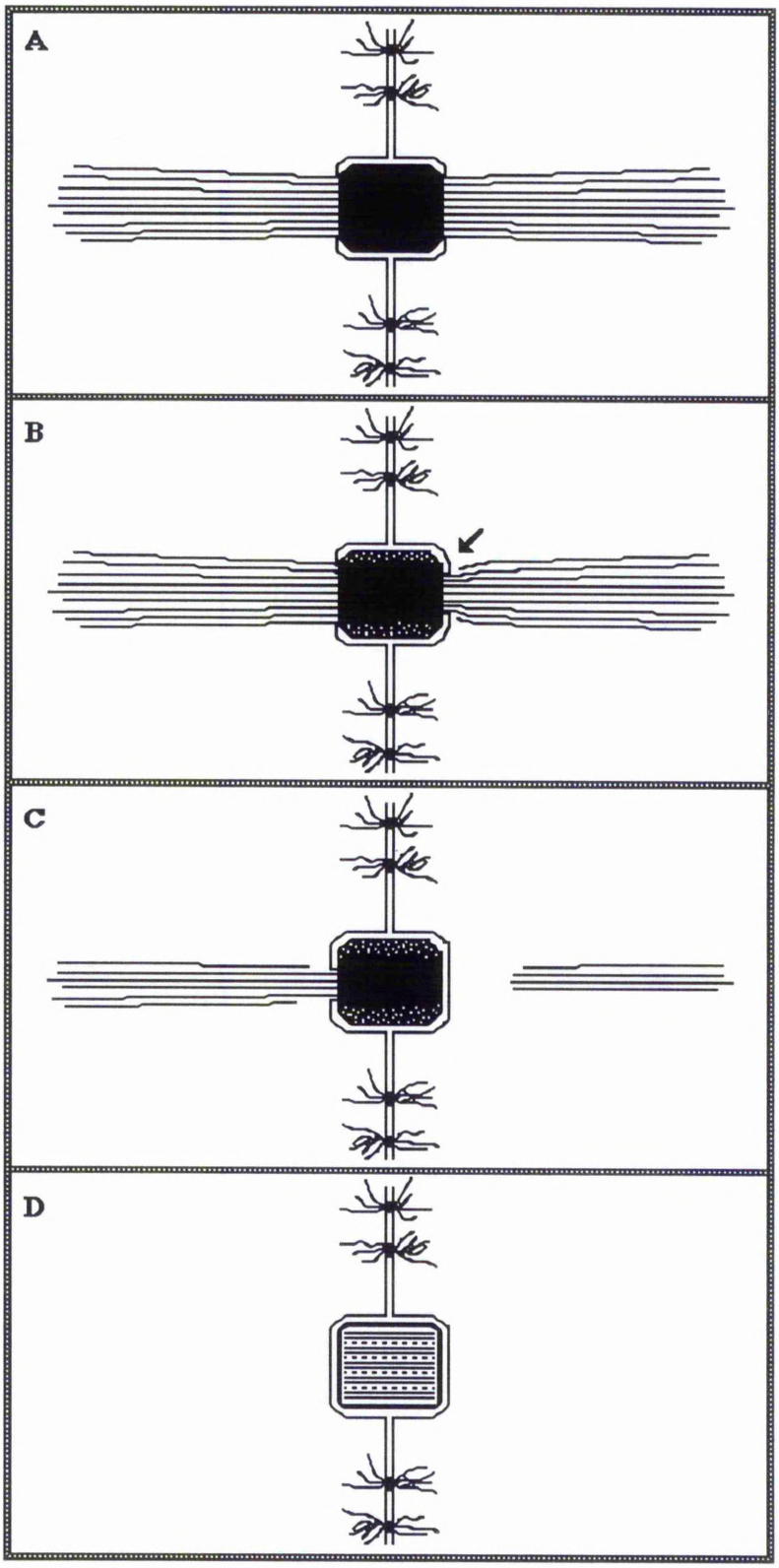
A
B
C
D

Chapter 6

Spatial and temporal localization of an antigen closely associated with the midbody of MDCK cells

6.1 Introduction

The plus ends of the two midbody-associated microtubule bundles interdigitate at the midbody (Euteneuer and McIntosh,1980). γ-Tubulin is concentrated at the minus ends of the two midbody-associated microtubule bundles of PtK2 cells (Julian *et al.*,1993). Therefore it has been suggested that microtubule nucleating sites at the margins of the intercellular bridge, which are not centriole containing centrosomes, nucleate the midbody-associated microtubules in PtK2 cells. In contrast, it is evident that a non-affinity purified *Xenopus*/gamma/C-terminus anti-γ-tubulin antiserum (NA XGC γ-tubulin antiserum) stains a region closely associated with both sides of the midbody in MDCK cells. The specificity of the localization of this antiserum has been investigated. The midbody-associated microtubule bundles appear to be involved in daughter cell separation (see chapter 5). Therefore, any difference in the organization of MDCK midbody-associated microtubule bundles, compared with that in other cell types, may affect daughter cell separation.

It has been determined that the antigen, stained with NA γ-tubulin antiserum, which is closely associated with both sides of the midbody is not γ-tubulin. However, the spatial and temporal localization of this antigen indicates that it may be a constituent of the recently discovered telophase disc.

6.2 Results

6.2.1 Centrosomal localization of NA XGC γ-tubulin antiserum in MDCK cells

NA XGC γ-tubulin antiserum stains a discrete spherical site next to the nucleus of each incipient daughter cell (Fig.1a). Anti-α-tubulin stains a network of microtubules which radiate from exactly the same site with which the antiserum is associated (Fig.1b). The stained spherical site is presumably occupied by the centrosome.

6.2.2 NA XGC γ-tubulin antiserum stains a region closely associated with both sides of the midbody

The different stages identified during cytokinesis and daughter cell separation of MDCK cells (see Chap.5) are employed in order to characterize the temporal and spatial changes of NA XGC γ-tubulin antiserum localization at the intercellular apparatus.

Stage 1

Stem bodies are aligned across the plane of the former spindle equator by early telophase (McIntosh and Landis,1971). NA XGC γ-tubulin antiserum stains a region closely associated with both sides of each stem body (Fig.1).

Stage 2

Stem bodies aggregate into a midbody (see Chap.5, Fig.3). NA XGC γ-tubulin antiserum stains a region closely associated with both sides of the midbody (Fig.2). The stained region increases in length but decreases in diameter and this appears to be correlated with the decrease in the diameter of the midbody during cytokinesis. Furrowing arrests when the cleavage constriction has a diameter of approximately 1μm and is occupied by the midbody (Fig.3). The intensity with which this region stains, is equivalent to that with which the centrosome stains. Occasionally, NA XGC γ-tubulin antiserum stains the outer end of each midbody-associated microtubule bundle (Fig.4). These stain with considerably less intensity than the centrosome and the regions closely associated with the sides of the midbody.

Stage 3

Anti-α-tubulin stains the entire midbody (see Chap. 5, Fig.9). NA XGC γ-tubulin antiserum no longer stains regions closely associated with the sides of the midbody. Instead, it stains the entire length of the midbody (Fig.5). The outer end of each midbody-associated microtubule bundle, no longer stains with the antiserum.

Stage 4

The first of the two midbody-associated microtubule bundles completely loses contact with one side of the midbody (Chap. 5, Fig.10). NA XGC γ-tubulin antiserum stains the detached end of this microtubule bundle and also continues to stain the midbody (Fig.6).

Stage 5

NA XGC γ-tubulin antiserum stains the remnant midbody with considerably less intensity than it stains the midbody at either stage 3 or 4. (Fig.7).

6.2.3 NA XGC γ-tubulin antiserum staining after detergent extraction

Detergent extraction, prior to fixation, completely destroys most microtubules of interphase and mitotic cells (Fig.8). However, anti-α-tubulin, still stains the centrosome and the remnants of midbody associated microtubule bundles. Anti-α-tubulin stains a discrete spherical site next to the nucleus in both interphase and dividing cells. NA XGC γ-tubulin antiserum stains exactly the same discrete spot as anti-α-tubulin (Fig.8). This site is presumably occupied by the centrosome. Only remnants of the midbody-associated microtubule bundles persist after detergent extraction (Fig.8). However NA XGC γ-tubulin antiserum stains a region which is closely associated with both sides of the midbody even after detergent extraction has been performed prior to fixation (Fig.8). Furthermore, the intensity with which NA XGC γ-tubulin antiserum stains this region is equivalent to that in untreated cells (cf. Fig's 8 and 3).

6.2.4 Localization of Human and *Drosophila* γ-tubulin antisera

Non-affinity purified Human anti-γ-tubulin antiserum (NA Human γ-tubulin antiserum) stains a discrete spherical site next to the nucleus of each incipient daughter cell (Fig.9). Anti-α-tubulin stains a network of microtubules which radiate from exactly the same site with which the antiserum is associated (Fig.9). The stained spherical site is

presumably occupied by the centrosome. However, NA Human γ-tubulin antiserum does not stain regions closely associated with the sides of each stem body and midbody.

An affinity-purified *Drosophila* anti-γ-tubulin antiserum does not stain regions closely associated with the sides of each stem body and midbody. However, it does not stain the centrosomes in MDCK cells either.

6.2.5 Centrosomal localization of affinity purified XGC γ-tubulin antiserum in MDCK cells

Affinity purified XGC γ-tubulin antiserum (AP XGC γ-tubulin antiserum) stains a discrete spherical site next to the nucleus of each incipient daughter cell (Fig.10,11). The stained spherical site is presumably occupied by the centrosome. The AP XGC γ-tubulin antiserum stains a pair of closely associated spheres in each interphase MDCK cell (Fig.10,11). The pairs of stained spherical sites presumably represent the centrosome in each interphase MDCK cell.

6.2.6 AP XGC γ-tubulin antiserum stains the outer ends of midbody-associated microtubule bundles.

AP XGC γ-tubulin antiserum does not stain regions closely associated with the sides of each stem body or with the midbody. However, the outer ends of the midbody-associated microtubule bundles stain with this antiserum from early telophase (Fig.10) up to and including stage 3 (Fig.11). AP XGC γ-tubulin antiserum stains the outer ends of the midbody-associated microtubule bundles much less intensely than the centrosome.

6.2.7 Specificity of antibody staining

Western Blot Analysis

Immunoblots of total MDCK protein content assayed for γ-tubulin with NA XGC γ-tubulin antiserum and AP XGC γ-tubulin antiserum are similar with the exception of two stained protein bands (Fig.12). NA XGC γ-tubulin antiserum stains protein bands at 80 and 88Kd which AP XGC γ-tubulin antiserum apparently does not. Both antisera stain a discrete protein band with a molecular weight that is approximately the same (48Kd) as that reported for γ-tubulin (Oakley and Oakley,1989). Both antisera also stain discrete protein bands at approximately 40, 37, and 35Kd.

Secondary Antibody

MDCK cells have been incubated with all the fluorescently conjugated secondary antibodies but without a previous incubation with the appropriate primary antibodies. After these procedures there is no detectable staining of these cells.

6.3 Discussion

6.3.1 Is γ-tubulin closely associated with both sides of each stem body and midbody?

The spatial and temporal localization with which the NA XGC γ-tubulin antiserum stains regions occupied by the midbody-associated microtubule bundles has

been characterized from late anaphase through to daughter cell separation. This antiserum stains regions which are closely associated with the sides of each stem body and midbody (it also stains the outer end of each midbody-associated microtubule array from stage 1 to stage 3 and is discussed in a subsequent section).

The presence of γ-tubulin closely associated with both sides of each stem body and the midbody is unlikely. This is because current evidence indicates that γ-tubulin associates with the minus ends of microtubules (Stearns and Kirschner,1994). Stem-bodies and midbodies are regions composed in part of interdigitating microtubule plus ends from each microtubule bundle (Euteneuer and Macintosh,1980).

It was essential to test the validity of NA XGC γ-tubulin antiserum staining of the regions closely associated with both sides of each stem body and midbody. Non-affinity purified antisera raised against human, and *Drosophila* γ-tubulin, do not stain a region closely associated with both sides of each stem body and the midbody. The laboratory responsible for the production of this antiserum (see Materials and Methods, section 2.4.3) was informed of the staining pattern obtained in MDCK cells with this antiserum. Consequently, a small volume of the affinity purified form of the antiserum (AP XGC γ-tubulin antiserum) was made available. The AP XGC γ-tubulin antiserum was used to determine whether it would stain regions closely associated with the sides of stem-bodies and midbodies. AP XGC γ-tubulin antiserum does not stain regions closely associated with the sides of stem bodies and midbodies. Therefore, it can be concluded that γ-tubulin is not closely associated with the sides of stem bodies and midbodies.

6.3.2 NA XGC γ-tubulin antiserum may recognise an 80 or 88Kd protein

Evidence from the localisation of AP XGC γ-tubulin antiserum indicates that γ-tubulin is not closely associated with both sides of each stem body and midbody. Therefore what antibody in the NA XGC γ-tubulin antiserum is responsible for the spatio-temporal staining pattern, and what protein does it recognise? Immunoblots of total

MDCK protein content assayed for γ-tubulin with NA XGC γ-tubulin antiserum exhibit a major protein band at approximately 48Kd; the molecular weight of γ-tubulin. There are also stained protein bands at the 88, 80, 40, 37 and 35 Kd positions. γ-Tubulin proteolysis is most likely responsible for the stained bands at 40, 37 and 35 Kd. This is because the immunoblot of total MDCK protein content assayed with AP XGC γ-tubulin antiserum not only exhibits a major stained protein band at 48Kd but also stained protein bands at 40, 37 and 35Kd. NA XGC γ-tubulin antiserum stains protein bands at 80 and 88Kd, which AP XGC γ-tubulin antiserum does not. It is therefore possible that NA XGC γ-tubulin antiserum recognises an 80 or 88Kd protein which is closely associated with both sides of the midbody. However, it can not be concluded that the antigen detected by immunofluorescence definitely has a molecular weight of 80 or 88Kd. This is because the antigen of interest may not be efficiently transferred by the western blot procedure. Alternatively, it may not be recognised on a Western blot by the NA XGC γ-tubulin antiserum.

The most likely possibility is that an antibody present in the rabbit serum prior to inoculation, recognises an antigen closely associated with both sides of each stem body and midbody. Rabbit pre-immune sera have been found previously to recognise specific antigens (Gosti-Testu *et al.*,1986; Connoly and Kalnins,1987; Gosti *et al.*,1987). However, it has not been possible to verify whether or not the antibody is present in the rabbit prior to inoculation as the pre-immune serum was not available. Therefore, the stained region on each side of the midbody could be due to an antibody from one of two other sources. It is possible that antibodies raised against the carrier protein may be responsible for the staining pattern. Furthermore, it is also possible, although unlikely, that an antibody in the NA XGC γ-tubulin antiserum which stains the region in question, may have a great affinity for γ-tubulin and thus could have been retained on the affinity chromatography column. Such an antibody may recognise, apart from γ-tubulin, a biologically unrelated protein and thus still be responsible for the 80 or 88Kd band. Such a phenomenon would not be without precedent (Schatten *et al.*,1987; Kallajoki *et al.*, 1991,1993; Paul and Quaroni,1993). The possible sources of the antibody responsible

for the spatio-temporal staining pattern closely associated with each side of a stem body and the midbody are summarised in Fig.13.

In conclusion, NA XGC γ-tubulin antiserum recognises an antigen closely associated with both sides of each stem body and midbody, which is not γ-tubulin. This antigen may have a molecular weight of either 80 or 88Kd. The antibody which recognises this antigen is possibly present in the rabbit pre-immune serum.

6.3.3 NA XGC γ-tubulin antiserum stains antigen associated with the telophase disc?

NA XGC γ-tubulin antiserum stains an antigen closely associated with the sides of stem-bodies and midbodies. It has been established that this antigen is unlikely to be a portion of the γ-tubulin protein. Even though this antigen is unidentified, its spatial and temporal localization is highly specific. During late anaphase, the antigen is closely associated with the sides of stem-body. During cytokinesis, it becomes concentrated into a region closely associated with the sides of the midbodies.

During the terminal stages of daughter cell separation the antigen localizes in the midbody. Subsequently, one microtubule bundle loses contact with the midbody (see Chap.5). At this point the antigen not only associates with the midbody but also the detached end of one of the microtubule bundles. Both the midbody and the detached end of the microtubule bundle must be regions with a relatively high concentration of microtubule plus ends. Finally, after the completion of daughter cell separation, a low concentration of the antigen is present in the remnant midbody. It would appear therefore that the antigen in question localizes at concentrations of microtubule plus ends in MDCK cells.

The antigen's localization is not disrupted by detergent extraction. This is a characteristic usually associated with cellular organelles (Andreassen *et al.*,1991). Interestingly, the localization of this antigen during late anaphase and telophase is

virtually identical to the localization of the TD-60 antigen which is a component of the recently discovered telophase disc (Margolis and Andreassen,1992). It has been established that the telophase disc is a mitotic organelle, although its function has not been determined. Therefore, could the antigen which NA XGC γ-tubulin antiserum stains possibly be a component of the telophase disc? This antigen is present in the region of the telophase disc. However this antigen is redistributed from its compact association with both sides of the midbody to the midbody itself which has not been reported for the TD-60 antigen. This would suggest that the antigen, identified in my investigation, is only transiently associated with the telophase disc (and as such is not an integral component). Alternatively, the redistribution of antigen may be a feature of the disassembly of the telophase disc.

It is interesting that the antigen is associated in regions where there is a high concentration of microtubule plus ends. This includes, the antigens localization in the vicinity of microtubule interdigitation and its localization at the midbody and the detached end of the midbody-associated microtubule bundle.

A molecular approach is now required to further characterize the antigen. For example, the antigen could be concentrated by adding affigel beads coated with the NA XGC γ-tubulin antiserum (or pre-immune serum, if the antibody proves to be present in this serum) to lysed MDCK cells. Subsequently, the antigen may be eluted from the beads and separated by SDS-gel electrophoresis. If a protein band is found at 88Kd this could be isolated from the gel and used to produce antibodies against the antigen. Furthermore, if the pre-immune serum proves to contain the antibody of interest, it could be used to screen a cDNA library and thus identify cDNA's related to this antigen. This would provide information about the structure of the protein, and could also be used to produce more specific antibodies. Furthermore, an affinity-purified antiserum against this antigen could be micro-injected into cells in order to establish what is the function of the protein .

6.3.4 AP XGC γ-tubulin antiserum localization at the outer ends of the midbody-associated microtubule bundles

γ-Tubulin is localized at the outer ends of the midbody-associated microtubule bundles of PtK2 cells (Julian *et al.*,1993) where the minus ends of microtubules are located (Euteneuer and McIntosh,1980). This occurs during telophase. AP XGC γ-tubulin antiserum stains the outer ends of some but not all midbody-associated microtubule bundles of MDCK cells. This was also the case for NA XGC γ-tubulin antiserum and NA Human γ-tubulin antiserum. The outer ends of the midbody-associated microtubule bundles stain from early telophase (stage 1) through to stage 3. γ-Tubulin is most likely present at this location in MDCK cells since: (1) It has been established that it is present at the margins of the intercellular bridge in PtK2 cells and (2) immunoblots exhibit a major stained protein band at 48Kd, the molecular weight of γ-tubulin (stained protein bands at 40, 37, and 35Kd are most likely due to proteolysis of γ-tubulin, see section 6.3.2).

Fig.1 (a) 'Dual image' and 'projected z-series' of NA XGC γ-tubulin antiserum localization (LHS) and anti-α-tubulin localization (RHS) in the same pair of incipient MDCK daughter cells during telophase. Scale bar, 5μm.

Fig.1 (b) 'Merged image' of Fig.1a. The NA XGC γ-tubulin antiserum (yellow) stains a discrete sphere which is located at the centre of a microtubule array (red) in each incipient daughter cell. The stained spherical sites are presumably occupied by the centrosome. The NA XGC γ-tubulin antiserum appears to be localized on both sides of the stem bodies which are aligned across the former spindle equator at telophase. Confocal laser scanning microscopy. Scale bar, 5μm.

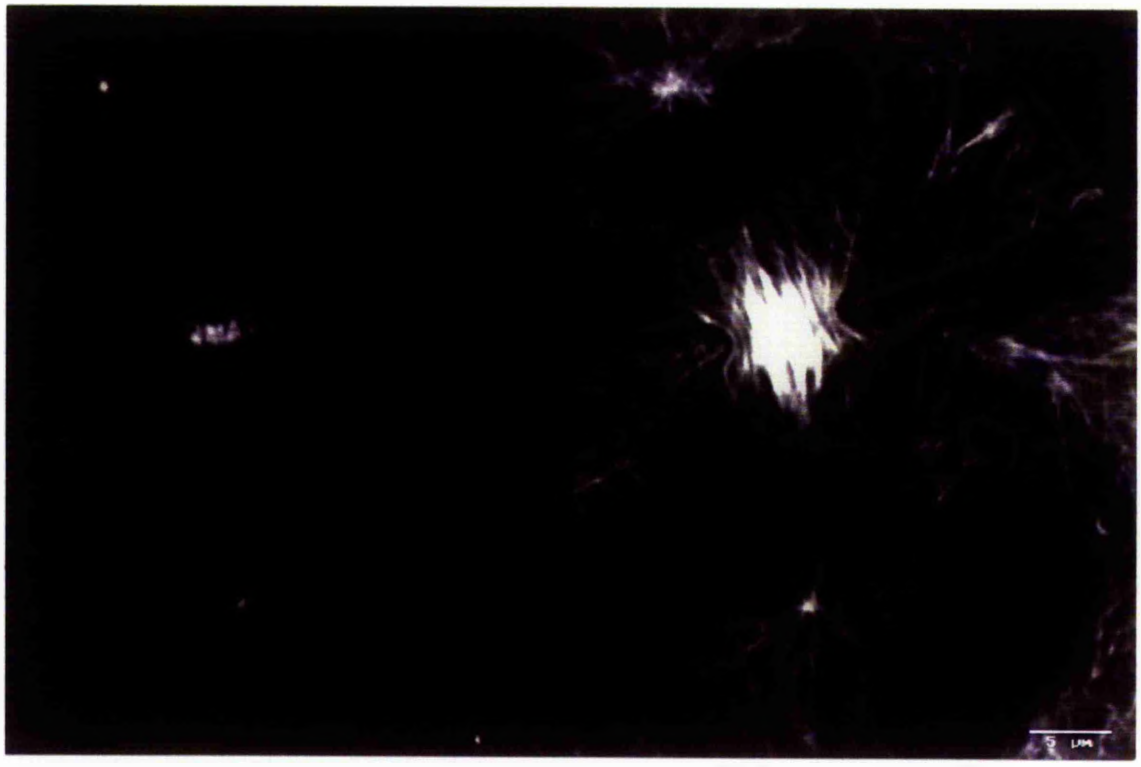
5 µm


5 µm

Fig.2 (a) 'Dual image' of NA XGC γ-tubulin antiserum localization (LHS) and anti-α-tubulin localization (RHS) in the same pair of incipient MDCK daughter cells during late telophase. Scale bar, 5μm.

Fig.2 (b) 'Merged image' of Fig.2a. The NA XGC γ-tubulin antiserum (yellow) stains a region on both sides of the midbody. Confocal laser scanning microscopy. Scale bar, 5μm.

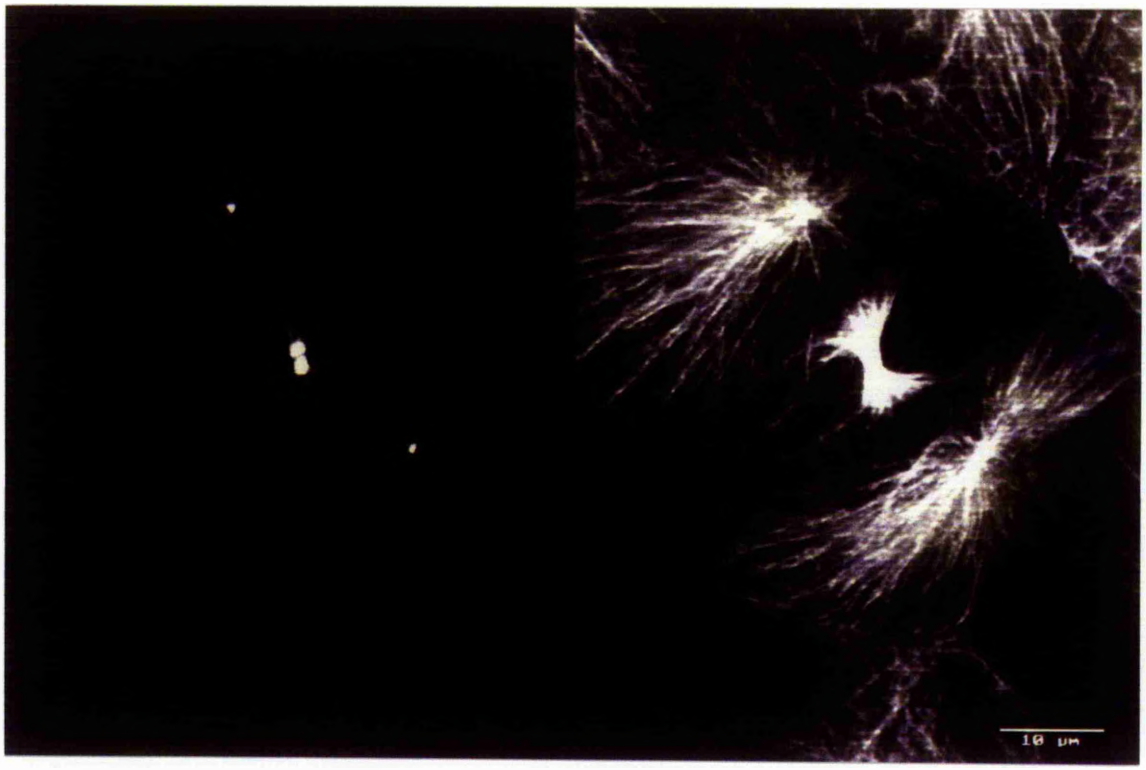
10 µm

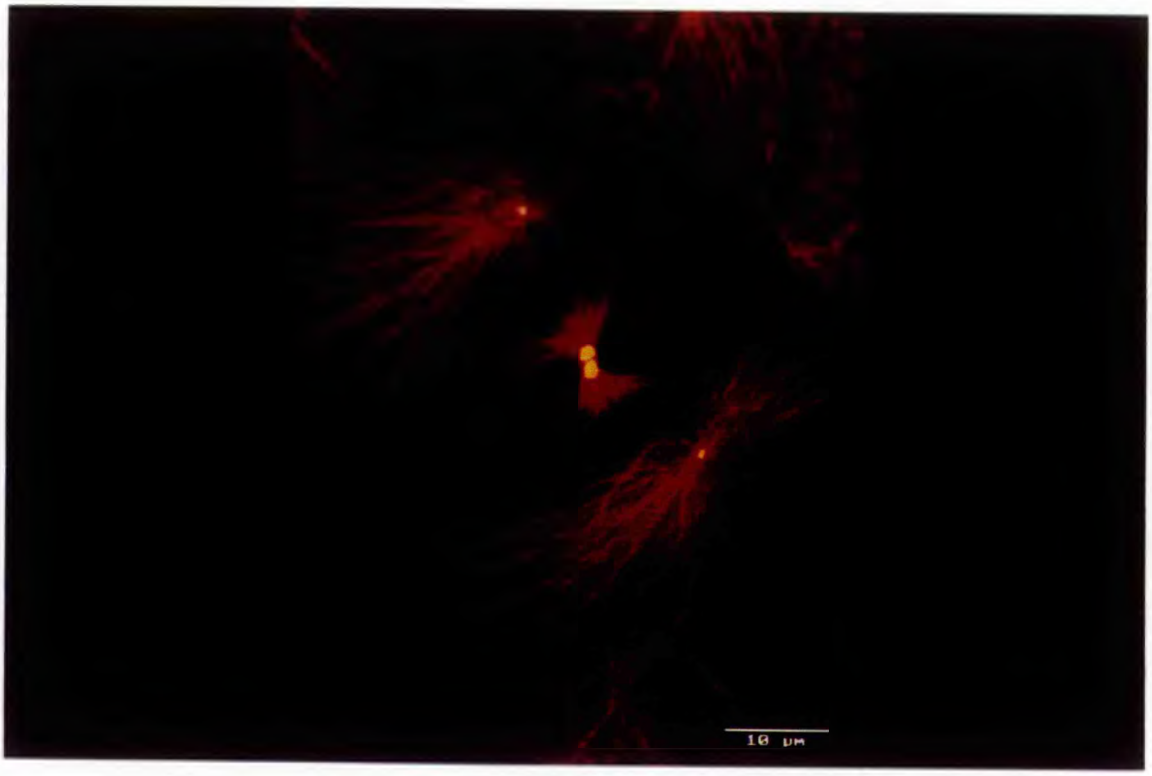
10 µm

Fig.3 (a) 'Dual image' and 'projected z-series' of NA XGC γ-tubulin antiserum localization (LHS) and anti-α-tubulin localization (RHS) in the same pair of incipient MDCK daughter cells after furrowing of the cleavage constriction has arrested. Scale bar, 5μm.

Fig.3 (b) 'Merged image' of Fig.3a. The NA XGC γ-tubulin antiserum (yellow) stains a discrete sphere which is located at the centre of a microtubule array in each incipient daughter cell. The stained spherical sites are presumably occupied by the centrosome. The NA XGC γ-tubulin antiserum also stains a region on both sides of the midbody. Confocal laser scanning microscopy. Scale bar, 5μm.

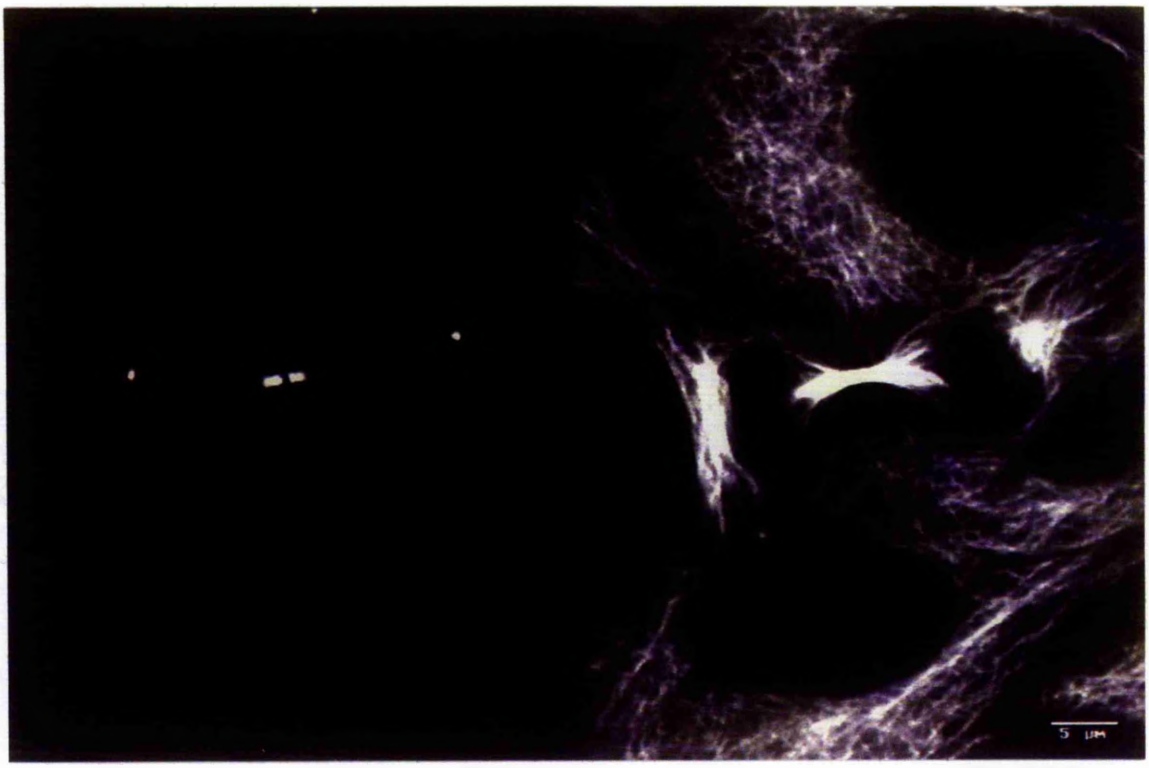
5 µm


5 µm

Fig.4 (a) 'Dual image' of NA XGC γ-tubulin antiserum localization (LHS) and anti-α-tubulin localization (RHS) in the same pair of incipient MDCK daughter cells during late telophase. Scale bar, 5μm.

Fig.4 (b) 'Merged image' of Fig.4a. The NA XGC γ-tubulin antiserum (yellow) stains a region on both sides of the midbody. It also stains the outer end of each midbody-associated microtubule bundle. Confocal laser scanning microscopy. Scale bar, 5μm.

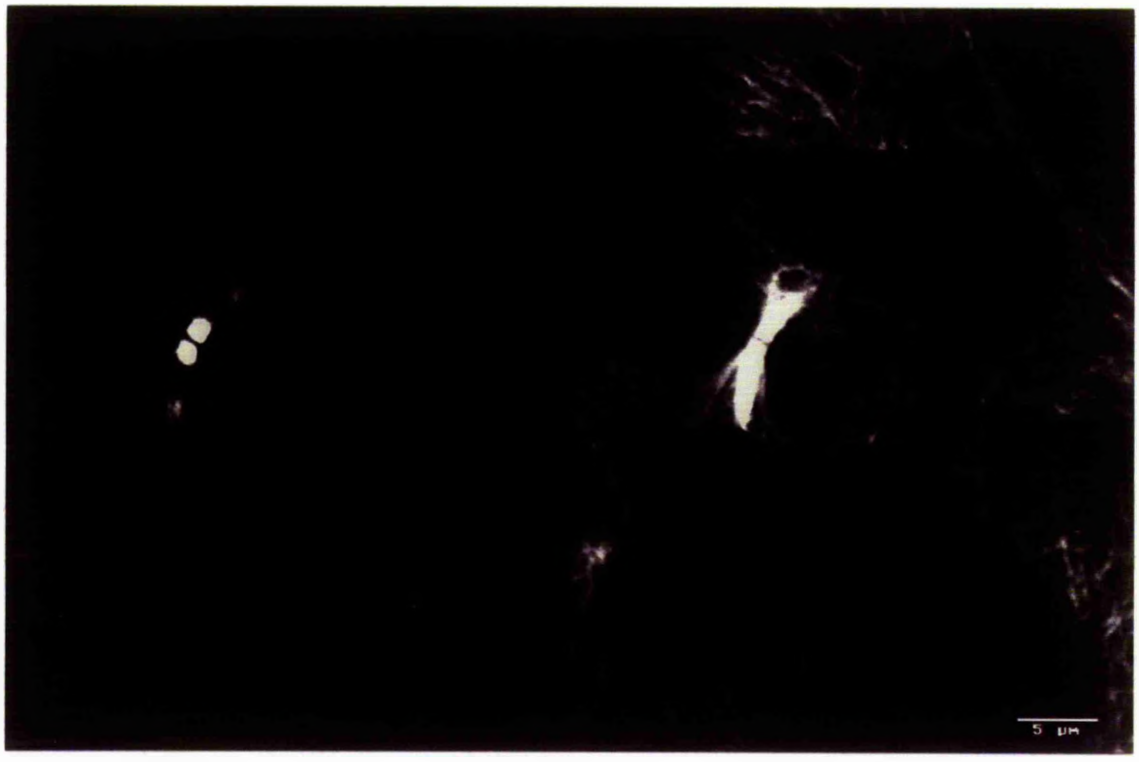
5 µm


5 µm

Fig.5 (a) 'Dual image' of NA XGC γ-tubulin antiserum localization (LHS) and anti-α-tubulin localization (RHS) in the same pair of incipient MDCK daughter cells just prior to the terminal stages of daughter cell separation. Scale bar, 5μm.

Fig.5 (b) 'Merged image' of Fig.5a. The NA XGC γ-tubulin antiserum (yellow) stains the entire length of the midbody. Confocal laser scanning microscopy. Scale bar, 5μm.


10 µm

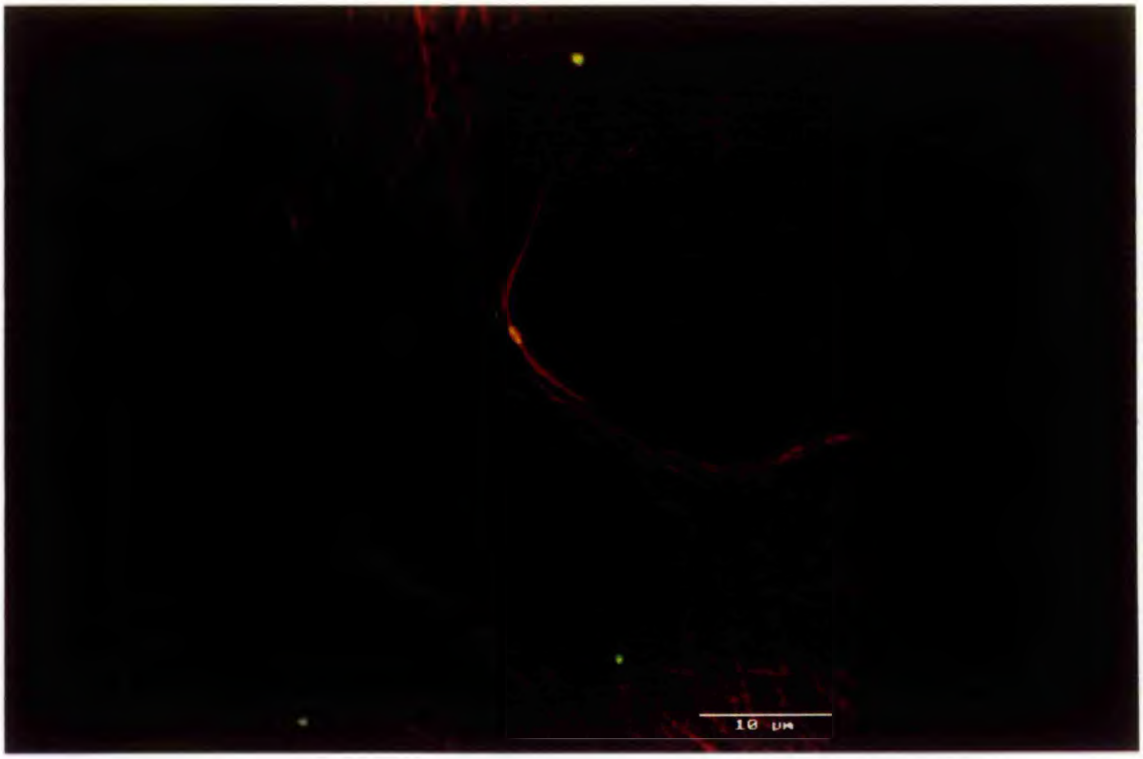
10 µm

Fig.6 (a) 'Dual image' and 'projected z-series' of NA XGC γ-tubulin antiserum localization (LHS) and anti-α-tubulin localization (RHS) in the same pair of incipient MDCK daughter cells after one microtubule bundle loses contact with the midbody. Scale bar, 5μm.

Fig.6 (b) 'Merged image' of Fig.6a. The NA XGC γ-tubulin antiserum (yellow) stains a discrete sphere which is not located at the centre of a microtubule array (see chapter 8) in each incipient daughter cell. The stained spherical sites are presumably occupied by the centrosome. The NA XGC γ-tubulin antiserum also stains the midbody and the end of the microtubule bundle which has lost contact with the midbody. Confocal laser scanning microscopy. Scale bar, 5μm.

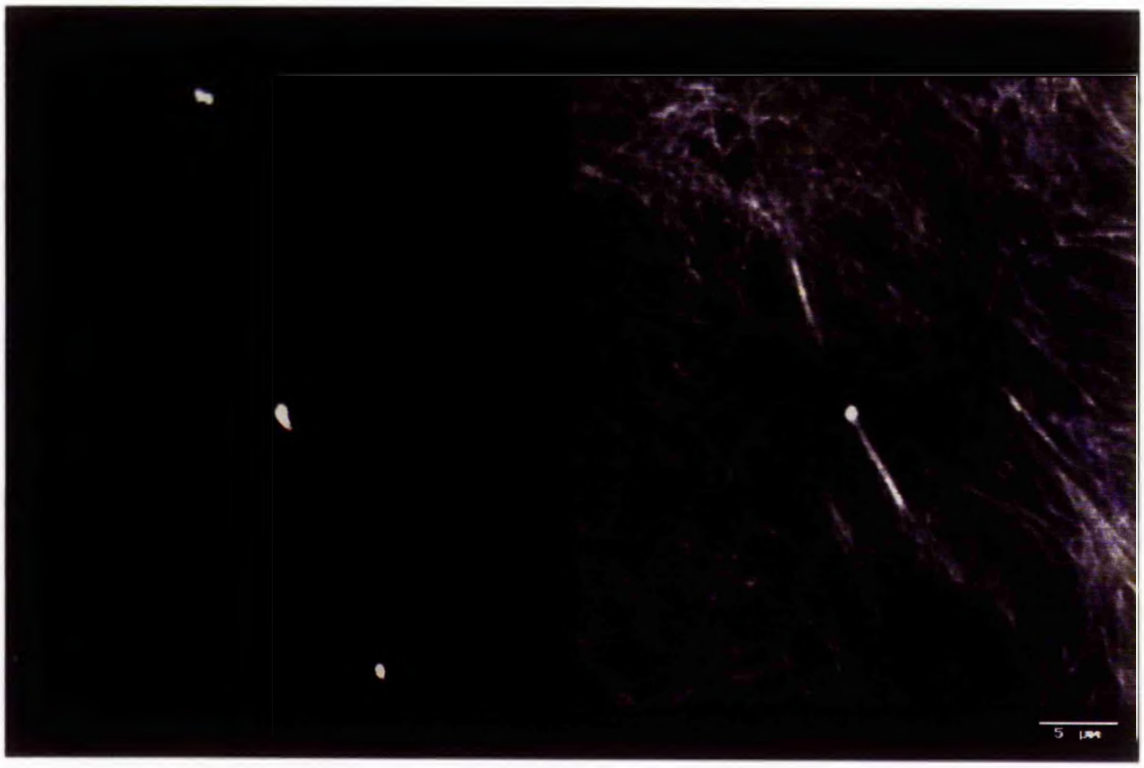
5 µm


5 µm

Fig.7 'Dual image' of NA XGC γ-tubulin antiserum localization (LHS) and anti-α-tubulin localization (RHS) in the same group of MDCK cells. The NA XGC γ-tubulin antiserum stains a discrete sphere which is not located at the centre of a microtubule array (see Chapter 8) in each MDCK cell. The stained spherical sites are presumably occupied by the centrosome. The NA XGC γ-tubulin antiserum also stains a region between a pair of separated daughter cells (arrow) which is the location of the remnant midbody (see arrow head on anti-α-tubulin image and inset). Confocal laser scanning microscopy. Scale bar, 5μm.

Inset - phase contrast image of the remnant midbody which is stained with NA XGC γ-tubulin antiserum (LHS) and anti-α-tubulin (RHS) in main picture. Scale bar 2μm.

Fig.8 (a) 'Dual image' and 'projected z-series' of NA XGC γ-tubulin antiserum localization (LHS) and anti-α-tubulin localization (RHS) in the same pair of detergent extracted incipient MDCK daughter cells at late telophase. Detergent extraction has almost completely destroyed the cytoplasmic microtubule array in each incipient daughter cell. Anti-α-tubulin and NA XGC γ-tubulin antiserum both stain one (or two closely associated) discrete sphere/s in each incipient daughter cell. The stained spherical sites are presumably occupied by a centrosome. The midbody-associated microtubule bundles have almost been completely destroyed. Remnants of each microtubule bundle are present within the midbody and at a region closely associated with both sides of the midbody. The NA XGC γ-tubulin antiserum intensely stains a region closely associated with both sides of the midbody. Scale bar, 5μm.

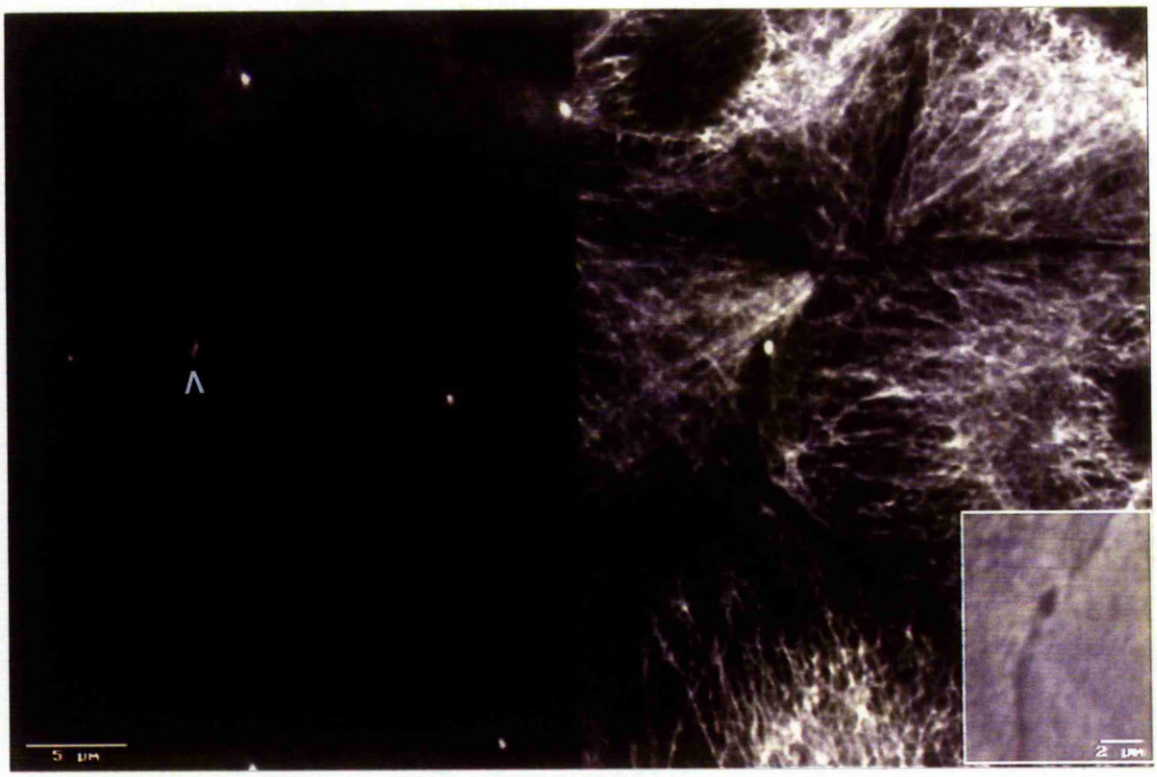
5 µm
2 µm


5 µm

Fig.8 (b) 'Merged image' of Fig.8a. Confirms that both anti-α-tubulin (red) and NA XGC γ-tubulin antiserum (yellow/green) stain the same sites in each incipient daughter cell. Confocal laser scanning microscopy. Scale bar, 5μm.

Fig.9 'Dual image' of NA Human γ-tubulin antiserum localization (LHS) and anti-α-tubulin localization (RHS) in the same pair of incipient MDCK daughter cells at telophase. The NA Human γ-tubulin antiserum stains a discrete sphere which is located at the centre of a microtubule array in each incipient daughter cell. The stained spherical sites are presumably occupied by the centrosome. The NA Human γ-tubulin antiserum does not stain a region closely associated with both sides of the midbody. Confocal laser scanning microscopy. Scale bar, 5μm.


5 µm

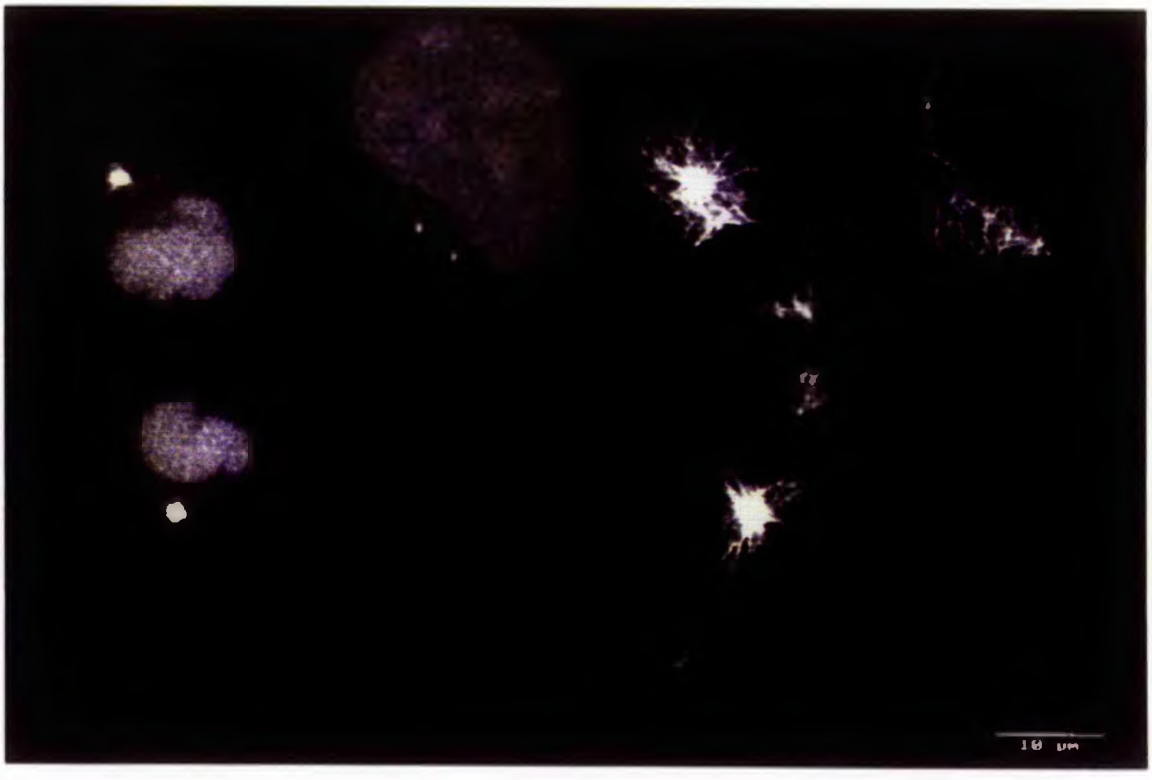
10 µm

Fig.10 'Projected z-series' of AP XGC γ-tubulin antiserum localization in a pair of incipient MDCK daughter cells at telophase. The AP XGC γ-tubulin antiserum stains a discrete sphere in each incipient daughter cell. The stained spherical sites are presumably occupied by the centrosome. The AP XGC γ-tubulin antiserum also stains a diffuse region in each incipient daughter cell which corresponds to the outer end of each midbody-associated microtubule bundle. The AP XGC γ-tubulin antiserum does not stain a region closely associated with both sides of the midbody. Pairs of closely associated stained spheres are presumably occupied by the centrosome in interphase MDCK cells. Confocal laser scanning microscopy. Scale bar, 5μm.

Fig.11 'Projected z-series' of AP XGC γ-tubulin antiserum localization in a pair of incipient MDCK daughter cells just prior to the terminal stages of daughter cell separation. The AP XGC γ-tubulin antiserum stains a pair of closely associated discrete spheres in each incipient daughter cell. The pairs of stained spherical sites are presumably occupied by the centrosome. The AP XGC γ-tubulin antiserum also stains a region in each incipient daughter cell which corresponds to the outer end of each midbody-associated microtubule bundle. The AP XGC γ-tubulin antiserum does not stain a region closely associated with both sides of the midbody. Confocal laser scanning microscopy. Scale bar, 5μm.

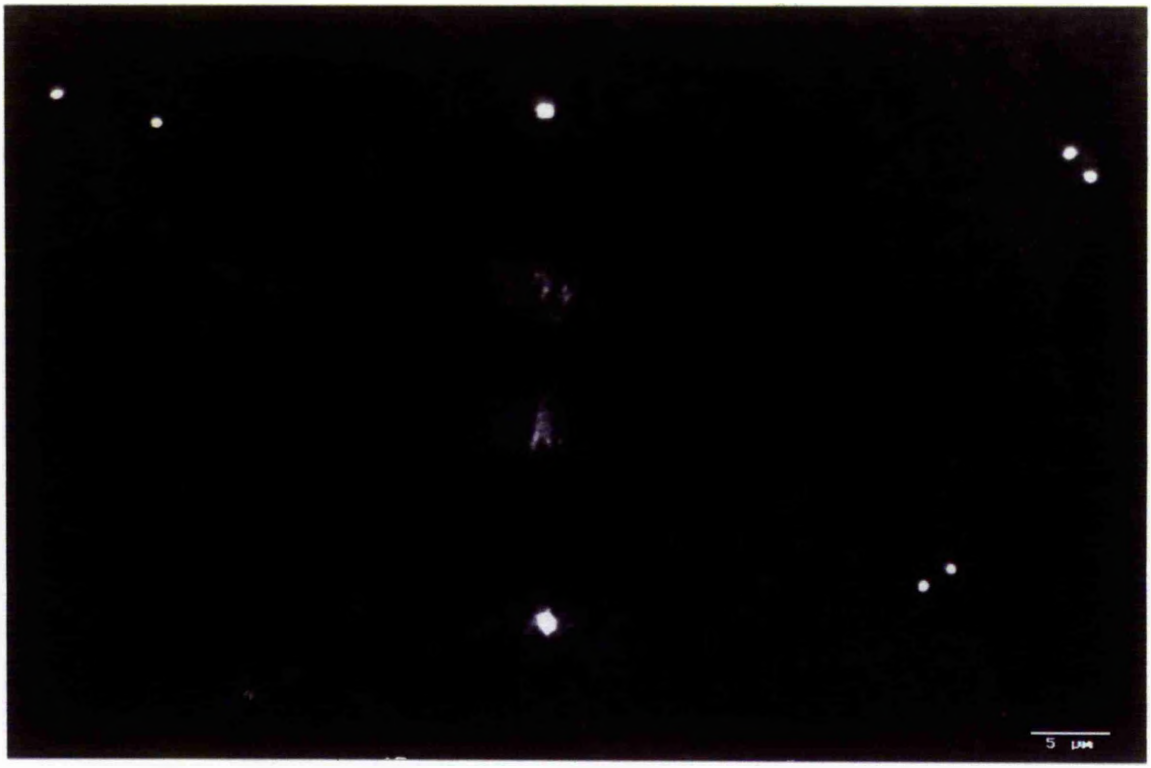
5 µm

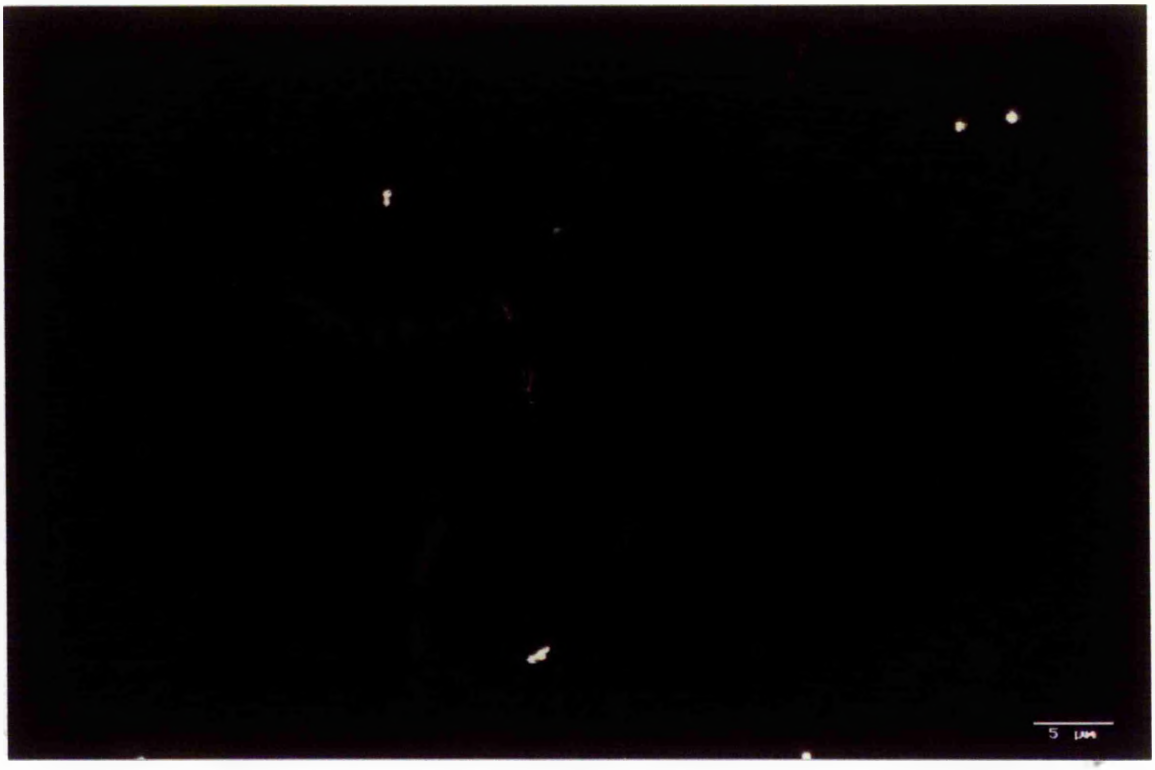
5 µm

Fig.12 Immunoblots of MDCK whole cell lysate assayed for gamma tubulin with either NA XGC γ-tubulin antiserum or AP XGC γ-tubulin antiserum. (**a**) Immunoblot of MDCK whole cell lysate stained with NA XGC γ-tubulin antiserum. Major stained protein band at approx. 48Kd (M.W. of γ-tubulin). Minor stained protein bands at approx. 88, 80, 40, 37 and 35Kd. (**b**) Immunoblot of MDCK whole cell lysate stained with AP XGC γ-tubulin antiserum. Major stained protein band at approx. 48Kd (M.W. of γ-tubulin). Minor stained protein bands at approx. 40, 37 and 35Kd.

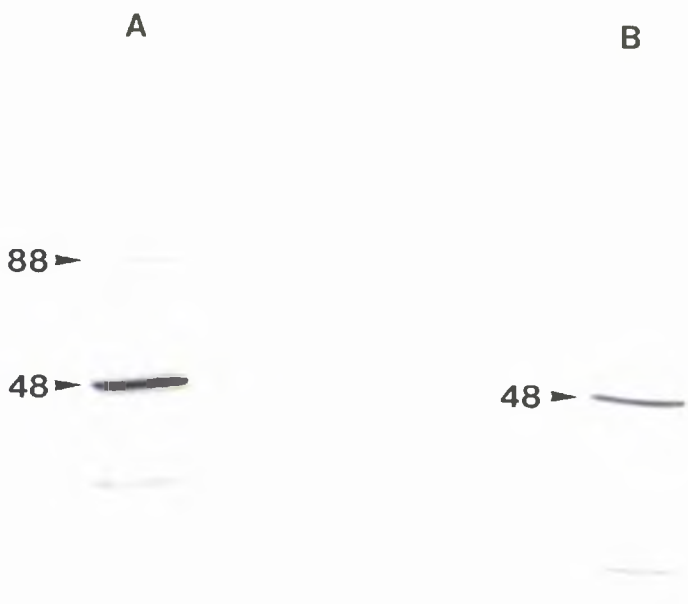
A
B
88
48
48

Fig.13 Possible sources of antibody responsible for the spatial-temporal staining pattern closely associated with both sides of the midbody. **A** - antibodies present in the rabbit prior to inoculation; **γ** - antibodies raised in the rabbit against the γ-tubulin peptide; **C** - antibodies raised in the rabbit against the carrier protein.

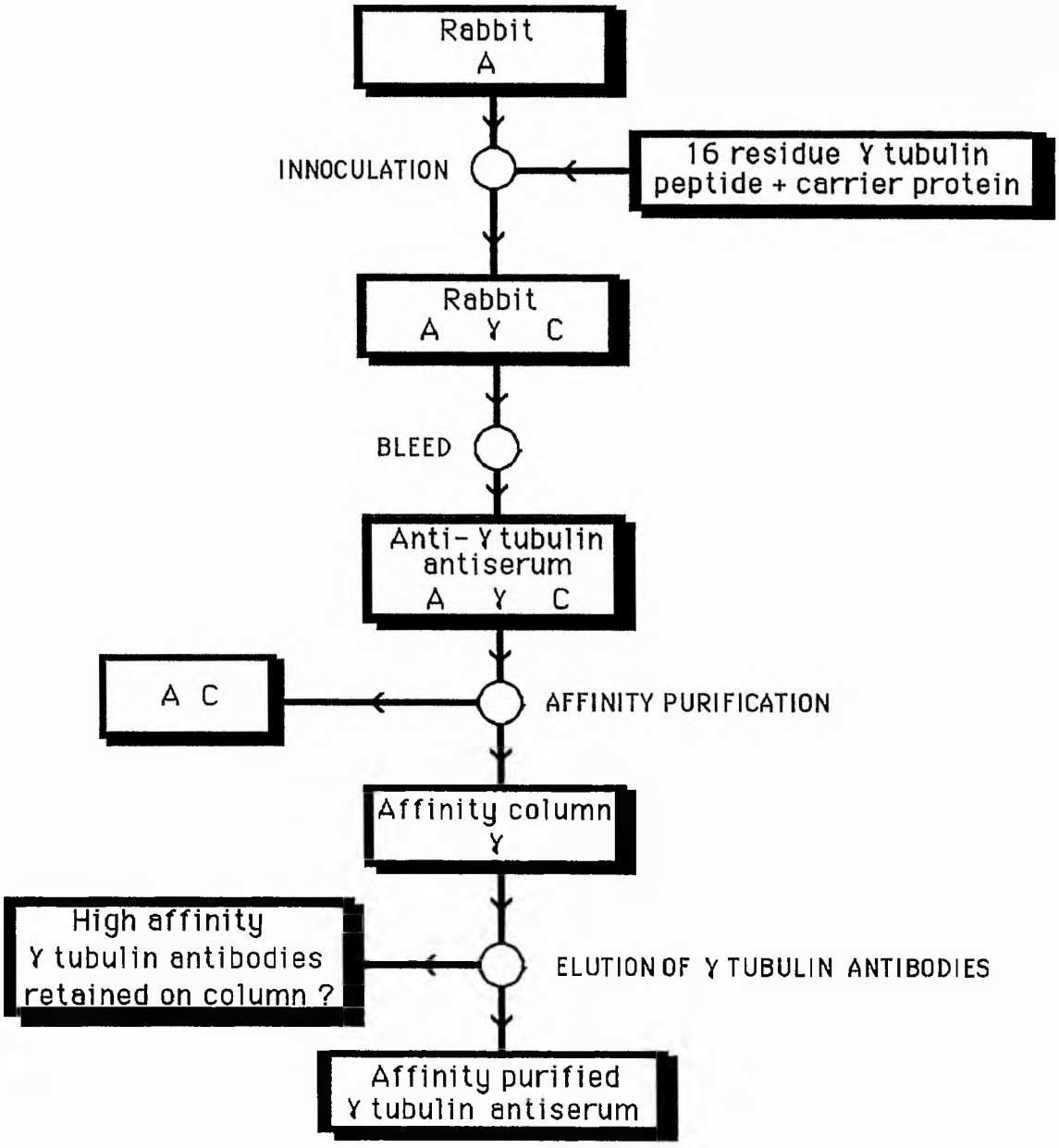
Rabbit
A
INNOCULATION
16 residue Y tubulin
peptide + carrier protein
Rabbit
A Y C
BLEED
Anti-Y tubulin
antiserum
A Y C
A C
AFFINITY PURIFICATION
Affinity column
Y
High affinity
Y tubulin antibodies
retained on column ?
ELUTION OF Y TUBULIN ANTIBODIES
Affinity purified
Y tubulin antiserum

Chapter 7

The effect of taxol on microtubule organization and protofilament number in *Drosophila* neuroblast cells

7.1 Introduction

Microtubules are nucleated from plasma membrane-associated MTOC's in the late-pupal wing epidermal cells of *Drosophila* (Mogensen *et al.*,1989). The vast majority of these microtubules are composed of 15 protofilaments. If these cells are incubated in taxol, microtubules are still nucleated from the plasma membrane-associated MTOC's. However, the vast majority of these microtubules have 12 instead of the normal 15 protofilaments. Is this effect confined to nucleating-sites which are not involved in exacting 13p fidelity? If established, this would indicate that nucleating MTOC's which do not specify 13p microtubules are different from those which do. Alternatively, are downshifts in protofilament number induced at all MTOC's in the presence of taxol? If all MTOC's are taxol sensitive this may indicate that taxol can interfere with the normal nucleation of microtubules. In this case, taxol could be a valuable drug with which to investigate the molecular mechanism of microtubule nucleation. Therefore, the principal objective of this investigation was to establish whether taxol induces a switch-down in microtubule protofilament number in cells which nucleate conventional 13 protofilament microtubules under normal conditions. Microtubule organization of neuroblast cells within the optic lobes of the *Drosophila* third instar larva has been examined. These cells contain conventional centriole-containing centrosomes. Therefore, they are likely to nucleate 13 protofilament microtubules (although this remains to be confirmed). Are microtubules nucleated at their usual MTOC (the neuroblast cell centrosome) in the presence of taxol as is the

case for *Drosophila* wing epidermal cells (Mogensen and Tucker,1990)? Alternatively, does taxol induce microtubule bundles and asters? This occurs in mammalian cells when they are exposed to taxol (De Brabander *et al.*,1981; Manfredi *et al.*,1986; Albertini,1987). Is microtubule protofilament number perturbed in neuroblast cells?

7.2 Results

7.2.1 Immunocytochemistry and ultrastructure of normal neuroblast cells

Microtubules are abundant in the cells of the late *Drosophila* 3rd instar larval central nervous system (CNS) (Fig.1a). Microtubules are particularly abundant in the cells of the optic lobe (a constituent of the larval CNS) (Fig.1b).

Interphase neuroblast cells stained with α-tubulin monoclonal antibody (anti-α -tubulin), reveal microtubules which are distributed around the periphery of each cell (Fig.2). Microtubules appear to focus at one end of each cell. Mitotic neuroblast cells stained with anti-α-tubulin, exhibit conventional mitotic spindles (Fig.3).

A pair of centrioles is located at one end of each interphase neuroblast cell, just below the plasma membrane (Fig.4). Microtubules radiate out from the region in the immediate vicinity of each centriole (Fig.4). Microtubule bundles occur below the surface of, and are oriented parallel to, the plasma membrane (Fig.5).

7.2.2 Immunocytochemistry and Ultrastructure of neuroblast cells incubated in taxol for 18 hours

Taxol induces one microtubule array and one microtubule aster, in interphase and mitotically arrested neuroblast cells respectively (Fig.6). Transmission electron

microscopy, confirms that one microtubule array is present in interphase neuroblast cells incubated in taxol (Fig.7). The taxol-induced interphase microtubule array always occurs next to the nuclear surface (Fig.7). Microtubules appear to be completely restricted to the array since none have been found elsewhere in the cytoplasm. Microtubule arrays contain microtubule 'chains' (Fig.8a). A dense layer of material is associated with the surface of these microtubules. It appears that adjacent microtubules share some of the same protofilaments (Fig.8b). There is no obvious difference in the diameters of microtubules in microtubule arrays (Fig.9). Sequential serial sections have not revealed any centrioles in these taxol incubated interphase cells.

Cells arrested in mitosis by taxol contain one central microtubule aster (Fig.10). Chromatin is present around the periphery of such asters. Sequential sections of several microtubule asters have not revealed any centrioles. Microtubules do not form 'chains' as occurs in interphase cells after taxol incubation.

7.2.3 Microtubule Protofilament Number

An attempt was made to reveal the protofilament number of microtubules in taxol-incubated neuroblast cells. However, this was not successful. It was clear that numerous modifications would be required to the protocol in order to increase the probability of success. It was concluded that it would be of greater value to spend time on devising a protocol which would establish the effect of taxol on microtubule protofilament number in mammalian cells.

7.3 Discussion

7.3.1 Microtubule organization in normal and 18hr taxol incubated neuroblast cells

A pair of centrioles are located just below the surface of the plasma membrane at one end of each untreated neuroblast cell. Microtubule ends are localized in the vicinity of each centriole pair. This indicates that microtubules are organised by a conventional centriole containing centrosome. Microtubules skirt around the periphery of each interphase neuroblast cell, just below the plasma membrane.

Microtubule organization in neuroblast cells incubated in taxol for 18hrs is considerably different from that in normal neuroblast cells. Neuroblast cells at interphase after an 18hr taxol incubation each contain one microtubule array which is next to the nucleus. There is no evidence that centrioles associate with these microtubule arrays. Microtubule ends do not appear to focus at a distinct region within these arrays. Furthermore, there is no evidence of any material which is similar in appearance to the pericentriolar material of centrosomes within these arrays. However, centrioles have not been found elsewhere in these taxol incubated interphase cells.

Neuroblast cells at mitotic arrest after an 18hr taxol incubation each contain one central microtubule aster. Microtubules radiate out from the centre of each aster towards the cell periphery. No evidence of centrioles or material which resembles pericentriolar material has been found in the mitotically arrested cells incubated in taxol.

It has not been determined whether microtubules in taxol incubated neuroblast cells at interphase and mitotic arrest are organized by conventional centriole-containing centrosomes. The presence of centriole-containing centrosomes in taxol incubated neuroblast cells could be confirmed by immunofluorescence with AP γ-tubulin antiserum and/or pericentrin antisera.

7.3.2 Taxol induced microtubule arrays and asters

Taxol lowers the threshold required for microtubule polymerization *in vitro* (Schiff *et al.*,1979). This may also occur *in vivo* (De Brabander *et al.*,1981; Verde *et al.*,1991). If microtubule nucleation in taxol incubated neuroblast cells is completely controlled by lowering the threshold for nucleation, then it would be anticipated that microtubules would polymerize at various locations in the cytoplasm. However, in taxol incubated interphase neuroblast cells microtubules are confined to a solitary array. Similarly, when these cells are mitotically arrested there is only one taxol induced aster per cell. This suggests that microtubule nucleation is favoured within a specific region of each cell. For example, specific microtubule nucleating proteins may concentrate at a specific site within each cell. If this is the case, is the centriole containing centrosome responsible for microtubule nucleation in the presence of taxol? This question remains to be answered.

7.3.3 Microtubule 'Chains'

Microtubule 'chains' are a characteristic feature of microtubule arrays in neuroblast cells which are at interphase after an 18hr taxol incubation. It appears that adjoining microtubules may share some of the same protofilaments. Zinc can also induce a peculiar polymorphic assembly form of tubulin. Zinc induces sheets of antiparallel rows of protofilaments (Kamimura and Mandlekow,1992). Microtubule 'chains' do not occur in normal interphase neuroblast cells. Therefore, microtubule 'chains' can be attributed to taxol incubation. Revealing and counting protofilaments in taxol incubated neuroblast cells would confirm whether adjoining microtubules of microtubule 'chains' share some of the same protofilaments.

Interestingly, microtubule 'chains' do not occur in the taxol induced microtubule asters of mitotically arrested neuroblast cells. Thus the effect of taxol on microtubule organization in neuroblast cells appears to depend on whether the cells are in mitosis or

at interphase. Why microtubule 'chains' occur in interphase and not mitotic neuroblast cells after taxol incubation has not been resolved. Can taxol directly or indirectly inhibit or enhance the function of specific proteins during interphase which results in the formation of microtubule 'chains' ?

Fig.1 (a) 'Projected z-series' of anti-α-tubulin localization in the central nervous system of a *Drosophila* 3rd instar larva. Microtubules are abundant in cells throughout the ventral ganglion (1), the two brain hemispheres (2) and the optic lobes (3). Confocal laser scanning microscopy. Scale bar, 100μm.

Fig.1 (b) 'Projected z-series' of anti-α-tubulin localization in the optic lobe of a *Drosophila* 3rd instar larva. Microtubules are abundant in the cells throughout the optic lobe. Scale bar, 50μm.


1
2
3
100 µm


50 µm

Fig.2 'Projected z-series' of anti-α-tubulin localization in interphase neuroblast cells of a *Drosophila* 3rd instar larva optic lobe. Microtubules are organized around the periphery of each neuroblast cell. The microtubules appear to radiate from a discrete site at one end of each cell. Confocal laser scanning microscopy. Scale bar, 5μm.

Fig.3 'Projected z-series' of anti-α-tubulin localization in a mitotic neuroblast cell and interphase neuroblast cells of a *Drosophila* 3rd instar larval optic lobe. The mitotic neuroblast cell exhibits a conventional mitotic spindle. Confocal laser scanning microscopy. Scale bar, 5μm.

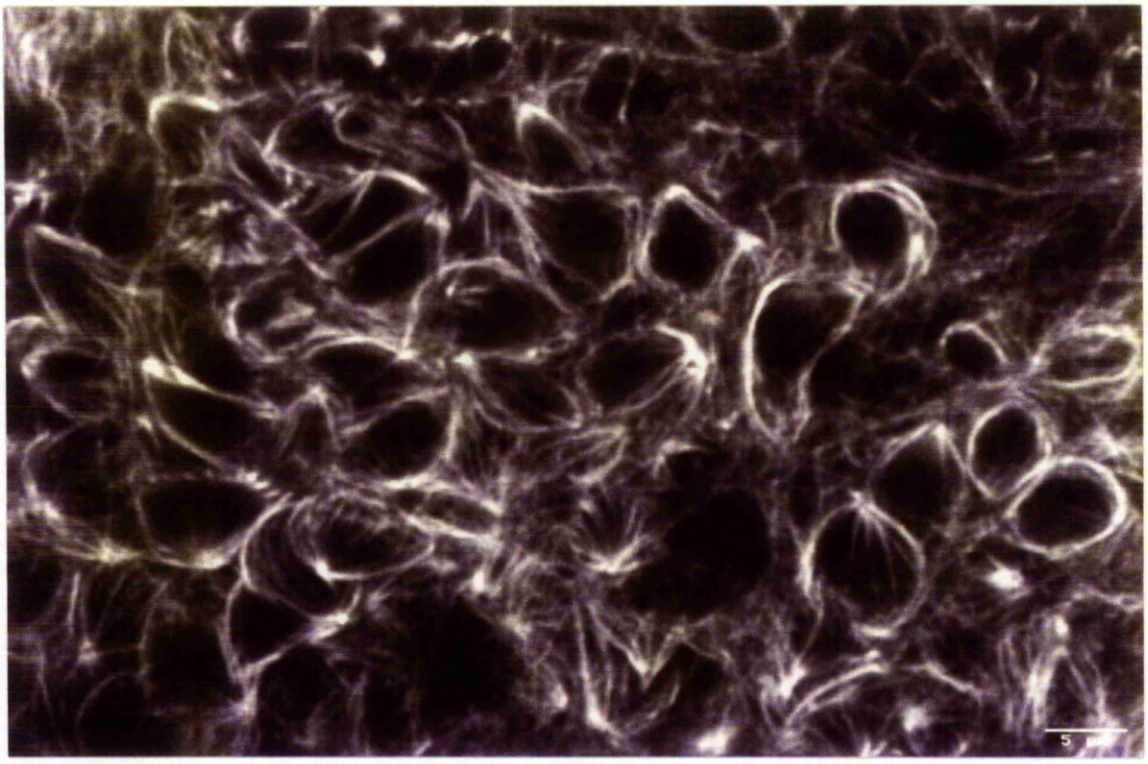

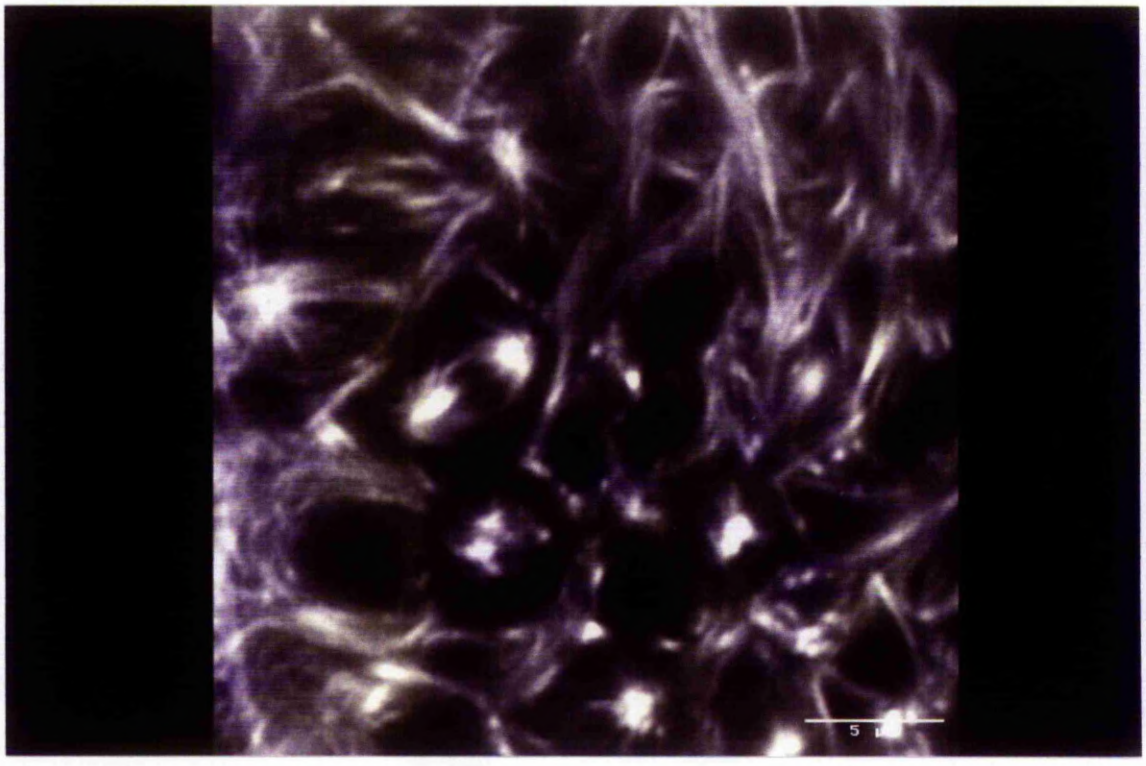

Fig.4 Interphase neuroblast cell in the optic lobe of a *Drosophila* 3rd instar larva. **(a)** Survey of one end of a neuroblast cell where the centrosome is located. Microtubules radiate from the centrosome and skirt just under the inner surface of the cell. Scale bar, 0.5μm. **(b)** Neuroblast cell centrosome located at one end of the cell. A conventional centriole-containing centrosome from which microtubules radiate. Scale bar, 0.2μm.

Fig.5 Two interphase neuroblast cells located side by side in the optic lobe of a *Drosophila* 3rd instar larva. Microtubules are located just below and oriented parallel to the plasma membrane in each cell. Scale bar, 0.2μm.

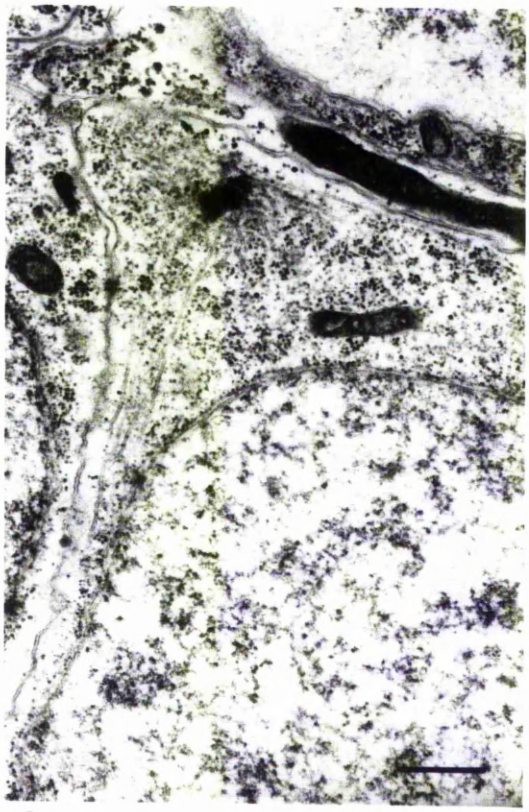

A

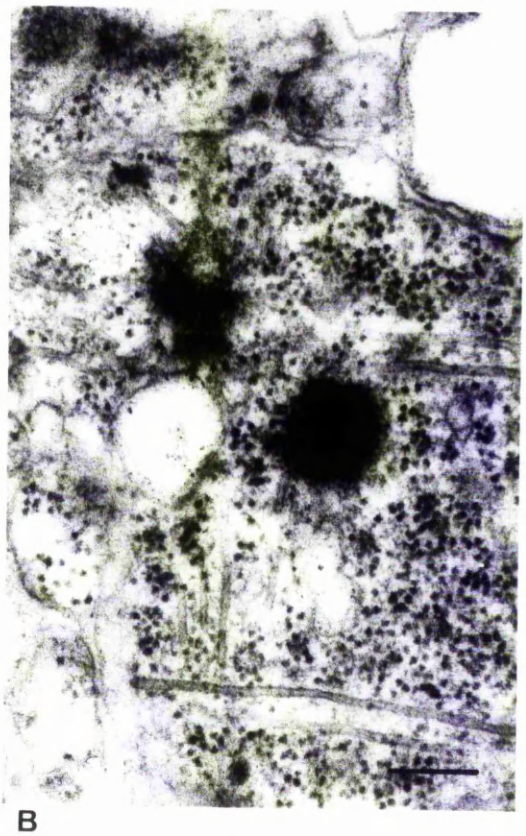

B

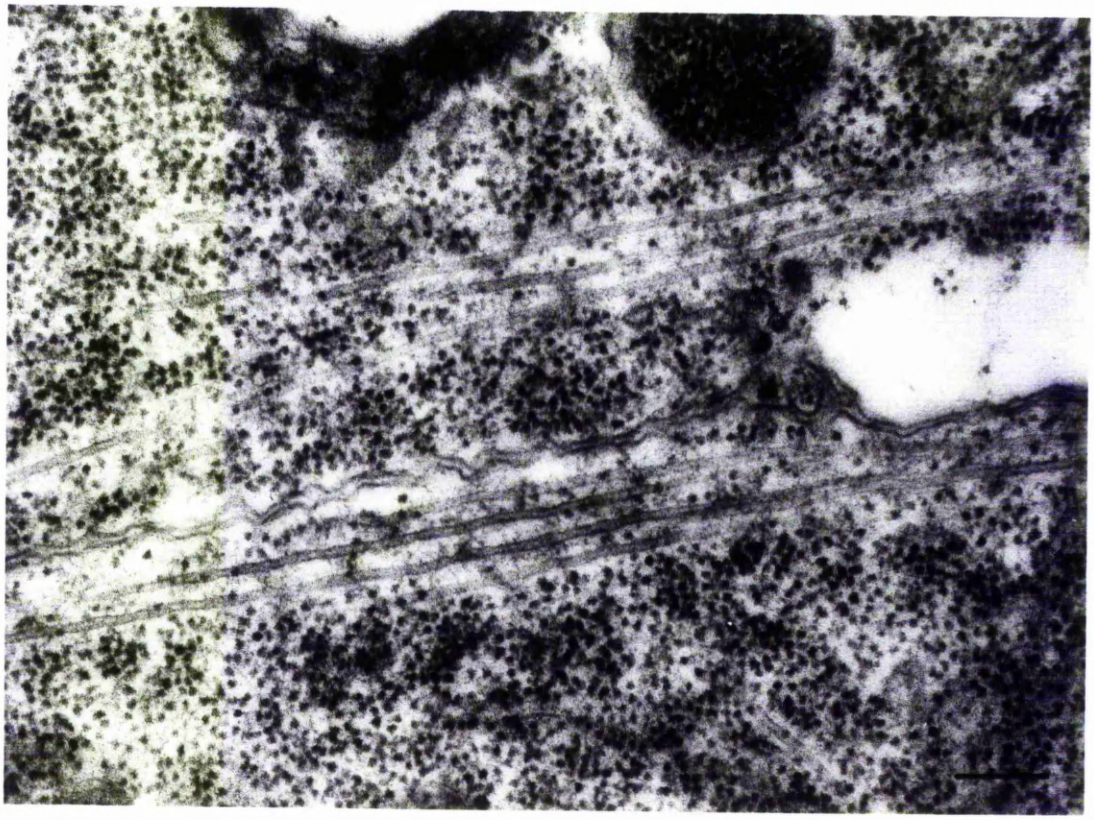

Fig.6 Confocal image of anti-α-tubulin localization in 18hr taxol incubated cells of the optic lobe of a *Drosophila* 3rd instar larva. One microtubule array or one microtubule aster is present in each cell. Confocal laser scanning microscopy. Scale bar, 10μm.

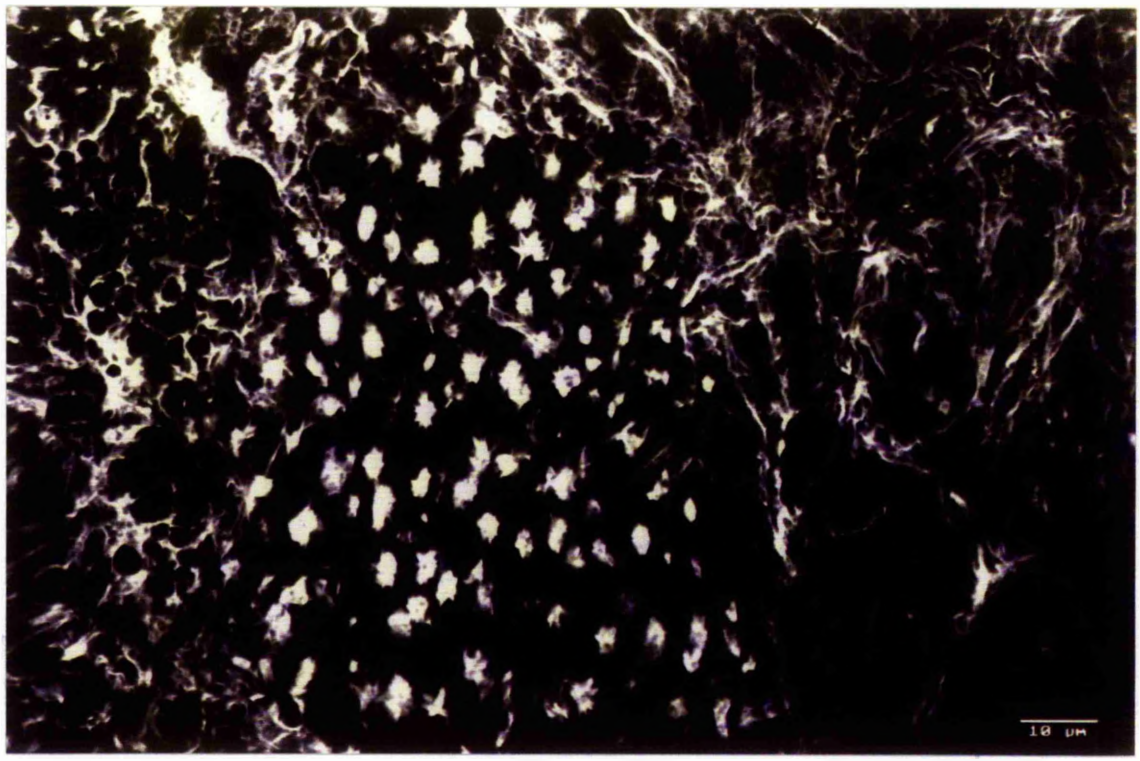
10 um

Fig.7 Neuroblast cell (in the optic lobe of a *Drosophila* 3rd instar larva) at interphase after an 18hr taxol incubation. Microtubules present as one large array next to the nuclear surface (arrow). No microtubules are present outside of this array. Scale bar, 1μm.

Fig.8 **(a)** Microtubule array in a neuroblast cell at interphase after an 18hr taxol incubation. Microtubule 'chains' are present within the array. Scale bar, 0.2μm. **(b)** Adjacent microtubules of microtubule 'chains' appear to share some of the same protofilaments. Scale bar, 0.1μm.

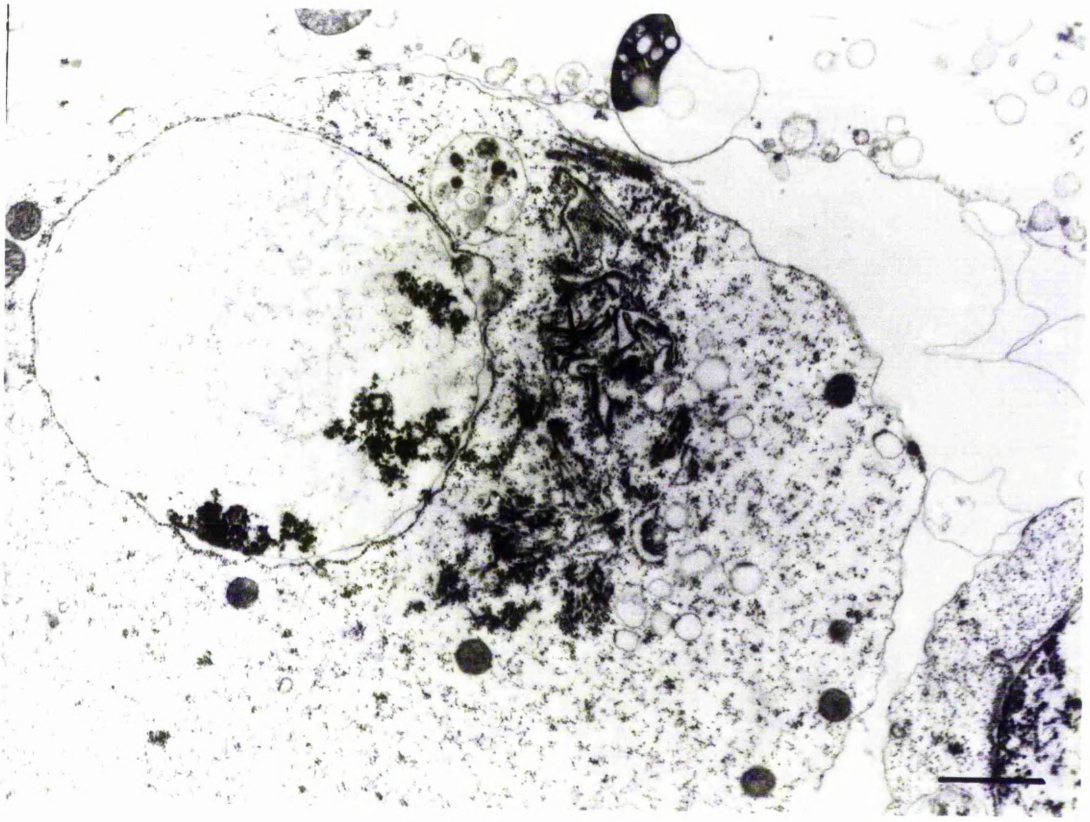

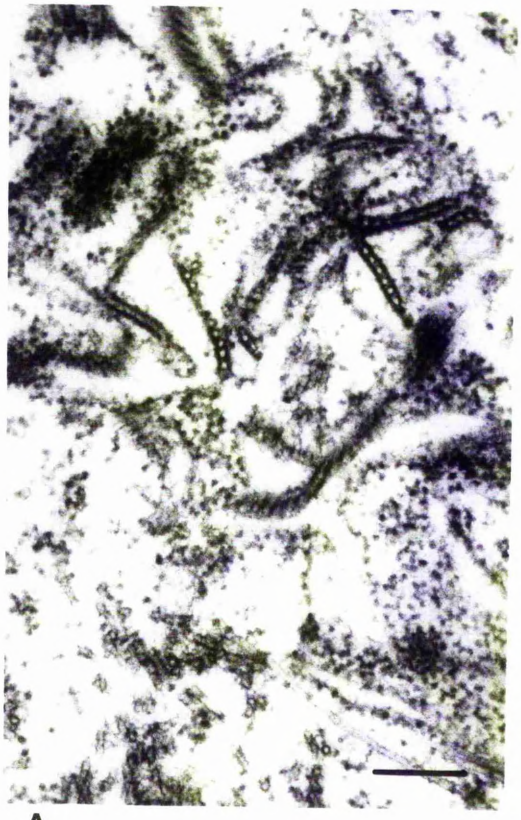

A

B

Fig.9 Neuroblast cell (in the optic lobe of a *Drosophila* 3rd instar larva) at interphase after an 18hr taxol incubation. Cross section of microtubules within a microtubule array. Scale bar, 0.2μm.

Fig.10 Neuroblast cell (in the optic lobe of a *Drosophila* 3rd instar larva) arrested in mitosis after an 18hr taxol incubation. A large microtubule aster. Chromatin is located around the periphery of the aster. Scale bar, 0.5μm.

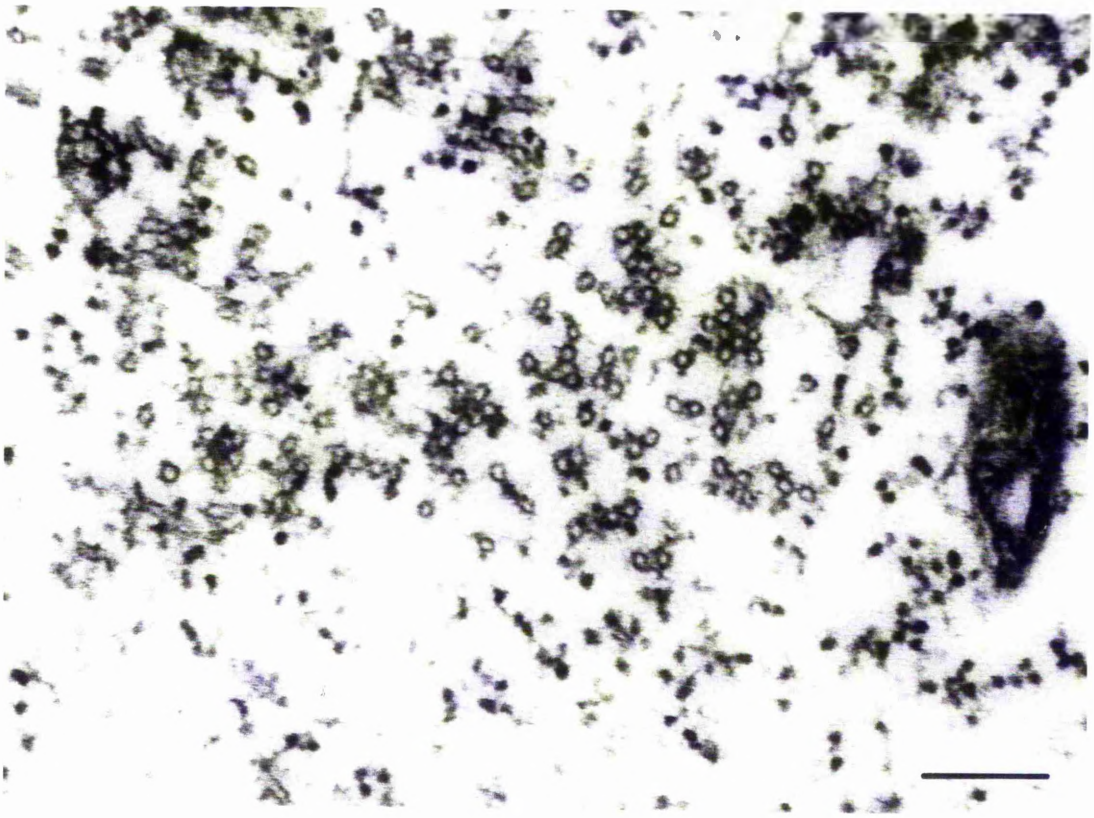

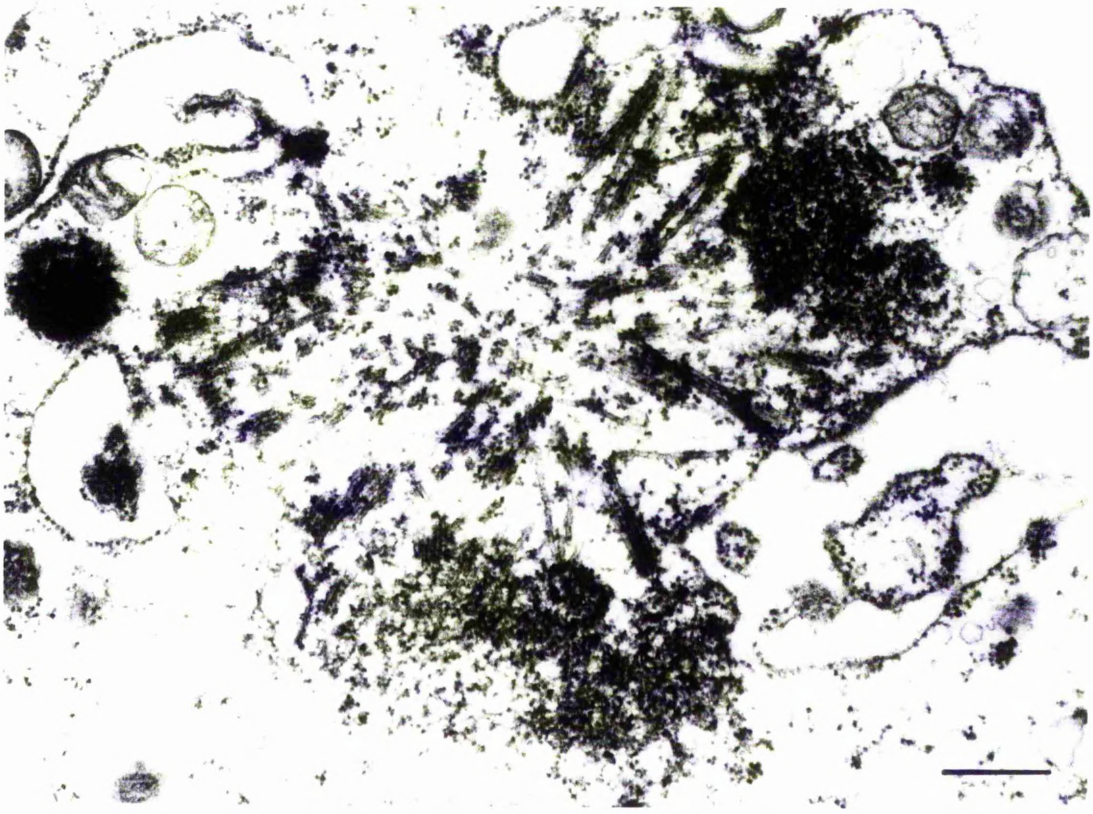

Chapter 8

The effect of taxol on centrosomal activity and protofilament number in MDCK cells

8.1 Introduction

This investigation deals with the same issue as that outlined in the Introduction of Chapter 7. Does taxol perturb microtubule protofilament number in cells which normally contain 13 protofilament microtubules? MDCK cells possess centriole containing centrosomes and therefore under normal circumstances are likely to nucleate 13 protofilament microtubules.

The question of the extent to which each cell's main nucleating-site (the centrosome) is involved during taxol induced microtubule assembly has also been addressed. It has been claimed that for certain mammalian cells in culture microtubules nucleated in the presence of taxol are not initiated at centriole-containing centrosomes (DeBrabander *et. al.*,1981).

Taxol incubation arrests mammalian cells in mitosis by disrupting the normal mitotic spindle (Schiff and Horwitz,1980) and induces many microtubule asters (DeBrabander *et al.*,1981). Are microtubule asters nucleated at typical microtubule nucleating sites? Are the proteins which nucleate microtubules at the centrosome present at the centres of microtubule asters? This is of particular importance in the case of γ–tubulin. This protein is apparently important for microtubule nucleation and may directly associate with the minus ends of microtubules (Stearns and Kirschner,1994). If γ–tubulin is present at microtubule nucleating sites in the form of 13 subunit rings it could specify protofilament number. This may explain why purified brain tubulin polymerizes into microtubules with various protofilament numbers *in vitro* (Wade et al.,1990). While

in contrast, microtubules that assemble onto centrosomes have 13 protofilament microtubules *in vitro* (Evans *et al.*, 1985).

Pericentrin as well as γ–tubulin is also apparently involved in microtubule nucleation (*Doxsey et al.*,1994). Therefore, the question of whether these two proteins are present at the centres of taxol induced asters has been investigated. Both γ–tubulin and pericentrin are apparently present at the centre of taxol and DMSO induced asters which do not contain centrioles in *Xenopus* meiotic egg extracts (Stearns and Kirschner,1994). Furthermore, a protein present at the spindle poles, which may play a role in spindle microtubule organization, is also present at the centre of each taxol induced aster in HeLa cells, CHO cells and PtK_2 cells (Kallajoki et al.,1992). Hence, there are indications that taxol-induced asters *in vivo* may be nucleated at typical microtubule-nucleating sites.

The effect of taxol on microtubule-organization in interphase MDCK cells has also been investigated and the localization of pericentrin and γ–tubulin established. Do pericentrin and γ–tubulin localize at any sites other than the centrosome after taxol incubation?

Sub-confluent populations of MDCK cells have been used throughout this investigation. The pair of centrioles in sub-confluent MDCK cells are separated by several micrometers (Bre *et al.*, 1987).

8.2 Results

8.2.1 Immunocytochemistry and ultrastructure of interphase MDCK cells

In the vast majority of MDCK cells microtubules are organised in a lattice which extends throughout the cytoplasm (Fig.1). Microtubules do not focus at a single site. Two spheres, which may be several micrometers apart, stain with affinity-purified XGC

anti-γ–tubulin antiserum (AP γ–tubulin antiserum) (Fig.2) and affinity-purified M8 anti-pericentrin antiserum (AP pericentrin antiserum) (Fig.3). Each of these stained spheres presumably represents a centriole with associated pericentriolar material. Microtubules do not radiate from the spheres which stain with AP pericentrin antiserum and AP γ–tubulin antiserum in interphase MDCK cells. Ultrastructural examination confirms the results obtained by immunocytochemistry. Very few microtubules associate with a region in the immediate vicinity of each centriole (Fig.4). Furthermore, there appears to be very little pericentriolar material around the centrioles. Microtubules are found throughout the cytoplasm (Fig.5).

8.2.2. Immunocytochemistry of mitotic MDCK cells

MDCK cells exhibit normal metaphase and anaphase mitotic spindle poles (Fig.6). The spindle poles stain with AP γ–tubulin antiserum (Fig.6b). At early telophase the microtubule array which radiates from each centrosome (Fig.7) is substantially larger than that which radiates from each spindle pole at anaphase (cf. Fig.6b and Fig.7). The early telophase array extends up to 10μm from each centrosome. At late telophase a microtubule array radiates from each centrosome (Fig.8) which is substantially larger than that which radiates from each centrosome at early telophase (cf. Fig.7 and Fig.8). At late telophase a microtubule array extends up to 30μm from each centrosome. Such a microtubule array extends throughout each incipient daughter cell at late telophase.

Up to and including telophase AP γ–tubulin antiserum stains one discrete sphere in each incipient daughter cell which is located at the centre of a microtubule array (see Chap.5, Fig.1). The stained spherical sites are presumably occupied by the centrosome. However, just prior to the completion of daughter cell separation (when the midbody-associated microtubule bundles have decreased substantially in diameter and the midbody stains with anti-α-tubulin) the AP γ–tubulin antiserum stains two closely associated

spheres in each incipient daughter cell (Fig.9). Each pair of stained spherical sites is presumably occupied by a centrosome. At this point an extensive microtubule array no longer radiates from each centrosome.

8.2.3 Immunocytochemistry and ultrastructure of taxol-incubated MDCK cells

Sub-confluent populations of MDCK cells have been incubated in 10μM taxol for periods of 30mins, 4hrs and 18hrs. The number of cells at interphase compared with the number at mitotic arrest depends on the length of time incubated in taxol (Table 1). This was determined by counting the number of interphase to mitotic arrested cells in the field of view at several randomly selected sites on each coverslip examined.

Table 1 : Proportion of cells at interphase and mitotic arrest after incubation in 10μM taxol for various lengths of time

Taxol Incubation	Interphase	Mitotic Arrest
30mins	95%	5%
4 hrs	75%	25%
18 hrs	20%	80%

8.2.4 Immunocytochemical studies of the effect of taxol on interphase microtubule organization and localization of γ–tubulin and pericentrin

8.2.4.1 MDCK cells at interphase after 30min taxol incubation

Microtubule organization is apparently no different from that of control cells (cf. Fig.1 and Fig.10). Furthermore, the localization of AP pericentrin antisera and AP γ–tubulin antiserum is the same as in the control cells (cf. Fig.2 and Fig.10).

8.2.4.2 MDCK cells at interphase after 4hr taxol incubation

Anti-α-tubulin staining reveals microtubules which are organized around the cell periphery in the vast majority of taxol incubated interphase cells (Fig.11). In many cells microtubules are organized in bundles which are oriented approximately perpendicular to the cell surface (Fig.11). In most cases the AP γ–tubulin antiserum does not stain the microtubule bundles (Fig.12). However, occasionally, one end of some of the microtubule bundles in a cell stain with AP γ–tubulin antiserum (Fig.13).

The AP γ–tubulin antiserum and AP pericentrin antisera, stain a pair of spheres, separated by several micrometers (Fig.12,14). Each stained sphere presumably represents a centriole and associated pericentriolar material. The ends of microtubules do not appear to be associated with these stained spheres.

8.2.4.3 MDCK cells at interphase after 18hr taxol incubation

Microtubules no longer predominate at the cell periphery. Anti-α-tubulin staining reveals microtubule bundles which are distributed throughout the cytoplasm at various

orientations (Fig.15). In most cases no staining of these microtubule bundles with γ–tubulin is detected. However, occasionally, one end of some of the microtubule bundles in a cell stain with AP γ–tubulin antiserum (Fig.16). The AP γ–tubulin antiserum and AP pericentrin antiserum, both stain a pair of spheres which may be several micrometers apart (Fig.17,18). Each stained sphere presumably represents a centriole and associated pericentriolar material. The ends of microtubules do not appear to be associated with these stained spheres.

8.2.5 Ultrastructural study of microtubule organization in MDCK cells at interphase after 18hr taxol incubation

Microtubule bundles at various orientations are apparent throughout the cytoplasm (Fig.19). No centrioles have been found associated with these microtubule bundles. Centrioles are surrounded by a small amount of pericentriolar material and have very few microtubules in their immediate vicinities (Fig.20).

8.2.6 Immunocytochemical study of the localization of pericentrin and γ–tubulin in mitotically arrested MDCK cells after taxol incubation

8.2.6.1 Mitotically arrested cells after 30min, 2hr, and 4hr taxol incubations

The results obtained for γ–tubulin and pericentrin localization were the same regardless of whether the cells had been incubated in taxol for 30mins or 4hrs. The majority of mitotically arrested cells have at least two microtubule asters (Fig.21) and it is not uncommon to find cells with up to 20 microtubule asters (Fig.22).

The AP γ–tubulin antiserum and AP pericentrin antiserum both stain two discrete spheres in each mitotically arrested cell (Fig's.21 and 22). Each stained sphere is located at the centre of a microtubule aster. The vast majority of mitotically arrested cells have more than two asters. However, the AP pericentrin antiserum only stains the centres of two asters in cases where there are more than two (Fig.22). The AP γ–tubulin antiserum always stains the centres of two microtubule asters and occasionally stains a diffuse region within the other asters in cases where there are more than two (Fig. 23).

8.2.6.2 Mitotically arrested cells after 18hr taxol incubation

Both AP γ–tubulin antiserum and AP pericentrin antiserum, stain two discrete spheres in each mitotically arrested MDCK cell. These stained spheres may be closely associated or several micrometers apart. Each stained sphere, of a pair of stained spheres which are several micrometers apart, is either located at the centre of a microtubule aster (Fig.24) or at the periphery of a microtubule aster (Fig.25). In contrast, pairs of stained spheres which are located side by side are clearly not associated with microtubule asters (Fig's.26 and 27).

The AP γ–tubulin antiserum occasionally stains a diffuse region within each microtubule aster which is not associated with a AP γ–tubulin antiserum stained sphere (Fig.28).

8.2.7 Ultrastructural study of microtubule organization in MDCK cells at mitotic arrest after 18hr taxol incubation

Sequential sections of several microtubule asters did not reveal any centrioles. there is no apparent difference in the diameters of microtubules present in the microtubule asters (Fig.29).

8.2.8 Microtubule protofilament number in MDCK cells at mitotic arrest after 18 hour taxol incubation

Numerous attempts to reveal microtubule protofilaments in MDCK cells initially proved unsuccessful. However, the protocol used to detect protofilaments was gradually modified from one experiment to the next. For example, several different detergent concentrations and detergent recipes have been used to extract MDCK cells. Also, different methods have been employed in order to maintain the experimental environment at 37^{o}C prior to the fixation of cells. Furthermore, both araldite (alcohol miscible resin) and nanoplast (aqueous miscible resin) resins have been used to embed cells. The protocol which best permits detection of protofilaments is detailed in the Material and Methods (see Chap.2, section 2.6.6). This modified protocol has only recently been established. Therefore, it is only now being fully exploited with regard to protofilament number in taxol incubated MDCK cells.

A preliminary investigation has been conducted of microtubule protofilament number in taxol induced microtubule asters. Some microtubule profiles have been found which reveal all of their protofilaments (Fig.30a). These microtubules appear to have 12 protofilaments (Fig.30b).

8.2.9 Specificity of antibody staining

MDCK cells have been incubated with all the fluorescently conjugated secondary antibodies used in the studies above but without incubation with the appropriate primary antibodies. After these procedures there is no detectable staining of these cells.

8.2.10 Controls

MDCK cells have been incubated in 0.1% DMSO for 30mins, 4hrs and 18hrs and subsequently stained with anti-α-tubulin, AP γ–tubulin antiserum, and AP pericentrin antiserum. The various 0.1% DMSO incubations had no apparent effect on microtubule organization or on γ–tubulin and pericentrin localization. Furthermore the ultrastructure of MDCK cells which have been incubated in 0.1% DMSO for 18hrs appears no different from that of normal MDCK cells.

8.3 Discussion

8.3.1 Microtubule organization and localization of pericentrin and γ–tubulin in normal interphase MDCK cells

γ-Tubulin and pericentrin are both present at two discrete sites, separated by several micrometers, in each cell. Each site presumably represents a centriole and its associated pericentriolar material. Microtubules are distributed throughout the cytoplasm and do not radiate from the centrioles and their associated pericentriolar material. Consequently, it has been suggested that centrosomes do not function as the principal microtubule nucleating-sites in MDCK cells (Bre´*et al.*,1987,1990). Both γ–tubulin and pericentrin are apparently involved in microtubule nucleation. However, neither protein appears to be present at any site in interphase MDCK cells other than around the centrioles. Is it possible that pericentriolar like material, which contains both proteins, is dispersed at a low concentration within a large region of the cytoplasm? If so, γ–tubulin and pericentrin may not be detected by immunofluorescence. Alternatively, can microtubules be nucleated without the involvement of either γ–tubulin or pericentrin in MDCK cells? In *S. pombe*, γ–tubulin is associated with the spindle pole bodies

throughout the cell cycle (Horio *et al.*, 1991). However, the spindle pole bodies only appear to nucleate microtubules during mitosis. It has been demonstrated that γ–tubulin alone is not sufficient for microtubule nucleation (Masuda *et al.*, 1992). This indicates that a γ–tubulin modification or alternatively an additional protein(s) is required for microtubule nucleation. If additional proteins are involved in nucleation this raises the possibility that in some cases such proteins could even function independently of γ–tubulin.

8.3.2 Microtubule organization and the localization of γ–tubulin and pericentrin in MDCK cells at interphase after taxol incubation

Microtubules predominate around the cell periphery in the vast majority of MDCK cells at interphase after taxol incubation. In most cells, bundles of microtubules are scattered around the cell periphery after a 4hr taxol incubation and throughout the cell after an 18hr taxol incubation. There is no evidence that pericentrin is present in the vicinity of microtubules located at the cell periphery or that it is associated with microtubule bundles. Occasionally, γ–tubulin appears to be present at one end of a microtubule bundle. However, this appears to be an exceptional rather than a common association. Soluble γ-tubulin within the cytoplasm (Stearns and Kirschner,1994) may occasionally nucleate microtubules in the presence of taxol and give rise to microtubule bundles which are associated with γ-tubulin. However, the vast majority of microtubule bundles are not associated with γ-tubulin. If γ-tubulin is essential for microtubule nucleation how are these microtubule bundles formed? One possibility is that taxol merely lowers the critical concentration of tubulin required for spontaneous self-assembly of tubulin sub-units without the requirement of centrosomally-associated proteins.

8.3.3 Taxol induced microtubule asters in mitotically arrested MDCK cells

γ–Tubulin and pericentrin are present at both spindle poles in normal mitotic MDCK cells. After a 30min, 4hr or 18hr taxol incubation, mitotically arrested MDCK cells contain several microtubule asters. After a 30min or 4hr taxol incubation, γ–tubulin and pericentrin are concentrated at a pair of discrete spheres in each mitotically arrested cell. Each γ-tubulin and pericentrin containing sphere is located at the centre of a microtubule aster. Therefore, each discrete sphere presumably represents a centriole-containing centrosome, which under normal conditions would have formed a spindle pole. Therefore, the nucleating activity of the centrosome does not appear to have been blocked after a 4hr taxol incubation.

After an 18hr taxol incubation γ–tubulin and pericentrin are concentrated at two discrete spheres which are either several micrometers apart or located side by side in each mitotically arrested cell. Each γ-tubulin and pericentrin containing sphere presumably represents a centriole-containing centrosome. Each centrosome, of a pair of centrosomes which are several micrometers apart, is either located at the centre of a microtubule aster or at the periphery of a microtubule aster. Centrosomes which are located side by side as a pair are not associated with microtubule asters. It is a possibility that the latter example represents cells that may have attempted, unsuccessfully, to revert to interphase which has resulted in the disassembly of the microtubule asters associated with the centrosomes. Taxol stabilizes microtubules *in vitro* (Schiff *et al.,* 1979; Wilson *et al.,*1985; Williams and Rone,1989). However, microtubules in the presence of taxol are still subject to dynamic instability *in vivo*, albeit at reduced levels (DeBrabander,1981,1986).

8.3.4 Are γ–tubulin and pericentrin present in taxol-induced asters which do not contain centrioles?

Microtubule asters can be induced if purified tubulin is added to meiotic egg extract (which does not contain centrioles) and subsequently incubated in taxol or high concentrations of DMSO *in vitro*. (Stearns and Kirschner,1994). Immunofluorescence has revealed that both γ–tubulin and pericentrin are present at these taxol and DMSO induced asters. Furthermore, biochemical studies have confirmed the presence of γ–tubulin in these asters (Stearns and Kirschner,1994). In contrast, this investigation has found no evidence whatsoever that pericentrin associates with taxol-induced asters, which do not contain centrioles, in MDCK cells. In addition, AP γ–tubulin antiserum does not consistently stain taxol induced asters which do not contain centrioles. The apparent difference in the *in vitro* and *in vivo* localization of pericentrin and γ–tubulin at taxol induced asters has not been accounted for. It is possible that pericentrin is always, and γ–tubulin is often, present at such low concentrations at MDCK cell taxol induced asters, that they are not detected by immunofluorescence. However, this would seem unlikely. There are large numbers of microtubules in these asters and therefore a high concentration of microtubule ends. Furthermore, γ–tubulin and pericentrin are detected by immunofluorescence in asters *in vitro* (Stearns and Kirschner,1994).

8.3.5 Microtubules escape from centrosomes in MDCK cells?

It is possible to interpret the results in this investigation in terms of microtubule escape from the centrosome.

8.3.5.1 Microtubules escape from interphase centrosomes of MDCK cells?

Microtubules do not radiate from the centrosome in interphase MDCK cells. However, γ–tubulin only appears to concentrate at the centrosome. If γ–tubulin is responsible for microtubule nucleation then it is a distinct possibility that microtubules are released and escape from interphase centrosomes. Two different lines of evidence support the possibility that microtubules are nucleated at, and subsequently released from, the centrosome to form the interphase cytoplasmic array in MDCK cells.

The microtubule array associated with the spindle poles increases in size from anaphase until late telophase. At late telophase the centrosomally associated microtubule array radiates across the entire incipient cell body. Just prior to the terminal stages of daughter cell separation, AP γ–tubulin antiserum stains two closely associated spheres in each incipient daughter cell. Prior to this point only one AP γ–tubulin antiserum stained sphere is present in each incipient daughter cell. Presumably, each pair of closely associated stained spherical sites is occupied by a centrosome, with one centriole located in each stained site. The pair of centrioles of a centrosome in an interphase MDCK cell are separated by up to several micrometers (Buendia *et al.*,1990). Consequently, it appears that the incipient daughter cells enter interphase prior to the completion of daughter cell separation. At this point an extensive microtubule array no longer radiates from the centrosome. Instead, a non-focused network of microtubules is present throughout the incipient cell body. Consequently, it appears that the centrosome may be responsible for the nucleation of microtubules which are subsequently released to form the non-focused cytoplasmic interphase array.

A 4hr taxol incubation results in a distribution of microtubules predominantly at the cell periphery. Such microtubules are sometimes organized into bundles; these appear to be rarely associated with γ–tubulin. Taxol may enable soluble γ–tubulin within the cytoplasm (Stearns and Kirschner *et al.*,1994) to occasionally nucleate microtubules. However, it is also possible that the predominance of microtubules around the cell

periphery is an indication that taxol induces an increase in microtubule initiation and escape at the centrosome.

Taxol induces microtubule bundles in PtK_2 cells which are not associated with the centrosome. Consequently, it has been claimed that microtubules are not nucleated at the centrosome in the presence of taxol (DeBrabander *et al.*,1981). However, evidence indicates that the centrosome is not blocked from nucleating microtubules during taxol induced mitotic arrest. It is clear that a pair of centrosomes nucleate two microtubule asters in taxol incubated mitotically arrested MDCK cells. Furthermore, microtubules are clearly nucleated from their normal acentriolar MTOC's in the presence of taxol in epidermal cells of the *Drosophila* wing blade (Mogensen and Tucker,1990). Therefore, since the spindle poles and acentriolar MTOC's nucleate microtubules in the presence of taxol then it would appear possible that the interphase centrosome would also nucleate microtubules in the presence of taxol.

It is unlikely that microtubules would be required to escape from the spindle poles of normal cells or from the acentriolar MTOC's of normal epidermal cells of the *Drosophila* wing blade. The majority of microtubule ends probably must remain anchored to the spindle poles to enable chromosomal separation to occur. In normal epidermal wing cells microtubule minus ends are anchored to the apical cell surface at their MTOC. Their plus ends are anchored to cell junctions at the basal cell surface. Therefore, these microtubules are most likely to be relatively stable and probably perform a structural role by maintaining cell shape. In both the above cases it would appear to be advantageous for microtubules to remain anchored to their nucleating sites. This may explain why microtubules are always associated with the spindle poles after a 4hr taxol incubation and why microtubules are associated with the acentriolar MTOC's in epidermal cells of the *Drosophila* wing blade after taxol incubation.

In contrast, it may be necessary for interphase microtubules to be released from the centrosome to establish the cytoplasmic array. For example, the number of reconstituted microtubules at the centrosome immediately after cold treatment exceeds the number of microtubules normally associated with the centrosome (Vorobjev and

Chentsov, 1983). Therefore, it has been suggested that microtubules disengage from the centrosome to form the cytoplasmic network. Microtubules are nucleated at the neuronal centrosome which is apparently the only site of γ–tubulin concentration (Bass and Joshi,1992). If neuronal microtubules require γ–tubulin for their nucleation then they must subsequently escape and be translocated into the nerve axon (Ahmad *et al.*,1994). γ– Tubulin is only concentrated at the centrosome in pillar cells in the mouse organ of Corti (personal communication, Mogensen and Tucker, University of St. Andrews). However the minus ends of several thousand microtubules are located approximately one micrometer from the centrosome (Tucker *et al.*,1992). Therefore, microtubule escape from the centrosome may account for the majority of microtubles in interphase MDCK cells after incubation in taxol. Taxol may directly or indirectly induce an increase in the rate of microtubule nucleation and release from the centrosome. Therefore, microtubules may be nucleated at and escape from the centrosome in normal interphase MDCK cells. This may be a phenomenon which occurs at interphase centrosomes generally but which is more pronounced in MDCK cells.

8.3.5.2. Microtubules released from mitotic spindle poles prior to depolymerization?

Apparently, dynamically unstable microtubules are subject to many short catastrophic events rather than a few long ones (McBeath and Fujiwara,1990). Consequently, the length of time required to completely disassemble a microtubule by catastrophic events is substantially greater than actually occurs. Therefore it has been suggested that the complete disassembly of a microtubule may also require minus end depolymerization. There is evidence that microtubules are released from the interphase centrosome and subsequently depolymerize from their minus ends in LT-cells from the goldfish scale (McBeath and Fujiwara,1990). Microtubule release from the spindle poles

and minus end depolymerization may also be occurring in MDCK cells. This phenomenon may have been revealed by taxol incubation.

γ–Tubulin and pericentrin are both present at a pair of discrete spheres in each mitotically arrested MDCK cell after an 18hr taxol incubation. Each stained sphere presumably represents a pair of centrioles and associated pericentriolar material which under normal circumstances would have formed the centrosome/spindle poles. In this investigation centrosomes have been found at the centre of microtubule asters, at the periphery of microtubule asters and completely isolated from microtubule asters. When centrosomes are at the centre of, or at the periphery of microtubule asters, a centrosomal pair is separated by several micrometers. However, a pair of centrosomes are always located side by side when they are completely isolated from microtubule asters.

One possible interpretation of these results is that centrosomally nucleated microtubule asters are released from their centrosomes. Subsequently, the microtubule asters may depolymerize as a pair of centrosomes migrate towards each other. This could represent mitotically arrested MDCK cells which attempt unsuccessfully to revert to interphase. Consequently, it is possible that the normal spindle poles must release spindle microtubules with 'uncapped' minus ends in order that they can be completely depolymerized at the end of mitosis.

Why has microtubule release not been detected at normal spindle poles if this phenomenon does occur? This phenomenon may not be apparent since identifying free minus ends would be very difficult due to the density of microtubules around the spindle poles. In addition, depolymerization events are likely to be rapid and the total number of such events may occur over a period of time rather than all at once. In contrast, if microtubules are released from the centrosomes of taxol incubated mitotically arrested MDCK cells they are likely to depolymerize relatively slowly. Taxol substantially reduces dynamic instability *in vivo* (DeBrabander *et al.*,1986). Consequently, the centrosomally nucleated microtubule asters may persist even after they have been released from the centrosome in the presence of taxol.

8.3.5.3 Model of microtubule release and escape from the centrosome

Microtubule release and escape from the centrosome may be important in order to establish the interphase microtubule array. A model is proposed for microtubule release from the centrosome based on microtubule severing by a protein such as centrin (which has been implicated in microtubule severing in lower eucaryotes (Sanders and Salisbury,1994) and is present at the centrosome of higher eucaryotes throughout the cell cycle (Errabolu *et al.*,1994) (Fig.31).

The model proposed for microtubule release and escape from the centrosome can be further developed to incorporate microtubules which may be released from the centrosome in order that they can be completely disassembled at the end of mitosis : if the newly exposed minus end of a severed microtubule is not 'capped' then this microtubule could disassemble from its minus end as well as its plus end.

8.3.5.4 Taxol perturbs protofilament number of centrosomally nucleated microtubules?

It is evident that pericentrin does not appear to be present at taxol induced microtubule asters which do not contain centrioles. Therefore, it is possible that other proteins which are involved in microtubule nucleation and other aspects of microtubule organization may not be present at those microtubule asters which do not contain centrioles. Consequently, those taxol induced microtubule asters which do not contain centrioles may not be nucleated by typical microtubule-nucleating sites. The absence of specific nucleating proteins, such as pericentrin, and perhaps other microtubule-organizing proteins as well, may effect the protofilament number of aster microtubules. This is different from the situation in *Drosophila* wing epidermal cells where microtubule

assembly was still nucleated in the presence of taxol at the normal sites (Mogensen and Tucker,1990).

The protofilament number of microtubules in taxol induced asters is nevertheless of interest. Pericentrin does not appear to be present in those asters which do not contain centrioles. What is the protofilament number of aster microtubules in the absence of certain nucleating proteins? If, for example, the protofilament number of these microtubules is thirteen this would indicate that pericentrin is unlikely to contribute towards the specification of protofilament number. Alternatively, the protofilament number may have a value different from thirteen. This could be the result of the absence of specific centrosomal proteins at microtubule asters or a taxol induced modification of a protein(s). Therefore, ascertaining which centrosomal proteins are present in taxol induced asters may give a valuable insight into the control of microtubule organization.

The ultrastructure of microtubule asters does not appear to reveal any obvious change in aster microtubule diameter. However, a down-regulation from 13 protofilaments to 12 protofilaments would be difficult to detect by conventional electron microscopy. A protocol which appears to reveal microtubule protofilaments in MDCK cells has only recently been successfully modified. Therefore only a preliminary investigation has been carried out. Preliminary results appear to suggest that 12 protofilament microtubules are nucleated at taxol induced asters. However, an extensive study is required in order to observe a significant number of microtubules which consistently reveal all of their protofilaments. Furthermore, it will be important to determine the protofilament number of microtubules in asters which contain and do not contain centrioles.

Taxol appears to perturb microtubule protofilament number in *Drosophila* neuroblast cells and MDCK cells. Preliminary results indicate that microtubules are composed of 12 instead of the normal 13 protofilaments in MDCK cells. The majority of microtubules may be nucleated at the centrosome and subsequently escape in MDCK cells incubated in taxol. Therefore, it is possible that taxol can directly or indirectly interfere with microtubule nucleation at the centrosome. This would be consistent with the finding

that microtubule protofilament number is perturbed when they are nucleated from their normal MTOC's in the presence of taxol in epidermal cells of the *Drosophila* wing blade (Mogensen and Tucker,1990). Microtubules are mostly composed of 15 protofilaments in the normal epidermal cells. However, mostly 12 protofilament microtubules are nucleated when incubated in the presence of taxol. It remains to be established whether the protofilament number of microtubules is perturbed in taxol induced asters which contain centrioles in MDCK cells.

Fig.1 Confocal image of anti-α-tubulin localization in a group of MDCK cells. Anti-α-tubulin stains a non-focused network of microtubules in the interphase cells. In contrast, microtubules in the telophase cell (which are not associated with the midbody) radiate from a discrete site in each cell body. Confocal laser scanning microscopy. Scale bar, 10μm.

Fig.2 (a) 'Dual image' and 'projected Z-series' of AP XGC γ-tubulin antiserum localization (LHS) and anti-α-tubulin localization (RHS) in a sub-confluent group of MDCK cells. Scale bar, 20μm.

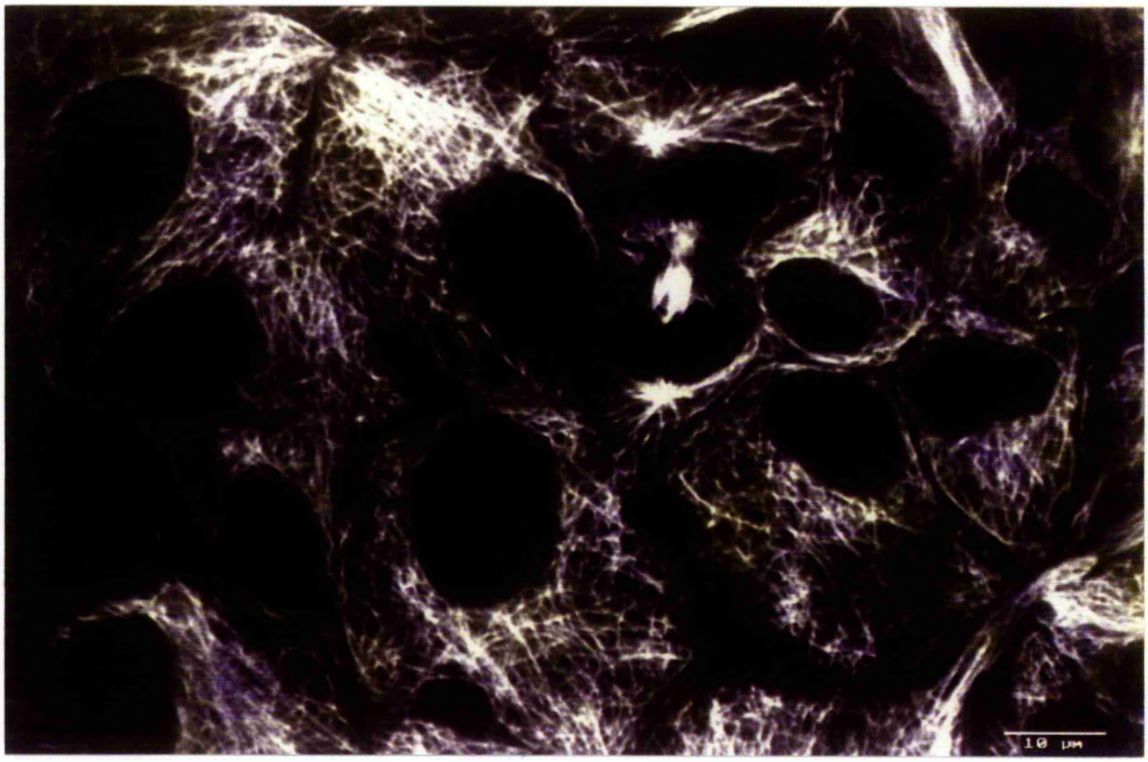
10 µm


20 µm

Fig.2 **(b)** 'Merged image' of Fig.2a. The AP XGC γ-tubulin antiserum (green) stains a pair of discrete spheres which are up to several micrometers apart in each interphase cell. Each stained spherical site is presumably occupied by one centriole and associated pericentriolar material. The anti-α-tubulin (red) stains a non-focused network of microtubules in the interphase cells. Confocal laser scanning microscopy. Scale bar, 10μm.

Fig.3 'Merged image' and 'projected Z-series' of AP M8 pericentrin antiserum localization (green) and anti-α-tubulin localization (red) in an interphase MDCK cell within a sub-confluent population. The AP M8 pericentrin antiserum stains a pair of discrete spheres. Each stained spherical site is presumably occupied by one centriole and associated pericentriolar material. The anti-α-tubulin stains a non-focused network of microtubules in the interphase cell. Confocal laser scanning microscopy. Scale bar, 10μm.

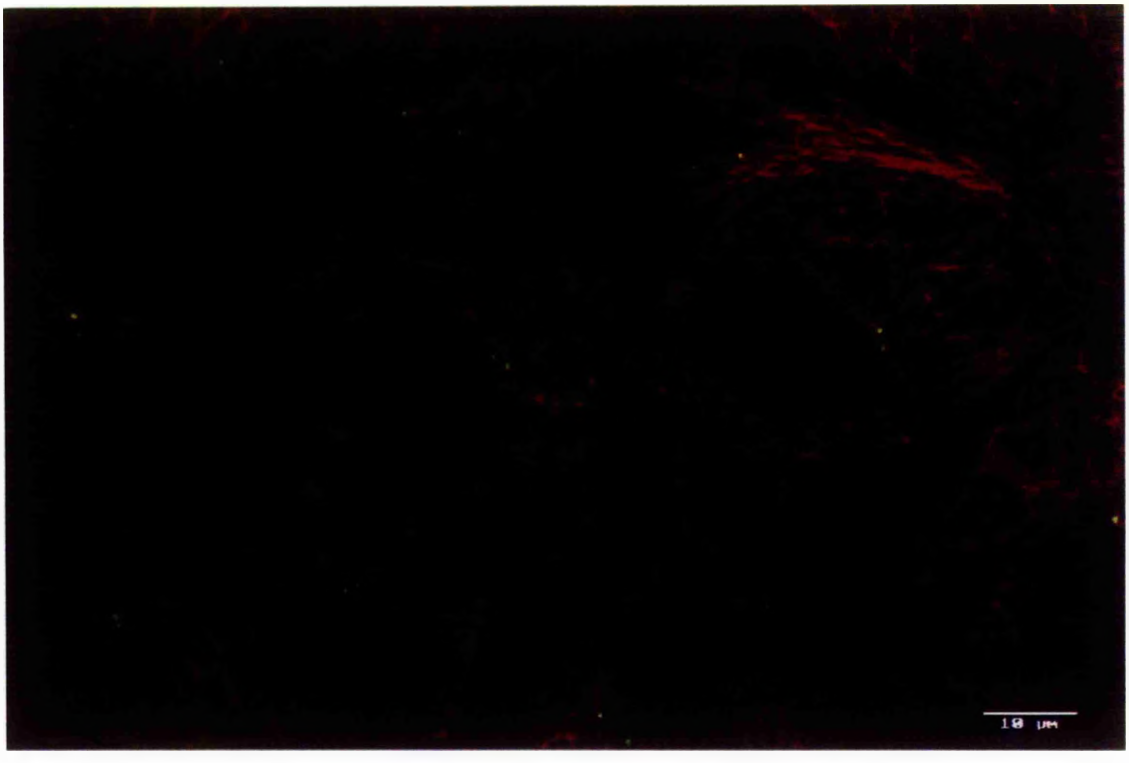
10 µm

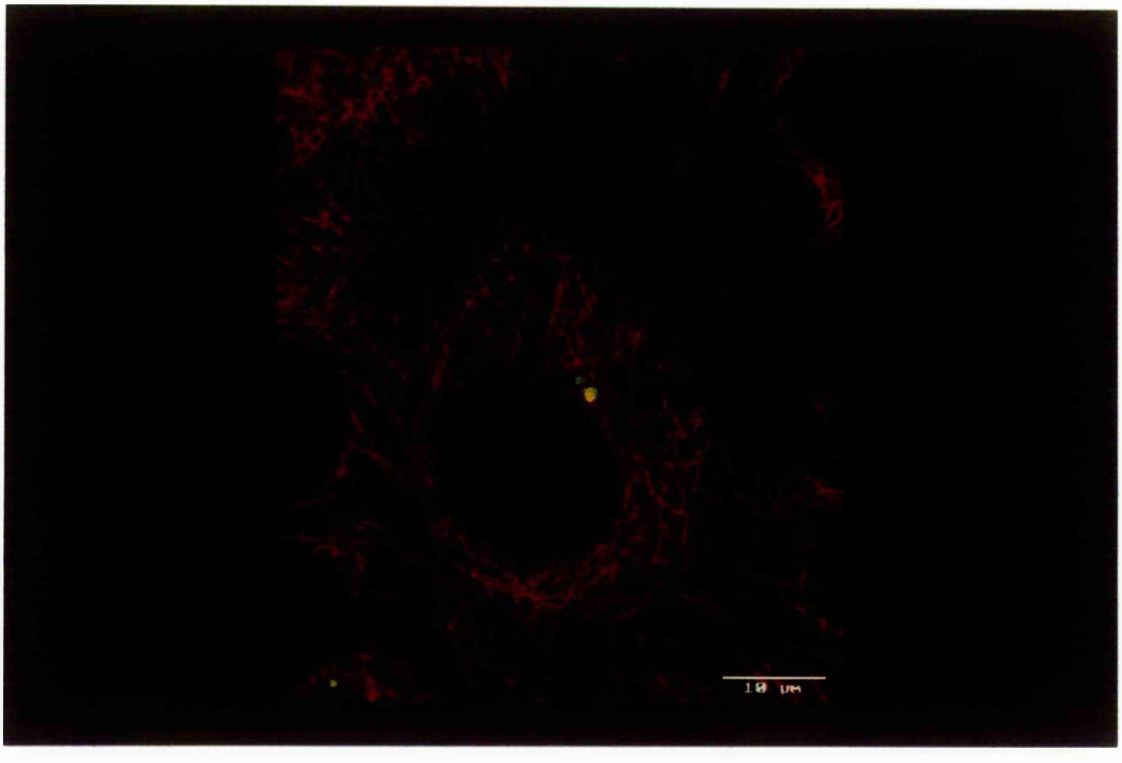
10 µm

Fig.4 Centriole and associated pericentriolar material in an interphase MDCK cell. Very few microtubule ends are located in the immediate vicinity of the centriole. Scale bar, 0.2μm.

Fig.5 Two interphase MDCK cells located side by side. Microtubules are distributed at various orientations within the cytoplasm of each cell. Scale bar, 0.5μm.

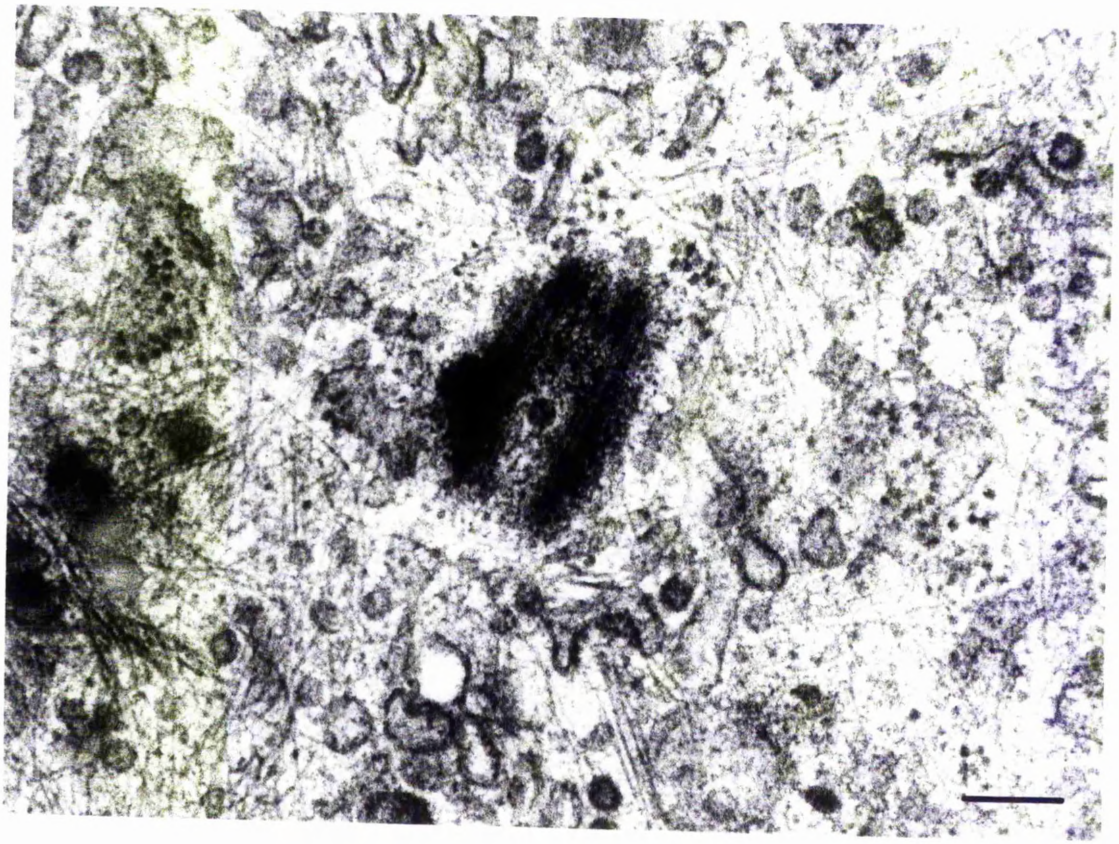

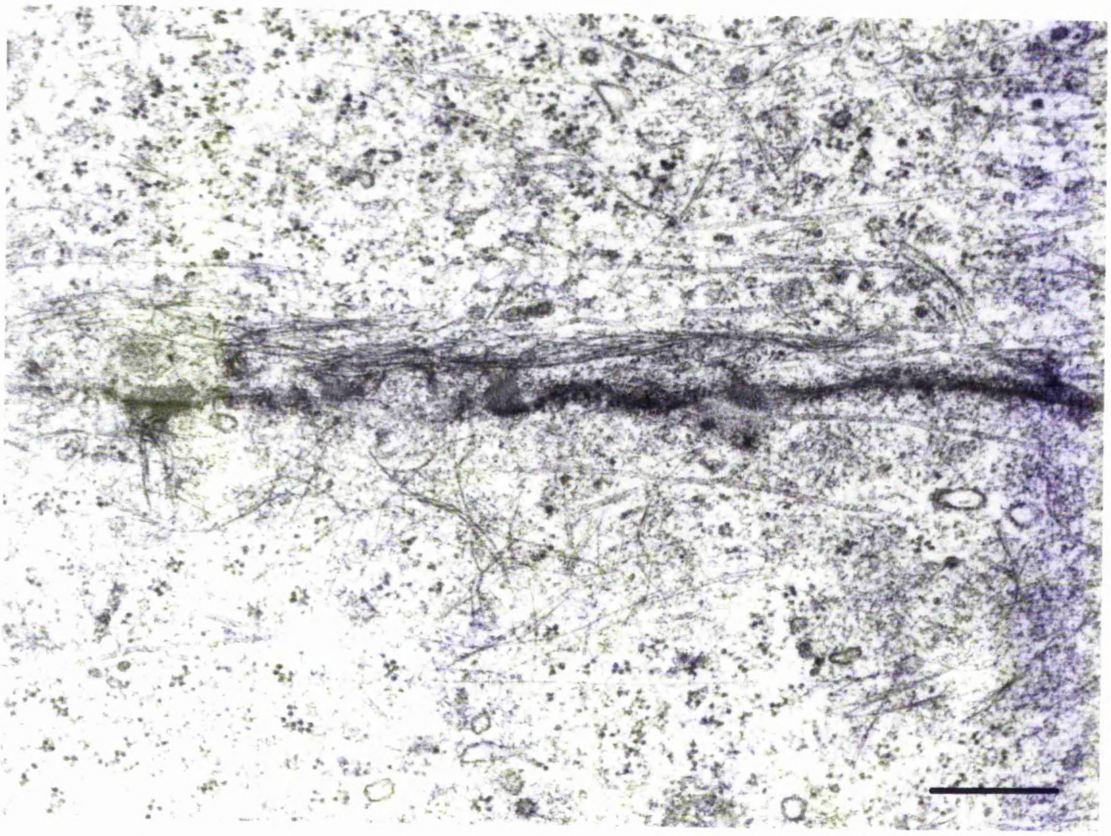

Fig.6 (a) 'Dual image' of an MDCK cell at metaphase. Phase contrast image (LHS) and confocal image of anti-α-tubulin localization (RHS) of the same MDCK cell at metaphase. The cell exhibits a conventional mitotic spindle. Scale bar, 10μm.

Fig.6 (b) 'Dual image' and 'projected Z-series' of AP XGC γ-tubulin antiserum localization (LHS) and anti-α-tubulin localization (RHS) in an MDCK cell at anaphase. The cell exhibits a conventional mitotic spindle. The spindle poles stain with the AP XGC γ-tubulin antiserum . Confocal laser scanning microscopy. Scale bar, 10μm.

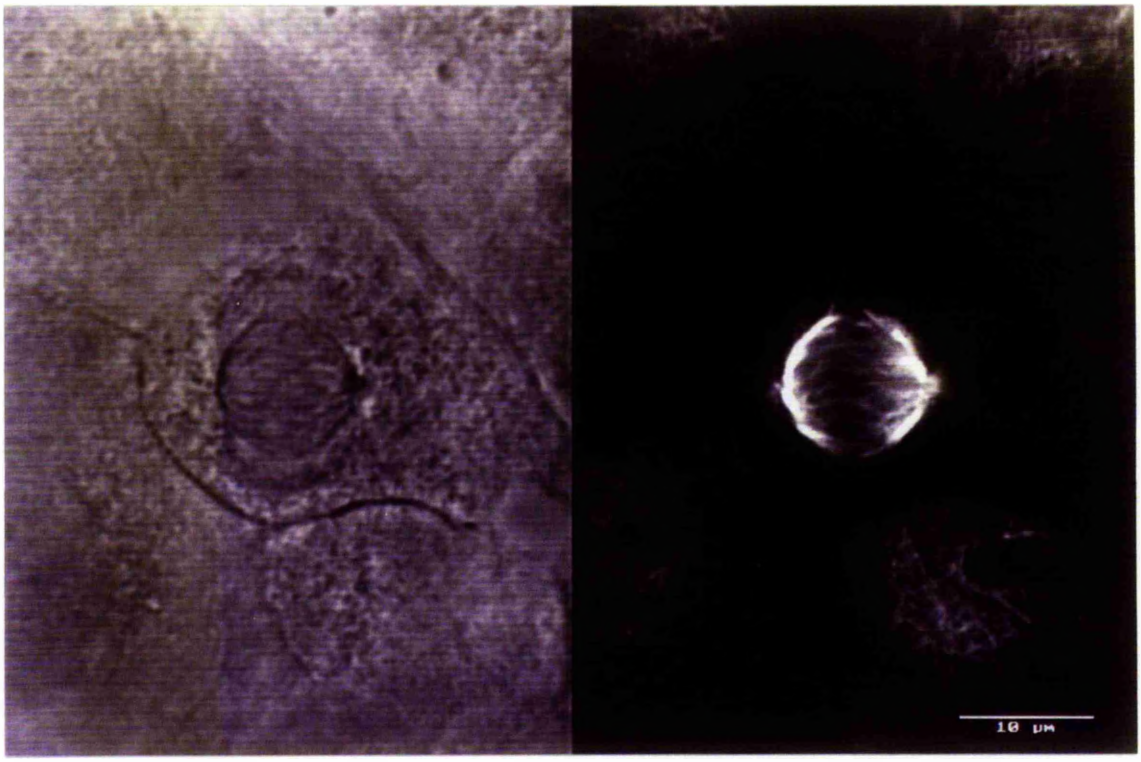
10 µm

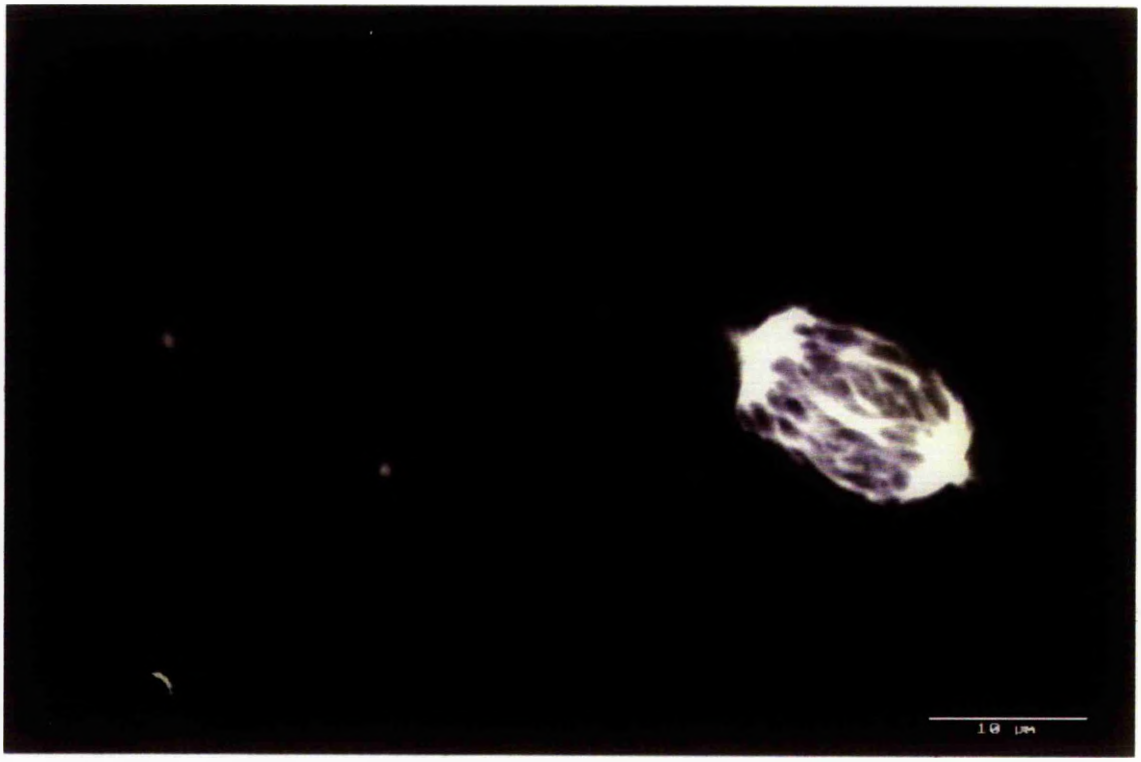
10 µm

Fig.7 'Projected Z-series' of anti-α-tubulin localization in an MDCK cell at early telophase. A microtubule array radiates from a site located beside the nucleus in each incipient daughter cell. Each array extends approximately 10μm from this site. Confocal laser scanning microscopy. Scale bar, 10μm

Fig.8 'Projected Z-series' of anti-α-tubulin localization in an MDCK cell at late telophase. A microtubule array radiates from a site located beside the nucleus in each incipient daughter cell. Each array extends approximately 30μm from this site. Confocal laser scanning microscopy. Scale bar, 10μm.

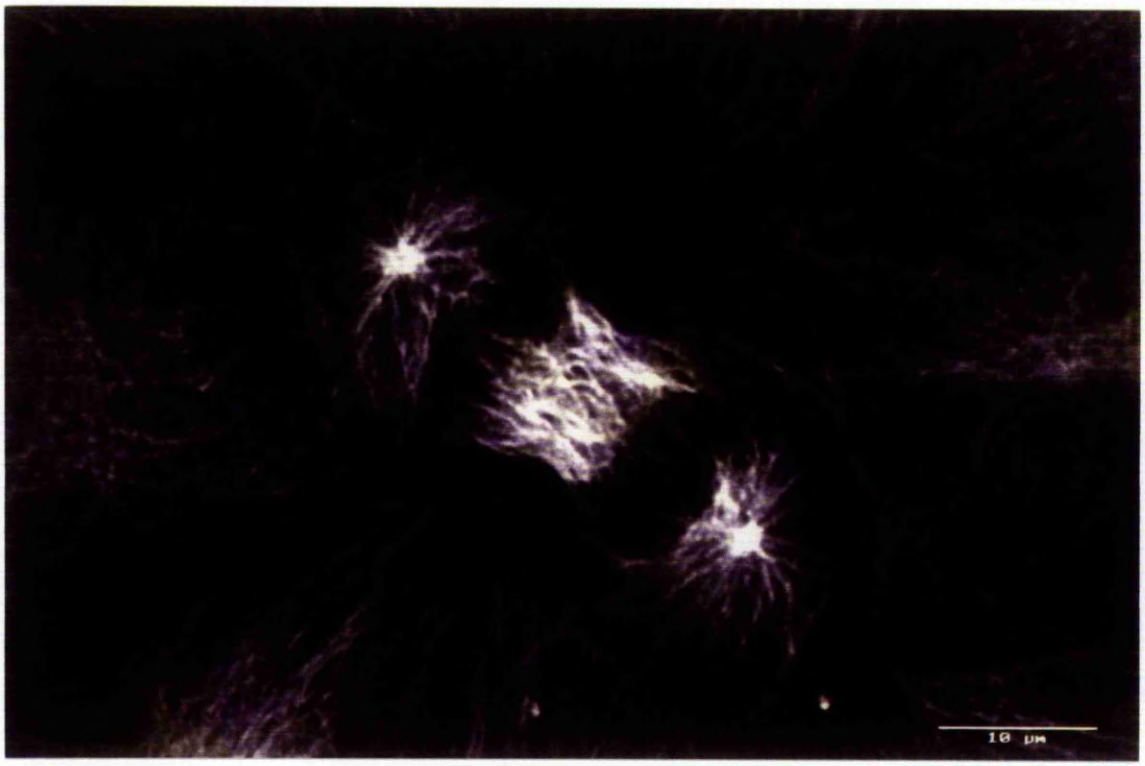
10 µm

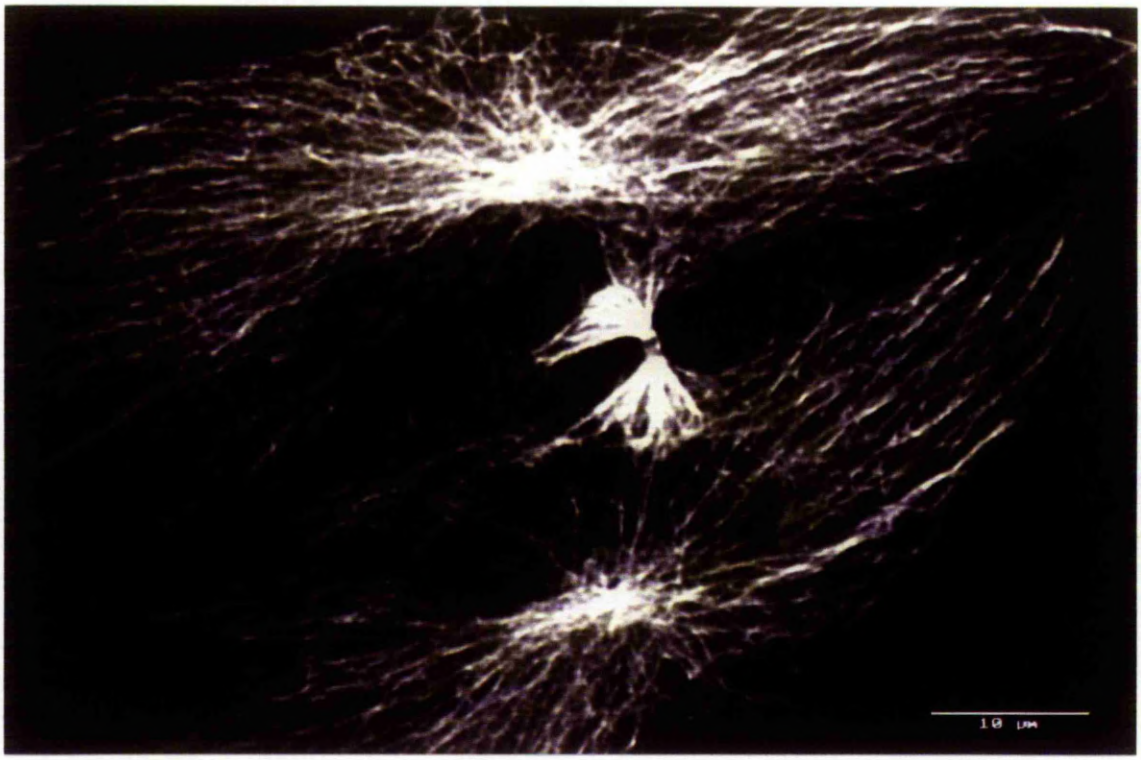
10 µm

Fig.9 'Dual image' and 'projected Z-series' of AP XGC γ-tubulin antiserum localization (LHS) and anti-α-tubulin localization (RHS) in the same incipient MDCK daughter cell just prior to the terminal stages of daughter cell separation. The AP XGC γ-tubulin antiserum stains a pair of closely associated discrete spheres which are not associated with an extensive microtubule array. Each stained spherical site is presumably occupied by one centriole and associated pericentriolar material. Scale bar, 5μm.

Fig.10 'Dual image' and 'projected Z-series' of AP XGC γ-tubulin antiserum localization (LHS) and anti-α-tubulin localization (RHS) in the same MDCK cell at interphase after a 30min, 10μM taxol incubation. The AP XGC γ-tubulin antiserum stains a pair of discrete spheres which are not associated with an extensive microtubule array. Each stained spherical site is presumably occupied by one centriole and associated pericentriolar material. Scale bar, 10μm.


AP gamma tubulin antiserum
Anti-alpha tubulin
5 µm

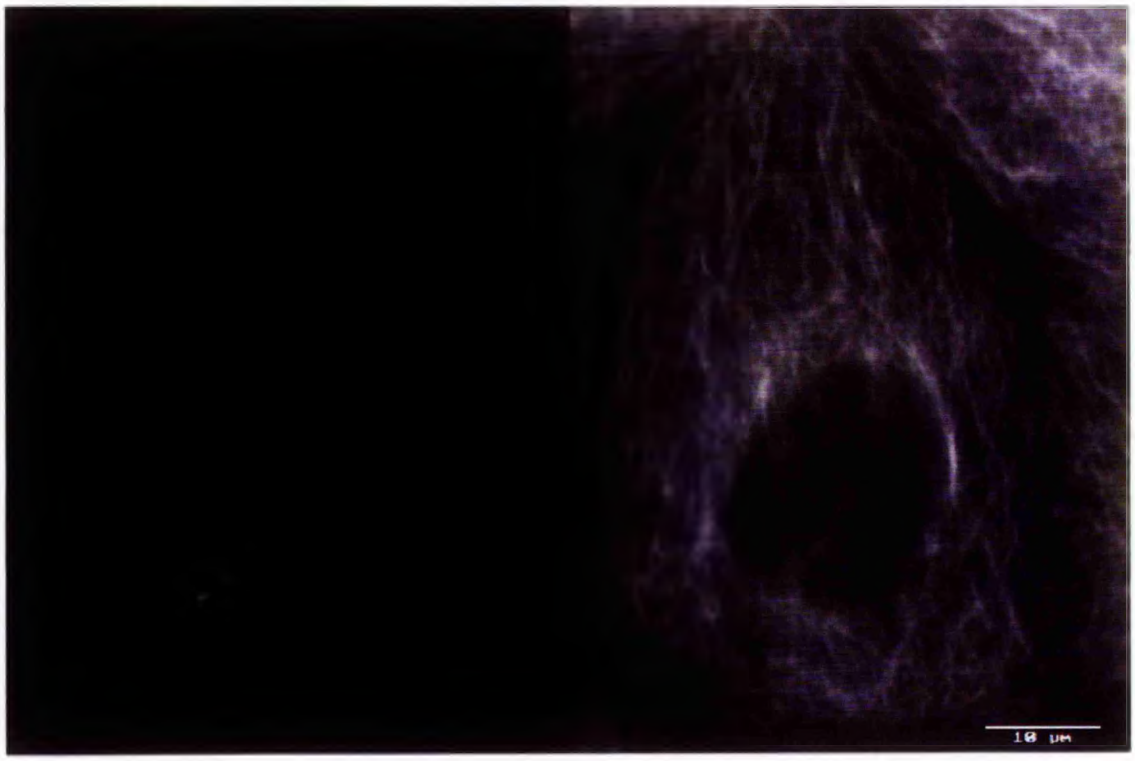
10 µm

Fig.11 **(a)** Confocal image of anti-α-tubulin localization in a group of MDCK cells at interphase (except one cell) after a 4hr, 10μM taxol incubation. Microtubules predominate around the cell periphery. In many cells the microtubules are oriented almost perpendicular to the cell surface. Confocal laser scanning microscopy. Scale bar, 20μm.

Fig.11 **(b)** Confocal image of anti-α-tubulin localization in a group of MDCK cells at interphase after a 4hr, 10μM taxol incubation. Microtubules predominate around the cell periphery. In many cells the microtubules are oriented almost perpendicular to the cell surface. Confocal laser scanning microscopy. Scale bar, 10μm.

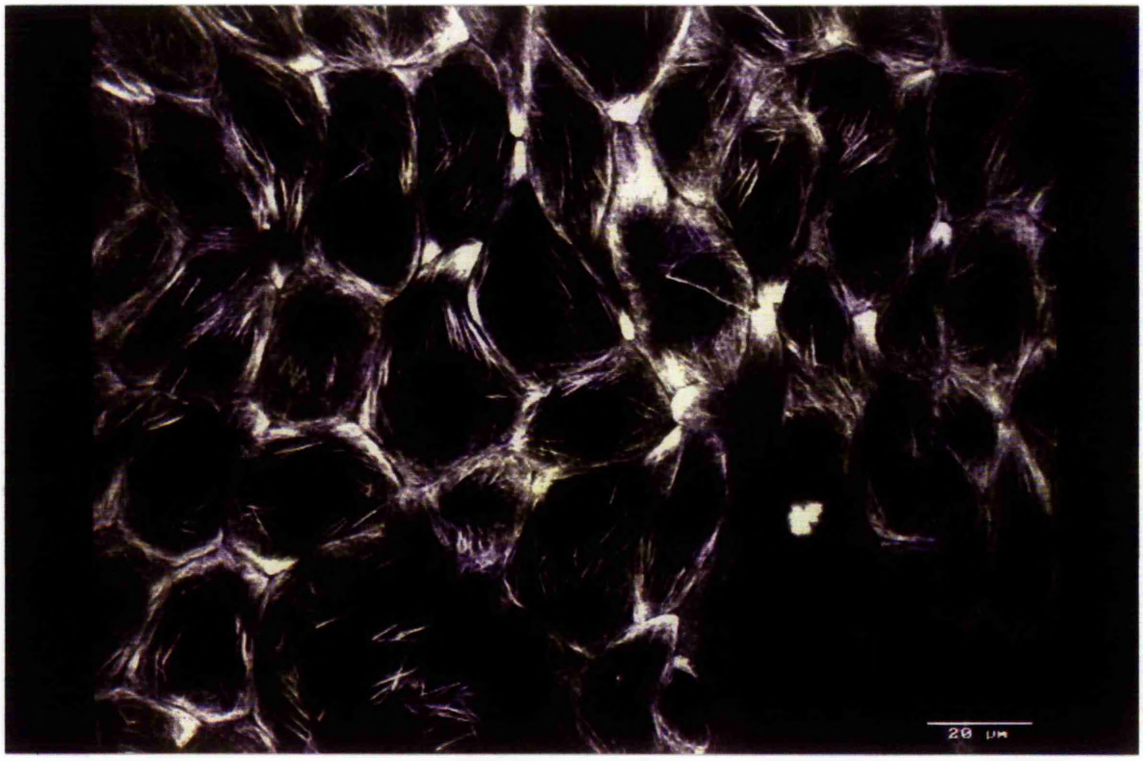
20 µm

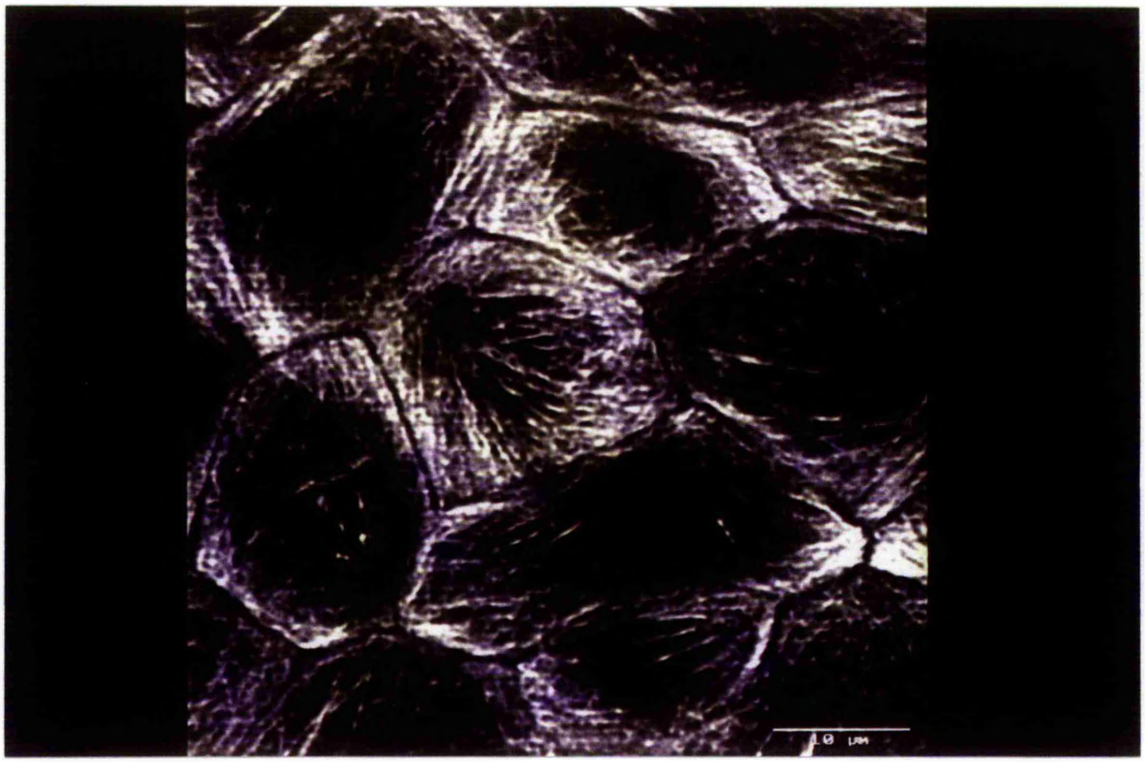
10 µm

Fig.12 'Merged image' of AP XGC γ-tubulin antiserum localization (yellow/green) and anti-α-tubulin localization (red) in the same MDCK cell at interphase after a 4hr, 10μM taxol incubation. The AP XGC γ-tubulin antiserum stains a pair of discrete spheres which are several micrometers apart. Each stained spherical site is presumably occupied by one centriole and associated pericentriolar material. The ends of microtubules do not appear to be associated with the stained spheres. The AP XGC γ-tubulin antiserum does not stain the ends of any of the microtubule bundles which are organized around the cell periphery. Confocal laser scanning microscopy. Scale bar, 5μm.

Fig.13 'Dual image' of AP XGC γ-tubulin antiserum localization (LHS) and anti-α-tubulin localization (RHS) in the same MDCK cell at interphase after a 4hr, 10μM taxol incubation. The AP XGC γ-tubulin antiserum stains one end of some microtubule bundles. Confocal laser scanning microscopy. Scale bar, 10μm.

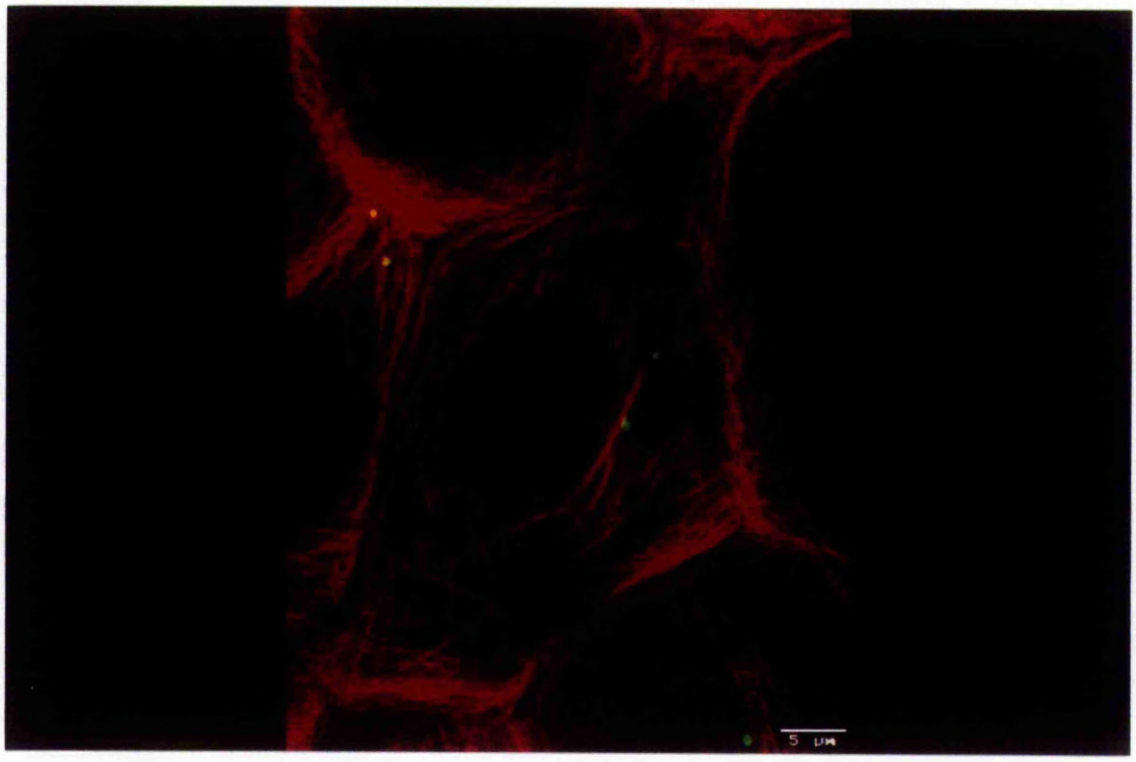
5 µm

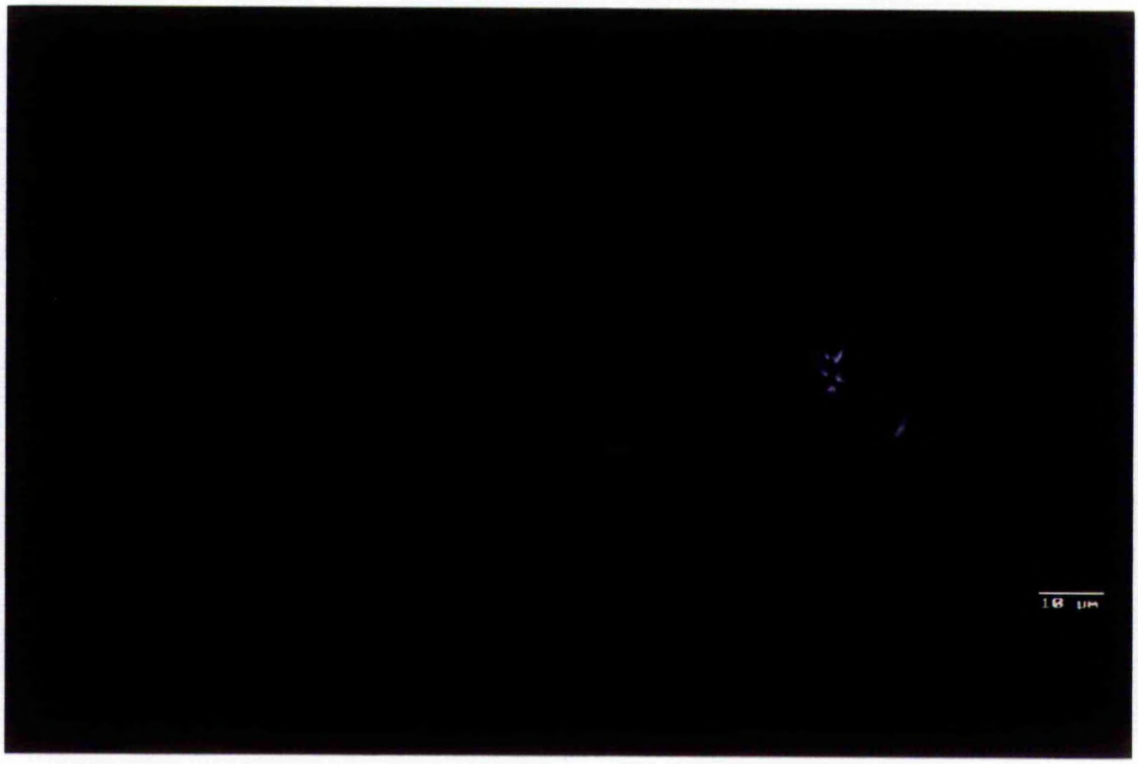
10 µm

Fig.14 'Merged image' of AP M8 pericentrin-antiserum localization (green) and anti-α-tubulin localization (red) in the same group of MDCK cells at interphase after a 4hr, 10μM taxol incubation. The AP M8 pericentrin-antiserum stains a pair of discrete spheres which are up to several micrometers apart in each interphase cell. Each stained spherical site is presumably occupied by one centriole and associated pericentriolar material. The ends of microtubules do not appear to be associated with the stained spheres. The AP M8 pericentrin-antiserum does not stain the ends of any of the microtubule bundles which are organized around the cell periphery. Confocal laser scanning microscopy. Scale bar, 10μm.

Fig.15 Confocal image of anti-α-tubulin localization in a group of MDCK cells after an 18hr, 10μM taxol incubation. Microtubule bundles are present throughout the cytoplasm at various orientations in interphase cells. Mitotically arrested MDCK cells each contain several microtubule asters which are stained intensely with anti-α-tubulin. Confocal laser scanning microscopy. Scale bar, 25μm.

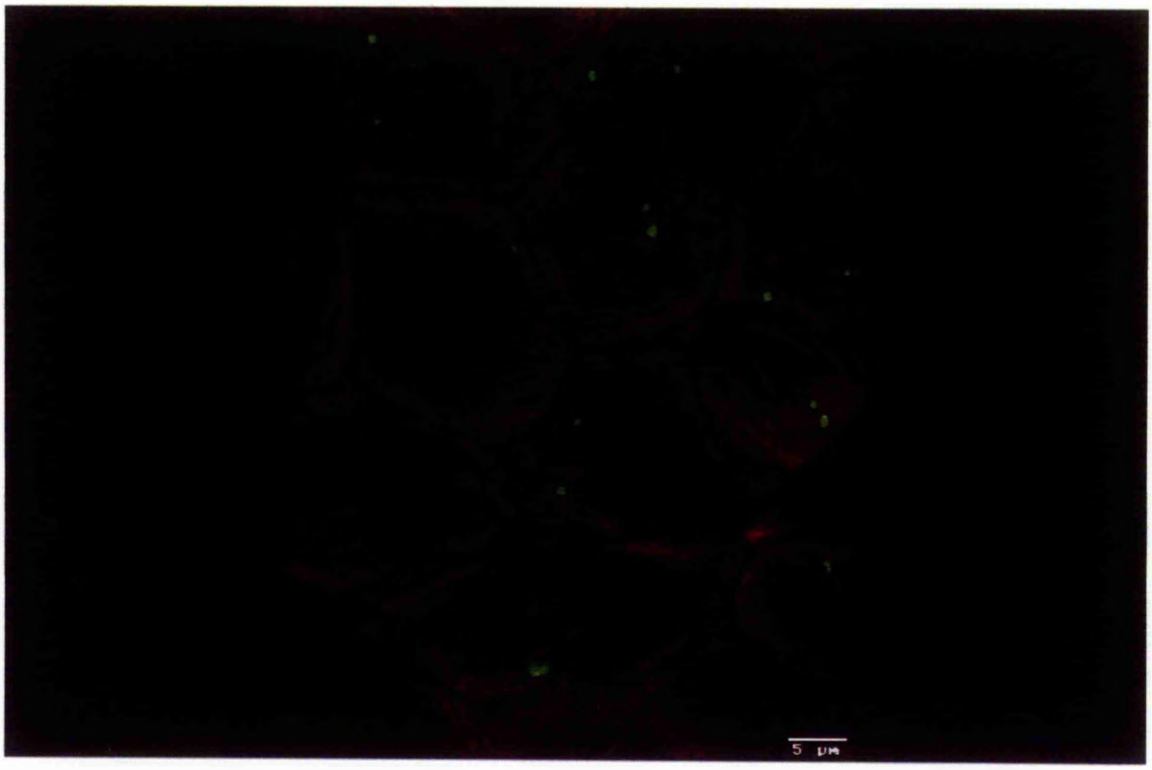
5 µm

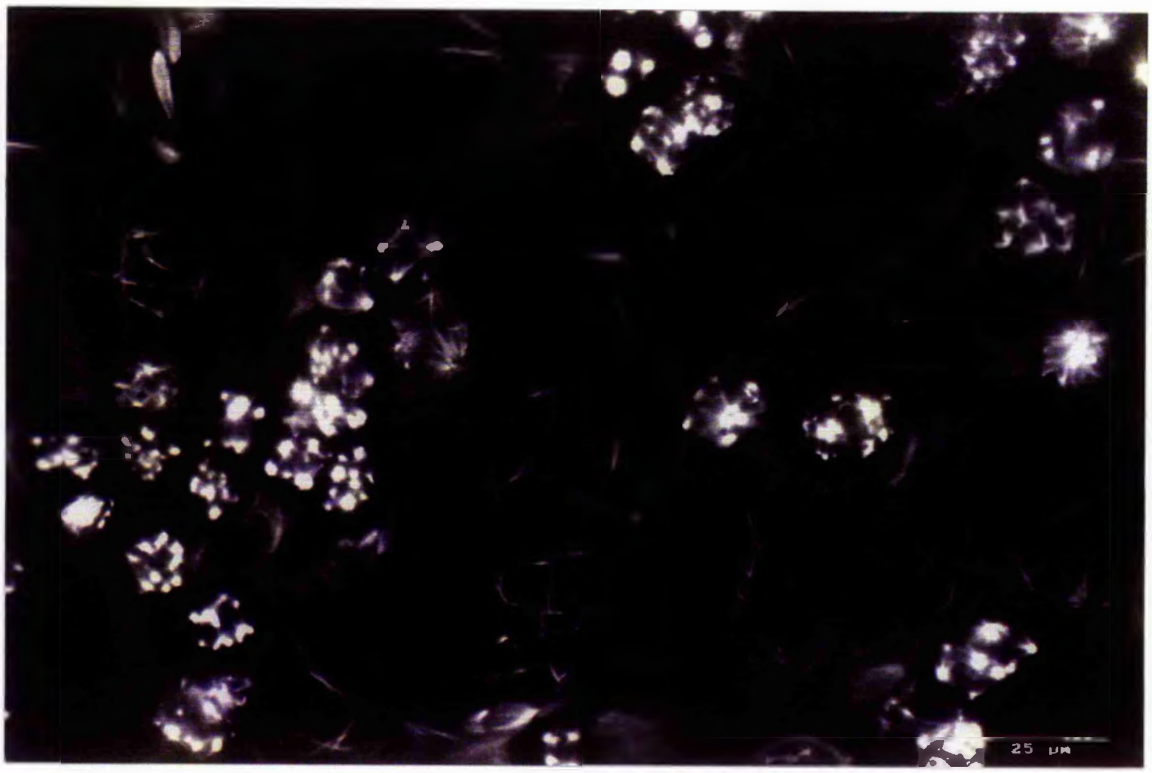
25 µm

Fig.16 'Merged image' of AP XGC γ-tubulin antiserum localization (yellow/green) and anti-α-tubulin localization (red) in the same MDCK cell at interphase after an 18hr, 10μM taxol incubation. The AP XGC γ-tubulin antiserum stains one end of a microtubule bundle. An AP XGC γ-tubulin antiserum stained sphere is also present in this image. This stained spherical site is presumably occupied by a centriole and associated pericentriolar material. Confocal laser scanning microscopy. Scale bar, 10μm.

Fig.17 'Merged image' of AP XGC γ-tubulin antiserum localization (yellow/green) and anti-α-tubulin localization (red) in the same MDCK cell at interphase after an 18hr, 10μM taxol incubation. The AP XGC γ-tubulin antiserum stains a pair of discrete spheres which are approximately 5μm apart. Each stained spherical site is presumably occupied by a centriole and associated pericentriolar material. The ends of the microtubule bundles are not associated with the spherical stained sites. The AP XGC γ-tubulin antiserum does not stain the ends of these microtubule bundles. Confocal laser scanning microscopy. Scale bar, 10μm.


10 µm

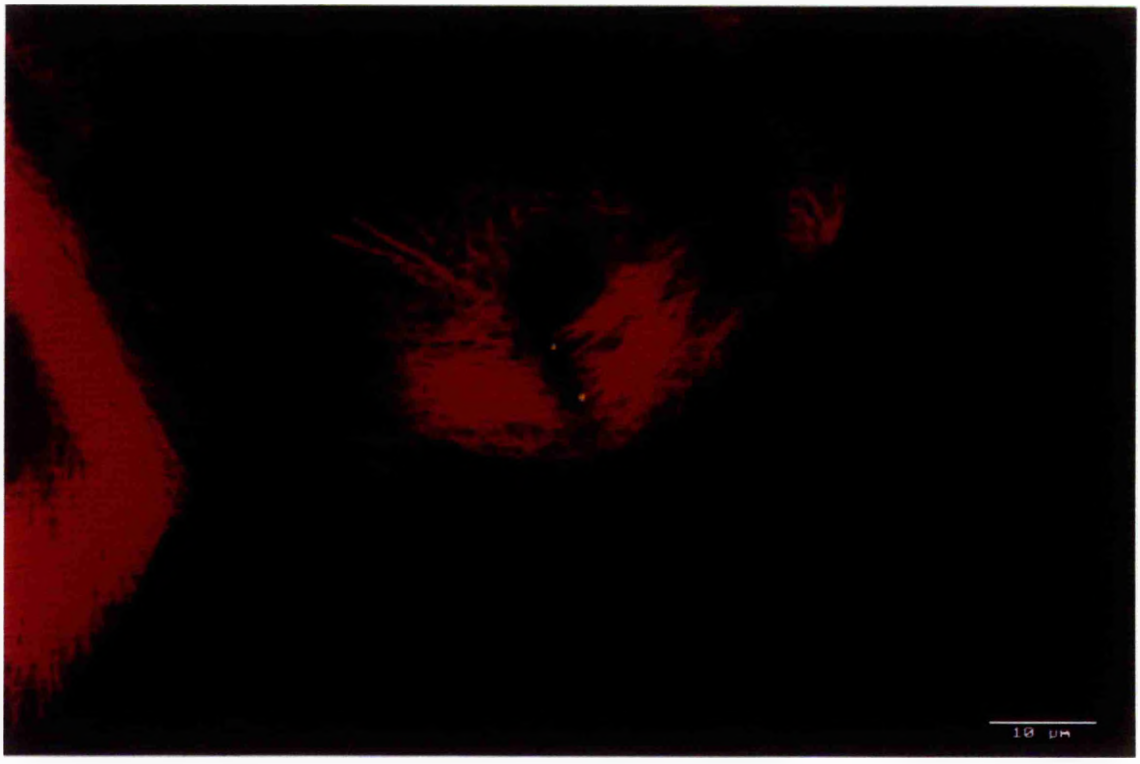
10 µm

Fig.18 'Merged image' of AP M8 pericentrin antiserum localization (yellow/green) and anti-α-tubulin localization (red) in the same MDCK cell at interphase after an 18hr, 10μM taxol incubation. The AP M8 pericentrin antiserum stains a pair of discrete spheres. Each stained spherical site is presumably occupied by a centriole and associated pericentriolar material. The ends of the microtubule bundles are not associated with the spherical stained sites. The AP M8 pericentrin antiserum does not stain the ends of these microtubule bundles. Confocal laser scanning microscopy. Scale bar, 5μm.


5 µm

Fig.19 MDCK cell at interphase after an 18hr, 10μM taxol incubation. Longitudinal section of one microtubule bundle and cross section of another microtubule bundle. Scale bar, 0.2μm.

Fig.20 MDCK cell at interphase after an 18hr, 10μM taxol incubation. Longitudinal section of a centriole surrounded by a small amount of pericentriolar material. Very few microtubule ends are present in the vicinity of the centriole. Scale bar, 0.2μm.

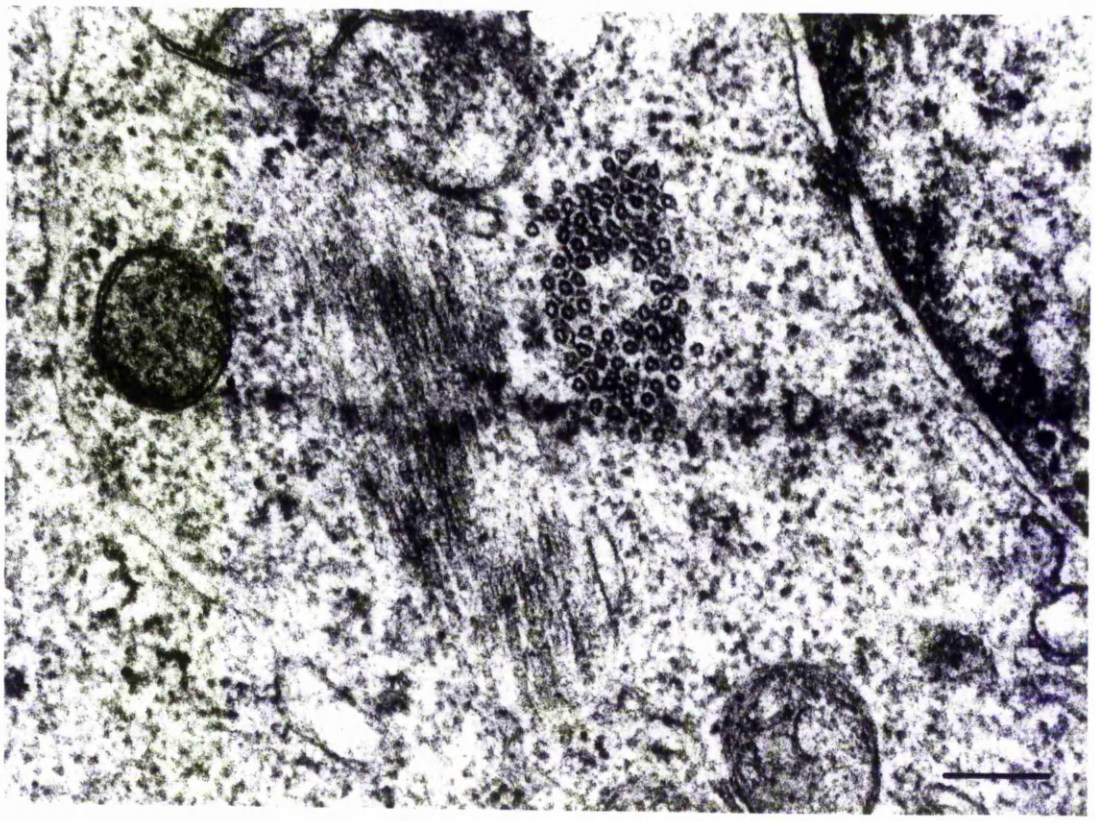

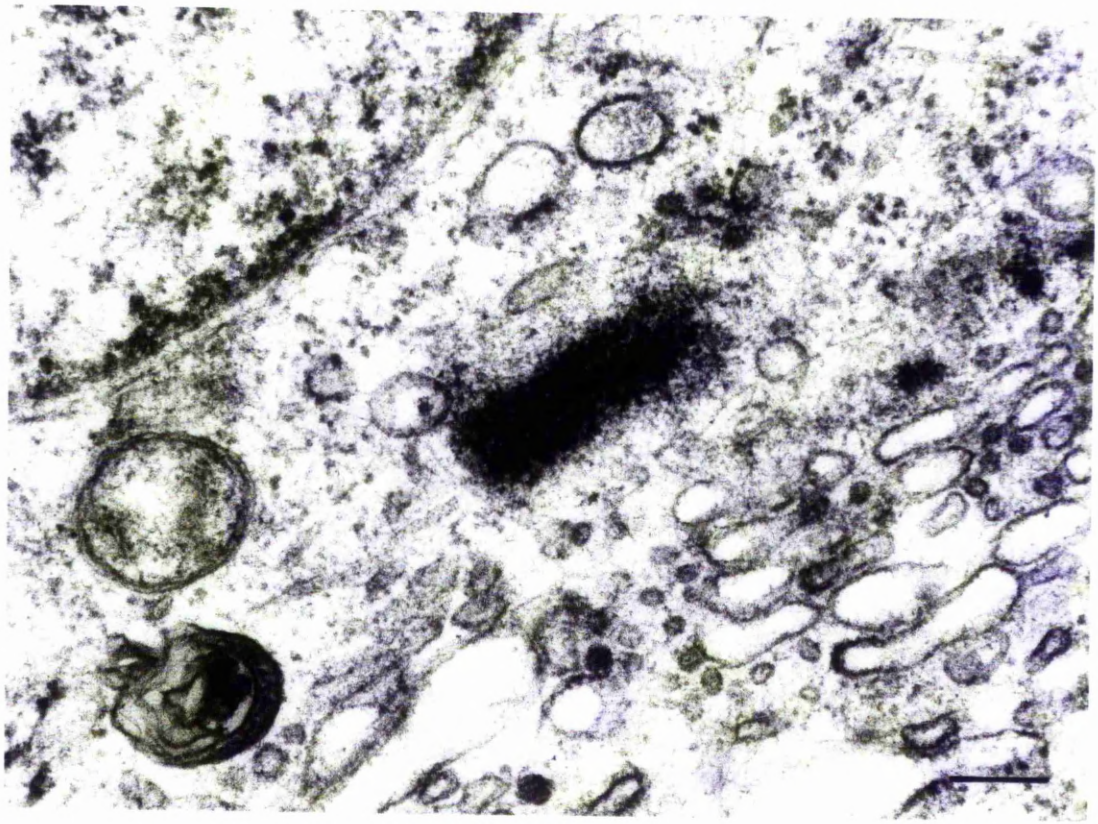

Fig.21 (a) 'Dual image' and 'projected Z-series' of AP XGC γ-tubulin antiserum localization (LHS) and anti-α-tubulin localization (RHS) in the same mitotically arrested MDCK cells after a 4hr, 10μM taxol incubation. The AP XGC γ-tubulin antiserum stains a pair of discrete spheres which are several micrometers apart. Four microtubule asters are present in this cell. Scale bar, 10μm.

Fig.21 (b) 'Merged image' of Fig.21a. Each AP XGC γ-tubulin antiserum stained spherical site (yellow) is located within a microtubule aster (red). Confocal laser scanning microscopy. Scale bar, 10μm.


10 µm


10 µm

Fig.22 'Merged image' and 'projected Z-series' of AP M8 pericentrin antiserum localization (LHS) and anti-α-tubulin localization (RHS) in the same mitotically arrested MDCK cells after a 4hr, 10μM taxol incubation. The AP M8 pericentrin antiserum stains a pair of discrete spheres which are several micrometers apart. Seventeen microtubule asters are present in this cell. Each of the two AP M8 pericentrin antiserum stained spherical sites (yellow) is located at the centre of a microtubule aster (red). The AP M8 pericentrin antiserum only stains the centre of two microtubule asters. Confocal laser scanning microscopy. Scale bar, 10μm.

Fig.23 'Dual image' and 'projected Z-series' of AP XGC γ-tubulin antiserum localization (LHS) and anti-α-tubulin localization (RHS) in two mitotically arrested MDCK cells after a 4hr, 10μM taxol incubation. The AP XGC γ-tubulin antiserum stains a pair of discrete spheres which are several micrometers apart in each mitotically arrested cell. Each stained spherical site is located at the centre of a microtubule aster. The AP XGC γ-tubulin antiserum also stains a diffuse region within each microtubule aster which does not contain a stained spherical site. Confocal laser scanning microscopy. Scale bar, 5μm.

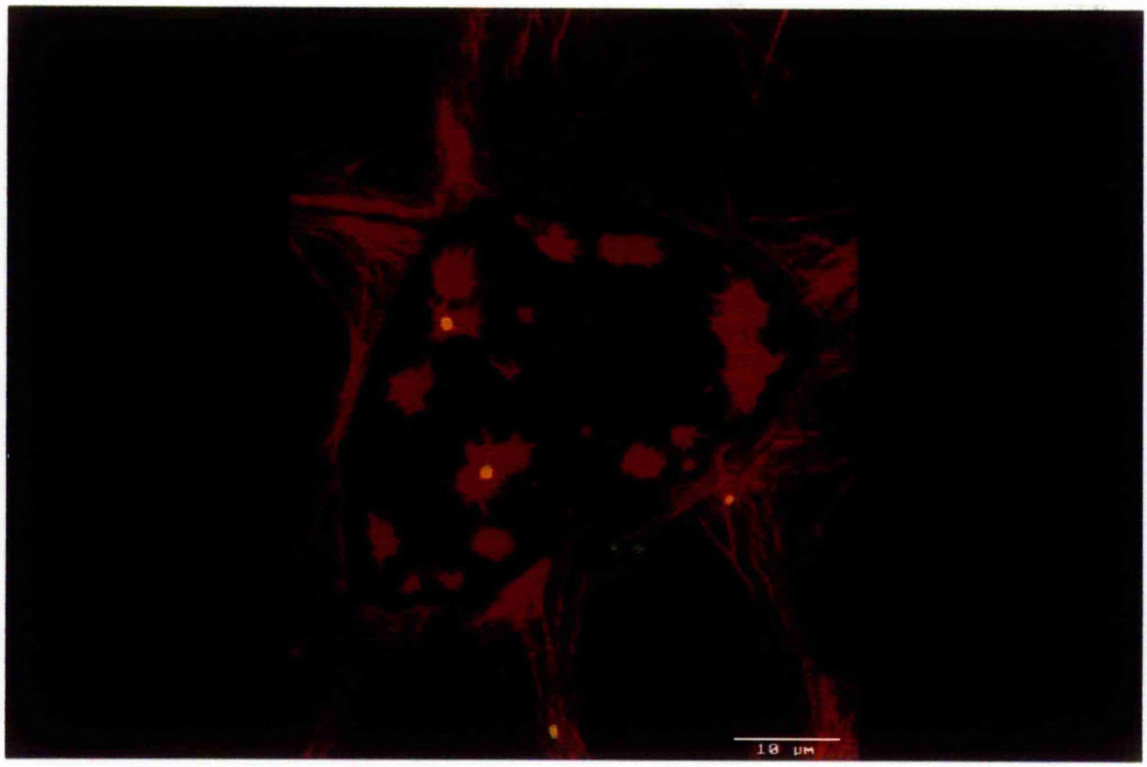
10 µm

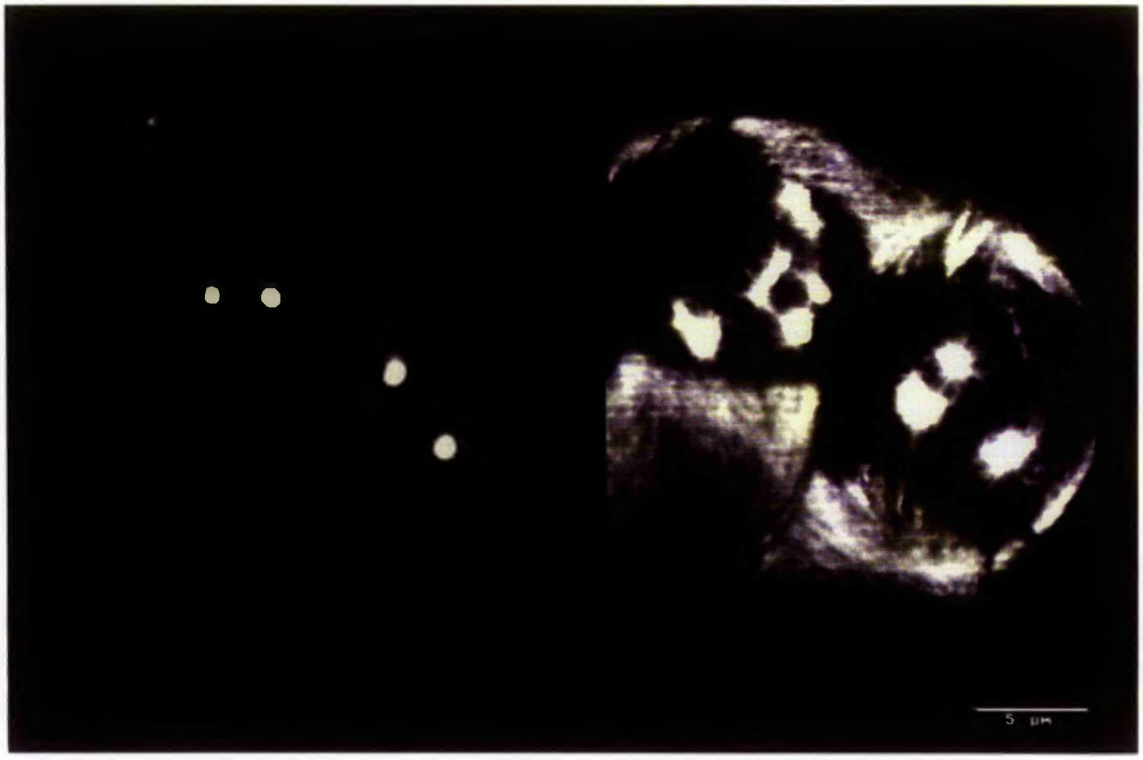
5 µm

Fig.24 'Merged image' and 'projected Z-series' of AP XGC γ-tubulin antiserum localization (LHS) and anti-α-tubulin localization (RHS) in the same mitotically arrested MDCK cells after an 18hr, 10μM taxol incubation. The AP XGC γ-tubulin antiserum stains a pair of discrete spheres (yellow/green) which are several micrometers apart. Each stained spherical site (yellow) is located at the centre of a microtubule aster (red) in the cell located on the right hand side of the confocal micrograph. Confocal laser scanning microscopy. Scale bar, 5μm.

Fig.25 'Merged image' and 'projected Z-series' of AP XGC γ-tubulin antiserum localization (LHS) and anti-α-tubulin localization (RHS) in the same mitotically arrested MDCK cells after an 18hr, 10μM taxol incubation. The AP XGC γ-tubulin antiserum stains a pair of discrete spheres which are several micrometers apart. Each stained spherical site (yellow) is located at the periphery of a microtubule aster (red). Confocal laser scanning microscopy. Scale bar, 5μm.

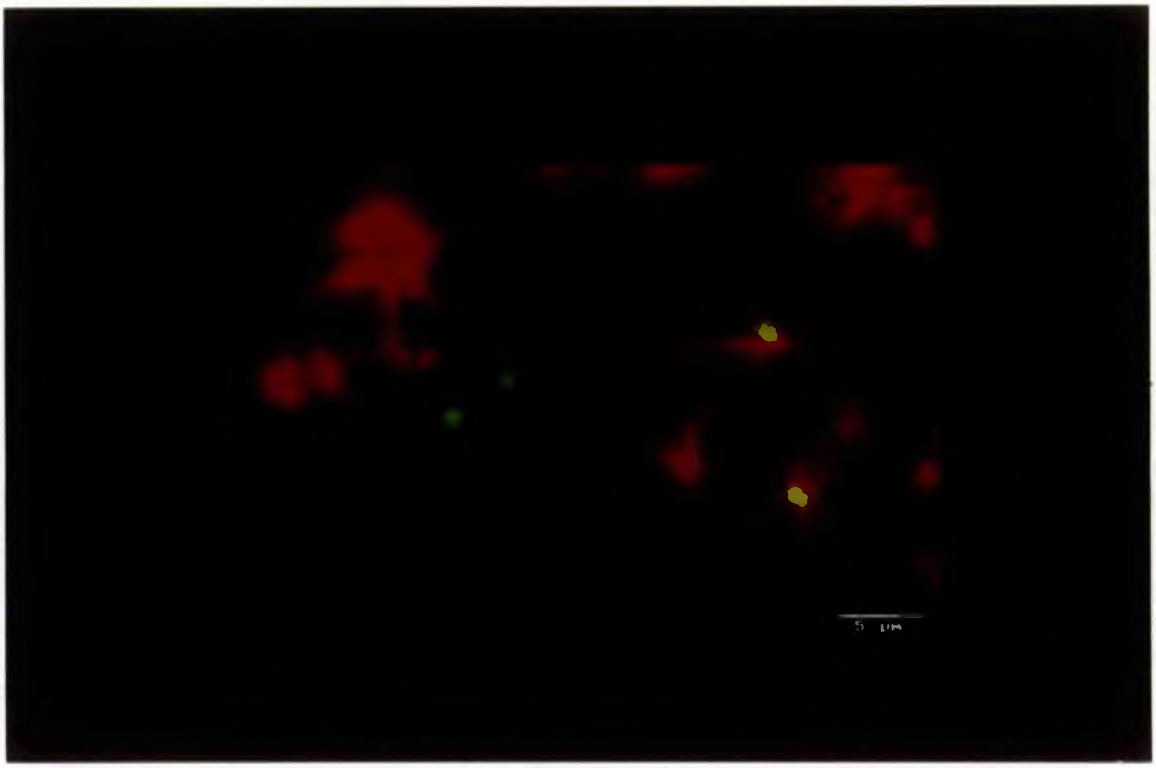
5 µm

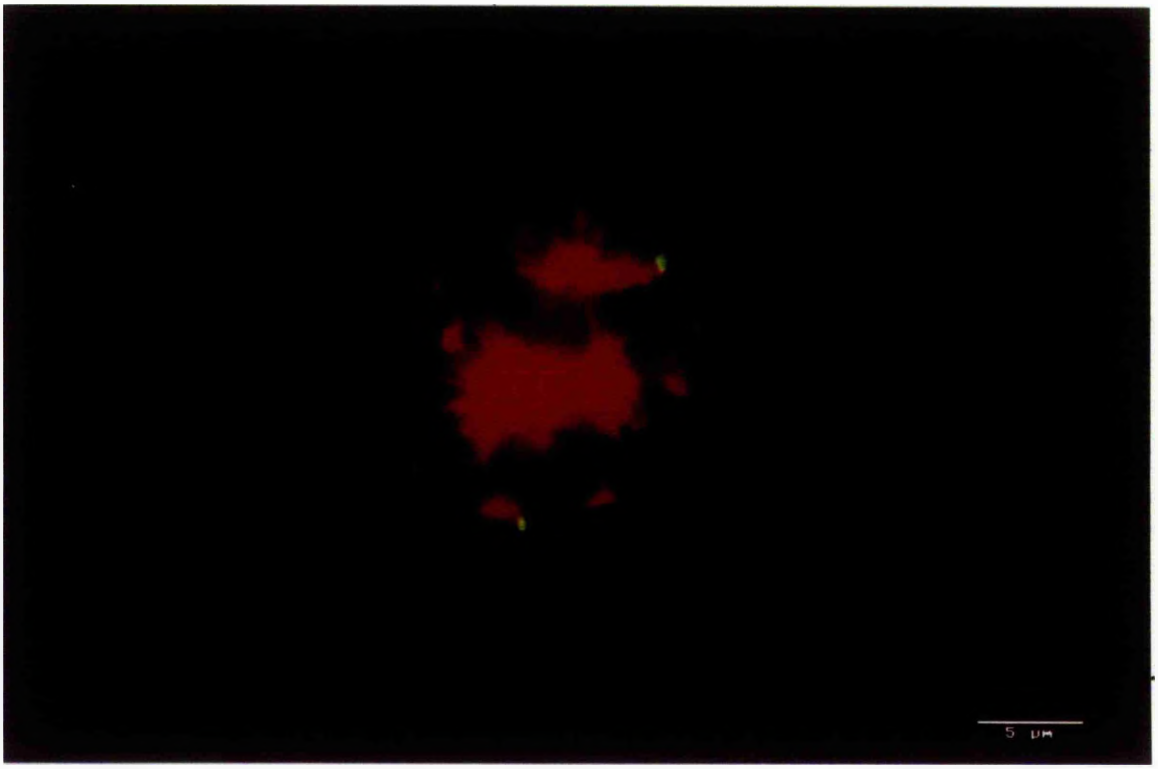
5 µm

Fig.26 (a) 'Dual image' and 'projected Z-series' of AP XGC γ-tubulin antiserum localization (LHS) and anti-α-tubulin localization (RHS) in a mitotically arrested MDCK cell after an 18hr, 10μM taxol incubation. The AP XGC γ-tubulin antiserum stains a pair of closely associated discrete spheres. Scale bar, 10μm.

Fig.26 (b) Merged image of Fig.26a. The pair of stained spherical sites are not associated with a microtubule aster. Confocal laser scanning microscopy. Scale bar, 5μm.


10 µm


5 µm

Fig.27 (a) 'Dual image' and 'projected Z-series' of AP M8 pericentrin antiserum localization (LHS) and anti-α-tubulin localization (RHS) in a mitotically arrested MDCK cell after an 18hr, 10μM taxol incubation. The AP M8 pericentrin antiserum stains a pair of closely associated discrete spheres. Scale bar, 5μm

Fig.27 (b) Merged image of Fig.27a. The pair of stained spherical sites are not associated with a microtubule aster. Confocal laser scanning microscopy. Scale bar, 5μm.

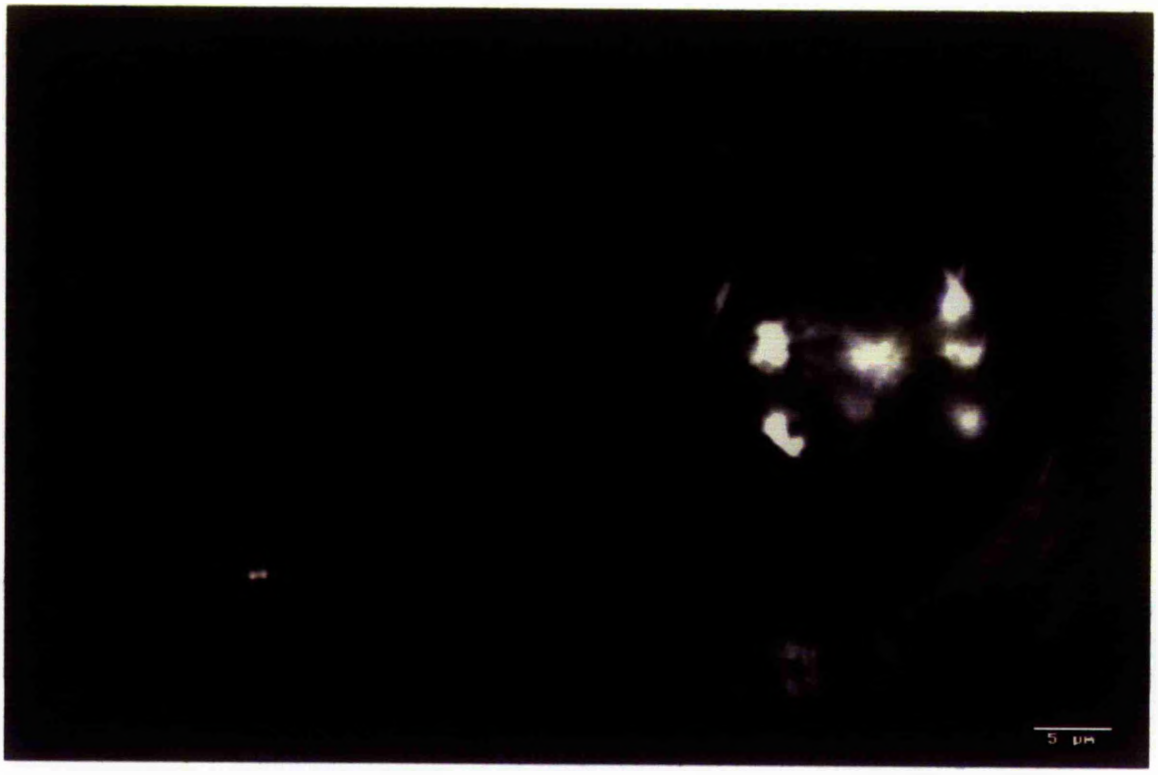
5 µm

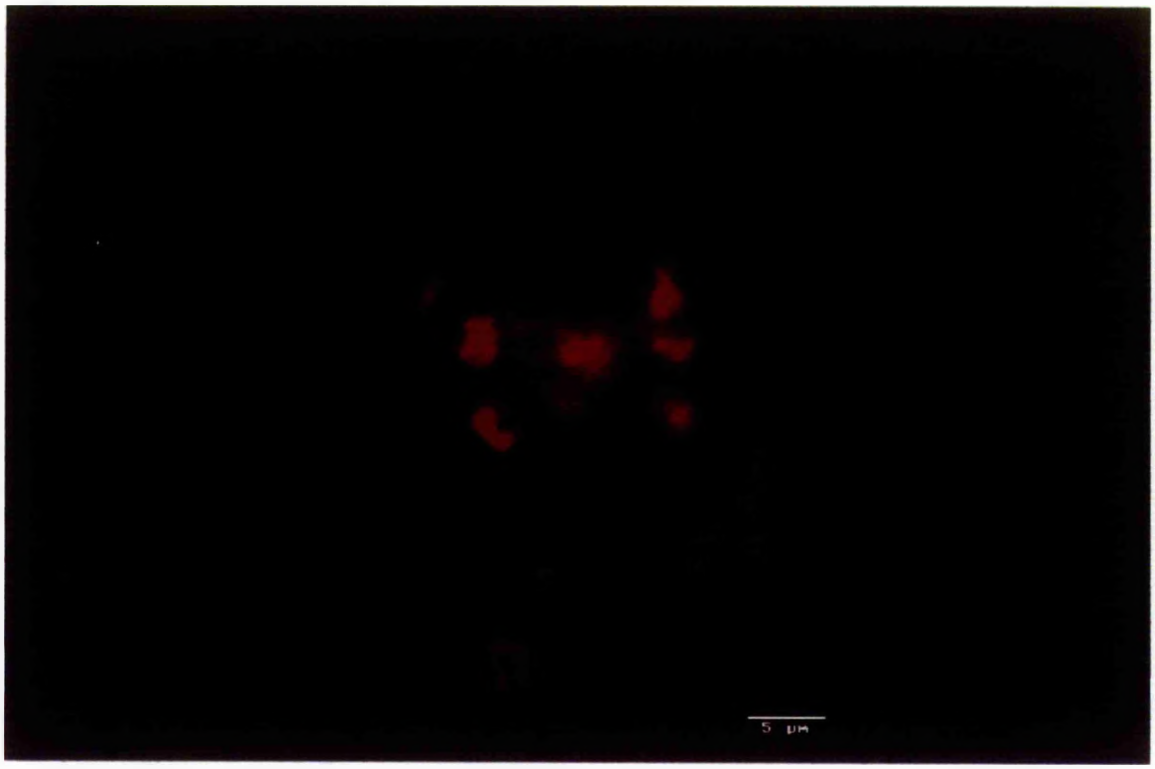
5 µm

Fig.28 **(a)** 'Dual image' and 'projected Z-series' of AP XGC γ-tubulin antiserum localization (LHS) and anti-α-tubulin localization (RHS) in a mitotically arrested MDCK cell after an 18hr, 10μM taxol incubation. Scale bar, 5μm.

Fig.28 **(b)** 'Merged image' of Fig.28a. The AP XGC γ-tubulin antiserum stains a pair of closely associated discrete spheres. The pair of stained spherical sites are not associated with a microtubule aster. The AP XGC γ-tubulin antiserum also stains a diffuse region within each microtubule aster. Confocal laser scanning microscopy. Scale bar, 5μm.

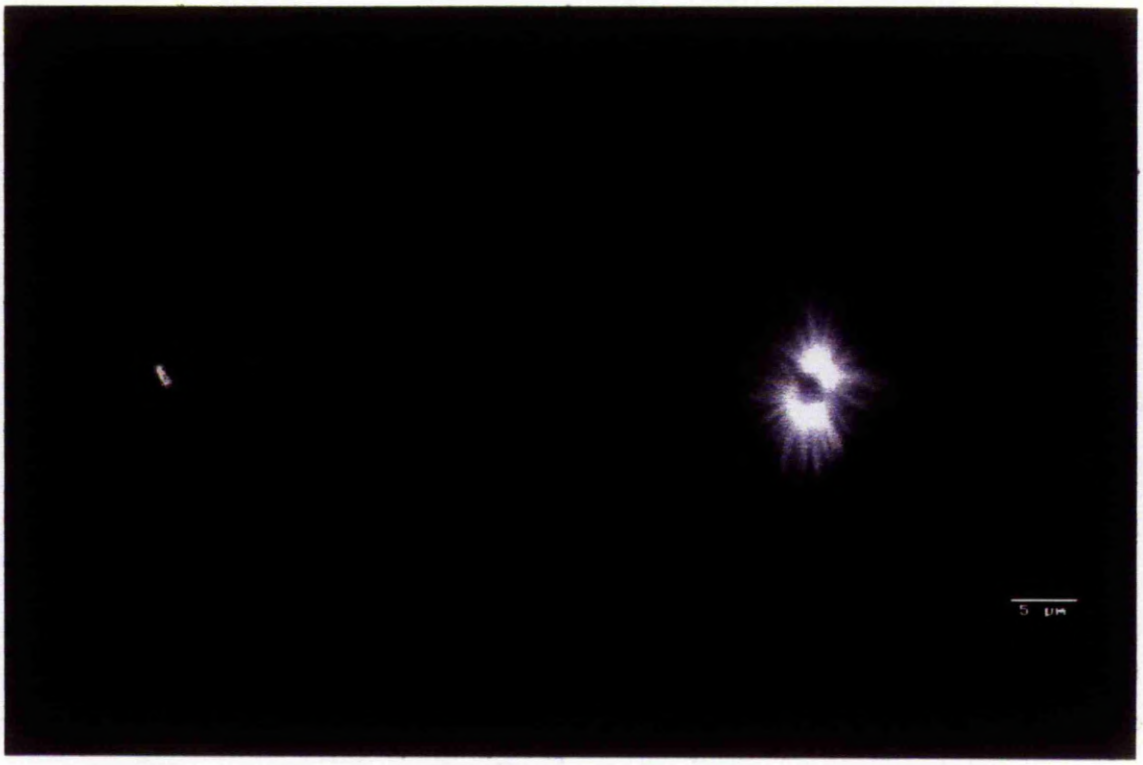
5 µm

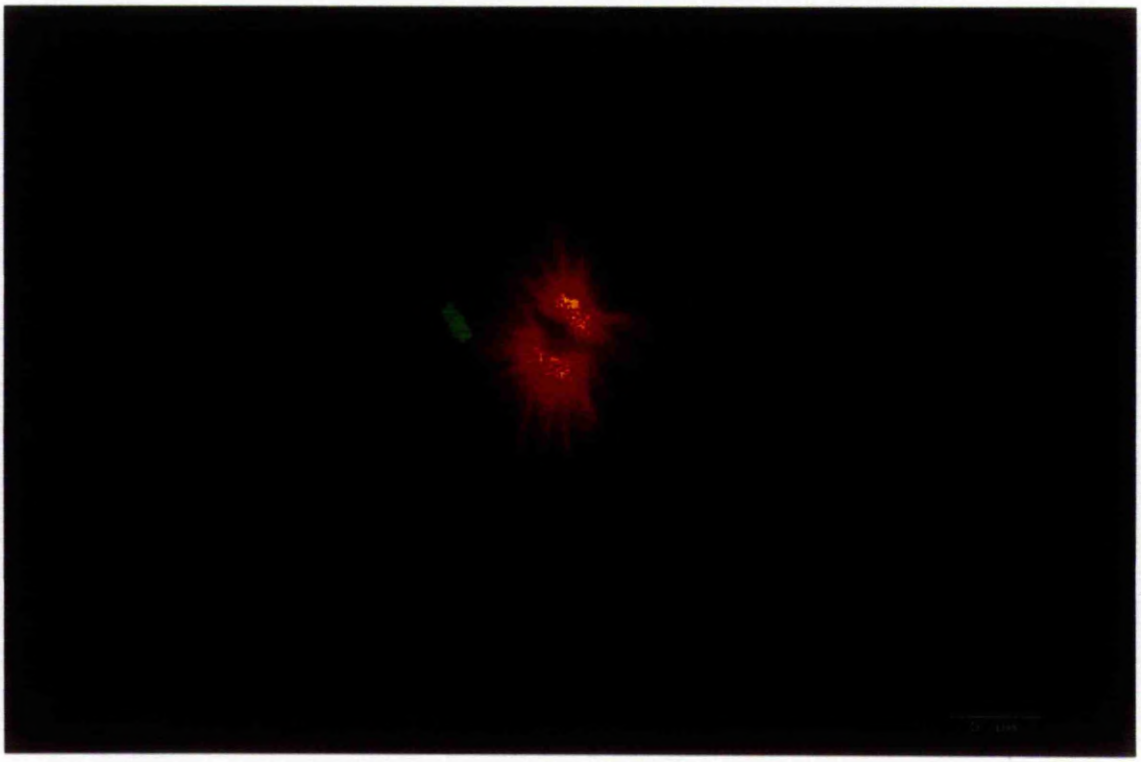

Fig.29 Microtubule aster in a mitotically arrested MDCK cell after an 18hr, 10μM taxol incubation. There is no apparent difference in the diameters of microtubules in the aster. Scale bar, 0.3μm.

Fig.30 (a) Cross sectional profiles of microtubules in a microtubule aster of a mitotically arrested MDCK cell after an 18hr, 10μM taxol incubation. Microtubules which have been stained with tannic acid to reveal protofilaments. Scale bar, 50nm.

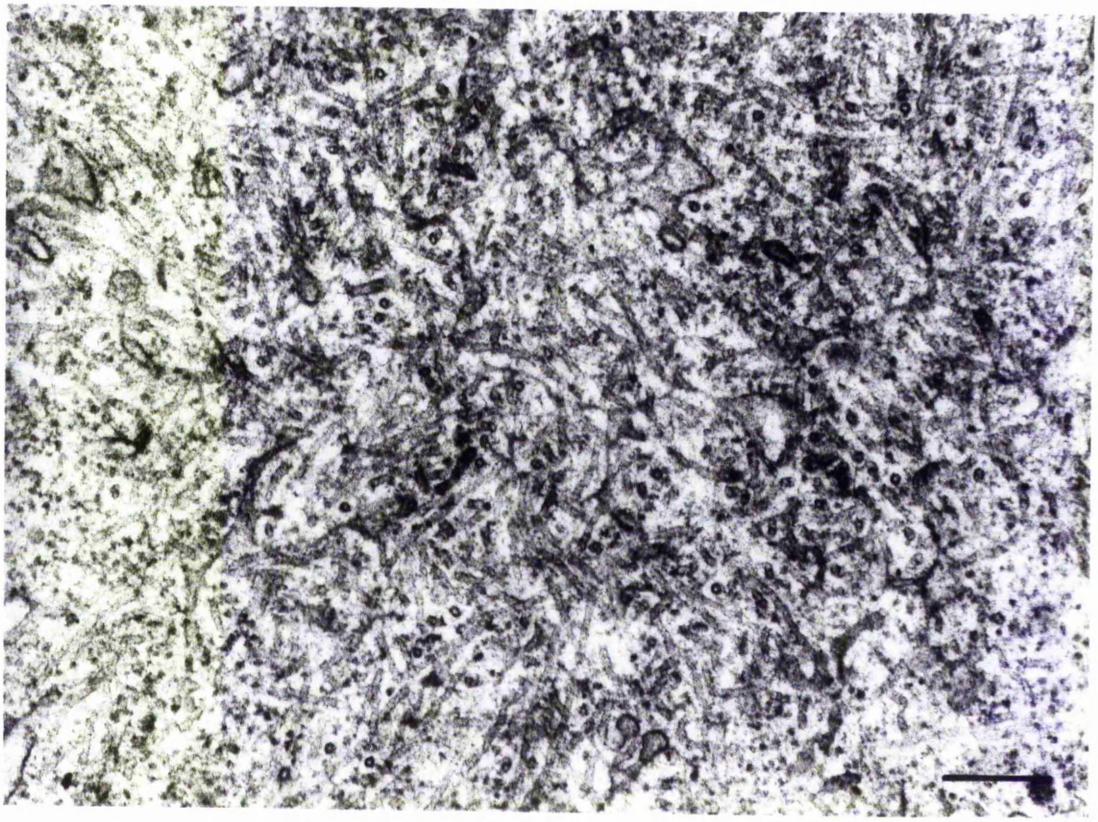

Fig.30 (b) Cross sectional profiles of microtubules in a microtubule aster of a mitotically arrested MDCK cell after an 18hr, 10μM taxol incubation. Microtubules composed of 12 protofilaments. Scale bar, 20nm.

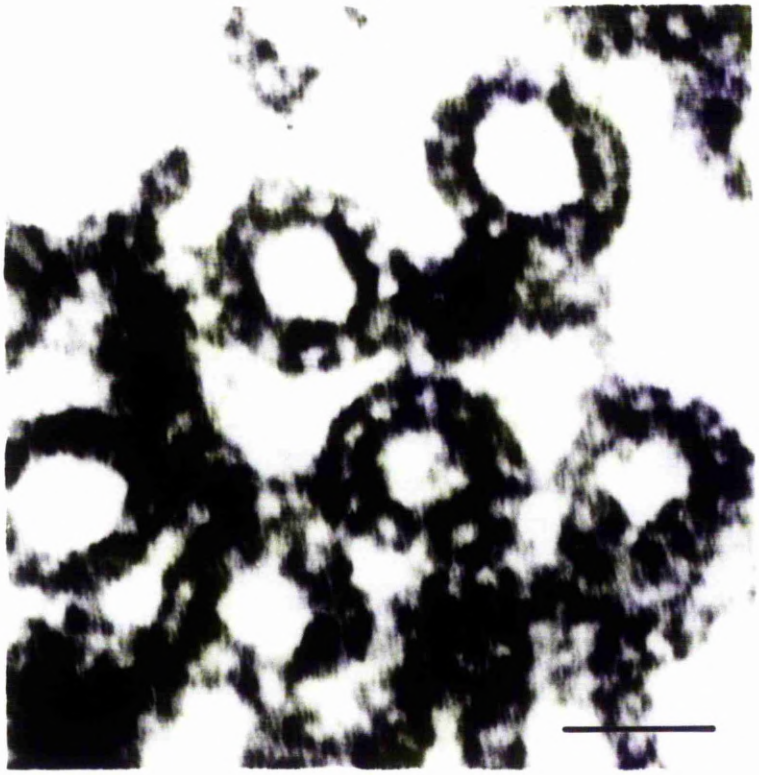

Fig.31 Hypothesis for microtubule severing activity and microtubule escape at the centrosome

(A) Microtubule nucleated in the centrosome at nucleating element (NE). Specific microtubule-associated proteins bind to an elongating microtubule close to its minus end. **(B)** Microtubule severing protein (e.g. centrin) severs microtubule just below the portion of a microtubule to which specific MAPs are bound **(C)** MAPs cap newly-exposed minus end of a microtubule. The newly exposed tubulin-GDP plus end is dynamically unstable and is subject to catastrophe. **(D)** The dynamically unstable microtubule is rescued and begins to elongate. **(E)** Specific MAPs associate with a portion of the rescued microtubule close to its minus end. The microtubule severing protein (e.g. centrin) subsequently severs the microtubule as described above. Minus end stabilized microtubules escape from the centrosome. The cycle of microtubule severing activity would enable the centrosome to nucleate more microtubules than the total number of nucleating elements and allow microtubule escape.

This hypothesis is compatible with several experimental results: (1) The number of reconstituted microtubules at the centrosome immediately after cold treatment exceeds the number of microtubules normally associated with the centrosome (Vorobjev and Chentsov,1983). Therefore, it has been suggested that microtubules disengage from the centrosome to form the cytoplasmic network. (2) Microtubules are nucleated at the neuronal centrosome which is apparently the only site of gamma tubulin concentration (Bass and Joshi,1992). If neuronal microtubules require gamma tubulin for their nucleation then they must subsequently escape and be translocated into the nerve axon (Ahmad *et al.*,1994). (3) Gamma tubulin is only concentrated in the centrosome of pillar cells in the mouse organ of Corti (personal communication, Mogensen and Tucker, University of St.Andrews). However the minus ends of several thousand microtubules are located approximately one micrometer from the centrosome (Tucker *et al.*,1992; 1995). (4) Microtubule ends do not focus at the centrosome in interphase MDCK cells (Bré *et al.*,1987; Peppercock *et al.*,1990). However, gamma tubulin is only concentrated at the centrosome (See Chap.8).

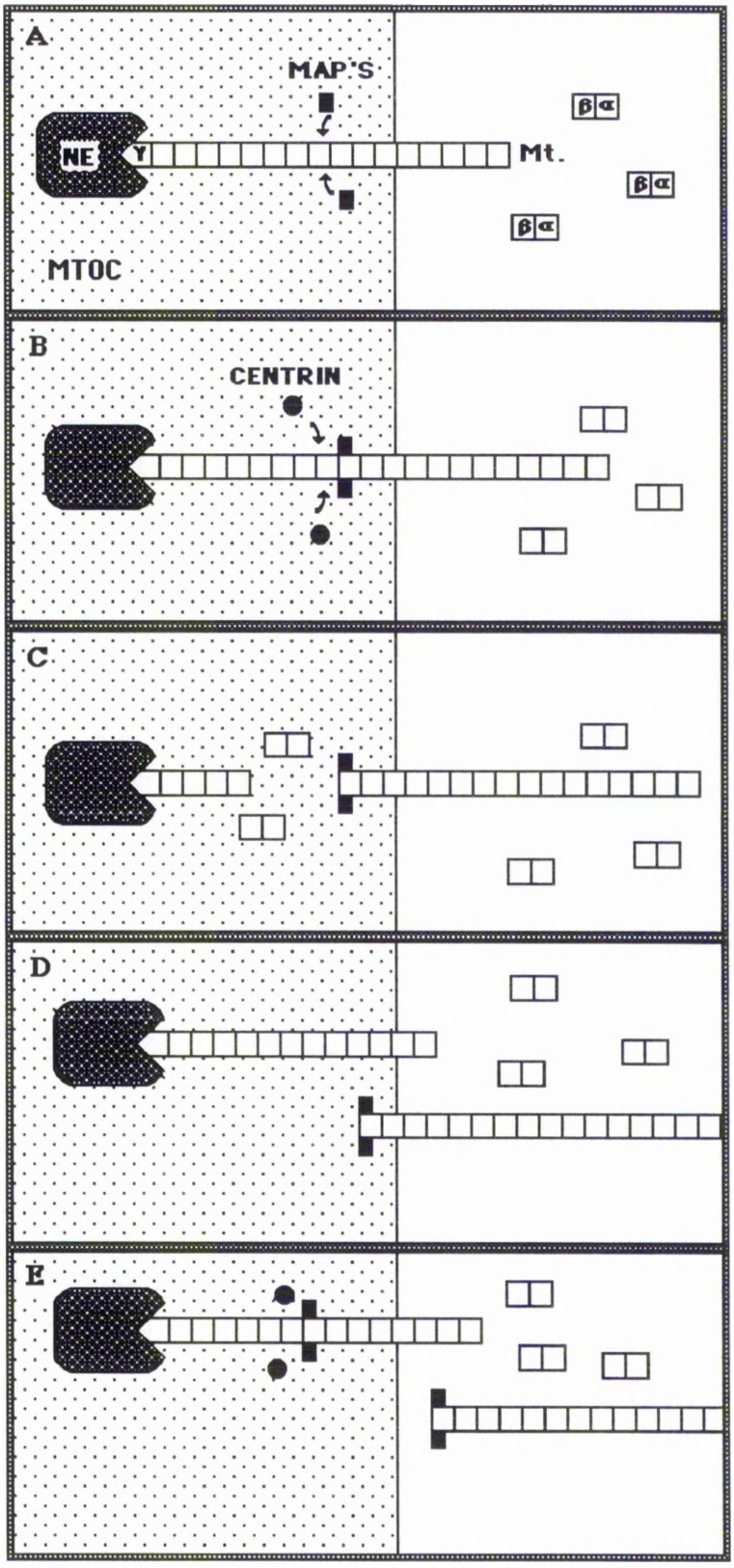
A
MAP'S
NE
Mt.
MTOC
B
CENTRIN
C
D
E

Chapter 9

Overview

The investigations reported in this thesis have dealt with control of microtubule assembly and positioning in a range of cell types (insect muscle, and insect neuroblast cells *in vivo,* and cultured MDCK cells), and in a range of microtubule arrays (transient 'interphase' arrays in differentiating muscle cells, more conventional interphase arrays in neuroblast cells and MDCK cells, mitotic spindles and telophase midbody-associated microtubule arrays). The investigations have revealed new aspects of the ways in which several different types of microtubule-organizing centres contribute to the control of microtubule-organization. Some of the MTOC's in question are centriole-containing centrosomes and others are acentriolar. There is no obvious unifying major theme which links each individual study. Each one has addressed a different issue. Thus the Thesis as a whole is a testament to the variety and complexity of the organization and the functions of MTOC's. The major advances reported here are as follows.

Drosophila indirect fibrillar flight muscles and epithelial tendon cells do not possess centriole-containing centrosomes. Microtubules appear to be organized by both surfaces of each myotendon junction. Do these sites nucleate or capture microtubules? Are these sites the counterpart of the perinuclear nucleating-sites of mammalian muscle cells? The investigation, using antisera against pericentrin, provides evidence that these sites do operate as microtubule nucleating-sites. The presence of pericentrin at the spindle poles of *Drosophila* embryos and cultured *Drosophila* epithelial cells confirms that pericentrin is expressed in *Drosophila* and increases the likelihood that pericentrin is present at the surface of myotendon junctions. However, it remains to be resolved whether or not γ-tubulin is localized at these sites.

MDCK cells are a highly differentiated cell line since, for example, they can establish cell polarity and form cellular junctions. Consequently, the manner in which the cleavage procedure is carried out during the terminal stages of daughter cell separation in MDCK cells may reflect that which occurs in epithelial sheets and tissues generally. It is apparent from this investigation that at least one midbody-associated microtubule bundle must detach from the midbody in order that cytokinesis can complete the separation of daughter cells. Evidence in this investigation indicates that midbody-associated microtubule bundles may be severed at their point of entry into the side of the midbody. It would be of interest to establish whether a microtubule severing protein concentrates at the midbody during the terminal stages of daughter cell separation. Furthermore, midbody-associated microtubule bundles could potentially be used to investigate the mechanism(s) and molecular biology of microtubule severing.

Microtubule escape from the centrosome maybe a more widespread phenomenon than is currently appreciated. This investigation provides indirect evidence which may indicate that microtubules are released and escape from the centrosome in MDCK cells. At interphase a non-focused cytoplasmic microtubule array is present in MDCK cells. However, γ-tubulin is only concentrated at the centrosome. If γ-tubulin is required for microtubule nucleation then it is a distinct possibility that microtubules are initiated at the centrosome and subsequently released. Taxol incubation of MDCK cells results in a microtubule organization, in both interphase and mitotically arrested MDCK cells, which may be consistent with microtubule escape from the centrosome. Microtubules may escape from interphase centrosomes to establish a non-focused cytoplasmic array while microtubules may be released from the centrosome at the end of mitosis in order that they can be completely depolimerized. Furthermore, during telophase a centrosomally-associated microtubule array increases substantially in size and subsequently a non-focused microtubule array is present. This may also be an indication that microtubules are nucleated at the centrosome and subsequently released to form the cytoplasmic array.

This investigation does not prove that microtubules are released from the centrosome of MDCK cells. However, it does provide evidence which strongly indicates

that this phenomenon may be operating in MDCK cells. Consequently, it would be extremely interesting to investigate further the possibility of microtubule escape from centrosomes of MDCK cells. One approach would be to depolimerize the microtubules of interphase MDCK cells with nocodazole and subsequently to micro-inject these cells with an anti-γ-tubulin antiserum or an antisense γ-tubulin RNA strand. This would prevent γ-tubulin from functioning and would establish whether it is required for microtubule nucleation in interphase MDCK cells. If microtubules are released from the centrosome, how is this achieved? One possibility is that microtubules could be severed at the centrosome and as a consequence released. If a severing protein is responsible for microtubule release at the centrosome an experimental procedure could be adopted in order to block the function of such a protein. It is possible that this may prevent a non focused interphase microtubule array from being established.

Preliminary results indicate that taxol down regulates the protofilament number of microtubules from thirteen to twelve in MDCK cells. If the centrosome is responsible for the nucleation of these microtubules, then taxol may cause this perturbation by interacting with a component of the centrosome.

Both microtubule release from the centrosome and microtubule severing have only recently been documented. The extent to which these phenomena operate has not been established. This investigation has provided further evidence to support both microtubule release from the centrosome and microtubule severing *in vivo*. Microtubule release and escape from the mammalian centrosome and severing of microtubules associated with the midbody (a structure common to most animal cells) indicates that these phenomena may be fundamental features of microtubule organization. Both microtubule release from the centrosome and microtubule severing could have a considerable effect on how microtubule arrays are organized. These phenomena may enable microtubules to be organized in regions of cells which are spatially distinct of the centrosome. Furthermore, microtubule severing could play an important role in the dynamics of microtubules by effecting their disassembly.

References

Ahmad, F.J., Joshi, H.C., Centonze, V.E, Bass, P.W. (1994). Inhibition of microtubule nucleation at the neuronal centrosome compromises axon growth. *Neuron.* **12**, 271-280.

Albertini, D.F. (1987). Cytoplasmic reorganization during the resumption of meiosis in cultured preovulatory rat oocytes. *Developmental Biol.* **120**, 121-131.

Alberts, B., Bray, D., Lewis, J., Raff, M., Roberts, K., Watson, J.D. (1989). *Molecular Biology of the Cell*, Chap. 14, pp791-836. New York, GarlandPublishing, Inc.

Allen, C., Borisy, G.G. (1974). Structural polarity and directional growth of microtubules of *Chlamydomonas* flagella. *J. Mol. Biol.* **90**, 381-402.

Allenspach, A.L., Roth, L.E. (1967). Structural variations during mitosis in the chick embryo. *J. Cell Biol.* **33**, 179-196.

Andreassen, P.R., Palmer, D.K., Wener, M.H., Margolis, R.L. (1991). Telophase disc: a new mammalian mitotic organelle that bisects telophase cells with a possible function in cytokinesis. *J. Cell Sci.* **99**, 523-534.

Andreu, J.M., Bordas, J., Diaz, J.F., Garcia de Ancos, J., Gil, R., Medrano, F.J., Nogales, E., Pantos, E., Towns-Andrews, E. (1992). Low resolution structure of microtubules in solution: synchrotron X-ray scattering and electron microscopy of taxol-induced microtubules assembled from purified tubulin in comparison with glycerol and MAP-induced microtubules. *J. Mol. Biol.* **226**, 169-184.

Asano, H., Kobayashi, M., Hoshino, T. (1991). Ultrastructural study of a cytoplasmic bridge connecting a pair of erythroblasts in mice. *Cell Tissue Res.* **264**, 215-219.

Auber, J. (1963). Ultrastructure de la junction myo-epidermique chez les Dipteres. *J. Microscopie.* **2**, 325-336.

Auber, J. (1969). La myofibrillogenese du muscle strie. I. Insectes. *J. Microscopie.* **8**, 197-232.

Bass, P.W., Deitch, J.S., Black, M.M., Banker, G.A. (1988). Polarity orientation of microtubules in hippocampal neurons: uniformity in the axon and nonuniformity in the dendrite. *Proc. Natl. Acad. Sci. USA.* **85**, 8335-8339.

Bass, P. W. and Joshi, H. C. (1992). γ-Tubulin distribution in the neuron: implications for the origins of neuritic microtubules. *J. Cell Biol.* **119**, 171-178.

Bacallao, R., Antony, C., Dotti, C., Karsenti, E., Stelzer E.H.K., Simons, K. (1989) The subcellular organization of Madin-Darby canine kidney cells during the formation of a polarized epithelium. *J. Cell Biol.* **109**, 2817-2832.

Bastmeyer, M., Russell, D.G. (1987). Characterization of *Pales* spermatocyte spindles, with reference to an MTOC-associated protein. *J. Cell Sci.*, **87**, 431-438.

Berman, L., Stulberg, C.S. (1956). Eight culture strains (Detroit) of human epithelial-like cells. *Proc. Soc. Exp. Biol. Med.* **92**, 730-735.

Bre, M-H., Kreis, T.E., Karsenti, E. (1987). Control of microtubule nucleation and stability in Madin-Darby canine kidney cells: The occurence of noncentrosomal, stable detyrosinated microtubules. *J. Cell Biol.* **105**, 1283-1296.

Bre, M-H., Pepperkok, R., Hill, A.M., Levilliers, N., Ansorge, W., Stelzer, E.H.K., Karsenti, E. (1990). Regulation of microtubule dynamics and nucleation during polarization in MDCK II cells. *J. Cell Biol.* **111**, 2013-3021.

Brinkley, B.R. (1975). Cold-labile and cold-stable microtubules in the mitotic spindle of mammalian cells. *Ann. N.Y. Acad. Sci.* **253**, 428-439.

Buck, R.C., Tisdale, J.M. (1962). The fine structure of the midbody of the rat erythroblast. *J. Cell biol.* **13**, 109-115.

Buendia, B., Antony, C., Verde, F., Bornens, M., Karsenti, E. (1990a). A centrosomal antigen localized on intermediate filaments and mitotic spindle poles. *J. Cell Sci.* **97**, 259-271.

Buendia, B., Bre, M-H., Griffiths, G., Karsenti, K. (1990b) Cytoskeletal control of centrioles movement during the establishment of polarity in Madin-Darby canine kidney cells. *J. Cell Biol.* **110**, 1123-1135.

Burgoyne, R.D., Cambray-Deakin, M.A., Lewis, S.A., Sarkar, S., Cowan, N.J. (1988) Differential distribution of β-tubulin isotypes in cerebellum. *EMBO J.* **7**, 2311-2319.

Byers, B., Abramson, D.H. (1968). Cytokinesis in HeLa : post-telophase delay and microtubule associated motility. *Protoplasma.* **66**, 413-435.

Calarco, P.D., Siebert, M.C., Hubble. R., Mitchison, T., Kirschner, M. (1983). Centrosome development in early embryos as defined by an autoantibody against pericentriolar material. *J. Cell Biol.* **101**, 319-324.

Callaini, G., Riparbelli, M.G. (1990). Centriole and centrosome cycle in the early *Drosophila* embryo. *J. Cell Sci.* **97**, 539-543.

Cande, W.Z., Lazarides, E., McIntosh, J.R. (1977). A comparison of the distribution of actin and tubulin in the mammalian mitotic spindle as seen by indirect immunofluorescence. *J. Cell Biol.* **72**, 552-567.

Carlier, M.F., Pantaloni, D. (1981). Kinetic analysis of guanosine 5'-triphosphate hydrolysis associated with tubulin polymerization. *Biochemistry.* **20**, 1918-1924.

Carlier, M-F., Hill, T.L., Chen, Y-D. (1984). Interference of GTP hydrolysis in the mechanism of microtubule assembly: an experimental study. *Proc. Natl. Acad. Sci. USA*. **81**, 771-775.

Cassimeris, L., Pryer, N.K., Salmon, E.D. (1988). Real-time observations of microtubule dynamic instability in living cells. *J. Cell Biol.* **107**, 2223-2231.

Cifuentes-Diaz, C. (1989). Mode of formation of the flight muscles in a butterfly *Pieris brassicae. Tissue and Cell.* **21**, 875-889.

Clark, S.W., Meyer, D.I. (1992). Centractin is an actin homologue associated with the centrosome *Nature*. **359**, 246-250.

Clayton, L., Black, C.M., Lloyd, C.W. (1985). Microtubule nucleating sites in higher plants identified by an autoantibody against pericentriolar material. *Cell.* **35**, 621-629.

Cohen, C., Parry, D.A.D. (1990). α-Helical coiled-coils and bundles: how to design a α-helical protein. *Prot. Struct. Funct. Genet.* **7**, 1-15.

Connolly, J.A., Kalnins, V.I. (1987). Specific visualization of centrioles and basal bodies by fluorescent staining with non-immune rabbit sera. *J. Cell Biol.* Abs. 288a.

Cooke, C.A., Heck, M.M.S., Earnshaw, W.C. (1987). The inner centromere protein (INCENP) antigens: movement from inner centromere to midbody during mitosis. *J. Cell Biol.* **105**, 2053-2067.

Crossley, A.C. (1978). The morphology and development of the *Drosophila* muscular system. In: *Genetics and biology of Drosophila Vol. 2b* (ed.: Ashburner, M., Wright, T.R.F.) pp.499-560. New York, Academic press.

Cullen, C.F., Milner, M.J., (1991). Parameters of growth in primary cultures and cell lines established from *Drosophila* imaginal discs. *Tissue and Cell.* **23**, 29-39.

Currie, D.A., Milner, M.J., Evans, C.W. (1988). The growth and differentiation *in vitro* of leg and wing imaginal disc cells from *Drosophila melanogaster.* Development. **102**, 805-814.

Davis, F.M., Tsao, T.Y., Fowler, S.K., Rao, P.N. (1983). Monoclonal antibodies to mitotic cells. *Proc. Natl. Acad. Sci. USA.* **80**, 2926-2930.

DeBrabander, M., Geuens, G., DeMay, J., Jonaiau, M. (1979). Light microscopic and ultrastructural distribution of immunoreactive tubulin in mitotic mammalian cells. *Biol. Cell.* **34**, 213-226.

DeBrabander, M., Geuens, G., Nuydens, R., Willebrords, R., De May, J. (1981). Taxol induces the assembly of free microtubules in living cells and blocks the organizing capacity of the centrosomes and kinetochores. *Proc. Natl. Acad. Sci. USA* **78**, 5608-5612.

DeBrabander, M., Geuens, G., Nuydens, R., Willebrords, R., Aerts, F. De May, J. and McIntosh, J.R. (1986). Microtubule dynamics during the cell cycle : the effects of taxol and nocodazole on the microtubule system of PtK2 cells at different stages of the mitotic cycle. *Int. Rev. of Cytol.* **101**, 215-277.

DeMey, J., Aerts, F., Moeremans, M., Geuens, G., Daneels, G., DeBrabander, M. (1984). Anti-MAP1 reacts with the centrosomes, kinetochores, midbody, and spindle of mitotic PtK_2 cells. *J. Cell Biol.* **99**, 447a. (Abstr.).

Doxsey, S.J., Stein, P., Evans, L., Calarco, P.D., Kirschner, M. (1994). Pericentrin, a highly conserved centrosome protein involved in microtubule organisation. *Cell* **76**, 639-650.

Drechsel, D.N., Kirschner, M.W. (1994). The minimum GTP cap required to stabilize microtubules. *Current Biol.* **4**, 1053-1061.

Edgar, B.A., O'Farrell, P.H. (1989) Genetic control of cell division patterns in the *Drosophila* embryo. *Cell* **57**, 177-187.

Erickson, H.P., O'Brien, E.T. (1992). Microtubule dynamic instability and GTP hydrolysis. *Annu. Rev. Biophys. Biomol. Struct.*, **21**, 145-166.

Errabolu, R., Sanders, M., Salisbury, J. (1994). Cloning of a cDNA encoding human centrin, a calcium-binding protein of centrosomes and mitotic spindle poles. J. Cell Sci. *In press*.

Euteneuer, U., McIntosh, J.R. (1980). Polarity of midbody and phragmoplast microtubules. *J. Cell Biol.* **87**, 509-515.

Euteneuer, U., McIntosh, J.R. (1981). Structural polarity of kinetochore microtubules in PtK1 cells. *J. Cell Biol.* **89**, 338-345.

Evans, T., Mitchison, T.M., Kirschner, M.W. (1985). Influence of the centrosome on the structure of nucleated microtubules. *J. Cell Biol.* **100**, 1185-1191.

Falconer M.M., Donalson, G., Seagull, R.W. (1988). MTOC's in higher plant cells: an immunofluorescent study of microtubule assembly sites following depolymerization by APM. Protoplasma **144**, 46-55.

Fawcett, D.W. (1961). Intercellular bridges. *Exp. Cell Res.* **8** (Suppl.), 174-187.

Fernandes, J., Bate, M., VijayRaghavan, K. (1991). Development of the indirect flight muscles of *Drosophila*. *Development.* **113**, 67-77.

Fiil, A. (1978). Follicle cell bridges in the mosquito ovary: syncytia formation and bridge mophology. *J. Cell Sci.* **31**, 137-143.

Finlayson, L.H. (1975). Development and degeneration. In: Insect muscle. pp 75-149. New York, Acad. Press.

Foe, V.E. (1993) Mitosis and morphogenesis in the *Drosophila* embryo: point and counterpoint. In: The Development of *Drosophila melanogaster* (Ed.: Bate, Martinez Arias) Volume I, pp. 149, Cold Spring Harbor Lab. Press, USA.

Foe, V.E., Alberts, B.M. (1983). Studies of nuclear and cytoplasmic behaviour during the five mitotic cycles that precede gastrulation in *Drosophila* embryogenesis. *J. Cell Sci.* **61**, 31-70.

Fullilove, S.L., Jacobsen, A.G. (1971). Nuclear elongation and cytokinesisin *Drosophila montana. Dev. Biol.* **26**, 560-577.

Fyrberg, E., Ball, E., Kelly, M., Fyberg, C., Reedy, M.C. (1990). Molecular genetics of *Drosophila* sarcomeric alpha-actinin : Mutant alleles disrupt Z-disc integrity and myofibrillar insertions. *J. Cell Biol.* **110**, 1999-2012.

Glover, D.M. (1989). Mitosis in *Drosophila. J. Cell Sci.* **92**, 137-146.

Goldstein, L.S.B. (1991). The kinesin superfamily : tails of functional redundancy. *Trends Cell Biol.* **1**, 93-98.

Gorbsky, G.J., Sammack, P.J., Borisy, G.G. (1988) Microtubule dynamics and chromosome motion visualized in living anaphase cells. *J. Cell Biol.* **106**, 1185-1192.

Gorbsky, G.J., Simerly, C., Schatten, G., Borisy, G.G. (1990). Microtubules in the metaphase-arrested mouse oocyte turn over rapidly. *Proc. Na. Acad. Sci. USA.* **87**, 6049-6053.

Gosti, F., Marty, M.C., Courvalin, J.C., Maunoury, R., Bornens, M. (1987). Centrosomal proteins and lactate dehydrogenase possess a common epitope in human cell lines. *Proc. Natl. Acad. Sci. USA.* **84**, 1000-1004.

Gosti-Testu, F., Marty, M.C., Berges, J., Maunoury, R., Bornens, M. (1986). Identification of centrosomal proteins in a human lymphoblastic cel line. *EMBO. J.* **5**, 2545-2550.

Gould, R.R., Borisy, G.G. (1977). The pericentriolar material in chinese hamster ovary cells nucleates microtubule formation. *J. Cell Biol.* **73**, 601-615.

Heidemann, S.R., Landers, J.M., Hamborg, M.A. (1981). Polarity orientation of axonal microtubules. *J. Cell Biol.* **91**, 661-665.

Hofbauer, A., Campos-Ortega, J.A. (1990). Proliferation pattern and early differentiation of the optic lobes in *Drosophila melanogaster. Roux's Arch. Dev. Biol.* **198**, 264-274.

Horio, T., Uzawa, S., Jung, M.K., Oakley, B.R., Tanaka, K. and Yanagida, M. (1991). The fission yeast γ-tubulin is essential for mitosis and is localized at microtubule organizing centres. *J. Cell Sci.* **99**, 693-700.

Joshi, H.C., Palacios, M.J., McNamara, L. and Cleveland, D.W. (1992). γ-Tubulin is a centrosomal protein required for cell cycle-dependent microtubule nucleation. *Nature* **356**, 80-83.

Julian, M., Tollon, Y., Lajoie-Mazenc, I., Moisand, A., Mazarguil, H., Puget, A., Wright, M. (1993). γ-Tubulin participates in the formation of the midbody during cytokinesis in mammalian cells. *J. Cell Sci.* **105**, 145-156.

Kahoh, K., Ishikawa, H. (1989) The cytoskeletal involvement in cellularization of the *Drosophila melanogaster* embryo. *Protoplasma* **150**, 83-95.

Kallajoki, M., Weber, K., Osborn, M. (1991). A 210Kd. nuclear matrix protein is a functional part of the mitotic spindle; a microinjection study using SPN monoclonal antibodies. *EMBO. J.* **10**, 3351-3362.

Kallajoki, M., Weber, K., Osborn, M. (1992). Ability to organize microtubules in taxol-treated PtK2 cels goes with the SPN antigen and not with the centrosome. *J. Cell Sci.* **102**, 91-102.

Kallajoki, M., Harborth, J., Weber, K., Osborn, M. (1993). Microinjection of a monoclonal antibody against SPN antigen, now identified by peptide sequences as the NUMA protein, induces micronuclei in PtK_2 cells. *J. Cell Sci.* **104**, 130-150.

Kalt, A. Schliwa, M. (1993). Molecular components of the centrosome. *Trends Cell Biol.* **3**, 118-128.

Kamimura, S., Mandlekov, E. (1992). Tubulin protofilaments and kinesin-dependent motility. *J. Cell Biol.* **118**, 865-875.

Karr, T.L., Alberts, B.M. (1986). Organization of the cytoskeleton in early *Drosophila* embryos. *J. Cell Biol.* **102**, 1494-1509.

Karsenti, E. (1993). Severing microtubules in mitosis. *Current Biol.* **3**, 208-210.

Khawaja, S., Gundersen, G.G., Bulinski,J.C. (1988). Enhanced stability of microtubules enriched in detyrosinated tubulin is not a direct function of detyrosination level. *J. Cell Biol.* **106**, 141-149.

Kidder, G.M., Barron, D.J., Olmsted, J.B. (1988). Contribution of midbody channels to embryogenesis in the mouse. *Roux's Arch. Dev. Biol.* **197**, 110-114.

Kimble, M., Incardona, J.P., Raff, E.C. (1989) A variant β-tubulin isoform of *Drosophila melanogaster* (β3) is expressed primarily in tissues of mesodermal origin in embryos and pupae, and is utilized in populations of transient microtubules. *Dev. Biol.* **131**, 415-429.

Kirschner, M.W., Mitchison, T.J. (1986) Beyond self-assembly: from microtubules to morphogenesis. *Cell* **45**, 329-342.

Kronebusch, P.J., Singer, S.J. (1987). The microtubule-organizing complex and the golgi apparatus are co-localized around the entire nuclear envelope of interphase cardiac myocytes. *J. Cell Sci.* **88**, 25-34.

Laemmli, U.K., (1970). Cleavage of the structral protins during the assembly of the head of bacteriophage T4. *Nature* **227**, 680-685.

Lai-Fook, J. (1967). The structure of developing muscle insertions in insects. *J. Morphol.* **123**, 503-528.

Lambert, A.M. (1993). Microtubule-organizing centres in higher plants. *Curr. Opin. Cell Biol* **5**, 116-122.

Lawrence, P.A. (1982). Cell lineage of the thoracic muscles of *Drosophila*. *Cell.* **29**, 493-503.

Le Dizet, M, Piperno, G. (1986). Cytoplasmic microtubules containing acetylated α-tubulin in *Chlamydomonas reinhardtii* spatial arrangement and properties. *J. Cell Biol.* **103**, 13-22.

Lee, G. (1993). Non-motor microtubule-associated proteins. *Curr. Opin. Cell Biol.* **5**, 88-94.

Lin, S.X.H., Collins, C.A. (1992). Immunolocalization of cytoplasmic dynein to lysosomes in cultured cells. *J. Cell Sci.* **101**, 125-137.

Liu, B., Joshi, H.C., Wilson, T.J., Silflow, C.D., Palevitz, B.A., Snustad, D.P. (1994). γ-Tubulin in *Arabidopsis* : Gene sequence, immunoblot, and immunofluorescence studies. *The Plant Cell.* **6**, 303-314.

Lupas, A., VanDyke, M., Stock, J. (1991). Predicting coiled-coils from protein sequences. *Science.* **252**, 1162-1164.

Maekawa, T., Leslie, R., Kuriyama, R. (1991). Identification of a minus end-specific microtubule-associated protein located at the mitotic poles in cultured mammalian cells. *Eur. J. Cell Biol.* **54**, 255-267.

Mandlekow, E., Mandlekow, E-M. (1994). Microtubule structure. *Current Opinion Structural Biol.* **4**, 171-179.

Manfredi, J.J., Parness, J., Horwitz, S.B. (1982). Taxol binds to cellular microtubules. *J. Cell Biol.* **94**, 688-696.

Manfredi, J.J., Fant, J., Horwitz, S.B. (1986). Taxol induces formation of unusual arrays of celluar microtubules in colchicine-pretreated J774.2 cells. *Eur. J. Cell Biol.* **42**, 126-134.

Margolis, R.L., Rauch, C.T., Pirollet, F., Job, D. (1990). Specific association of STOP protein with microtubules *in vitro* and with stable microtubules in mitotic spindles of cultured cells. *EMBO J.* **9**, 4095-4102.

Margolis, R.L., Andreassen, P.R. (1993). The telophase disc: its possible role in mammalian cell cleavage. *BioEssays.* **15**, 201-207.

Masuda, H., Sevik, M., Cande, W.Z. (1992). In vitro microtubule-nucleating activity of spindle pole bodies in fission yeast *Schizosaccharomyces pombe*: cell cycle-dependent activation in *Xenopus* cell free extracts. *J. Cell Biol.* **117**, 1055-1066.

McBeath, E., Jujiwara, K. (1990). Microtubule detachment from the microtubule-organizing centre as a key event in the complete turnover of microtubules in cells. *European J. Cell Biol.* **52**, 1-16.

McDonald, A.R., Liu, B., Joshi, H.C. and Palevitz, B.A. (1993). γ-Tubulin is associated with a cortical microtubule organizing zone in the developing gaurd cells of *Allium-Cepa L. Planta.* **191**, 357-361.

McIntosh, J.R., Landis, S.C. (1971). The distribution of spindle microtubules during mitosis in cultured human cells. *J. Cell Biol.* **49**, 468-497.

McIntosh, J.R., Cande, Z., Snyder, J., Vanderslice, K. (1975). Studies on the mechanism of mitosis. *Ann. N.Y. Acad. Sci.* **253**, 407-427.

McIntosh, J.R., Euteneuer, U. (1984). Tubulin hooks as probes for microtubule polarity : an analysis of the method and evaluation of data on microtubule polarity in the mitotic spindle. *J. Cell Biol.* **98**, 525-533.

McNally, F.J., Vale, R.D. (1993). Identification of Katanin, an ATPase that severs and disassembles stable microtubules. *Cell.* **75**, 419-429.

McQuilkin, W.T., Earle, W.R. (1962). Cinemicrographic analysis of cell populations *in vitro*. *J. Natl. Cancer Inst.* **28**, 763-782.

Mitchison T.J., Sedat, J. (1983). Localization of antigenic determinants in whole *Drosophila* embryos. *Developmental Biology.* **99**, 261-264.

Mitchison, T. J. and Kirschner, M.W. (1984). Dynamic instability of microtubule growth. *Nature.* **312**, 237-242.

Mitchison, T.J., Kirschner, M.W. (1985). Properties of the kinetochore *in vitro*. II. Microtubule capture and ATP-dependent translocation. *J. Cel Biol.* **101**, 766-777.

Mogensen, M. M., Tucker, J. B. (1987). Evidence for microtubule nucleation at plasma membrane-associated sites in *Drosophila*. *J. Cell Sci.* **88**, 95-107.

Mogensen, M.M., Tucker, J.B. (1988). Intermicrotubular actin filaments in the transalar cytoskeletal arrays of *Drosophila*. *J. Cell Sci.* **91**, 431-438.

Mogensen, M.M., Tucker, J.B., Stebbings, H. (1989). Microtubule polarities indicate that nucleation and capture of microtubules occurs at cell surfaces in *Drosophila*. *J. Cell Biol.* **108**, 1445-1452.

Mogensen, M.M., Tucker, J.B. (1990). Taxol influences control of protofilament number at microtubule-nucleating sites in *Drosophila*. *J. Cell Sci.* **97**, 101-107.

Mogensen, M.M., Tucker, J.B., Baggaley, T.B. (1993). Multiple plasma membrane-associated MTOC system in the acentrosomal cone cells of *Drosophila* ommatidia. *Eur. J. Cell Biol.* **60**, 67-75.

Moudjou, M., Paintrand, M., Vigues, B., Bornens, M. (1991). A human centrosomal protein is immunologicaly related to basal body-associated proteins from lower eucaryotes and is involved in the nucleatio of microtubules *J. Cell Biol.* **115**, 129-140.

Mullins, J.M., Biesele, J.J. (1973). Cytokinetic activities in a human cell line: the midbody and intercellular bridge. *Tissue Cell.* **5**, 47-61.

Mullins, J.M., Biesele, J.J. (1977). Terminal phase of cytokinesis in D-98S cells. *J. Cell Biol.* **73**, 672-684.

Mullins, J.M., McIntosh, J.R. (1982). Isolation and initial characterization of the mammalian midbody. *J. Cell Biol.* **94**, 654-661.

Multigner, L., Gagnon, J., Van Dorsselaer, A., Job, D. (1992). Stabilization of sea urchin flagellar microtubules by histone H1. *Nature.* **360**, 33-39.

Murray, A.W., Kirschner, M.W. (1989). Cyclin synthesis drives the early embryonic cell cycle. *Nature.* **339**, 275-280.

Neighbors, B.W., Williams, R.C. Jr, McIntosh, J.R. (1988). Localization of kinesin in cultured cells. *J. Cell Biol* **106**, 1193-1204.

Oakley, B.R., Morris N.R. (1981). A β-tubulin mutation in *Aspergillus nidulans* that blocks microtubule function without blocking microtubule assembly. *Cell* **24**, 837-845.

Oakley, C.E., Oakley, B.R. (1989). Identification of γ-tubulin, a new member of the tubulin superfamily encoded by mipA gene of *Aspergillus nidulans*. *Nature*, **338**, 662-664.

Oakley, B.R., Oakley, C.E., Yoon, Y., Jung, M.K. (1990). γ-Tubulin is a component of the spindle pole body that is essential for microtubule function in *Aspergillus nidulans*. *Cell* **61**, 1289-1301.

Oakley, B.R. (1994). γ-Tubulin. In: *Microtubules*. (ed's.: Hyams, J.S., Lloyd, C.W.), pp. 27-45, Chichester, Uk, Wiley-Liss.

Olmsted, J.B. (1986). Microtubule-associated proteins. *Annu. Rev. Cell Biol.* **2**, 421-457.

Oppenheim, D.S., Hauschka, B.T., McIntosh, J.R. (1973). Anaphase motions in dilute colchicine. Evidence of two phases in chromosome separation. *Exp. Cell Res.* **79**, 95-105.

Palacious, M.J., Joshi, H.C., Simerly, C. and Schatten, G. (1993). γ-Tubulin reorganisation during mouse fertilization and early development. *J. Cell Sci.* **104**, 383-389.

Parness, J., Horwitz, S. (1981). Taxol binds to polymerized tubulin *in vitro*. *J. Cell Biol.* **91**, 479-487.

Paschal, B.M., Vallee, R.B. (1987). Retrograde transport by the microtubule-associated protein MAP-1C. *Nature.* **330**, 181-183.

Paul, E.C.A., Quaroni, A. (1993). Identification of a 102KDa protein (cytocentrin) immunologically related to keratin 19, which is a cytoplasmically derived component of the mitotic spindle pole. *J. Cell Sci.* **106**, 967-981.

Pepperkok, R., Bre, M-H., Davoust, J., Kreis, T.E. (1990). Microtubules are stabilized in confluent epithelial cells but not in fibroblasts. *J. Cell Biol.* **111**, 3003-3012.

Peristianis, G., Gregory, D. (1971). Early stages of flight muscle development in the blowfly Lucilia cuprina: a light and electron microscope study. *J. Insect Physiol.* **17**, 1005-1022.

Piperno, G. and Fuller, M.T. (1985). Monoclonal antibodies specific for an acetylaated form of a-tubulin recognize the antigen in cilia and flagella from a variety of organisms. *J. Cell Biol.* **101**, 2085-2094.

Poodry, C.A., Schneiderman, H.A. (1970). The ultrastructure of the developing leg of *Drosophila melanogaster. Wilhelm Roux Arch. EntwMech. Org.* **166**, 1-44.

Prokop, A., Technau, G.M. (1991) The origin of postembryonic neuroblasts in the ventral nerve cord of *Drosophila melanogaster. Development* **111**, 79-88.

Pryer, N., Walker, R., Skeen, B., Bourns, B., Soboeiro, M., Salmon, E.D. (1992). Brain microtubule-associated proteins modulate microtubule dynamic instability in vitro : real-time observations using video microscopy. *J. Cell Sci.* **103**, 965-976.

Raff, E.C. (1984). Genetics of microtubule systems. *J. Cell Biol.* **99**, 1-10.

Rao, S., Horwitz, S.B., Ringel, I. (1992). Direct photoaffinity labelling of tubulin with taxol. *J. Natl. Cancer Inst.* **84**, 785-788.

Ratner, J.B. (1992). Mapping the mammalian intercellular bridge. *Cell Motility Cytoskeleton* **23**, 231-235.

Reedy, M.C., Beall, C. (1993a). Ultrastructure of developing flight muscles in *Drosophila*. I. Asembly of myofibrils. *Developmental Biol.* **160**, 443-465.

Reedy, M.C., Beall, C. (1993b). Ultrastructure of developing flight muscles in *Drosophila*. II. Formation of the myotendon junction. *Develop. Biol.* **160**, 466-479.

Reynolds, E.S. (1963). The use of lead citrate at high pH as an electron-opaque stain in electron microscopy. *J. Cell Biol.* **17**, 527-531.

Rowinsky, E.K., Donehower, R.C. (1991). The clinical pharmacology and use of antimicrotubule agents in cancer chemotherapeutics. *Pharmacol. Ther.* **52**, 35-84.

Sager, P.R., Rothfield, N.L., Oliver, J.M., Berlin, R.D. (1986). A novel mitotic spindle pole component that originates from the cytoplasm during prophase. *J. Cell Biol.* **103**, 1863-1872.

Saito, K., Hama, K. (1982). Structural diversity of microtubules in the supporting cells of the sensory epithelium of guinea pig organ of Corti. *J. E.Microsc.* **31**, 278-281.

Salmon, E.D., Goode, D., Maugel, T.K., Bonar, D.B. (1976). Pressure-induced depolymerization of spindle microtubules. III. differential stability in HeLa cells. *J. Cell Biol.* **69**, 443-454.

Sammak, P.J., Gorbsky, G.J., Borisy, G.G. (1987). Microtubule dynamics *in vivo* : a test of mechanisms of turnover. *J. Cell Biol.* **104**, 395-405.

Sammak, P.J., Borisy, G.G. (1988). Direct observation of microtubule dynamics in living cells. *Nature.* **332**, 724-726.

Sanders, M.A., Salisbury, J.L. (1989). Centrin-mediated microtubule severing during flagellar excision in *Chlamydomonas reinhardtii. J. Cell Biol.* **108**, 1751-1760.

Sanders, M.A., Salisbury, J.L. (1994). Centrin plays an essential role in microtubule severing during flagellar excision in *Chlamydomonas reinhardtii. J. Cell Biol.* **124**, 795-805.

Sanger, J.M., Pochapin, M.B., Sanger, J.W. (1985). Midbody sealing after cytokinesis in the embryos of the sea urchin *Arabacia punctulata. Cell Tiss. Res.* **240**, 287-292.

Saxton, W.M., Stemple, D.L., Leslie, R.J., Salmon, E.D., Zavortink, M., McIntosh, J.R. (1984). Tubulin dynamics in cultured mammalian cells. *J. Cell Biol.* **99**, 2175-2186.

Saxton, W.M., McIntosh, J.R (1987). Interzone microtubule behavior in late anaphase and telophase spindles. *J. Cell Biol.* **105**, 875-886.

Schatten, G., Schatten, H., Bestor, T.H., Balczon, R. (1982). Taxol inhibits the nuclear movements during fertilization and induces asters in unfertilized sea urchin eggs. *J. Cell Biol.* **94**, 455-465.

Schatten, H., Walter, M., Mazia, M., Biessmann, D., Paweletz, H., Coffe, G., Schatten, J. (1987). Centrosome detection in sea urchin egs with a monoclonal antibody against *Drosophila* intermediate filament proteins: Characterization of stages of the division cycle. *Proc. Nat. Acad. Sci. USA.* **84**, 8488-8492.

Scheele, R.B., Bergen, L.G., Borisy, G.G. (1982). Control of the structural fidelity of microtubules by initiation sites. *J. Mol. Biol.* **154**, 485-500.

Schiff, P.B., Fant, J., Horwitz, S.B. (1979). Promotion of microtubule assembly *in vitro* by taxol. *Nature* **277**, 665-667.

Schiff, P.B., Horwitz, S.B. (1980). Taxol stabilizes microtubules in mouse fibroblast cells. *Proc. Nat. Acad. Sci. USA.* **77**, 1561-1565.

Schulze, E.S., Blose, S.H. (1984). Passage of molecules across the intercellular bridge between post-mitotic daughter cells. *Exp. Cell Res.* **151**, 367-373.

Schulze, E. Asai, D.J., Bulinski, J.C., Kirschner, M. (1987). Posttranslational modifications and microtubule stability. *J. Cell Biol.*, **81**, 624-634.

Sellitto, C., Kuriyama, R. (1987). Analysis of MTOC-components with monoclonal antibodies. *J. Cell Biol.* **105**, 282a. (Abstr.).

Sellitto, C., Kuriyama, R. (1988). Distribution of matrix component of the midbody during the cell cycle in Chinese hamster ovary cells. *J. Cell Biol.* **106**, 431-439.

Shafiq, A. (1963). Electron microscopic studies on the indirect flight muscles of *Drosophila melanogaster*. II. Differentiation of myofibrils. *J. Cell Biol.* **17**, 363-371.

Shelden, E., Wadsworth, P. (1990). Interzone microtubules are dynamic during spindle elongation. *J. Cell Sci.* **97**, 273-282.

Song, Y-H., Mandlekow, E. (1995). The anatomy of flagellar microtubules: polarity, seam, junctions, and lattice. *J. Cell Biol.* **128**, 81-94.

Stearns, T., Evans, L., Kirschner, M. (1991). γ-Tubulin is a highly conserved component of the centrosome. *Cell* **65**, 825-836.

Stearns, T. and Kirschner, M. (1994). *In vitro* reconstitiution of centrosome assembly and function - the central role of γ-tubulin. *Cell* **76**, 623-637.

Sullivan, K.F. (1988). Structure and utilization of tubulin isotypes. *Annu. Rev. Cell Biol.* **4**, 687-716.

Sunkel, C.E., Gomes, R., Sampaio, P., Perdigao, J., Gonzalez, C. (1995). γ-Tubulin is required for the structure and function of the microtubule organizing centre in *Drosophila* neuroblasts. *EMBO J.* **14**, 28-36.

Tassin, A-M., Maro, B., Bornens, M. (1985). Fate of microtubule-organizing centers during myogenesis *in vitro*. *J. Cell Biol.* **100**, 35-46.

Thompson, W.C., Wilson, L., Purich, D.L. (1981). Taxol induces microtubule assembly at low temperature. *Cell Motil.* **1**, 445-454.

Thompson, W.C. (1982). The cyclic tyrosination/detyrosination of α-tubulin. *Methods Cell Biol.* **24**, 235-255.

Tilney, L.G., Bryan, J., Bush, D.J., Fujiwara, K., Mooseker, M.S., Murphy, D.R., Snyder, D.H. (1973). Microtubules: evidence for 13 protofilaments. *J. Cell Biol.* **59**, 267-275.

Todorov, I.T., Philipova, R.N., Joswig, G., Werner, D. and Ramaekers, F.C.S. (1992). Detection of the 125-KDA nuclear-protein mitotin in centrosomes, the poles of the mitotic spindle, and the midbody. *Experimental Cell Research.* **199**, 398-401.

Truman, J.W., Taylor, B.J. (1993) Formation of the adult nervous system. In: The Development of *Drosophila melanogaster* (Ed.: Bate, Martinez Arias) Volume II, pp. 1245, Cold Spring Harbor Lab. Press, USA.

Tucker, J.B. (1982). Microtubule-organizing centres and assembly of intricate microtubule arrays in protozoans. In: Microtubules in micro-organisms. (eds.: Cappuccinelli, P., Morris, N.R.) Marcel Dekker,Inc., New York. 351-375.

Tucker, J.B. (1984). Spatial organization of microtubule-organizing centres and microtubules. **99**, 55s-62s.

Tucker, J.B., Milner, M.J., Currie, D.A., Muir, J.W., Forrest, D.A., Spencer, M.J. (1986). Centrosomal microtubule-organizing centres and a switch in the control of protofilament number for cell surface-associated microtubules during *Drosophila* wing morphogenesis. *Eur. J. Cell Biol.* **41**, 279-289.

Tucker, J.B., Paton, C.C., Richardson, G.P., Mogensen, M.M., Russell, I.J. (1992). A cell surface-associated centrosomal layer of microtubule-organizing material in the inner pillar cell of the mouse cochlea. *J. Cell Sci.* **102**, 215-226.

Tuffanelli, D.L., McKeon, F., Kleinsmith, D.M., Burnham, T.K. Kirschner, M. (1983). Anti-centrosome and anti-centriole antibodies in the scleroderma spectrum. *Arch. Dermatol.* **119**, 560-566.

Vale, R.D., Schnapp, B.J., Mitchison, T., Steuer, E., Reese, T.S., Sheetz, M.P. (1985). Different axoplasmic proteins generate movement in opposite directions along microtubules *in vitro*. *Cell* **43**, 623-632.

Vale, R.D. (1987). Intracellular transport using microtubule-based motors. *Ann. Rev. Cell Biol.*, **3**, 347-378.

Vandre, D., Davis, F., Rao., P., Borisy, G. (1984). Phosphoproteins are components of mitotic microtubule organizing centres. *Proc. Natl. Acad. Sci. USA* **81**, 4439-4443.

Verde, F., Berrez, J-M., Antony, C., Karsenti, E. (1991). Taxol induced microtubule asters in mitotic extracts of *Xenopus* eggs: requirement for phosphorylated factors and cytoplasmic dynein. *J. Cell Biol.* **112**, 1177-1187.

Verde, F., Dogterom, M., Stelzer, E., Karsenti, E., Leibler, S. (1992) Control of microtubule dynamics and length by cyclin A-dependent and cyclin B-dependent kinases in *Xenopus* egg extracts. *J. Cell Biol.* **118**, 1097-1108.

Wade, R.H., Chretien, D., and Job, D. (1990). Characterization of microtubule protofilament numbers - how does the surface lattice accomodate. *J. Mol. Biol.* **212**, 775-786.

Walker R.A., O'Brien E.T., Pryer N.K., Soboeiro M.F., Voter W.A., Erickson H.P., Salmon E.D. (1988). Dynamic instability of individual MAP-free microtubules analysed by video light microscopy : rate constants and transition frequencies. *J. Cell Biol.* **107**, 1437-1448.

Wani, M.C., Taylor, H.L., Wall, M.E., Coggon, P., McPhail, A.T. (1971). Plant antitumour agents. VI. The isolation and structure of taxol, a novel antileukemic and antitumor agent from Taxus brevifolia. *J. Am. Chem. Soc.* **93**, 2325-2327.

Warn, R.M., Magrath, R., Webb, S. (1984) Distribution of F-actin during cleavage of the *Drosophila* syncytial blastoderm. *J. Cell Biol.* **98**, 156-162.

Warn, R.M., Warn A. (1986). Microtubule aray present during the syncitial and cellular blastoderm stages of the early *Drosophila* embryo. *Exp. Cell Res.* **163**, 201-210.

Warn, R.M., Flegg, L., Warn, A. (1987). An investigation of microtubule organization and functions in living *Drosophila* embryos by injection of a fluorescently labeled antibody against tyrosinated α-tubulin. *J. Cell Biol.* **105**, 1721-1730.

Weber, J.E., Russell, L.D. (1987). A study of intercellular bridges during spermatogenesis in the rat. *Am. J. Anat.* **180**, 1-24.

Weil, C.F., Oakley, C.E., Oakley, B.R. (1986). Isolation of mip (microtubule-interacting protein) mutations of *Aspergillus nidulans*. *Mol. Cell Biol.* **6**, 2963-2968.

Westphal, C., Frosch, D. (1984). Electron-phase-contrast imaging of unstained biological materials, embedded in a water soluble melamine resin. *J. Ultrastruct. Res.* **88**, 282-286.

Wieschaus, E., Nusslein-Volhard, C. (1986). Looking at embryos. In : *Drosophila* a practical approach (ed.: Roberts, D.B.) Oxford.

Wilson, L., Miller, H.P., Farrell, K.W., Snyder, K.B., Thompson, W.C., Purich, D.L. (1985). Taxol stabilization of microtubules *in vitro* : Dynamics of tubulin addition and loss at opposite microtubule ends. *Biochemistry.* 24, 5254.

Wolf, N., Regan, C.L., Fuller, M.T. (1988) Temporal and spatial pattern of differences in microtubule behavior during *Drosophila* embryogenesis revealed by distribution of a tubulin isoform. *Development* **102**, 311-324.

Yu, W., Centonze, V.E., Ahmad, F.J., Bass, P.W. (1993). Microtubule nucleation and release from the neuronal centrosome. *J. Cell Biol.* **122**, 349-359.

Zheng, Y., Jung, M.K. and Oakley, B.R. (1991a). γ-Tubulin is present in *Drosophila melanogaster* and Homo-sapiens and is associated with the centrosome. *Cell* **65**, 817-823.

Zheng, Y, Oakley, C.E., Oakley, B.R. (1991b). Identification of a second γ-tubulin gene in *Drosophila melanogaster*. *J. Cell Biol.* **115**, 382a.